



**Determining the mechanism of
dichloroacetate-regulated processing of the
Alzheimer's disease-related amyloid precursor
protein.**

Hannah Victoria Simmons BSc (Hons).

Supervised by Dr. Ed Parkin.

This thesis is submitted in fulfilment of the degree of masters by Research in Biomedical
Science.

The work presented in this thesis is entirely my own work and has not been submitted in
substantially the same form of the award of a higher degree elsewhere.

March 2019.

Acknowledgements.

I would like to thank everyone in the BLS department at Lancaster University for helping me throughout both my undergraduate and Masters degrees. Particular thanks go to my supervisor, Dr Ed Parkin, for his guidance whilst in the laboratory and whilst compiling my thesis.

I would also like to thank my parents, friends and family for all the help they have given me over the years; both financially and emotionally. I couldn't have done it without you!

Abstract.

Alzheimer's disease (AD) is the most common form of dementia caused, arguably, by the accumulation in the brain of 'sticky' protein fragments called amyloid beta (A β)-peptides. These fragments are formed through the proteolytic cleavage of the amyloid precursor protein (APP) by β - and γ -secretases. However, in an alternate non-amyloidogenic pathway, α -secretase (ADAM10) cleaves APP within the A β -domain thereby precluding the formation of intact toxic peptides.

We have recently shown that orphan drug dichloroacetate (DCA) can inhibit the detrimental amyloidogenic APP processing pathway whilst boosting the beneficial non-amyloidogenic processing pathway. However, the mechanism(s) by which DCA exerts these effects are, as yet, unknown and, therefore, the current study aims to elucidate these mechanisms. Hence, through manipulating pH, p53 levels, lactate dehydrogenase (LDH) activity, pyruvate and lactate levels, mitochondrial autophagy and oxidative stress, we aimed to investigate each potential mechanism by characterising the resultant effects on APP expression and proteolysis. Furthermore, we also investigated the potential effects of DCA on the subcellular localisation of APP and the activity of BACE1. However, none of these potential mechanisms proved to be involved in the DCA mechanism of action. Therefore, in conclusion, the mechanism(s) behind DCA-mediated changes in APP proteolysis/expression have not yet been identified but could still provide valuable insights in relation to future potential AD treatments.

Contents.

1.	Literature Review.	1.
1.1.	Alzheimer's Disease.	2.
1.2.	Amyloid precursor protein proteolysis.	3.
1.2.1.	α -secretases.	6.
1.2.2.	β -secretase.	9.
1.2.3.	γ -secretase.	10.
1.3.	The amyloid cascade hypothesis.	14.
1.4.	Dichloroacetate.	16.
1.4.1.	Mode of DCA action.	17.
1.5.	DCA as a regulator of APP expression and proteolysis.	19.
1.5.1.	Altered pH as a potential mechanism by which DCA regulates APP proteolysis.	19.
1.5.2.	Altered p53 levels as a potential mechanism by which DCA regulates APP proteolysis.	21.
1.5.3.	Altered metabolite levels as potential mechanisms by which DCA regulates APP proteolysis.	22.
1.5.3.1.	Lactate Dehydrogenase.	22.
1.5.3.2.	Pyruvate.	23.

1.5.3.3. Lactic acid.	24.
1.5.4. Altered APP subcellular localisation as a potential mechanism by which DCA regulates APP proteolysis.	24.
1.5.5. Mitochondrial autophagy as a potential mechanism by which DCA regulates APP proteolysis.	27.
1.5.6. Oxidative stress as a potential mechanism by which DCA regulates APP proteolysis.	29.
1.6. Project Aims.	31.
2. Materials and Methods.	32.
2.1. Materials.	33.
2.2. Methods.	33.
2.2.1. Cell culture.	33.
2.2.2. Resurrecting and freezing cell lines.	34.
2.2.3. Cell treatments.	35.
2.2.4. Small interfering RNA (siRNA) treatments.	38.
2.2.5. Preparing conditioned medium and cell lysate samples.	39.
2.2.6. Bicinchoninic acid (BCA) protein assay.	40.
2.2.7. Sodium dodecylsulphate–polyacrylamide gel electrophoresis.	41.
2.2.8. Immunoblotting.	42.

2.2.9.	Amido black staining of membranes.	43.
2.2.10.	Quantification of immunoblots.	43.
2.2.11.	MTS (3-(4,5-dimethylthiazol-2-yl)-5-(3-carboxymethoxyphenyl)-2-(4-sulfophenyl)-2H-tetrazolium) cell viability assays.	43.
2.2.12.	Trypan Blue Assay.	44.
2.2.13.	BACE1 activity fluorescence assay.	44.
2.2.14.	Immunofluorescence microscopy.	45.
2.2.15.	Statistical analysis.	47.
3.	The role of pH in the DCA-mediated regulation of APP proteolysis.	48.
3.1.	The effect of different DCA treatment regimes on APP proteolysis.	49.
3.1.1.	24 h DCA treatment regime.	49.
3.1.2.	Extended time course DCA treatment regime.	55.
3.2.	The effect of pH altering compounds structurally related to DCA on APP expression/proteolysis.	59.
3.2.1.	Sodium acetate.	60.
3.2.2.	Acetic acid.	68.
3.3.	Summary.	76.

4.	DCA-mediated changes in p53 levels and the regulation of APP proteolysis.	78.
4.1.	Reactivating p53 and Inducing Tumour Apoptosis (RITA) enhancement of p53 levels.	79.
4.1.1.	Optimisation of RITA concentrations.	80.
4.1.2.	The effect of RITA on the DCA-mediated regulation of APP expression/proteolysis.	86.
4.2.	siRNA knockdown of p53.	92.
4.2.1.	Transfection optimisation.	92.
4.2.2.	The effect of p53 siRNA knockdown on DCA-mediated changes in APP expression/proteolysis.	95.
4.3.	Summary.	99.
5.	Altered pyruvate and lactic acid metabolism as factors in the DCA-mediated regulation of APP proteolysis.	100.
5.1.	Lactate dehydrogenase inhibition.	101.
5.1.1.	GSK2837808A (LDH-A and LDH-B inhibitor).	102.
5.1.2.	FX11 (LDH-A inhibitor).	106.
5.2.	Pyruvate and lactic acid supplementation.	112.

5.2.1.	Pyruvate.	112.
5.2.2.	Lactic acid.	118.
5.3.	Summary.	130.
6.	The effects of DCA on BACE1 activity and APP subcellular localisation.	132.
6.1.	The effect of DCA on BACE1 activity.	133.
6.2.	The effect of DCA on APP subcellular localisation.	134.
6.3.	Summary.	141.
7.	Mitochondrial autophagy and oxidative stress as possible mechanisms through which DCA regulates APP proteolysis.	142.
7.1.	Mitochondrial autophagy and DCA-regulated APP processing.	143.
7.1.1.	Ammonium chloride.	144.
7.1.2.	Chloroquine.	149.
7.2.	Oxidative stress and DCA-regulated APP processing.	153.
7.2.1.	DMSO.	154.
7.2.2.	NAC.	159.
7.3.	Summary.	163.

8.	Discussion.	165.
8.1.	Characterisation of DCA action in SH-SY5Y cells.	166.
8.2.	pH as a possible mediator of DCA action.	167.
8.3.	The interaction between p53 and APP expression/proteolysis.	170.
8.4.	The association between lactic acid, pyruvate and APP processing.	172.
8.5.	DCA and APP localisation.	176.
8.6.	DCA-induced mitophagy and APP expression/proteolysis.	177.
8.7.	ROS production as a potential mediator of DCA-regulated APP proteolysis.	178.
8.8.	Concluding remarks and future perspectives.	178.
9.	Appendices.	180.
9.1.	Appendix I.	181.
10.	References.	182.

Abbreviations:

A β , Amyloid- β .

AcD, acidic domain.

AD, Alzheimer's disease.

ADAM, a disintegrin and metalloprotease.

Acetyl-coA, acetyl coenzyme A.

AICD, amyloid precursor protein intracellular domain.

APH-1, anterior pharynx defective-1.

APP, amyloid precursor protein.

APP CTF, amyloid precursor protein carboxy-terminal fragment.

BACE1, β -site cleaving enzyme-1.

BCA, bicinchoninic acid.

BSA, bovine serum albumin.

CAPPD, central amyloid precursor protein domain.

CHO, chinese hamster ovary.

CTF, carboxy-terminal fragment.

CuBD, copper binding domain.

DCA, dichloroacetate.

DMEM, Dubecco's modified Eagle's medium.

DMSO, dimethyl sulphoxide.

DTT, dithiothreitol.

EC, endothelial cells.

ECL, enhanced chemiluminescence reagent.

FBS, foetal bovine serum.

FL, full length.

GFLD, growth factor like domain.

Gpx4, glutathione peroxidase 4.

Grp78, glucose-regulated protein 78.

GSMs, γ -secretase modulators.

JMR, juxtamembrane region.

KO, knock-out.

KPI, Kunitz-type protease inhibitor.

LDH, lactate dehydrogenase.

LDLR, low-density lipoprotein receptor.

MEF, mouse embryonic fibroblast.

M₁AChR, M1 muscarinic acetylcholine receptor.

NAC, N-acetyl cysteine.

NCT, nicastrin.

NF- κ B, nuclear factor- κ B.

NICD, notch intracellular domain.

NT, non-targeting.

PBS, phosphate buffered saline.

PC12, pheochromocytoma cell line 12.

PDC, pyruvate dehydrogenase complex.

PDK, pyruvate dehydrogenase kinase.

PDVF, polyvinylidene difluoride.

PEN-2, presenilin enhancer-2.

PFA, paraformaldehyde.

PKC, protein kinase C.

PM, plasma membrane.

PS, presenilin.

RITA, reactivating p53 and inducing tumour apoptosis.

ROS, reactive oxygen species.

SDS-PAGE, sodium dodecylsulfate – polyacrylamide gel electrophoresis.

siRNA, small interfering RNA.

TGN, trans-Golgi network.

Chapter 1.

Literature review.

1. Literature Review.

1.1. Alzheimer's Disease.

The ageing global population has driven a dramatic increase in neurodegenerative disease within the last 20 years, reaching an estimated 50 million dementia patients in 2018 (World Health Organisation, 2018). This figure is expected to triple over the next 30 years, reaching approximately 150 million patients by 2050 (Dementia Statistics Hub, 2018), highlighting the importance of research in this field.

Alzheimer's disease (AD), which accounts for 60–70 % of dementia cases, was initially described by Alois Alzheimer in 1907 (Sanabria-Castro *et al.*, 2017). Through studying his patient, Auguste Deter, Alzheimer defined AD as an “unusual disease of the cerebral cortex”, resulting in hallucinations, memory loss and death. It has since been determined that the brains of AD patients are characterised by the degradation of neurons and synapses (Robinson *et al.*, 2018), resulting in several clinical features. These clinical features develop slowly and progressively, initially affecting short-term memory, advancing to aphasia, apraxia and agnosia, and eventually resulting in premature death (Macdonald *et al.*, 2018).

The pathological hallmarks of AD include deposition of amyloid- β ($A\beta$) plaques and neurofibrillary tangles within the brain (Sanabria-Castro *et al.*, 2017) (Fig. 1.1.). The $A\beta$ plaques are composed of thick fibrils consisting of 40–43 amino acid $A\beta$ -peptides, whereas neurofibrillary tangles consist of paired helical filaments made up of hyperphosphorylated tau protein (Kamat *et al.*, 2014).

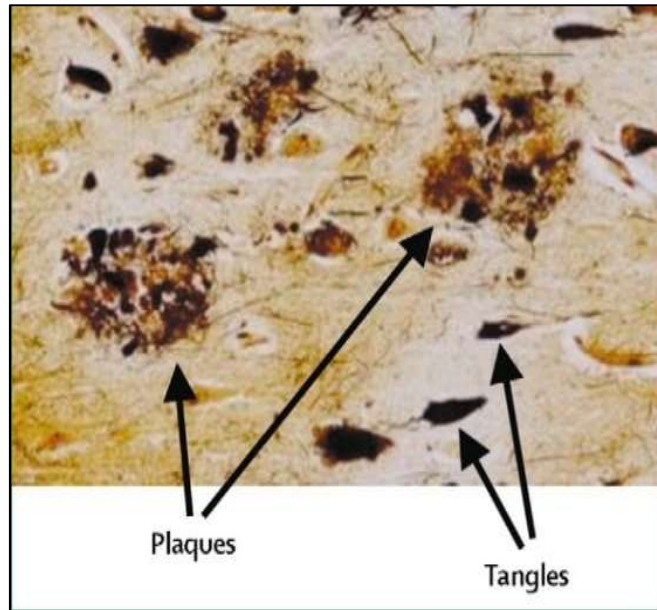


Figure 1.1. Pathology of an AD brain. Hallmark amyloid plaques and tau tangles visualised within an AD brain. (Image adapted from Blennow *et al.*, 2006).

One of the leading theories as to the causation of AD, called the “Amyloid Hypothesis”, suggests that the widespread degradation of neuronal matter observed in AD is a result of A β plaque formation (Hardy and Selkoe, 2002; Sanabria-Castro *et al.*, 2017). It suggests that the other hallmarks associated with AD arise due to the disproportional rates of A β formation and degradation, following changes in the proteolytic processing of the amyloid precursor protein (APP) (Hardy and Allsop, 1991).

1.2. Amyloid precursor protein proteolysis.

APP is a type-1 membrane protein containing a large extracellular amino-terminal region and a small cytosolic carboxyl-terminal region (Coronel *et al.*, 2018). Composed of 170 kb and 19 exons, the *APP* gene is alternatively spliced to generate 8 isoforms ranging in length from 365 to 770 amino acids (Holsinger *et al.*, 2013). The predominant transcript within the

central nervous system is the 695 amino acid isoform, whereas the predominant forms within other cell types are the 751 and the 770 amino acid isoforms (Coronel *et al.*, 2018).

APP contains several different domains (Pandey *et al.*, 2016). The large extracellular region consists of two domains, called E1 and E2 (Fig. 1.2.), connected by the acidic domain (AcD). The E1 domain is further divided into the growth-factor-like domain (GFLD) and the copper-binding domain (CuBD), whereas the E2 domain consists of the central APP domain (CAPPD). E2 is attached to the juxtamembrane region (JMR), which is adjoined to the APP intracellular domain (AICD) via a single transmembrane helix. The longer 751 and 770 amino acid APP isoforms also contain an additional Kunitz-type protease inhibitor domain (KPI) and the latter further possesses an OX-2 sequence (Coburger *et al.*, 2013).

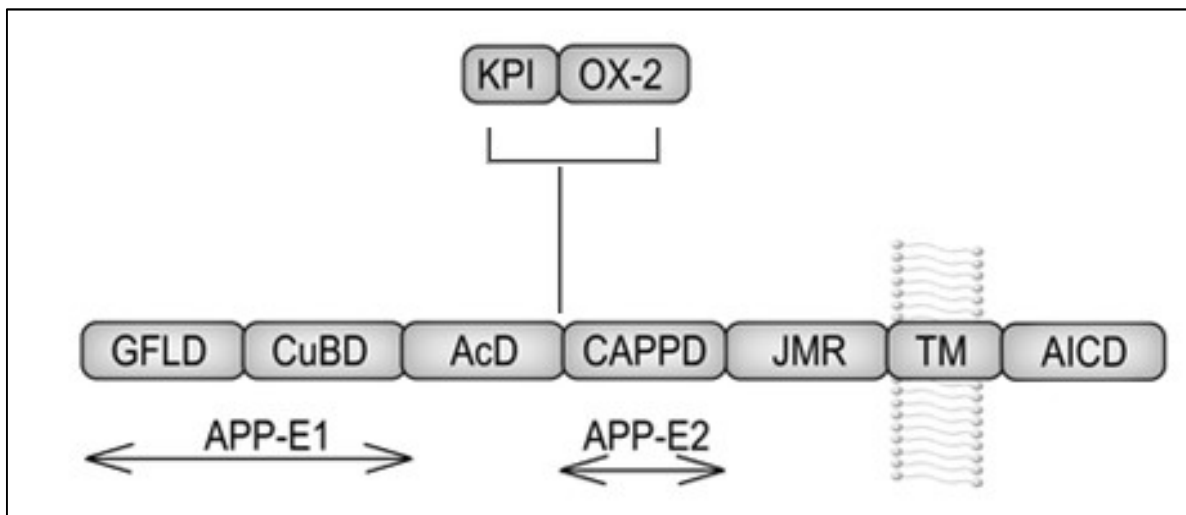


Figure 1.2. The domain composition of the amyloid precursor protein. The extracellular domain is composed of the E1 and E2 domains which are linked by an acidic domain (AcD). E1 is composed of a growth-factor-like-domain (GFLD) and a copper-binding-domain (CuBD). E2 is composed of a central APP domain (CAPPD). Additionally, a juxtamembrane domain (JMR) is bound to a single transmembrane helix which is bound to the APP intracellular domain (AICD). The longer 751 and 770 amino acid APP isoforms also contain an additional Kunitz-type protease inhibitor domain (KPI) and the latter further possesses an OX-2 sequence. (Image adapted from Coburger *et al.*, 2013).

After it is synthesised within membrane-bound polysomes, APP undergoes post-translational alterations (such as glycosylation, phosphorylation and sulphonation) and is transported to the surface membrane, or remains within the trans-Golgi network (TGN) (Plácido *et al.*, 2014).

APP is then cleaved via several proteolytic pathways including the 'amyloidogenic' and 'non-amyloidogenic' pathways (Fig. 1.3.). The former of these two pathways occurs primarily in the late endosomes and leads to the production of the neurotoxic A β -peptides found in plaques (Coronel *et al.*, 2018). Here, β -secretase cleaves APP to produce sAPP β and a carboxy-terminal fragment (β -CTF or C99). This β -CTF is then cleaved by γ -secretase to produce A β (4 kDa) and soluble AICD, which is involved in nuclear signalling (Eggert *et al.*, 2018). Conversely, in the non-amyloidogenic pathway (Fig. 1.3.), α -secretase cleaves APP to produce sAPP α and a truncated CTF (α -CTF or C83). This α -CTF lacks the N-terminal region of the A β domain, and so γ -secretase cleavage leads to the production of a truncated A β protein called p3 (3 kDa), along with soluble AICD. The sAPP α produced during the non-amyloidogenic pathway has neuroprotective qualities, boosting memory and preventing A β -related degeneration (Mattson *et al.*, 1993; Coronel *et al.*, 2018).

The amyloidogenic and non-amyloidogenic pathways are thought to be reciprocal in nature, with α -secretase enhancement inducing reductions in A β production (Nitsch *et al.*, 1992; Postina *et al.*, 2004). Therefore, it has been suggested that inhibiting the activity of β - or γ -secretase, or enhancing the activity of α -secretases, could be possible therapeutic targets for AD (Wang *et al.*, 2016; Gu *et al.*, 2017; Bhatt *et al.*, 2018).

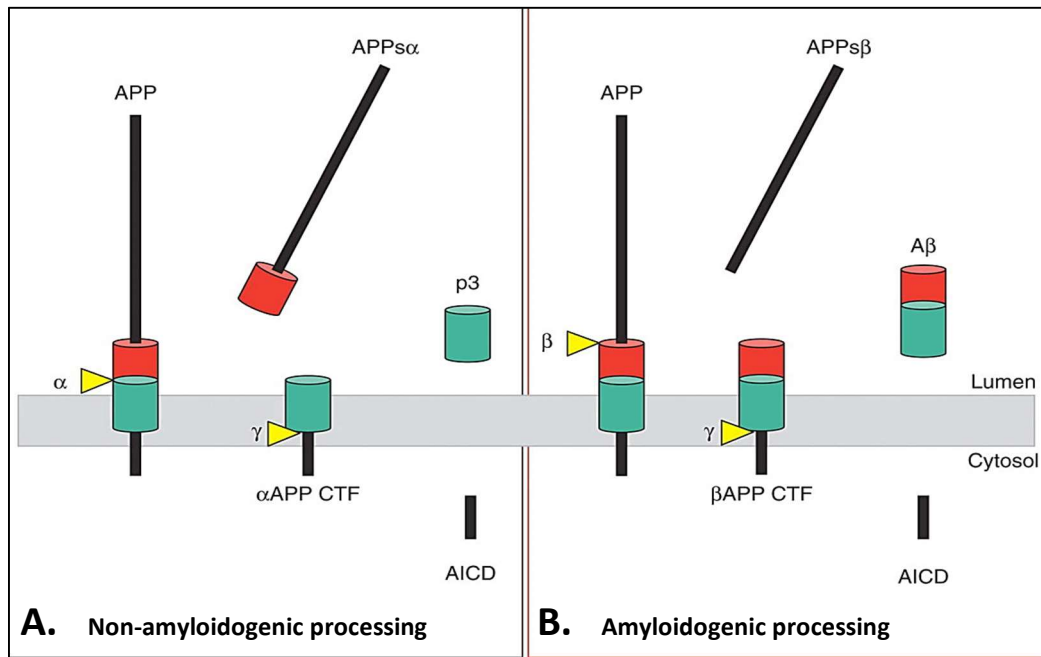


Figure 1.3. The non-amyloidogenic and amyloidogenic APP processing pathways. (A) The non-amyloidogenic pathway generates sAPP α , p3 and AICD through APP cleavage by the α - and γ -secretases. **(B)** The amyloidogenic pathway generates sAPP β , A β and AICD through APP cleavage by the β - and γ -secretases. (Image from Haass *et al.*, 2012).

1.2.1. α -secretases.

In most cells, >90 % of APP is processed via the non-amyloidogenic pathway, in which APP is cleaved between Lys16 and Leu17 of the A β sequence by an α -secretase activity (Yuan *et al.*, 2017; Eggert *et al.*, 2018). This enzymatic activity can be described as having both basal/constitutive and regulated forms; the latter being stimulated by phorbol ester activators of protein kinase C (PKC) (Wang *et al.*, 2016).

Several different enzymes have been implicated in α -secretase activity, primarily members of the a disintegrin and metalloprotease (ADAM) family (Wang *et al.*, 2016). For example, Lammich *et al.* (1999) observed an increase in both basal and PKC-stimulated sAPP α production in ADAM10-overexpressing HEK293 cells. The authors also demonstrated that endogenous α -secretase activity was inhibited by transfecting HEK293 cells with a dominant

negative form of ADAM10, containing a point mutation in the zinc binding site. Postina *et al.* (2004) also demonstrated the role of ADAM10 as an α -secretase, using transgenic mice overexpressing ADAM10 to show that the enzyme reduced brain plaque load and improved spatial learning relative to control animals, whereas overexpression of a dominant negative form of the enzyme led to an enhanced plaque load. Furthermore, Jorissen *et al.* (2010) generated conditional ADAM10 knockout mice by crossing Nestin-Cre transgenic mice with LoxP flanked ADAM10 mice. Global ADAM10 knockout mice usually die at embryonic day 9.5, but this system ablated ADAM10 expression specifically within neuronal cells, significantly enhancing the survival of the embryos. Although the mice died perinatally, they survived long enough for the identification of dramatically lower α -secretase activity in the embryonic brain, confirming the identity of ADAM10 as an α -secretase and suggesting it was responsible for a large proportion of basal α -secretase processing.

ADAM9 was also put forward as a potential α -secretase by Koike *et al.* (1999), who demonstrated that APP was cleaved specifically at the α -secretase site when co-expressed with ADAM9 in COS cells. The authors also found that inhibiting ADAM9 with the hydroxamate-based metalloprotease inhibitor, SI-27, enhanced β -secretase processing of APP, suggesting a reciprocal relationship between the non-amyloidogenic and amyloidogenic pathways. Additional studies have demonstrated that ADAM9 does not function as a secretase directly, but instead mediates the cleavage of APP through ADAM10 (Parkin and Harris, 2009; Tousseyn *et al.*, 2009). Parkin and Harris (2009) showed that ADAM10 itself could be shed by ADAM9 from the surface of HEK293 cells and that the shed form of the former enzyme was unable to cleave APP. Additional work by Tousseyn *et al.* (2009) found that ADAM10 shedding was decreased in ADAM9-deficient mouse embryonic fibroblast (MEF) cultures, and almost completely ablated in cells lacking both ADAMs 9 and 15, suggesting that

these two latter enzymes are both involved in ADAM10 shedding. As such, it would appear that ADAMs 9 and 15 are not true α -secretases but somehow work through ADAM10 to enhance the production of sAPP α .

Buxbaum *et al.* (1998) showed that primary embryonic fibroblasts from ADAM17 knockout mice had much lower regulated α -secretase function. Additionally, Slack *et al.* (2001) found that, when ADAM17 expression was enhanced in HEK293 cells, so too was sAPP α production. Caccamo *et al.* (2006) then suggested that ADAM17 acts as a regulated α -secretase, as M1 muscarinic acetylcholine receptor (M₁AChR) activation in a mouse model resulted in downstream PKC activation and enhanced activity of an α -secretase, subsequently identified as ADAM17.

It is now widely accepted that ADAM10 is the physiological constitutive α -secretase and ADAM17 probably a regulated secretase. However, it is worth noting that further studies have also implicated several other ADAM family members including ADAMs 8, 12 and 19 (Wang *et al.*, 2016).

As previously mentioned, boosting α -secretase activity has been suggested as a possible treatment for AD (Kumar *et al.*, 2018). For example, acitretin is a vitamin A analogue which has recently been investigated both in mouse models and clinical trials. In APP/PS1 transgenic mice, this drug led to a significant reduction in A β and enhanced activity of ADAM10 (Tippmann *et al.*, 2009). Phase II clinical trials, however, saw severe side effects such as cheilitis, peeling, alopecia and hepatotoxicity (Kumar *et al.*, 2018).

1.2.2. β -secretase.

The enzyme responsible for APP β -secretase cleavage is a 55.8 kDa transmembrane aspartyl protease called β -site APP cleaving enzyme-1 (BACE1) (Vassar *et al.*, 1999; Yan *et al.* 1999). Cai *et al.* (2001) demonstrated that this enzyme is the sole β -secretase in mice by showing that neurons from BACE1 knockout animals exhibited complete ablation of β -CTF and A β -peptide production.

BACE1 is initially synthesised within the ER and contains a short prodomain. This prodomain is then removed by post-translational modification within the Golgi and the protein is subject to several other modifications (such as glycosylation, phosphorylation, palmitoylation, ubiquitination and acetylation), allowing correct folding of the protease domain and enhanced enzymatic function (Araki, 2016; Sun and Roy, 2018). The mature BACE1 enzyme is membrane-bound and ubiquitously expressed in all tissues, with the highest levels identified in the pancreas and the brain (Prox *et al.*, 2012). The relevance of high levels in the pancreas is not yet fully understood, but the high levels in the brain help to explain why this organ is susceptible to AD.

BACE1 is localised in several subcellular sites including the endosomal compartments, TGN and endoplasmic reticulum (Sun and Roy, 2018). Whilst non-amyloidogenic processing primarily occurs at the surface membrane (Plácido *et al.*, 2014), cleavage by BACE1 mainly occurs upon re-internalisation to the endosomes or the TGN (Vassar *et al.*, 2004).

BACE1 inhibition has been suggested as a potential therapeutic target for AD, preventing the production of A β . However, this enzyme is thought to have other important physiological roles with several additional substrates, such as low-density lipoprotein receptor (LDLR) -related protein, identified in a study by von Arnim *et al.* (2005). Studies have

also shown that BACE1 has an important role in myelination and that inhibition can lead to hypomyelination (Willem *et al.*, 2006; Sankaranarayanan *et al.*, 2008). Although this may not be a problem in humans as neurons are fully myelinated by adulthood when AD develops, studies have identified other toxic effects of BACE1 inhibition, such as vascular dysregulation and retinal pathology (Cai *et al.*, 2001).

More recently, BACE1 inhibition has been tested in various clinical trials. However, none of these have shown any positive effect on slowing or restoring cognitive decline despite reducing A β and sAPP β levels (Kumar *et al.*, 2018). For example, Verubecestat was designed as a BACE1 inhibitor which selectively prevented the deposition of A β in various animal models (rats, mice and monkeys). However, a recent stage III clinical trial in mild-to-moderate AD patients by Merck was abandoned in February 2018 following findings that patients had no improvements in cognition despite a reduction in A β levels (Kumar *et al.*, 2018). Furthermore, these patients had increased falls, injuries, weight loss, and neuropsychiatric issues, including suicidal thoughts and sleep deprivation (Egan *et al.*, 2018).

1.2.3. γ -secretase.

The final proteolytic step in both the amyloidogenic and non-amyloidogenic pathways is performed by a 230 kDa intra-membrane cleaving aspartyl proteinase complex called γ -secretase (Aguayo-Ortiz *et al.*, 2018). This complex is composed of several distinct subunits: presenilins (PS) 1 or 2, nicastrin (NCT), anterior pharynx-defective 1 (APH-1) and presenilin enhancer 2 (PEN-2) (Zhang *et al.*, 2014).

The presenilins, which comprise the active component of the enzyme, were initially identified through genetic linkage analyses in familial AD families (Schellenberg *et al.*, 1992; Levylahad *et al.*, 1995). These studies identified two loci which were frequently mutated in AD patients on chromosomes 1 and 14, later identified through cloning and sequencing studies as *PSEN1* which encodes PS1 (on chromosome 14) and *PSEN2* which encodes PS2 (on chromosome 1) (Rogaev *et al.*, 1995; Sherrington *et al.*, 1995). The role of the presenilins in γ -secretase cleavage of APP was then directly demonstrated by De Strooper *et al.* (1998), who analysed γ -secretase function in PS1-deficient mouse embryos. They found that γ -secretase cleavage was almost completely ablated when PS1 was deleted, with no effect on α - and β -secretase function but a 5-fold reduction in A β production. Subsequently, studies have identified over 180 familial AD-linked mutations in the *PS* genes (Bursavich *et al.*, 2016).

Nicastrin was identified as a component of the γ -secretase complex through studies in *C.elegans*, in which the suppression of nicastrin expression resulted in the loss of γ -secretase function (Yu *et al.*, 2000). This component functions as a co-factor, binding to substrates and functioning as a γ -secretase receptor (Zhang *et al.*, 2014). Two additional co-factors, APH-1 and PEN-2, have also been identified through genetic screening in *C.elegans* (Francis *et al.*, 2002). Although the presenilins are the active components of the γ -secretase complex, all four protein components are required for the γ -secretase to mature and function correctly (Fraering *et al.*, 2004; Zoltowska and Berezovska, 2018). For example, one study identified that nicastrin is involved in the stability and trafficking of the mature complex (Zhang *et al.*, 2005), whereas another showed that APH-1 maintains the physical interactions between the different components of the secretase complex (Lee *et al.*, 2004).

The γ -secretase complex has relaxed specificity and APP CTFs are cleaved at several sites (ϵ , ζ , and γ -sites) resulting in the production of final A β peptides containing between 37 and 43 amino acids (Zoltowska and Berezovska, 2017). Approximately 90 % of A β produced is A β ₁₋₄₀ and <10 % is A β ₁₋₄₂, the latter of which aggregates more readily to form the A β oligomers observed in AD (Duggan *et al.*, 2016).

The exact process of APP CTF cleavage by γ -secretase is not fully understood. However, it has been suggested that the process occurs via a step-wise sequence of cleavages (Takami *et al.*, 2009) starting with cleavage at one of two ϵ -sites, followed by cleavage at one of two ζ -sites and followed, finally, by cleavage at one of the γ -sites (Fig. 1.4.). The final cleavage at one of the possible γ -sites occurs most commonly at amino acid 42 or 40 (but may occur at amino acid 37, 38 or 39 instead), resulting in the generation of A β ₁₋₄₂ or ₁₋₄₀ which is released into the extracellular space (Aguayo-Ortiz and Dominguez, 2017).

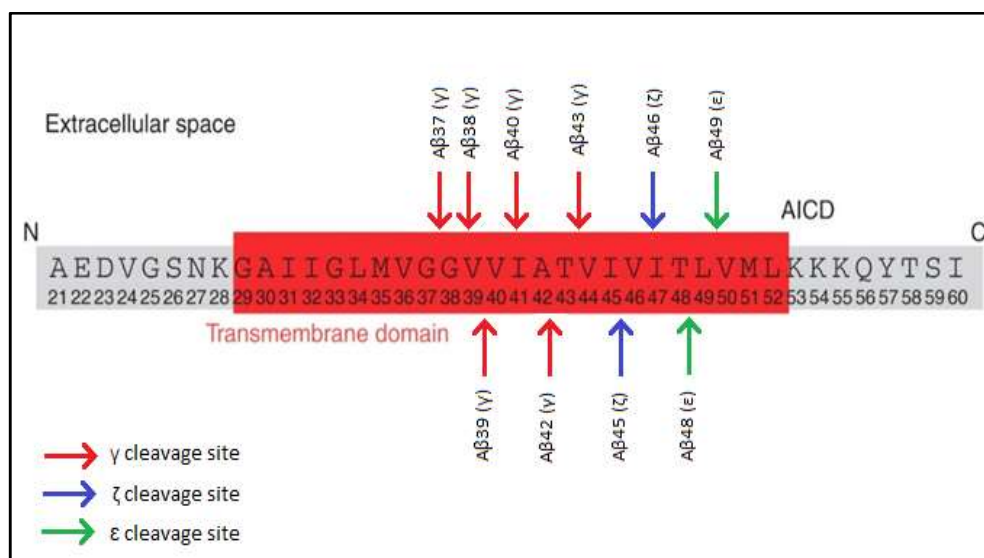


Figure 1.4. Cleavage of APP by γ -secretase. APP is cleaved at three distinct but relaxed sites (ϵ -, ζ -, and γ -sites) by γ -secretase, resulting in the production of A β , containing between 37- 43 amino acids. Initially, APP is cleaved at one of the possible ϵ -sites (green), either at amino acid 48 or 49. Next, the protein is cleaved at one of the possible ζ -sites (blue), either at amino acid 45 or 46. The final γ -site can occur at one of several sites (red), generating the final A β peptide of between 37 and 42 amino acids. (Image adapted from Haass *et al.*, 2012).

Several γ -secretase inhibitors have been investigated as possible AD treatments. For example, early clinical trials of Semagacestat saw significant dose-dependent decreases in A β plaque levels in the brains of AD patients (Henley *et al.*, 2009). However, in a phase III clinical trial, several side effects were observed including skin cancers and reduced lymphocyte counts (Doody *et al.*, 2013). These side effects are thought to be attributable to the role of γ -secretase in the cleavage of Notch, which is processed in a similar manner to APP, producing transcriptionally active Notch intracellular domain (NICD) (Kumar *et al.*, 2018). The trial was eventually abandoned because patients receiving Semagacestat also exhibited reductions in memory and cognitive function compared to placebo-treated patients, despite the reductions in A β generation. Another γ -secretase inhibitor, Avagacestat, has also been shown to result in a significant cognitive decline, brain atrophy and an increase in the incidence of skin cancers in AD patients treated with the drug relative to those receiving placebo (Coric *et al.*, 2015).

Largely in order to bypass the off-target effects, such as Notch signalling inhibition, γ -secretase modulators (GSMs) (as opposed to inhibitors) have recently been developed (Kumar *et al.*, 2018). Rather than inhibiting the γ -secretase, these drugs interact allosterically either with the γ -secretase complex or the APP CTF substrates. Clinical trials of several of these modulators have resulted in decreased A β formation and enhanced non-amyloidogenic APP processing (Bursavich *et al.*, 2016). These drugs commonly exhibit low efficacy and require very high doses (Kumar *et al.*, 2018) but a newer generation of GSMs show promise as they have been developed to have improved bioavailability and stability, therefore requiring lower doses.

1.3. The amyloid cascade hypothesis.

Although currently the subject of great discussion due to the failure of multiple β - and γ -secretase inhibitors/modulators in clinical trials, the amyloid cascade hypothesis (Fig. 1.5.) suggests that AD is initially caused by an increase in $A\beta$ generation from APP which exceeds the clearance of these peptides (Hardy and Allsop, 1991). This initial event then triggers a cascade resulting, ultimately, in neuronal dysfunction, the corresponding symptoms of AD and death.

The first clues in the identification of $A\beta$ -peptides as the putative toxic entity in AD came in the form of similarities between dementia observed in Down syndrome and the former disease. $A\beta$ was isolated and sequenced from the meningeal blood vessels of both AD and Down syndrome patients, suggesting a link between this peptide and the neurodegeneration observed in both conditions (Glenner and Wong, 1984). The following year, $A\beta$ -peptides were also identified in senile plaques from AD brains (Masters *et al.*, 1985). Sequencing studies then demonstrated that the *APP* gene was located on chromosome 21 and that mutations in this gene could lead to AD (Goldgaber *et al.*, 1987; Robakis *et al.*, 1987; Hardy, 1992). These findings also agreed with previous observations in Down syndrome cases, as these patients have an additional copy of chromosome 21 and, therefore, have an additional *APP* gene (Querfurth *et al.*, 2010).

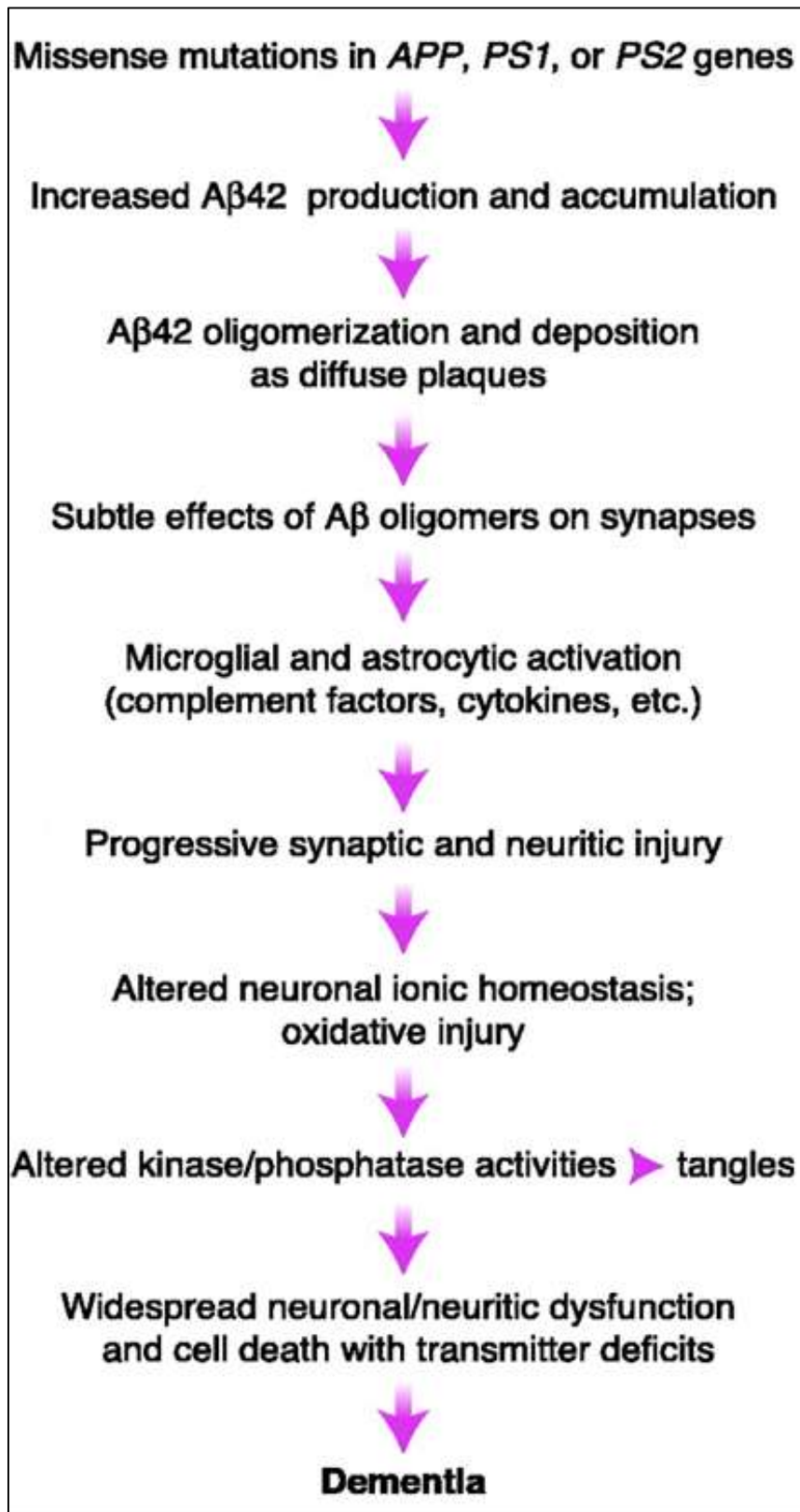


Figure 1.5. The Amyloid Cascade Hypothesis. When the production of A β 42 exceeds its clearance, the peptides aggregate and form plaques. This event then triggers a cascade which eventually results in AD. (Image from Hardy and Selkoe, 2002).

1.4. Dichloroacetate.

Dichloroacetate (DCA) (Fig. 1.6.) is an orphan drug which was originally studied as a possible treatment for mitochondrial diseases, such as lactic acidosis (James and Stacpoole, 2016), and has subsequently been investigated as a treatment for several other conditions including cancer, diabetes (Michelakis *et al.*, 2008) and, more recently, AD (Parkin *et al.*, unpublished data).

This small biomolecule (150 Da) can penetrate the blood-brain barrier with high bioavailability and is immediately absorbed when orally consumed (Stacpoole, 2017). The potential use of DCA in the treatment of lactic acidosis emanated from its identification as an indirect activator of the pyruvate dehydrogenase (PDH) (Kankotia and Stacpoole, 2014). Early studies in this field were promising and, in clinical trials, DCA reduced lactate levels and increased blood pH in lactic acidosis patients. However, these changes were later shown to have no significant effect on patient survival or disease-associated symptoms (Stacpoole *et al.*, 1992) and further research revealed that many patients experienced long-term cumulative DCA toxicity (Stacpoole *et al.*, 2012). Therefore, research into the use of DCA for the treatment of lactic acidosis was curtailed but the drug still shows promise for other applications.

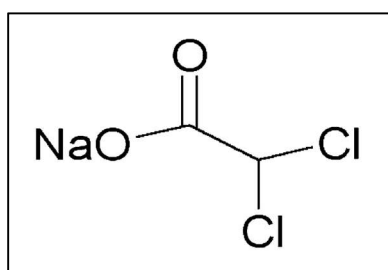


Figure 1.6. Molecular structure of DCA. (Image adapted from Kato *et al.*, 2007)

1.4.1. Mode of DCA action.

The most important site of DCA action is at the PDH, an enzyme found within the mitochondria which catalyses the decarboxylation of pyruvate to acetyl-coenzyme A (acetyl-coA) (Fig. 1.7.).

The activity of the PDH is tightly regulated to ensure that the correct levels of aerobic and anaerobic oxidation are carried out in the cell. This regulation is largely through the action of two types of enzymes; pyruvate dehydrogenase phosphatases which dephosphorylate and activate the PDH, and pyruvate dehydrogenase kinase (PDK) which phosphorylates and deactivates the complex (Fig. 1.7.) (James and Stacpoole, 2016).

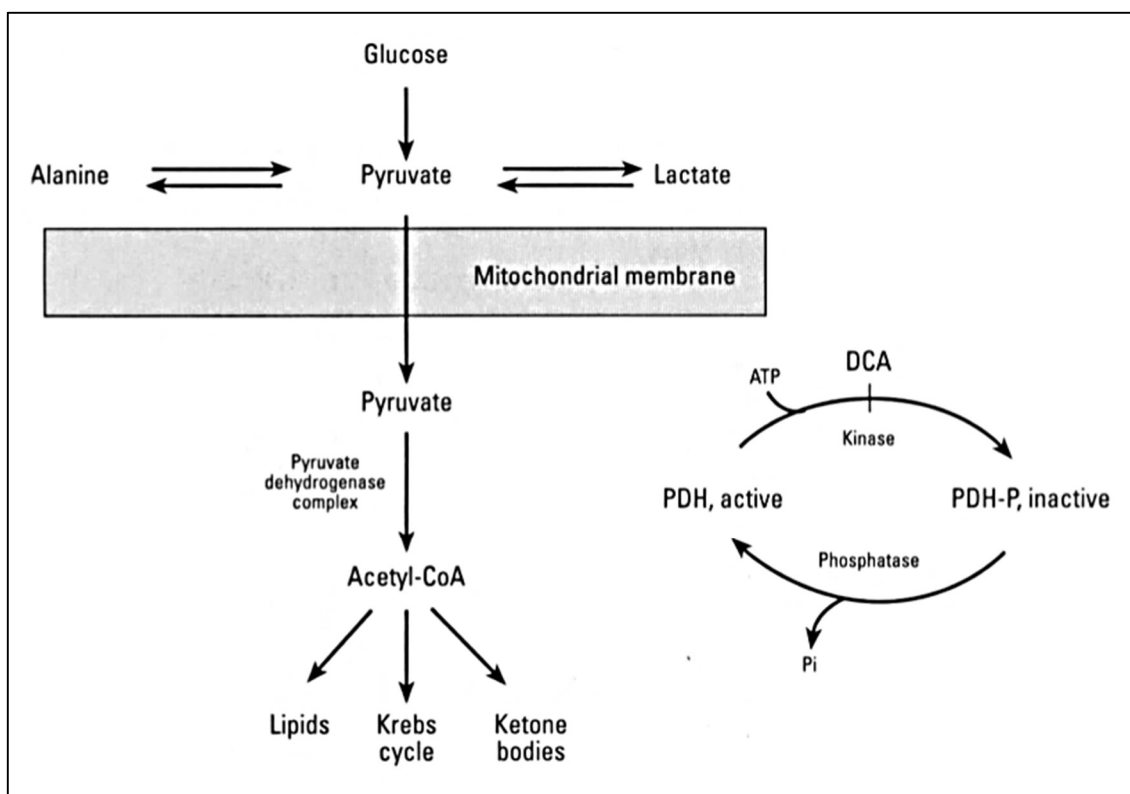


Figure 1.7. The mechanism of dichloroacetate (DCA) action. DCA inhibits PDH kinase and, therefore, maintains PDH in its active, dephosphorylated form. As a result, there is an increased generation of acetyl-coA from pyruvate catalysed by PDH. (Image from Mann *et al.*, 2000).

The primary mechanism through which DCA stimulates the PDH is through the inhibition of PDK, thereby ensuring that PDH is maintained in a dephosphorylated and active form (Neveu *et al.*, 2016). The drug binds to the hydrophobic binding pocket in the N-terminal domain of PDK, preventing the kinase from binding to the lipoyl E2 domain of PDH and hence preventing phosphorylation (Mann *et al.*, 2000; Stacpoole, 2017). Additionally, DCA can also cause a conformational change in the structure of PDK1, thereby blocking it from binding and phosphorylating the PDH (Kankotia and Stacpoole, 2014). Finally, DCA also inhibits the turnover of the PDH, preventing it from being broken down; however, the mechanism behind this latter process is currently unknown (Kankotia and Stacpoole, 2014). These mechanisms combine to result in an overall reduction in lactate levels, more acetyl-coA production and, therefore, more tricarboxylic acid cycle activity.

In recent years, DCA has been investigated as a possible treatment for cancer due to its ability to minimise the Warburg effect (Warburg *et al.*, 1927), whereby cancerous cells switch energy generation away from oxidative phosphorylation in the mitochondria to glycolytic energy generation in the cytosol (Sun *et al.*, 2018). DCA can reverse this process by minimising the availability of pyruvate, due to its enhanced utilisation by PDH (Stacpoole, 2017). This leads to a greater production of acetyl-coA, more tumour dependency on oxygen and, therefore, more susceptibility to hypoxia-specific chemotherapy (Wang *et al.*, 2017).

DCA also enhances free radical generation and associated cellular oxidative stress through the increased aerobic respiration resulting from PDH activation (Hassoun and Cearfoss, 2011). The drug minimises the ability of the mitochondrial membranes to hyperpolarise and opens transition pores within them, driving an increase in ROS production (Dai *et al.*, 2014). This enhanced ROS production and the associated increase in oxidative

stress have been proposed as another mechanism by which DCA promotes cancer cell death. It should, however, be noted that some studies have shown that specific tumour types have different responses to DCA and resistance to the drug can develop (Kankotia and Stacpoole, 2014).

1.5. DCA as a regulator of APP expression and proteolysis.

Recent studies in our laboratory (Parkin *et al.*, unpublished data) have demonstrated that DCA can enhance the non-amyloidogenic processing of APP in SH-SY5Y cells whilst impairing sAPP β and A β generation via the amyloidogenic pathway. However, the molecular mechanisms regulating this phenomenon are not yet known and are, therefore, the subject of the current study. The theories/background underlying the specific mechanisms tested are discussed in the following sections.

1.5.1. Altered pH as a potential mechanism by which DCA regulates APP proteolysis.

Sodium dichloroacetate is a sodium salt of dichloroacetic acid and, when in solution, acts as a base and raises the pH, making it more alkaline. DCA has also been shown to increase both extracellular and intracellular pH, most likely through decreased lactate levels as a consequence of drug treatment (Robey *et al.*, 2011; Albatany *et al.*, 2018).

Most studies suggest that, in Alzheimer's disease, there is an increase in cerebral acidosis and lactate accumulation within the cerebral spinal fluid, overall leading to a large decrease in neural pH. Bowen and Davison (1986) and Yates *et al.* (1990) reported a decreased tissue pH in the AD-afflicted brain and the former study suggested that this was due to an

accumulation of lactate and an alteration of anion exchange protein expression. Decreased pH has also been directly implicated in A β -peptide generation and aggregation. Brewer (1997) showed that increased acidity led to enhanced A β levels in cultured rat hippocampal neurons, whilst acidification has also been shown to promote aggregation of these peptides in rodent models and immobilised A β fibrils (Atwood *et al.*, 1998; Pirchl *et al.*, 2006; Brannstrom *et al.*, 2014).

The activity of APP cleaving secretases has been shown to be directly regulated by changes in pH (Brown *et al.*, 1998). For example, BACE1 is known to function optimally at pH 6 (Lin *et al.*, 2000; Xiang *et al.*, 2010). Furthermore, Hoefgen *et al.* (2015) showed that APP undergoes a conformational switch which is pH dependent and could affect proteolysis of the protein.

Schrader-Fischer *et al.* (1996) investigated the effect of alkalisising agents on the processing of APP in HEK293 cells and showed that, when cells were treated with ammonium chloride (which raise extracellular pH), amyloidogenic processing of APP was inhibited, suggesting a possible inhibition of BACE1. However, it should be noted that the same report showed that chloroquine and bafilomycin (which have a similar effect on pH) did not alter BACE1 activity in the same manner.

Collectively, these studies suggest that pH reductions promote amyloidogenic APP processing and provide evidence supporting the theory that alkalisising agents, such as DCA, might impair these processes through a simple change in pH.

1.5.2. Altered p53 levels as a potential mechanism by which DCA regulates APP proteolysis.

The p53 protein, otherwise known as the “guardian of the genome”, is a tumour-suppressing transcription factor which protects cells against uncontrolled division. Upon detection of stress, p53 transcriptionally activates various genes involved in cell cycle control and induces cycle arrest, DNA repair or apoptosis (Chira *et al.*, 2018; Labuschagne, Zani and Vousden, 2018). Over 50 % of cancers contain a mutation within the *TP53* gene, allowing cells to divide uncontrollably and evade cell death (Sabapathy and Lane, 2018). The function of the p53 protein has, therefore, been extensively investigated in this context. The expression of p53 has also been shown to be regulated by DCA (Agnoletto *et al.*, 2014) and to be regulated by APP proteolysis (Alves Da Costa *et al.*, 2006). Therefore, it is possible that there may be links between altered p53 levels and the ability of DCA to regulate APP proteolysis.

An increase in p53 levels, potentially leading to an increase in apoptosis and loss of neuronal cells, has been demonstrated in AD-afflicted brain tissues (Ganju *et al.*, 1998; Ohyagi *et al.*, 2005; Checler *et al.*, 2011). However, the direct link between p53 and APP processing is currently not fully understood.

Alves da Costa *et al.* (2006) demonstrated that the inhibition of γ -secretase function in various cells resulted in a significant reduction in p53 transcription, expression and function. The authors also showed that cells transfected with AICD displayed an increase in p53 transcription and function, and that *APP* knockout mice had lower brain p53 levels. Collectively, this study suggested that the AICD generated from APP CTFs by γ -secretase activity enhanced *TP53* promoter activity leading to increased p53 protein expression.

Whilst the preceding studies imply that APP can regulate p53 levels, it has also been shown that the latter protein can regulate the expression of the former. Cuesta *et al.* (2009) showed that increasing p53 expression and function led to a decrease in APP expression in murine N2a neuroblastoma cells. The authors went on to suggest that p53 prevented the binding of transcription factor Sp1 to the *APP* promotor, thereby impairing transcription of the gene. More recently, it has also been suggested that p53 may be able to regulate members of the γ -secretase complex (Checler *et al.*, 2010), which may, therefore, alter the processing of APP.

1.5.3. Altered metabolite levels as potential mechanisms by which DCA regulates APP proteolysis.

The indirect activation of the PDH by DCA is likely to have a significant impact on the levels of various cellular metabolites, not least lactic acid and pyruvate. We, therefore, hypothesised that the supplementation of cell cultures with these metabolites, or the inhibition of enzymes involved in their metabolism, might be able to mimic the effects of DCA on APP proteolysis. The background relating to this hypothesis is discussed in the following sections.

1.5.3.1. Lactate Dehydrogenase.

Initially, we sought to determine whether manipulating cellular levels of pyruvate or lactate through inhibition of lactate dehydrogenase (LDH) might mimic the effects of DCA on APP expression/proteolysis.

LDH is a vital enzyme involved in the reversible conversion of pyruvate to lactate in the glycolytic pathway (Fig. 1.7.). This enzyme is composed of two different monomers (A and B) which combine to form five different tetramers (LDH1–5), each with different properties and compositions of A and B monomers (Ding *et al.*, 2017). LDH-B, which is predominantly expressed in the heart, is thought to be responsible for the conversion of lactate to pyruvate (as it has a higher affinity for the former compound) (Dawson *et al.*, 1964). Conversely, LDH-A is highly expressed in skeletal muscle and has a higher affinity for pyruvate. Therefore, this monomer is thought to catalyse the conversion of pyruvate into lactate (Dawson *et al.*, 1964).

A link between the action of LDH and AD has been suggested following findings that neuronal cells with higher LDH function are resistant to A β (Soucek *et al.*, 2003). The most resistant cells showed a greater reliance on glucose availability, suggesting that the resistance to A β toxicity was due to reduced reliance on aerobic respiration. Furthermore, the brains of AD patients demonstrate increased LDH-A activity and increased PDK activity relative to age-matched controls (Bigl *et al.*, 1999).

1.5.3.2. Pyruvate.

We hypothesised that DCA might alter APP processing by reducing the pool of intracellular pyruvate levels due to the activation of the PDH (Fig. 1.7.). No previous studies have investigated how pyruvate may alter APP proteolysis, but the compound has been shown to protect neuronal cells against A β -induced toxicity in several studies (Alvarez *et al.*, 2003; Wang *et al.*, 2011).

1.5.3.3. Lactic acid.

Given that DCA promotes the conversion of pyruvate to acetyl-coA, and that the former compound is used to generate lactic acid (Fig. 1.7.), it was possible that DCA might mediate APP processing by reducing the intracellular pool of lactic acid.

Lactic acid has previously been shown to enhance levels of A β and lower sAPP α production in SH-SY5Y cell cultures (Xiang *et al.*, 2010). The authors also showed that full-length APP levels increased following lactic acid treatment and the protein exhibited an abnormal interaction with ER-chaperones, binding to glucose-regulated protein 78 (Grp78). It was suggested that this unusual binding led to an increased retention of APP in the ER/Golgi, enhanced co-localisation of APP and BACE1 and, therefore, an increased generation of A β and reduction of sAPP α production. Conversely, other studies have demonstrated a significant decrease in A β production following APP-Grp78 interaction (Yang *et al.*, 1998; Kudo *et al.*, 2006). It has also been suggested that excessive production of lactic acid may enhance the activity of BACE1 by lowering pH of the brain and cerebral spinal fluid, potentially influencing APP amyloidogenic processing and the production of A β (Xiang *et al.*, 2010).

1.5.4. Altered APP subcellular localisation as a potential mechanism by which DCA regulates APP proteolysis.

Given that the proteolysis of APP via the amyloidogenic and non-amyloidogenic pathways occurs in different subcellular compartments (discussed below), we hypothesised that DCA might exert its influence on APP processing by altering the subcellular distribution of the APP substrate protein.

It is widely accepted that APP is synthesised within membrane-bound polysomes before post-translational alterations (such as glycosylation, phosphorylation and sulphonation) within the ER and Golgi (Fig. 1.8.). Mature APP is then transported to either the cell surface (10 %) or remains within the TGN (90 %) (Plácido *et al.*, 2014; Zhang *et al.*, 2016; Toh *et al.*, 2017).

APP is subject to non-amyloidogenic processing at the plasma membrane (Jiang *et al.*, 2014). APP which is not shed from the plasma membrane is then rapidly reinternalised, where it is either returned to the TGN, broken down in the lysosome or recycled back to the PM (Fig. 1.8.). The precise location of amyloidogenic processing, however, is still under debate. Numerous studies have shown that it predominantly occurs following reinternalisation into the cell, either within the ER and Golgi complex, endosomal compartments or the TGN (Cook *et al.*, 1997; Greenfield *et al.*, 1999; Huse *et al.*, 2002; Kaether *et al.*, 2006).

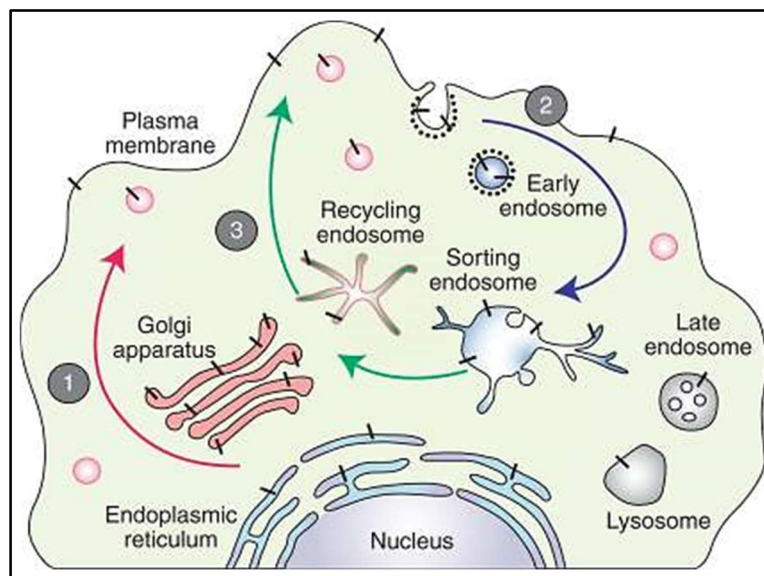


Figure 1.8. The intracellular processing of APP. (1) Initially, APP is transported to the PM, whilst undergoing posttranslational modifications. (2) The APP which is not released from the PM is reinternalised and sorted. (3) It is then either degraded in the lysosome, transported to the TGN or returned to the PM via recycling endosomes. (Image adapted from Haass *et al.*, 2012).

The findings that non-amyloidogenic and amyloidogenic APP processing occur in distinct subcellular compartments have led to several studies investigating how altering the subcellular localisation of the protein impacts on its processing. Perez *et al.* (1999) showed that inhibiting APP reinternalisation in Chinese hamster ovary (CHO) cells by mutating the APP C-terminal motif required for reinternalisation, led to reduced A β production due to a reduced interaction between APP and BACE1. Similarly, Carey *et al.* (2005) inhibited APP endocytosis in HEK293 cells by transfection with a dominant negative mutation within dynamin I and saw a decrease in A β formation. The influence of APP location on the processing of the protein was also investigated in HEK293 cells by Choy *et al.* (2012), who identified that retention of APP within the early endosomes, by depleting trafficking proteins Hrs and Tsg101 through shRNA treatments, led to a decrease in amyloidogenic processing. Additionally, the authors identified that retention of APP within the TGN, by depleting ESCRT subunit trafficking proteins CHMP6 and VPS4A/B through shRNA treatments, led to an increase in amyloidogenic processing. Furthermore, it has been identified that adaptor protein X11-deficient mice have an increase in APP and BACE1 colocalisation and an increase in A β production (Sano *et al.*, 2006). The adaptor protein X11 usually binds to APP in the C-terminal region and retains it within detergent-sensitive membranes which are devoid of BACE1 (Sun and Roy, 2018). Therefore, this ultimately demonstrates that the correct trafficking of APP is vital for the appropriate processing of the protein.

1.5.5. Mitochondrial autophagy as a potential mechanism by which DCA regulates

APP proteolysis.

In a recent study by Pajuelo-Reguera *et al.* (2015), DCA was shown to stimulate mitophagy in a dose-dependent manner and to alter the mitochondrial network morphology in SH-SY5Y cells. As such we hypothesised that, in the context of the current study, DCA might exert its influence on APP expression/proteolysis through similar alterations in the mitochondrial network.

Mitochondria are preserved via a specific form of autophagy, called mitophagy, through which abnormal or damaged mitochondria are engulfed by autophagosomes and compartmentalised. These mitochondria are then broken down when lysosomes fuse with the compartment (Pajuelo-Reguera *et al.*, 2015). This process is highly selective and tightly controlled to ensure that the correct mitochondria are degraded.

Cole *et al.* (1989) previously showed that the inhibition of lysosomal enzymes and, therefore, mitophagy using ammonium chloride and leupeptin in a pheochromocytoma cell line (PC12) led to reduced A β production. This was additionally supported by Siman *et al.* (1993) who inhibited mitophagy using a variety of inhibitors (including ammonium chloride, chloroquine, E64, or Z-Phe-Ala-CHN₂) in HCT293 cells overexpressing APP, also identifying a reduction in APP processing. This, therefore, suggests that inhibition of mitophagy also inhibits APP proteolysis (Salminen *et al.*, 2013). However, many studies suggest that A β accumulation leads to mitochondrial damage and mitophagy, rather than suggesting that mitochondrial damage alters amyloidogenic processing. For example, Cha *et al.* (2012) showed that, when the immortalised mouse hippocampal neuronal cell line HT22 was treated with exogenous A β , there was a significant change in both the activity and morphology of

mitochondria. Similar results have also been shown in several other APP overexpression studies using M17 neuroblastoma cells and transgenic mice (Wang *et al.*, 2008; Wu *et al.*, 2014). Furthermore, the morphology of mitochondria has been shown to be highly altered in AD-afflicted brain tissue (Trimmer and Borland, 2005).

The detrimental effect of A β aggregation on mitochondrial morphology has also been shown to contribute to the pathogenesis of AD. Firstly, Chen *et al.* (2007) showed that the loss of mitochondrial fusion resulted in poor mitochondrial dynamics and neurodegeneration. Mitochondrial fusion involves the integration of discrete, individual mitochondrion to form a single organelle, used to overcome stress-induced damage. This study used a mouse model with conditionally inactivated alleles of *Mfn1* and *Mfn2* (ATPases involved in fusion) and showed an associated increase in neurodegeneration.

Two other studies (Manczak *et al.*, 2006; Petersen *et al.*, 2008) also suggested that the neurotoxicity observed in AD-afflicted brains is partly due to the impact of A β accumulation upon mitochondrial function in that the peptides prevented proteins within the cytoplasm, for example the β -subunit of the F₁-ATPase precursor protein, from entering the mitochondrial matrix. The authors found that this inhibition led to impaired electron transport chain function and increases in ROS production and oxidative DNA damage (Petersen *et al.*, 2008).

1.5.6. Oxidative stress as a potential mechanism by which DCA regulates APP proteolysis.

There are numerous publications relating to the role of oxidative stress in AD and these have been reviewed recently in Cheignon *et al.* (2018) and Chen and Zhong (2014). Of particular relevance to the current study are those publications which relate directly to the effect of oxidative stress on secretase-mediated proteolysis of APP.

It has recently been demonstrated that oxidative stress enhances the levels of BACE1 expression, thereby enhancing amyloidogenic processing (Arimon *et al.*, 2015). For example, in a study by Mouton Liger *et al.* (2012), SH-SY5Y cells were subjected to oxidative stress through hydrogen peroxide treatment and the levels of BACE1 dramatically increased. Furthermore, in a study by Guglielmotto *et al.* (2009), ischaemic rats were shown to have increased BACE1 expression and ROS production. The link between ROS and the altered BACE1 expression was then confirmed in a second experiment where ischaemic rats treated with antioxidants SOD/Cat and α -tocopherol, which prevented ROS production, were shown not to exhibit the same increases in BACE1. Additionally, in a study by Muche *et al.* (2017), oxidative stress was shown to enhance sAPP β production in primary endothelial cells following hydrogen peroxide treatment. Taken together, these results suggest that oxidative stress enhances BACE1 production and leads to an increase in amyloidogenic processing.

Similar observations were also seen in a study by Kanamaru *et al.* (2015) who developed mice with enhanced oxidative stress due to a dominant-negative mutation within the mitochondrial aldehyde dehydrogenase 2. These mice exhibited increased A β deposition and decreased cognitive function, further suggesting that oxidative stress levels play a fundamental role in AD development. Tamagno *et al.* (2008) also demonstrated increased

γ -secretase and β -secretase levels in SK-N-BE neuroblastoma cells treated with the oxidative stress enhancers, 4-hydroxynonenal and H₂O₂.

Oxidative stress can also lead to peroxidation of lipids (Cheignon *et al.*, 2018). These lipids are thought to contribute to the progression of AD as they have been shown to upregulate the production of BACE1 (Chen *et al.*, 2008). This study found that, when glutathione peroxidase 4 (Gpx4) (which usually protects against lipid peroxidation) was knocked out in mice through a targeted mutation in the *Gpx4* gene, there was a dramatic increase in BACE1 expression and A β aggregation.

Nuclear factor- κ B (NF- κ b), a protein which is activated by oxidative stress and ROS, has also been linked to BACE1 expression and amyloidogenic proteolysis of APP. Chen *et al.* (2012) found that various types of neuroblastoma cells transfected with NF- κ B had enhanced expression of BACE1 due to enhanced promoter activity and, therefore, displayed increased amyloidogenic proteolysis. Additionally, the authors demonstrated that the frontal cortex of AD patients exhibited a significant increase in both NF- κ B and BACE1 activity.

Furthermore, it has been suggested that A β production may lead to an increase in oxidative stress, which further enhances A β production, resulting in a positive feedback cycle (Smith *et al.*, 2007). For example, Sheng *et al.* (2009) demonstrated significant reductions in both A β production and oxidative stress in mouse N2a neuroblastoma cells following inhibition of γ -secretase by expression of loss-of-function PS1 mutant D385A.

As previously discussed in section 1.4.1., DCA enhances oxidative stress and production of ROS. Therefore, as there is clearly a link between oxidative stress and APP proteolysis, it was hypothesised, in the current study, that this may be the mechanism by which DCA mediates APP processing.

1.6. Project Aims.

The overarching aim of the current project was to identify the molecular mechanisms whereby dichloroacetate regulates APP proteolysis. In this respect, the effects of manipulating pH, p53 expression, LDH activity, pyruvate and lactate levels, mitochondrial autophagy and oxidative stress were all investigated in terms of their abilities to impact on APP expression and proteolysis. Furthermore, we also investigated the potential effects of DCA on the subcellular localisation of APP and the activity of BACE1.

Whilst the concentrations of DCA required to alter APP proteolysis might well be too high to make the drug a viable treatment for the disease, studies such as this into the cellular mechanisms whereby the drug effects such changes may well open avenues for the development of future AD therapeutics.

Chapter 2.

Materials and Methods.

2. Materials and Methods.

2.1. Materials.

Anti- β -actin mouse monoclonal, anti-APP C-terminal rabbit polyclonal and anti-amyloid- β WO-2 mouse monoclonal antibodies were purchased from Sigma-Aldrich Ltd (Poole, UK). Anti-sAPP β rabbit polyclonal, anti-p53 mouse monoclonal, and anti-APP 6E10 mouse monoclonal antibodies were purchased from Biolegend (San Diego, USA). Anti-APP N-terminal 22C11 antibody was purchased from Merck Millipore (Darmstadt, Germany). Anti-LAMP1 rabbit polyclonal, anti-GM-130 rabbit polyclonal and anti-RAB6A rabbit polyclonal antibodies were purchased from Abcam (Cambridge, UK). Secondary peroxidase-conjugated antibodies were purchased from Sigma-Aldrich Ltd (Poole, UK). Secondary AlexaFluor-conjugated antibodies were purchased from Abcam (Cambridge, UK).

All cell culture reagents were purchased from Lonza Ltd (Basel, Switzerland), except for foetal bovine serum (FBS) which was supplied by Fisher Scientific (Loughborough, UK).

Unless otherwise stated, all other reagents were from Sigma-Aldrich Ltd (Poole, UK).

2.2. Methods.

2.2.1. Cell culture.

Human neuroblastoma SH-SY5Y cells were cultured at 37 °C and 5 % CO₂ in Dulbecco's modified Eagle's medium (DMEM) containing 4 mM L-glutamine, 25 mM glucose, 10 % (v/v) filter-sterilised FBS, 50 μ g/ml streptomycin and 50 U/ml penicillin. For sub-culturing, confluent cells were washed with 2 ml trypsin (200 mg/l versene EDTA, 170,000 U Trypsin/l)

Table 2.1. Quantities of culture medium used to resuspend SH-SY5Y cell pellets prepared from an initial confluent T75 cm² flask, and the volume of this cell resuspension and fresh medium used when seeding out new cultures.

Resuspension volume for initial pellet (μl)	Type of subculture to be seeded	Volume of resuspension seeded in subculture (μl)	Volume of culture medium added to subcultures (μl)
1000 per subculture	T75 cm ² flask	1000	10000
1000 per subculture	T25 cm ² flask	1000	8000
30000 total	6 well plate	100	3000
30000 total	96 well plate	50	150

which was then replaced with a fresh 2 ml of trypsin and incubated for 5 min at 37 °C. After tapping the flask to ensure all cells had detached, 20 ml culture medium was added to neutralise the trypsin and the cells were pelleted in an Allegra X-22R centrifuge (Beckman Coulter Ltd, High Wycombe, UK) at 500 rpm for 3 min. Once pelleted, the supernatant was decanted and cells were resuspended and seeded as described in Table 2.1.

2.2.2. Resurrecting and freezing cell lines.

In order to resurrect a cell line from liquid nitrogen, cells were thawed at 37 °C and transferred into a Falcon tube containing 20 ml of culture medium. After centrifuging for 3 min at 500 rpm in an Allegra X-22R centrifuge, the supernatant was decanted, and the cells were resuspended and seeded as described in Table 2.1.

For freezing cells, a confluent T75 cm² flask was pelleted as previously described in section 2.2.1. The pellet was then resuspended in 1.5 ml of culture medium containing 10 %

(v/v) dimethyl sulphoxide (DMSO) in a cryovial. This suspension was then frozen at -80 °C for at least 24 h, before being placed into liquid nitrogen for permanent storage.

2.2.3. Cell treatments.

For the dichloroacetate (DCA) treatments, 0.3 g of sodium dichloroacetate (MW 150.92) was dissolved in 5 ml UltraMEM and filter-sterilised, giving a stock solution of approximately 400 mM DCA. This meant that adding 500 µl stock to 10 ml UltraMEM gave a treatment concentration of approximately 20 mM and adding 250 µl stock (with an additional 250 µl UltraMEM) gave a final treatment concentration of approximately 10 mM DCA. Further dilutions of the stock were performed in order to achieve lower DCA concentrations whilst still adding a total of 500 µl to each 10 ml culture. Control cells were incubated in a total of 10.5 ml UltraMEM.

For the acetic acid treatments, 115 µl acetic acid (99.5 % solution; 17.4 M) was added to 4885 µl UltraMEM and filter-sterilised to give a final stock concentration of approximately 400 mM. This meant that adding 500 µl stock to 10 ml UltraMEM gave a treatment concentration of 20 mM and adding 250 µl stock (with an additional 250 µl UltraMEM) gave a treatment concentration of 10 mM.

For the sodium acetate (MW = 82.034) treatments, 0.16406 g was dissolved in 5 ml UltraMEM and filter-sterilised to give a final stock concentration of approximately 400 mM. This meant that adding 500 µl stock to 10 ml UltraMEM gave a treatment concentration of 20 mM and adding 250 µl stock (with an additional 250 µl UltraMEM) gave a treatment concentration of 10 mM.

For the Reactivating p53 and Inducing Tumour Apoptosis (RITA) treatments, RITA (CAY10006426- Cambridge Bioscience; MW = 292.37) was obtained as a 10 mg lyophilised sample. DMSO (1369.86 μ l) was added to this sample, giving a stock concentration of 25 mM. The stock (10 μ l) was then added to 90 μ l DMSO, to give a final stock concentration of 2.5 mM. This meant that adding 10 μ l of final stock on 10 ml UltraMem gave a treatment concentration of 25 μ M, 4 μ l of final stock gave a treatment concentration of 10 μ M, and 2 μ l of final stock gave a treatment concentration of 5 μ M. This stock was then serially diluted 10-fold, meaning that adding 2 μ l of the first serial dilution gave a treatment concentration of 0.5 μ M and 2 μ l of the second serial dilution gave a treatment concentration of 0.05 μ M.

For the GSK2837808A lactate dehydrogenase inhibitor (Tocris, Abingdon, UK; MW = 649.62) treatment, 10 mg of inhibitor was reconstituted in 30.5754 ml DMSO, which was then divided into 1 ml aliquots and frozen at -20 °C in order to give a 10 x stock. One of these aliquots was diluted 10-fold with DMSO to give 1 x stocks which were divided into 200 μ l aliquots and frozen. When using 10 ml culture volumes, 10 μ l of the 1 x stock was added to the medium to give a final inhibitor concentration of 50 nM. All other final concentrations were produced by further dilution of the 1 x stock with DMSO, prior to adding 10 μ l of these dilutions to the cultures. For 96 well plate cultures containing 200 μ l medium per well, the 1 x stock was diluted 10-fold with DMSO and 2 μ l of this was added to the wells to give a final inhibitor concentration of 50 nM.

For the FX11 lactate dehydrogenase inhibitor (Merck Millipore, Darmstadt, Germany; MW = 350) treatment, 10 mg FXII LDHA compound was dissolved in 285.71 μ l DMSO, giving a stock concentration of 1 mM. This meant that adding 10 μ l stock to 10 ml UltraMEM gave a final treatment concentration of 100 μ M in T75 cm² flasks. For all other inhibitor

concentrations, the stock was diluted such that the same volume (10 μ l) could be added to cultures to give lower final inhibitor concentrations. For 96 well plate cultures containing 200 μ l of medium per well, the stock was diluted 10-fold with DMSO and 2 μ l of this was added to each well to give a 100 μ M final inhibitor concentration.

For the pyruvate treatments, it is worth noting initially that the basal concentration of pyruvate in UltraMEM is 1 mM. As such, the UltraMEM 'control' for these experiments actually represented 1 mM pyruvate and the mass calculations for all other pyruvate concentrations were performed taking this initial 1 mM concentration into account. As such, 0.54648 g of sodium pyruvate (Sigma-Aldrich Ltd, Pool, UK; MW = 110.4) was dissolved in 50 ml UltraMEM and filter-sterilised. Cells were cultured directly in this solution without any further dilution, such that the final pyruvate concentration was 100 mM. Other final pyruvate concentrations were obtained simply by adjusting the weight of dry powder dissolved in the UltraMEM in which the cells were cultured.

For the lactic acid treatments, 0.54048 g of lactic acid (Sigma-Aldrich Ltd, Poole, UK; MW = 90.08) was dissolved in 10 ml UltraMEM and filter-sterilised to give a final stock solution of 600 mM. This meant that adding 200 μ l of stock solution to 10 ml UltraMEM gave a final treatment concentration of 12 mM.

For the N-acetyl cysteine (NAC) treatments, 0.163195 g NAC (Sigma-Aldrich Ltd, Poole, UK; MW = 163.195) was dissolved in 10 ml distilled water and filter-sterilised to give a final stock concentration of 100 mM. This meant that adding 100 μ l of stock solution to 10 ml UltraMEM gave a final treatment concentration of 1 mM.

For the ammonium chloride treatments, 0.5349 g of ammonium chloride (Sigma-Aldrich Ltd, Poole, UK; MW = 53.49) was dissolved in 10 ml UltraMEM and

filter-sterilised to give a stock solution of 1 M. This meant that adding 100 µl of stock to 10 ml UltraMEM gave a final treatment concentration of 10 mM.

For the chloroquine diphosphate treatments, 0.25793 g of chloroquine diphosphate (Sigma-Aldrich Ltd, Poole, UK; MW = 515.86) was dissolved in 100 ml UltraMEM to give a final stock concentration of 5 mM. This meant that adding 100 µl of stock solution to 10 ml UltraMEM gave a final treatment concentration of 50 µM.

For the batimastat treatments, 10 mg batimastat (Biotechne, Abingdon, UK; MW = 78.13) was dissolved in 12.7992 ml DMSO to give a stock solution of 10 mM. This meant that adding 5 µl to 10 ml UltraMEM gave a final treatment concentration of 5 µM.

2.2.4. Small interfering RNA (siRNA) treatments.

siRNAs were obtained from Dharmacon (Cambridge, UK) and were as follows:

Control siRNA: Cat. No. D-001810-10-05, ON-TARGETplus Non-Targeting Pool, (5 nM)

p53 siRNA: Cat. No. J-003329-15-0020 On target plus siRNA (*TP53* gene) (20 nM)

The following method is based on the transfection of cells in a single well of a 6 well plate (with a surface area of 10 cm²) and will yield a final Dharmafect transfection reagent concentration of 5 µl/ml and a final siRNA concentration of 37.5 nM. If higher concentrations of either Dharmafect or siRNA were required, then the volumes of UltraMEM in tubes A and B were reduced accordingly. Similarly, for transfecting larger scale cell cultures, the volumes of all reagents were simply increased in a manner proportionate to the surface area of the culture vessel used.

The siRNAs supplied from the manufacturer were made up to 5 μ M stocks using RNase-free water. Dharmafect (10 μ l) was diluted with 190 μ l of UltraMEM in Tube A and then 15 μ l of siRNA stock was diluted with 185 μ l of UltraMEM in Tube B. After incubating both tubes at room temperature for 5 min, the two tubes were combined and incubated for a further 20 min at the same temperature. Complete medium lacking antibiotic (1.6 ml) was then added to the mixture to make a total volume of 2 ml. The existing medium was removed from 70 % confluent cultures in 6 well plates and replaced with the 2 ml of transfection mixture described above. The cultures were then grown for a further 24 h before replacing the medium with 2 ml of normal (antibiotic containing) complete growth medium. Cultures were then grown for a further 48–72 h prior to drug treatments.

2.2.5. Preparing conditioned medium and cell lysate samples.

Cell debris was removed from conditioned cell culture medium by centrifuging in a Rotana 460R centrifuge at 3000 rpm at 4 °C for 5 min. Amicon Ultra-4 centrifugal filters (Merck Millipore, Darmstadt, Germany) were equilibrated by spinning through 4 ml d.H₂O for 10 min at 4000 rpm and 4 °C. Equilibrated filters were then used to concentrate 8 ml of medium supernatant to 250 μ l for approximately 50 min at 3500 rpm and 4 °C.

In order to prepare cell lysates, cells were washed *in situ* with 10 ml phosphate-buffered saline (PBS; 0.15 M NaCl, 2 mM NaH₂PO₄, 2 mM Na₂HPO₄, pH 7.4). The cells were then covered with a fresh 10 ml PBS, scraped from the base of the flask and transferred into a Falcon tube. An additional 10 ml PBS was then used to wash the remaining cells from the flask into the same Falcon tube. The cells were pelleted at 1500 *g* for 3 min at 4 °C. The cell pellet was resuspended in 1.5 ml of lysis buffer (50 mM Tris, 150 mM NaCl, 1 %

(v/v) Igepal, 0.1 % (w/v) sodium deoxycholate, 5 mM EDTA, pH 7.4) containing 1 % (v/v) protease inhibitor cocktail (1.04 mM AEBSF, 0.02 mM leupeptin, 0.8 μ M Aprotinin, 0.04 mM Bestatin, 0.0014 mM E-64, and 0.015 mM pepstatin A) and sonicated for 30 s using a probe sonicator (MSE, Crawley, UK) set at half power. The sonicated sample (1 ml) was then transferred into an eppendorf and insoluble material was pelleted at 11,600 *g* for 10 min, before the supernatant was transferred into a new eppendorf and the pellet was discarded. Once the protein levels were assayed and equalised (section 2.2.6.), lysate samples were frozen at -80 °C in 150 μ l aliquots.

2.2.6. Bicinchoninic acid (BCA) protein assay.

Standard bovine serum albumin (BSA) concentrations were prepared at concentrations of 0, 0.2, 0.4, 0.6, 0.8, and 1 mg/ml. BSA standards (10 μ l) and appropriate volumes of lysate samples were pipetted into a 96-well microtitre plate in duplicate. BCA protein assay reagent (Fisher Scientific, Loughborough, UK) and 4 % (w/v) $\text{CuSO}_4 \cdot 5\text{H}_2\text{O}$ were combined at a 50:1 volume ratio to produce the BCA assay working reagent, 200 μ l of which was added to each well. Samples were then mixed by tapping the plate, before incubating at 37 °C for 30 min. After sufficient colour development, the absorbance was read at 570 nm using a Victor² 1420 multilabel counter microplate reader (Lab Merchant Ltd, London, UK). The means of each pair of BSA standards were then used to generate a calibration curve which was used to determine the concentration of protein in each lysate sample. Concentrations of each sample were then equalised using lysis buffer containing 1 % (v/v) protease inhibitor cocktail.

2.2.7. Sodium dodecylsulphate – polyacrylamide gel electrophoresis (SDS-PAGE).

Stacking and resolving gel solutions were prepared as described in Table 2.2. Continuous gradient gels were poured using a mixing chamber and peristaltic pump. The resolving gel was covered with isobutanol and left to set for 30 min, following which the isobutanol was removed and the stacking gel was poured and left to set for a further 30 min.

Samples were mixed with dissociation buffer (3.5 ml 1 M Tris/HCl pH 6.8, 2.5 g sodium dodecyl sulfate (SDS), 0.3085 g dithiothreitol (DTT), 5 ml glycerol, 16.5 ml d.H₂O, 0.05 g bromophenol blue) at a volume ratio of 2:1. Molecular weight markers standards (GE Healthcare Ltd, Hatfield, UK) were prepared in the same manner. All samples and standards were boiled at 100 °C for 3 min. Samples and MW standards (30 µl) were loaded and resolved at 35 mA per gel in running buffer (25 mM Tris, 192 mM glycine, 0.1 % (w/v) SDS; Scientific Laboratory Supplies Ltd, Nottingham, UK) until the loading dye reached the base of the gel.

Table 2.2. Gel solution components.

	7 %	17 %	5 %	20 %	Stacking gel
Sucrose	-	0.37 g	-	0.37 g	-
Distilled H₂O	1.36 ml	-	1.44 ml	-	7.65 ml
1 M Tris/HCl, pH 8.8	1.39 ml	1.39 ml	1.39 ml	-	-
1 M Tris/HCl, pH 6.8	-	-	-	-	1.25 ml
1.5 M Tris, pH 8.8	-	-	-	0.93 ml	
10 % (w/v) SDS	37 µl	37 µl	37 µl	37 µl	100 µl
30 % acrylamide, 0.8 % Bis	0.88 ml	2.1 ml	2.5 ml	0.63 ml	1 ml
1.5 % (w/v) ammonium persulfate	100 µl	220 µl	71 µl	220 µl	0.5 ml
TEMED	3 µl	3 µl	3 µl	3 µl	10 µl

2.2.8. Immunoblotting.

Immobilon P polyvinylidene difluoride (PDVF) membrane (Merck Millipore, Darmstadt, Germany) was equilibrated in methanol for 10 s, d.H₂O for 2 min and Towbin transfer buffer (800 ml methanol, 150 mM glycine, 20 mM Tris, 3200 ml d.H₂O, pH 8.3) for 20 min. Proteins were then transferred in Towbin buffer at 115 V for 60 min. The membrane was then washed in PBS for 5 min followed by blocking with 50 ml of 5 % (w/v) marvel in PBS containing 0.1 % (v/v) Tween 20 (PBS-Tween) for 60 min at RT. All RT incubations were performed on a rocking platform. The membranes were then washed in PBS for an additional 5 min before incubating in primary antibody overnight at 4 °C on a roller mixer spiralizer (Stuart, Staffordshire, UK). Primary antibodies were prepared in 0.2 % (w/v) BSA in PBS-Tween at the dilutions shown in Table 2.3.

The next day, membranes were washed in PBS-Tween for 1 x 1 min and 2 x 15 min. Membranes were then incubated in secondary antibody for 60 min at RT. Secondary antibodies were prepared in 0.2 % (w/v) BSA in PBS-Tween at the concentrations shown in Table 2.3. This was then followed by washing in PBS for 1 x 1 min and 2 x 15 min.

The blots were then developed with Enhanced Chemiluminescence reagent (ECL) (Fisher Scientific, Loughborough, UK). They were submerged in ECL reagent for 3 min, sandwiched between acetate sheets and exposed to CL-XPosure™ clear blue X-ray film (Fisher Scientific, Loughborough, UK). This was then developed manually using Carestream® Kodak® autoradiography GBX fixer and replenisher (Sigma-Aldrich, Poole, UK).

Table 2.3. Concentrations of antibodies used in Western blotting.

Antibodies	Concentration
p53	1/4000
6E10	1/4000
Actin	1/5000
APP-CT	1/5000
22C11	1/5000
sAPP β	1/1000
Rabbit anti-mouse	1/4000
Goat anti-rabbit	1/4000

2.2.9. Amido black staining of membranes.

Proteins on membranes were visualised using amido black stain (0.1 % (w/v) amido black, 1 % (v/v) acetic acid, 40 % (v/v) methanol). Membranes were then destained in tap water.

2.2.10. Quantification of immunoblots.

X-ray films were scanned, and image files were imported in to 'ImageJ' quantification software. Images were converted to greyscale before the areas of bands were quantified.

2.2.11. MTS 3-(4,5-dimethylthiazol-2-yl)-5-(3-carboxymethoxyphenyl)-2-(4-sulfo phenyl)-2H-tetrazolium) cell viability assays.

MTS viability assays were performed in 96 well microtitre plates. Medium was removed from the cells and replaced with 200 μ l UltraMEM. This was then further replaced

with a fresh 100 µl of UltraMEM before adding 20 µl of CellTiter 96® AQueous One Cell Proliferation Assay solution (Promega, Wisconsin, USA). Background control wells contained just UltraMEM and MTS reagent. The plate was covered in foil and incubated at 37 °C (with mixing every 2 min) until there was sufficient colour development. Absorbances were then read at 490 nm using a Victor2 1420 multilabel counter microplate reader (Lab Merchant Ltd, London, UK).

2.2.12. Trypan Blue Assay.

Cells from cultures were trypsinised and pelleted as described in section 2.2.1. and resuspended in 15 ml of PBS. Cell suspension (20 µl) and trypan blue (20 µl) were combined and the solution was incubated for 2 min before placing 20 µl of this solution onto a haemocytometer and counting the cells. The cell counts in four large grids were averaged and multiplied by 400 to give the number of cells in 20 µl, and then by 750 to give the amount in 15 ml. Finally, the amount was multiplied by 2, to account for the original 1:1 dilution with trypan blue.

2.2.13. BACE1 activity fluorescence assay.

BACE1 activity in cell lysates was measured using the Fluorometric Beta Secretase Activity Kit (Abcam, Cambridge, UK) according to the manufacturer's instructions. Fluorescence was read at 335/495 nm using an infinite M200 pro tecan plate reader (Tecan Trading, Männedorf, Switzerland).

2.2.14. Immunofluorescence microscopy.

Glass coverslips (24 mm²) were submerged in sterile 0.01 % (w/v) poly-L-lysine solution (Sigma-Aldrich Ltd., Poole, UK.) for 45 min on a rocking platform at RT, before being washed 10 times in d.H₂O. The coverslips were allowed to dry and then either stored at room temperature at this stage or the process was continued by rinsing them, under aseptic conditions, in absolute ethanol. After drying under aseptic conditions, each coverslip was then placed in an individual well of a 6 well plate. SH-SY5Y cells were seeded in growth medium lacking antibiotics as described in Table 2.1. Once the cells reached 60 % confluency, if required, they were treated with DCA or batimastat for 24 h as described in section 2.2.3. before being processed for immunofluorescence (below).

Paraformaldehyde (4% w/v) was prepared by heating 80 ml of PBS to 60 °C and, whilst stirring, adding 4 g of paraformaldehyde. The pH was then slowly increased by adding 1 M NaOH until the paraformaldehyde dissolved. The solution was then brought to 100 ml with PBS and the pH adjusted to 6.9. Once cooled, the solution was filter-sterilised before use.

Coverslips were transferred to the wells of a fresh 6 well plate and washed with 2.5 ml ice-cold PBS which was then immediately replaced with 2 ml of 4 % (w/v) paraformaldehyde and the cells were fixed for 30 min. The paraformaldehyde was then removed and the coverslips were washed 3 times in 2.5 ml ice-cold PBS. Following removal of the last wash solution, the cells were permeabilised by incubating in 2.5 ml of 0.1 % (v/v) Triton X-100 in PBS for 10 min at RT. The coverslips were then washed 3 times in 2.5 ml PBS for 5 min and then inverted on to 500 µl of 5 % (v/v) goat serum in PBS containing 0.1 % Tween

for 1 h at RT on parafilm. Coverslips were then transferred to fresh 6-well plates and washed 3 times for 5 min in 2.5 ml PBS.

Primary antibodies (Table 2.4.) were made up in 100 μ l of 5 % (v/v) goat serum in PBS-0.1 % (v/v) Tween. Following the final PBS wash, coverslips were removed from the 6 well plates and placed, cell side up, on parafilm squares. The primary antibodies were then placed on the coverslips and covered with another parafilm square to ensure even distribution of the antibodies. Primary antibody incubations were conducted for 1 h at RT after which the coverslips were transferred back into 6 well plates and washed 3 times with 2.5 ml PBS for 5 min. Secondary fluorophore-conjugated antibody incubations (Table 2.4.) were performed as described above in relation to the primary antibodies except that the incubations were performed in the dark. The coverslips were then transferred back into 6 well plates and washed 3 x 5 min in the dark with 2.5 ml PBS. Before being mounted on to slides, the coverslips were dipped briefly in to distilled water to remove excess salt and then the edges of the slides were blotted in order to remove excess liquid. Finally, the coverslips were inverted on to two drops of Vectashield (containing DAPI; Vectorlabs, Peterborough, UK) on slides and allowed to set for 30 min at RT before storing at -80 °C in the dark. Slides were visualised using a Zeiss LSM880 Laser scanning confocal microscope (Zeiss, Denmark).

Table 2.4. Concentrations of antibodies used in immunofluorescence microscopy.

Antibody	Concentration
Anti-amyloid beta WO-2	1/50
Anti-LAMP1	1/140
Anti-RAB6A	1/100
Anti-GM-130	1/200
Goat-anti mouse IgG H+L (AlexaFluor 488) preabsorbed	1/200
Goat-anti mouse IgG H+L (AlexaFluor 594) preabsorbed	1/200

2.2.15. Statistical analysis.

Microsoft Excel was used to perform unpaired, two-tailed homoscedastic student's *t*-tests. Standard deviations/errors and levels of significance are detailed in individual figure legends.

Chapter 3.

The role of pH in the DCA-mediated regulation of APP proteolysis.

3. The role of pH in the DCA-mediated regulation of APP proteolysis.

In order to examine the mechanism by which DCA regulates APP proteolysis, it was first necessary to characterise the effects of the compound on the endogenous protein in the human neuroblastoma cell line, SH-SY5Y. It was then hypothesised that a simple change in cell culture medium pH mediated by DCA might alter APP processing. To this end, structurally-related compounds which also altered pH were tested in terms of their abilities to alter APP expression and/or proteolysis.

3.1. The effect of different DCA treatment regimes on APP proteolysis.

In order to subsequently examine the mechanism of DCA in the regulation of APP proteolysis, the effects of the compound on the endogenous protein in the human neuroblastoma cell line, SH-SY5Y, were characterised over different treatment regimes (24 h and extended time course treatments).

3.1.1. 24 h DCA treatment regime.

Cells were initially grown to confluence and treated for 24 h with UltraMEM containing DCA. Cells and medium were subsequently harvested and analysed, as described in the Materials and Methods section, in order to determine the effects of DCA on cell viability and APP expression/proteolysis.

The cell viability results (Fig. 3.1.) showed that, when using the MTS assay as a means of assessing viability, there were no changes in viable cell number when the cells were treated with DCA for 24 h. The situation was similar when using trypan blue, although this method showed a slight but significant decrease in viable cell number when cultures were treated for 24 h with 10 mM DCA.

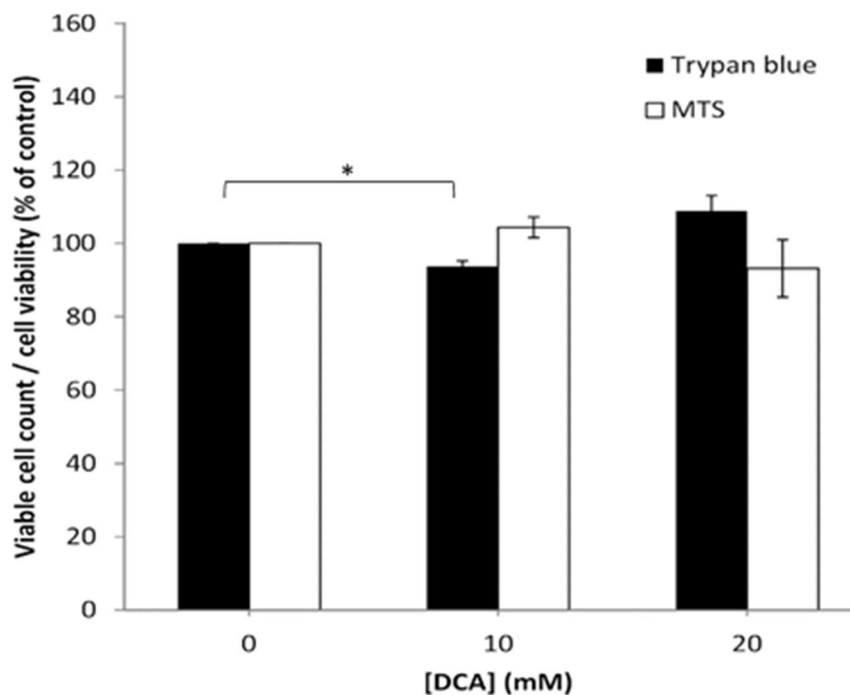


Figure 3.1. The effect of 24 h DCA treatment on SH-SY5Y cell viability. SH-SY5Y cells were treated with DCA at the concentrations indicated for 24 h. Cells were either trypsinised and counted via trypan blue or quantified using an MTS assay *in situ*. Results are means \pm S.D. (n=3). Significant results are indicated: * = significant at $p \leq 0.05$.

When lysates from cells treated for 24 h with 10 mM DCA were immunoblotted with the anti-APP C-terminal antibody (Fig. 3.2.), no significant change in full-length APP expression was observed. However, when cells were treated with 20 mM DCA, a significant increase in the expression of full-length APP was observed (111.72 ± 19.70 % increase, relative to controls).

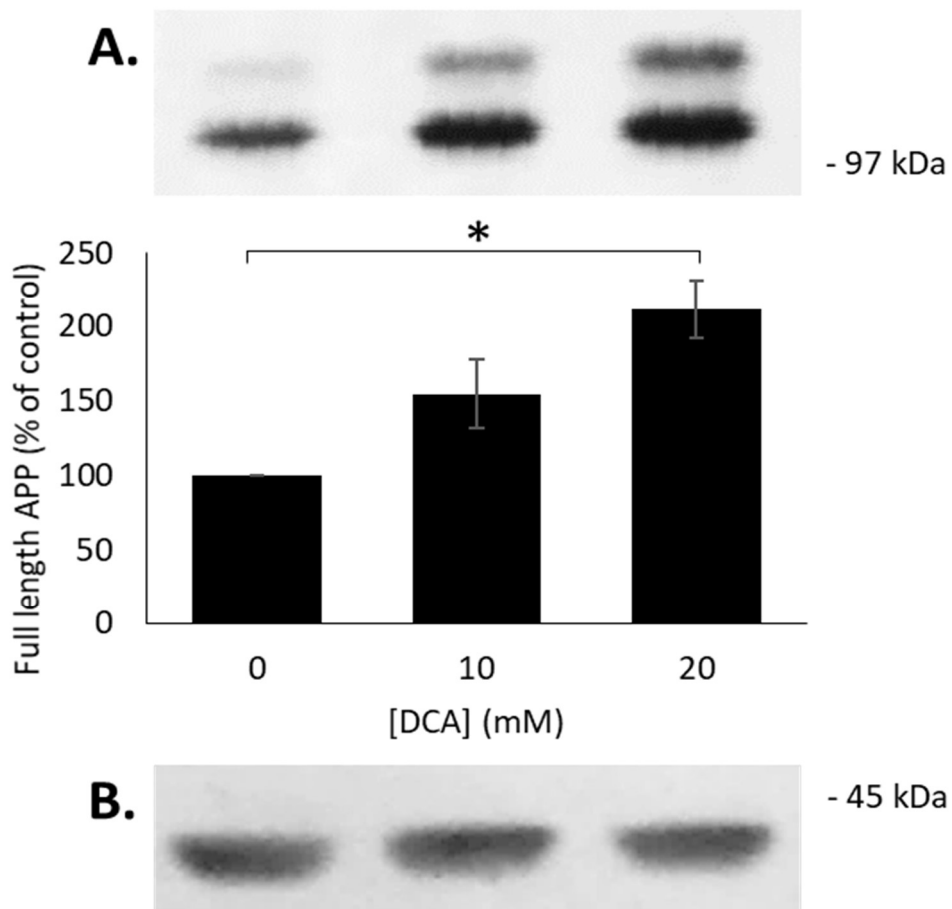


Figure 3.2. The effect of 24 h DCA treatment on the expression of full-length APP in SH-SY5Y cells. SH-SY5Y cells were treated with DCA at the concentrations indicated for 24 h. Equal amounts of lysate protein were then immunoblotted with (A) anti-APP C-terminal and (B) anti-actin antibodies. Results are means \pm S.D. (n=3). Significant results are indicated: * = significant at $p \leq 0.05$.

When 24 h DCA-treated cell lysates were immunoblotted with anti-p53 antibody (Fig. 3.3.), significant increases in p53 levels were observed with both 10 and 20 mM DCA treatments (113.71 ± 36.37 and 228.74 ± 32.89 % increases, respectively, relative to controls).

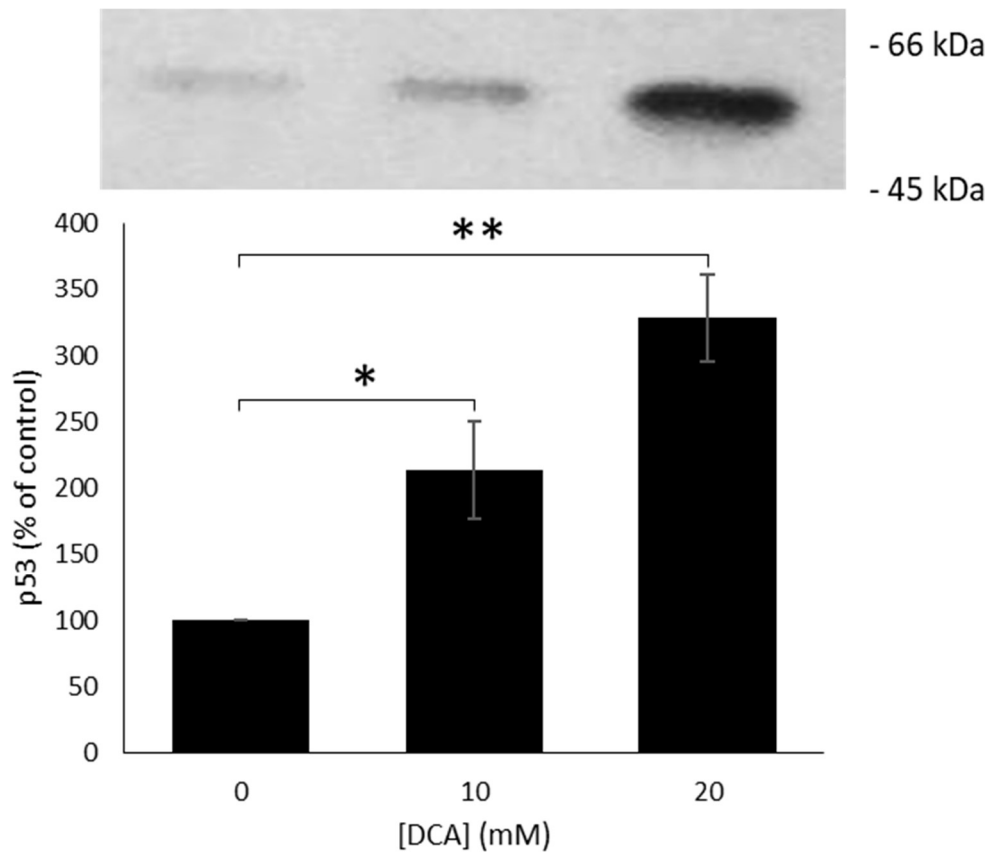


Figure 3.3. The effect of 24 h DCA treatment on the levels of p53 in SH-SY5Y cells. SH-SY5Y cells were treated with DCA at the concentrations indicated for 24 h. Equal amounts of lysate protein were then immunoblotted with anti-p53 antibody. Results are means \pm S.D. (n=3). Significant results are indicated: * = significant at $p \leq 0.05$, ** = significant at $p \leq 0.01$.

Next, the effects of 24 h DCA treatment on the levels of sAPP α and sAPP β production in conditioned medium were examined. To detect the former fragment, concentrated conditioned medium was first immunoblotted with the anti-APP 6E10 antibody. The results (Fig. 3.4.) revealed that, when cells were treated with 10 mM DCA, there were significant increases in both sAPP695 α and sAPP751/770 α levels in the medium (114.00 ± 34.40 and 267.23 ± 94.83 % increases, respectively, relative to controls). Cells treated with 20 mM DCA also generated more of both sAPP695 α and sAPP751/770 α (216.93 ± 9.85 and 396.25 ± 32.40 % increases, respectively, relative to controls).

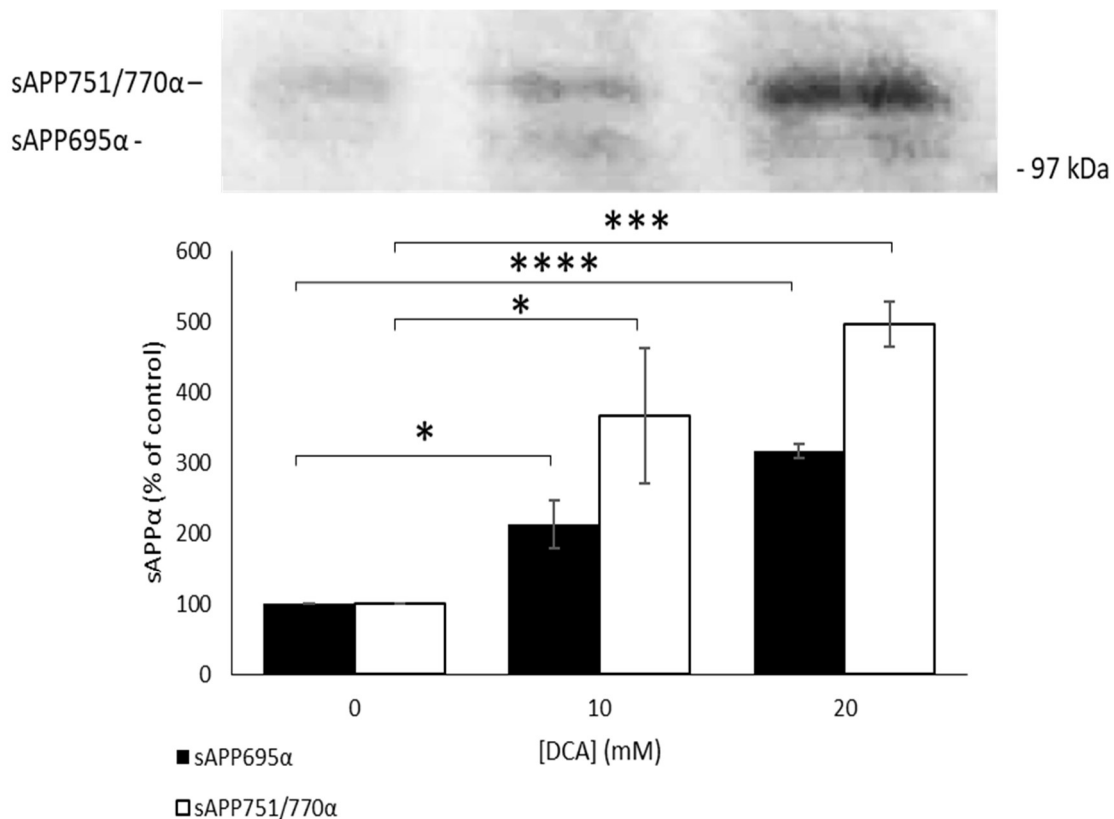


Figure 3.4. The effect of 24 h DCA treatment on the production of sAPP α by SH-SY5Y cells. SH-SY5Y cells were treated with DCA at the concentrations indicated for 24 h. Equal volumes of concentrated medium were then immunoblotted with the anti-sAPP α 6E10 antibody. Results are means \pm S.D. (n=3). Significant results are indicated: * = significant at $p \leq 0.05$, *** = significant at $p \leq 0.005$, **** = significant at $p \leq 0.001$.

When medium from 24 h DCA-treated cells was immunoblotted with the anti-sAPP β antibody, the results (Fig. 3.5.) revealed that culture treatments of 10 and 20 mM DCA both led to a significant decrease in sAPP β production, relative to control cultures (45.37 ± 6.98 and 60.63 ± 10.31 % reductions, respectively).

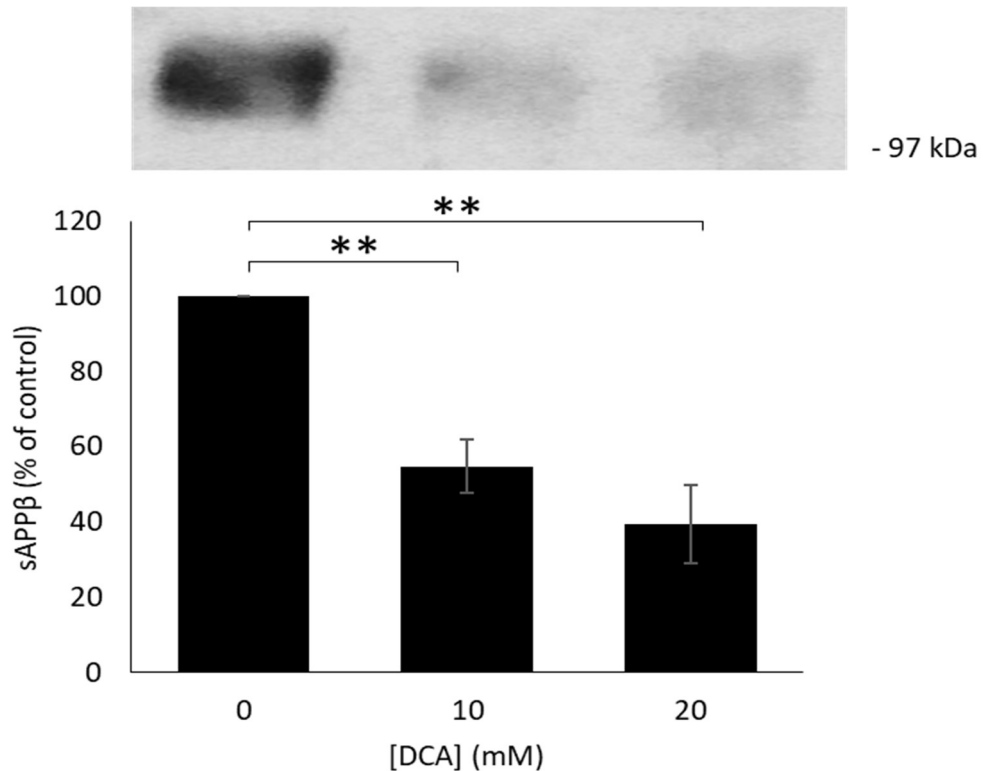


Figure 3.5. The effect of 24 h DCA treatment on the production of sAPP β by SH-SY5Y cells. SH-SY5Y cells were treated with DCA at the concentrations indicated for 24 h. Equal volumes of concentrated medium were then immunoblotted with the anti-sAPP β antibody. Results are means \pm S.D. (n=3). Significant results are indicated: ** = significant at $p \leq 0.01$.

3.1.2. Extended time course DCA treatment regime.

Previously, only two DCA concentrations (10 and 20 mM) had been investigated in terms of the ability of the drug to alter APP proteolysis over a 24 h period. In order to determine whether cells could be grown effectively in the presence of DCA and to examine whether lower concentrations of the compound could alter APP proteolysis, the effects of long-term DCA exposure on APP expression/proteolysis in SH-SY5Y cells were characterised. Here, cells were seeded and cultured in the presence of 0, 0.1, 1 or 10 mM DCA (as opposed to growing them to confluence before treatment) for 3 passages. Once each set of cells had reached confluency following the third passage, the DCA-containing growth medium was replaced with UltraMEM containing the same drug concentrations. The cells were then cultured for a further 24 h, after which lysates and concentrated conditioned medium samples were prepared as described in the Materials and Methods section.

When extended time course DCA-treated cell lysates were immunoblotted with the anti-APP C-terminal antibody (Fig. 3.6.), no significant increases in full-length APP expression were observed in either 0.1 or 1 mM DCA treated cells. Cells treated with 10 mM DCA, however, exhibited a significant increase in full-length APP expression (114.28 ± 24.27 % increase, relative to controls).

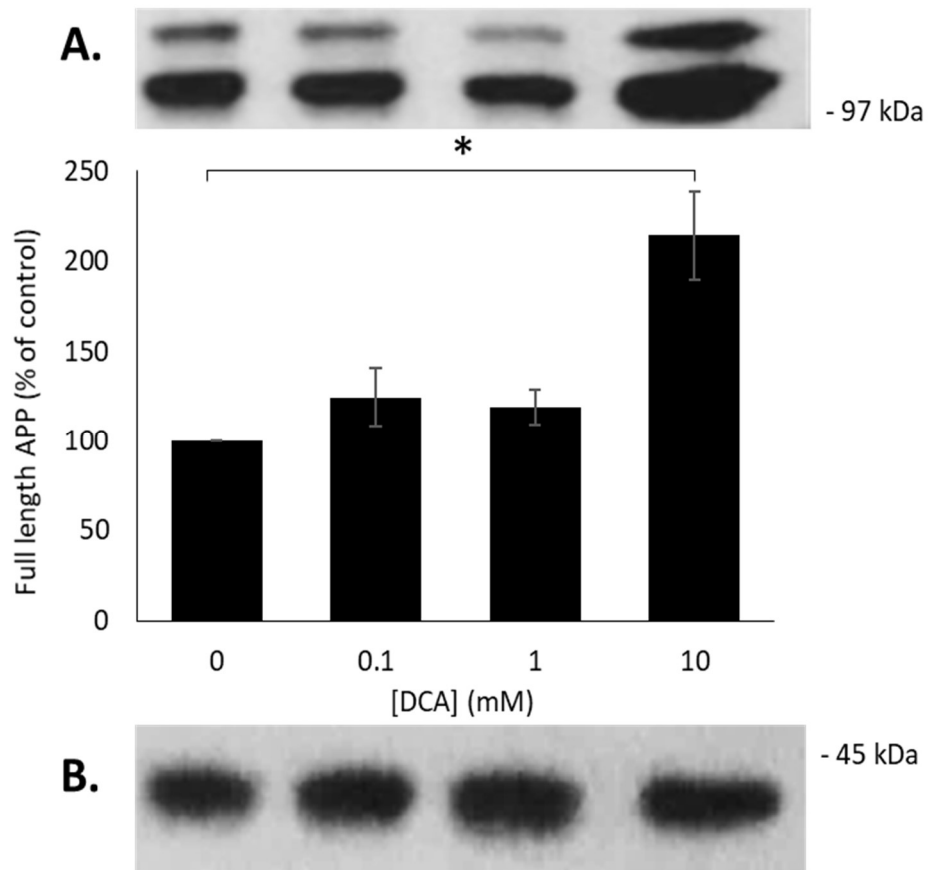


Figure 3.6. The effect of extended time course DCA treatment on full-length APP expression. SH-SY5Y cells were cultured in the presence of the indicated DCA concentrations for 3 passages, before a final 24 h treatment with DCA in UltraMEM. Equal amounts of lysate protein were then immunoblotted with **(A)** anti-APP C-terminal and **(B)** anti-actin antibodies. Results are means \pm S.D. (n=3). Significant results are indicated: * = significant at $p \leq 0.05$.

When the same cell lysates were immunoblotted with anti-p53 antibody (Fig. 3.7.), no significant increases in p53 levels were observed in either 0.1 or 1 mM DCA-treated cells. However, cells treated with 10 mM DCA saw a significant increase in p53 levels of 142.51 ± 33.98 %, relative to controls.

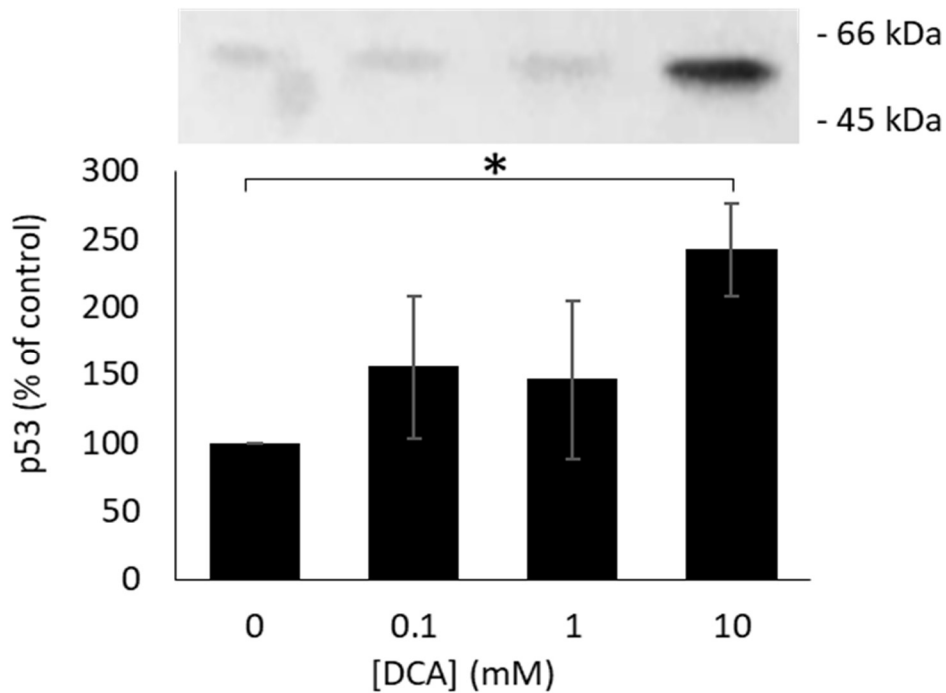


Figure 3.7. The effect of extended time course DCA treatment on p53 levels. SH-SY5Y cells were cultured in the presence of the indicated DCA concentrations for 3 passages, before a final 24 h treatment with DCA in UltraMEM. Equal amounts of lysate protein were then immunoblotted with anti-p53 antibody. Results are means \pm S.D. (n=3). Significant results are indicated: * = significant at $p \leq 0.05$.

Next, the effects of extended time course DCA treatment on the generation of sAPP α and sAPP β by SH-SY5Y cells were examined. When the concentrated conditioned medium from the final 24 h UltraMEM incubation was immunoblotted with anti-APP 6E10 antibody, the results (Fig. 3.8.) revealed that cells treated with 0.1, 1 and 10 mM DCA all generated significantly more sAPP α compared to control cells (20.41 ± 6.04 , 38.58 ± 17.16 , and 58.47 ± 28.93 % increases, respectively, relative to controls).

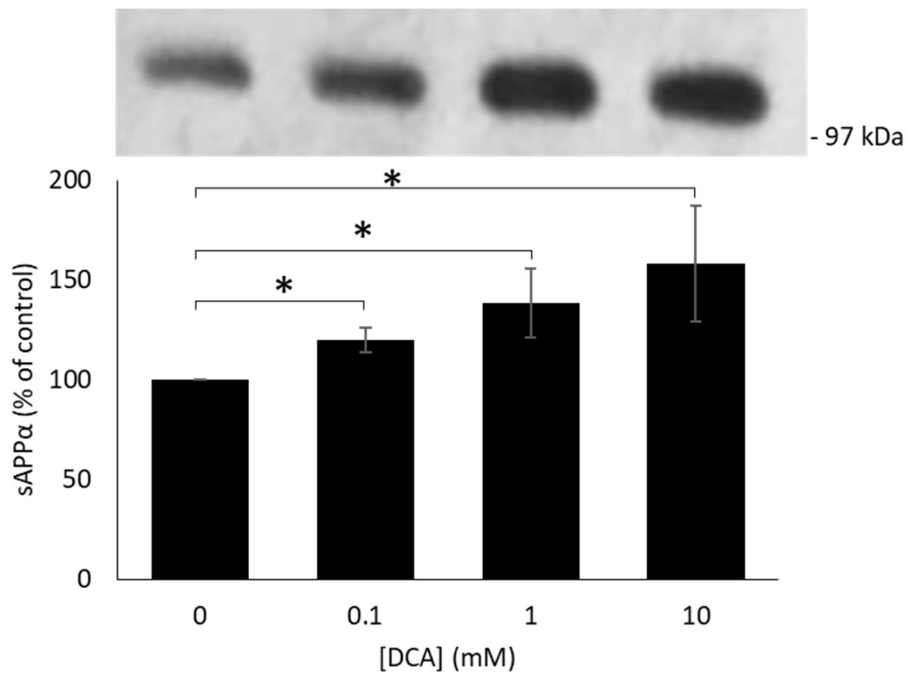


Figure 3.8. The effect of extended time course DCA treatment on sAPP α production by SH-SY5Y cells. Cells were cultured in the presence of the indicated DCA concentrations for 3 passages, before a final 24 h treatment with DCA in UltraMEM. Equal volumes of this final concentrated conditioned medium were then immunoblotted with the anti-sAPP α 6E10 antibody. Results are means \pm S.D. (n=3). Significant results are indicated: * = significant at $p \leq 0.05$.

When the same medium was immunoblotted with the anti-sAPP β antibody, the results (Fig. 3.9.) actually showed a significant increase in the generation of this fragment by cells cultured in the presence of the lowest (0.1 mM) concentration of DCA (26.24 ± 5.51 % increase, relative to controls). However, at the previously studied 10 mM concentration, the amount of sAPP β generated was, as previously observed, decreased relative to control cultures (46.03 ± 13.36 % decrease, relative to controls).

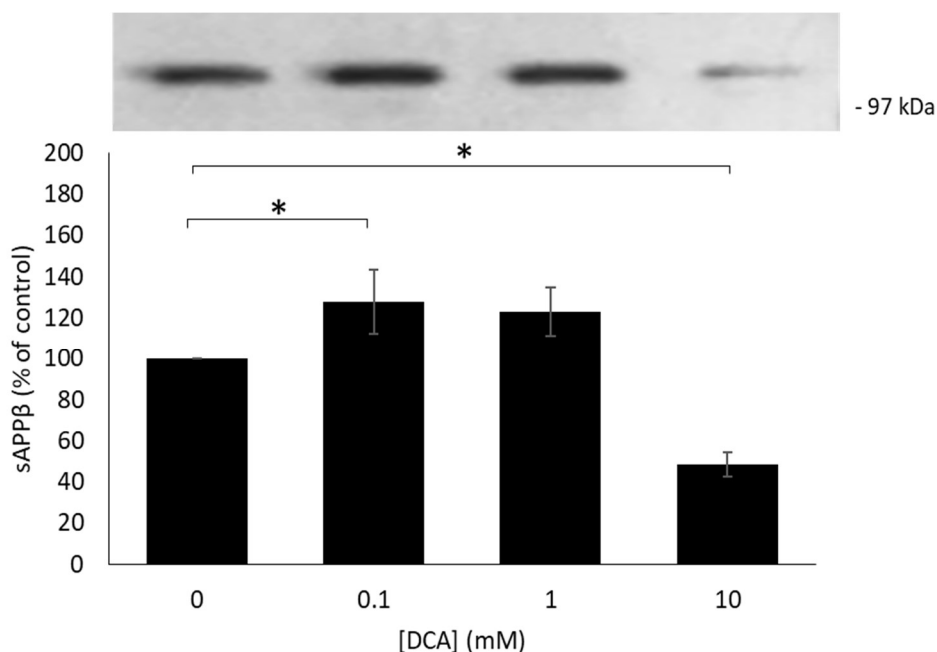


Figure 3.9. The effect of extended time course DCA treatment on sAPP β production by SH-SY5Y cells. Cells were cultured in the presence of the indicated DCA concentrations for 3 passages, before a final 24 h treatment with DCA in UltraMEM. Equal volumes of this final concentrated conditioned medium were then immunoblotted with the anti-sAPP β antibody. Results are means \pm S.D. (n=3). Significant results are indicated: * = significant at $p \leq 0.05$.

3.2. The effect of pH altering compounds structurally related to DCA on APP expression/proteolysis.

Having established that either short-term (24 h) or chronic exposure to DCA enhanced non-amyloidogenic and decreased the amyloidogenic processing of APP in SH-SY5Y cells, it was hypothesised that these effects might be mediated by simple changes in medium pH brought about by the drug. As such, the pH of the conditioned medium from 24 h DCA-treated cells was initially examined. The results (Fig. 3.10.) showed a significant increase in the pH of conditioned medium from cells treated with both 10 and 20 mM DCA, with the pH of control cultures being 6.96 ± 0.09 and that in the 10 and 20 mM DCA-treated cultures being 7.14 ± 0.03 and 7.23 ± 0.01 , respectively.

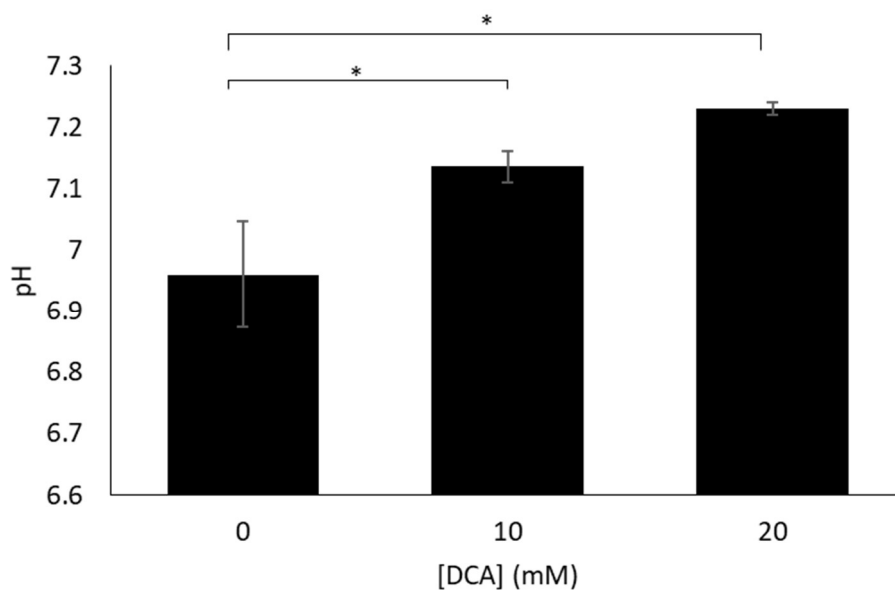


Figure 3.10. The effect of 24 h DCA treatment on the pH of conditioned medium. SH-SY5Y cells were treated with DCA at the concentrations indicated in UltraMEM for 24 h before measuring the pH of the medium. Results are means \pm S.D. (n=3). Significant results are indicated: * = significant at $p \leq 0.05$.

Given that DCA significantly enhanced the pH of the conditioned medium at the same drug concentrations as those which impacted on APP expression/proteolysis, it was then decided to investigate the effects of structurally related pH altering compounds on pH, cell viability and APP expression/proteolysis.

3.2.1. Sodium acetate.

In order to compare any potential effects of sodium acetate on APP expression/proteolysis to those mediated by sodium DCA (structures shown in Fig. 3.11.), SH-SY5Y cells were grown to confluence and treated for 24 h with UltraMEM containing molar concentrations of sodium acetate equivalent to those previously employed with DCA. Cells and medium were subsequently harvested, processed and analysed, as described in the

Materials and Methods section. Prior to concentrating, the pH of the conditioned medium was analysed. The results (Fig. 3.12.), similar to those observed with DCA (Fig. 3.10.), showed a significant increase in the pH of medium containing sodium acetate. Here, the pH of the medium from control cultures was 7.00 ± 0.03 and increased to 7.11 ± 0.02 and 7.19 ± 0.03 , respectively, in medium containing 10 and 20 mM sodium acetate.

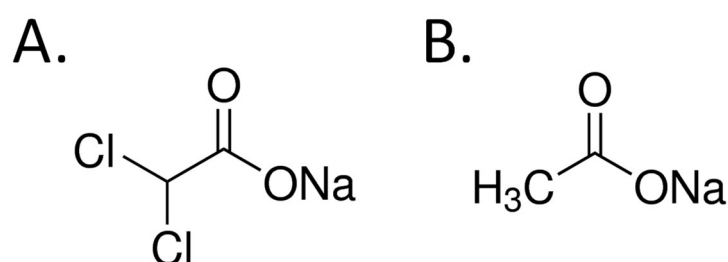


Figure 3.11. The structures of sodium dichloroacetate (A) and sodium acetate (B).

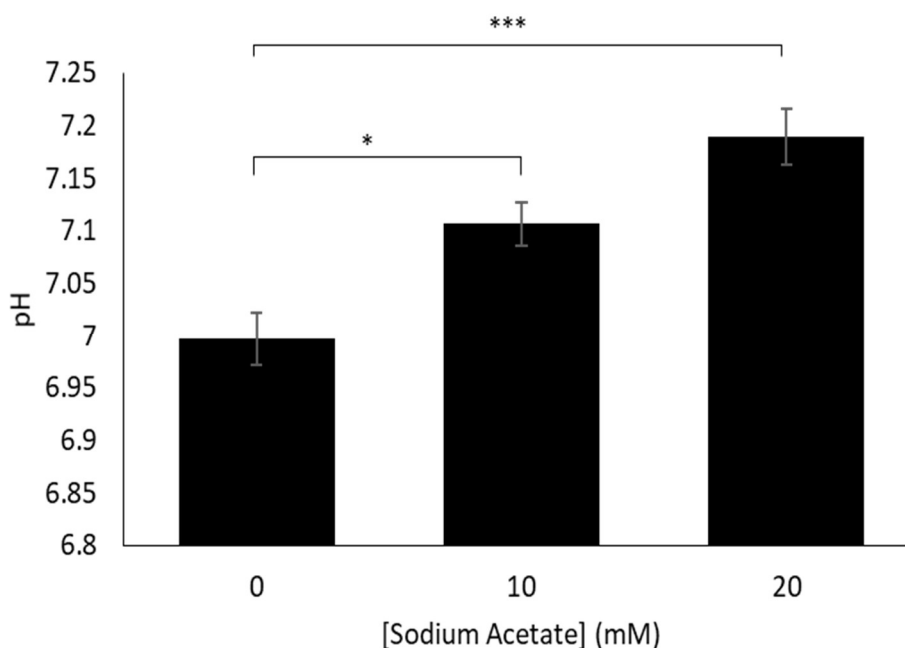


Figure 3.12. The effect of 24 h sodium acetate treatment on the pH of conditioned medium. SH-SY5Y cells were treated with sodium acetate at the concentrations indicated in UltraMEM for 24 h before measuring the pH of the medium. Results are means \pm S.D. (n=3). Significant results are indicated: * = significant at $p \leq 0.05$, *** = significant at $p \leq 0.005$.

Given that sodium acetate had an almost identical effect on the pH of conditioned medium to that of DCA, the viability of SH-SY5Y cells treated with the former compound was also investigated using the MTS assay, as described in the Materials and Methods section. The results (Fig. 3.13.) showed that whilst there was no significant effect of 10 mM sodium acetate on viability, there was a significant decrease of 16.92 ± 3.73 %, relative to control cultures, in the viability of 20 mM compound-treated cells. Hence, as with DCA, only relatively minor effects on cell viability were observed in sodium acetate-treated cultures.

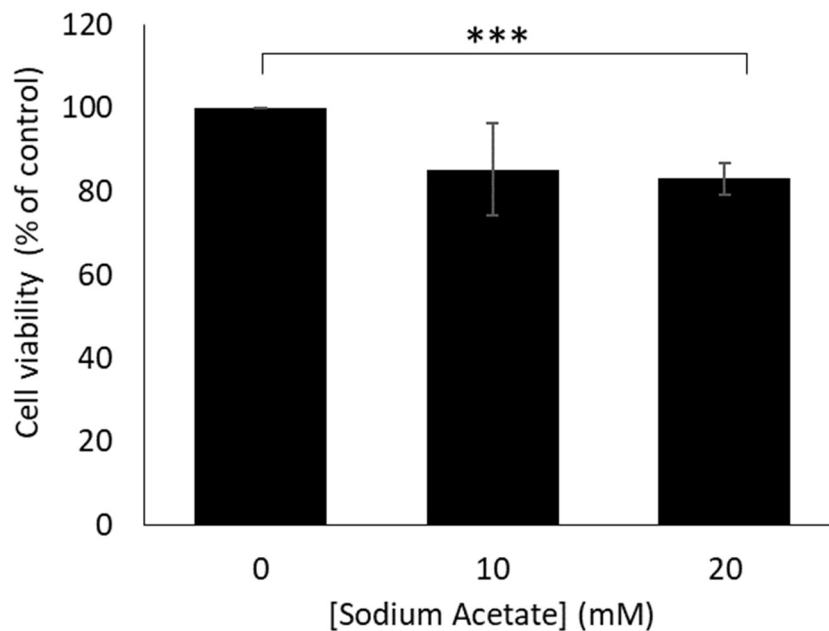


Figure 3.13. The effect of 24 h sodium acetate treatment on the viability of SH-SY5Y cells. Cells were treated with sodium acetate at the concentrations indicated for 24 h. Cell viability was then assessed through an MTS assay *in situ*. Results are means \pm S.D. (n=3). Significant results are indicated: *** = significant at $p \leq 0.005$.

Next, the effects of 24 h sodium acetate treatment on the expression of APP and p53 and proteolysis of the former protein were examined. To this end, lysates prepared from drug-treated cells were firstly immunoblotted with the anti-APP C-terminal antibody. The results (Fig. 3.14.) revealed no significant differences in the expression of full-length APP following the treatment of cells with sodium acetate (in contrast to clear increases observed previously with DCA).

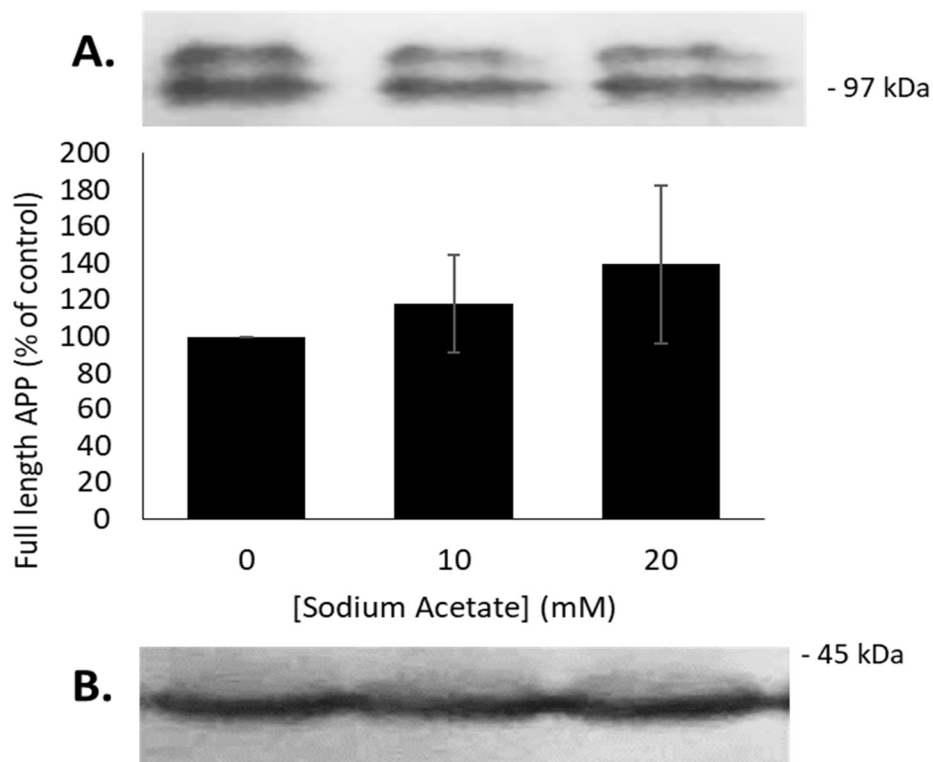


Figure 3.14. The effect of sodium acetate treatment on full-length APP expression. SH-SY5Y cells were cultured in the presence of the indicated sodium acetate concentrations in UltraMEM for 24 h. Equal amounts of lysate protein were then immunoblotted with **(A)** anti-APP C-terminal and **(B)** anti-actin antibodies. Results are means \pm S.D. (n=3).

When 24 h sodium acetate-treated cell lysates were immunoblotted with anti-p53 antibody (Fig. 3.15.), the results revealed a 68.89 ± 8.11 % decrease in the levels of this protein in 20 mM drug-treated cell lysates, relative to controls. Interestingly, despite the pH changes induced by sodium acetate being similar to those affected by DCA, the effect of the former compound on p53 levels was the complete opposite to that of DCA (which enhanced p53 levels).

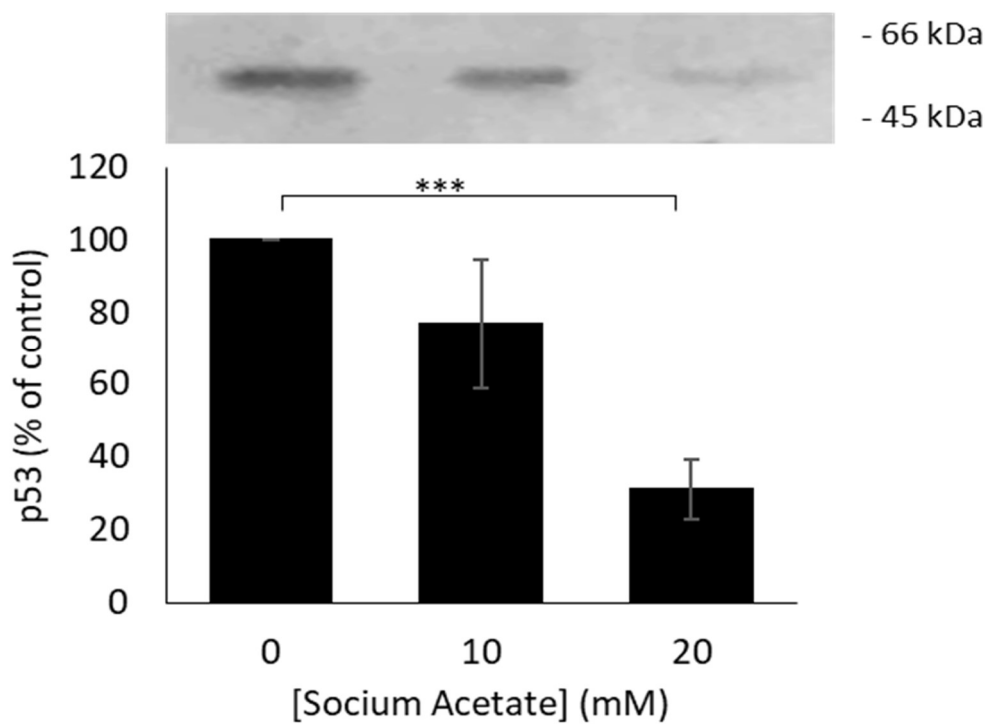


Figure 3.15. The effect of sodium acetate treatment on p53 levels. SH-SY5Y cells were cultured in the presence of the indicated sodium acetate concentrations in UltraMEM for 24 h. Equal amounts of lysate protein were then immunoblotted with anti-p53 antibody. Results are means \pm S.D. ($n=3$). Significant results are indicated: *** = significant at $p \leq 0.005$.

Next, conditioned medium from the 24 h sodium acetate-treated cells was immunoblotted with the anti-APP 6E10 antibody to detect sAPP α . Initially, the results were quantified in terms of the absolute amount of the protein fragment released by cells (Fig. 3.16A.). Here, cells treated with 10 mM sodium acetate demonstrated a 34.40 ± 9.68 % increase specifically in the generation of sAPP695 α but this difference was not significant at a 20 mM compound concentration. Conversely, although levels of sAPP751/770 α appeared to increase at both sodium acetate concentrations, the increase was only significant at 20 mM (34.40 ± 9.68 % increase relative to controls). The results were also standardised to account for the minor decreases observed in cell viability previously in Fig. 3.14. These latter results (Fig. 3.16B.) gave similar results but with higher levels of significance. As such, like DCA, sodium acetate appears to enhance sAPP α generation.

The same conditioned medium samples were then immunoblotted for sAPP β and the results (Fig. 3.17) clearly showed a significant increase in sAPP β generation by sodium acetate-treated cells. Non-standardised results (Fig. 3.17A.) revealed 24.50 ± 7.96 and 44.27 ± 14.72 % increases in 10 and 20 mM sodium acetate-treated cultures, respectively. When these results were corrected to account for changes in cell viability (Fig. 3.17B.) these differences were even more apparent. It is of note that, despite having similar effects on cell viability and sAPP α generation to DCA, sodium acetate increased rather than decreased sAPP β generation.

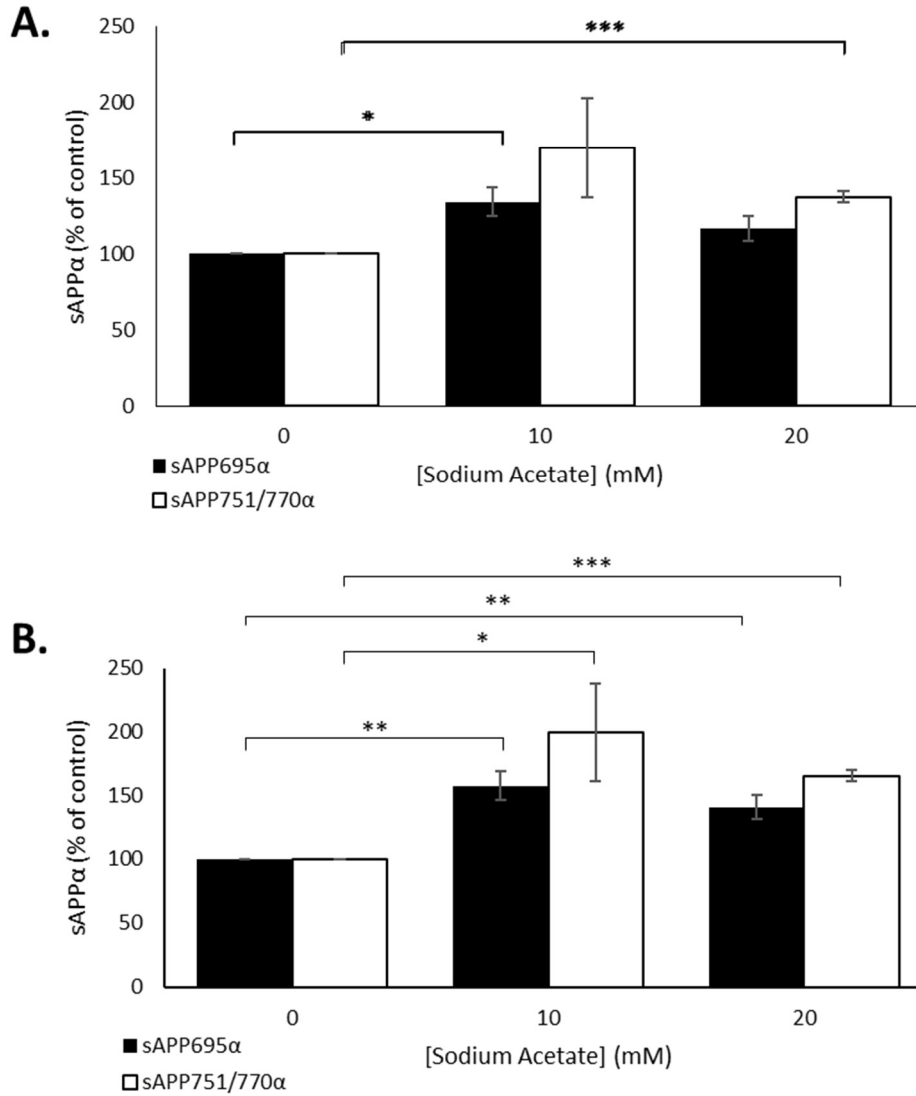


Figure 3.16. The effect of 24 h sodium acetate treatment on the production of sAPPα by SH-SY5Y cells. Cells were treated with sodium acetate at the concentrations indicated for 24 h. Equal volumes of concentrated medium were then immunoblotted with the anti-sAPPα 6E10 antibody. **(A)** Absolute levels and **(B)** levels standardised for cell viability. Results are means ± S.D. (n=3). Significant results are indicated: * = significant at $p \leq 0.05$, ** = significant at $p \leq 0.01$, *** = significant at $p \leq 0.005$.

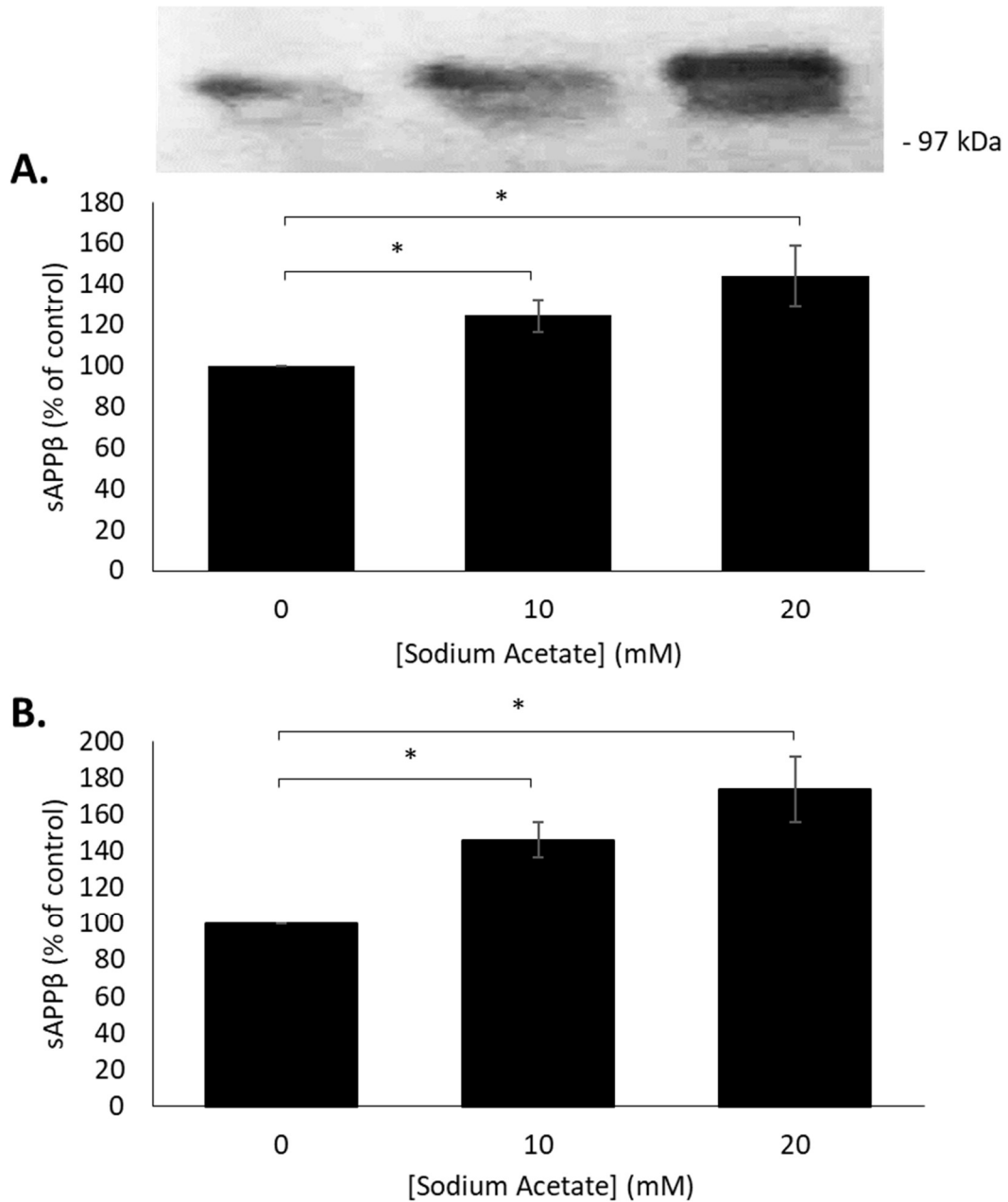


Figure 3.17. The effect of 24 h sodium acetate treatment on the production of sAPPβ by SH-SY5Y cells. Cells were treated with sodium acetate at the concentrations indicated for 24 h. Equal volumes of concentrated medium were then immunoblotted with the anti-sAPPβ antibody. **(A)** Absolute levels and **(B)** levels standardised for cell viability. Results are means ± S.D. (n=3). Significant results are indicated: * = significant at $p \leq 0.05$.

3.2.2. Acetic acid.

To further evaluate any potential role of pH in the DCA-mediated changes in APP expression/proteolysis, the effects of acetic acid on these processes were also examined (the structures of DCA and acetic acid are compared in Fig. 3.18.). Initially, SH-SY5Y cells were grown to confluence and treated for 24 h with UltraMEM containing molar concentrations of acetic acid equivalent to those previously employed with DCA. Cells and medium were subsequently harvested, processed and analysed, as described in the Materials and Methods section. Prior to concentrating, the pH of the conditioned medium was analysed. In contrast to the results obtained from medium treated with DCA (Fig. 3.10.) and sodium acetate (Fig. 3.12.), the results (Fig. 3.19.) showed a significant decrease in the pH of medium containing acetic acid. Here the pH of the medium from control cultures was 7.03 ± 0.01 , which decreased to 6.81 ± 0.01 and 6.64 ± 0.04 , respectively, in medium containing 10 and 20 mM acetic acid.

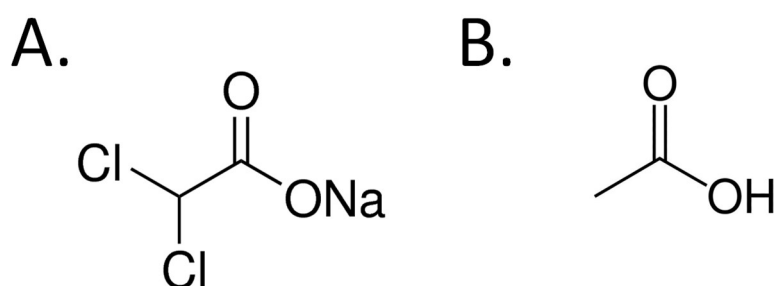


Figure 3.18. The structures of sodium dichloroacetate (A) and acetic acid (B).

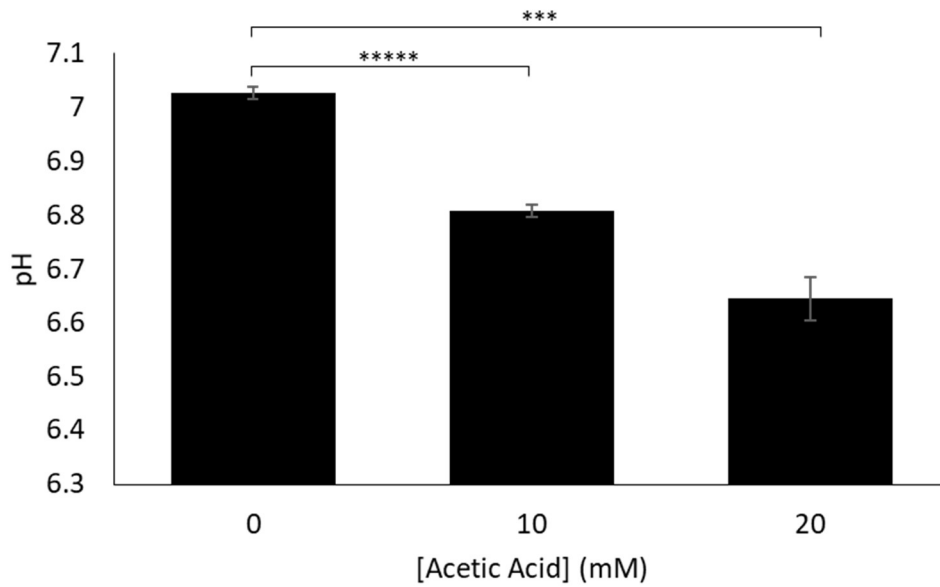


Figure 3.19. The effect of 24 h acetic acid treatment on the pH of conditioned medium. SH-SY5Y cells were treated with acetic acid at the concentrations indicated in UltraMEM for 24 h and the pH of the conditioned medium was measured. Results are means \pm S.D. (n=3). Significant results are indicated: *** = significant at $p \leq 0.05$, **** = significant at $p \leq 0.0005$.

Given that acetic acid had the complete opposite effect on medium pH to that of DCA, the viability of SH-SY5Y cells treated with the former compound was also investigated using the MTS assay as described in the Materials and Methods section. The results (Fig. 3.20.) showed that acetic acid treatment led to a significant decrease in cell viability in both 10 and 20 mM treated cultures (24.47 ± 2.02 and 58.98 ± 2.46 % decreases, respectively, relative to controls).

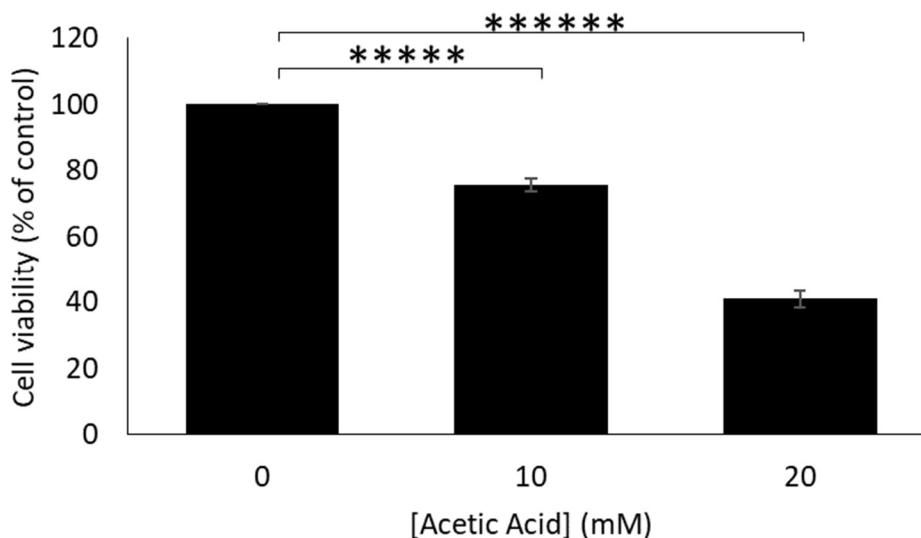


Figure 3.20. The effect of 24 h acetic acid treatment on cell viability. SH-SY5Y cells were treated with acetic acid at the concentrations indicated in UltraMEM for 24 h. Cells were then quantified using an MTS assay *in situ*. Results are means \pm S.D. (n=3). Significant results are indicated: ***** = significant at $p \leq 0.0005$, ***** = significant at $p \leq 0.00005$.

Next, the effects of 24 h acetic acid treatment on the expression of APP and p53 and proteolysis of the former protein were examined. To this end, lysates prepared from drug-treated cells were first immunoblotted with the anti-APP C-terminal antibody. The results (Fig. 3.21.) revealed no significant differences in the expression of full-length APP following the treatment of cells with 10 mM acetic acid. However, cells treated with 20 mM acetic acid saw a significant increase in full-length APP expression (154.33 ± 17.83 % increase, relative to controls). Therefore, like DCA, acetic acid treatment leads to a significant increase in full-length APP expression despite the latter compound having an opposite effect to DCA on pH.

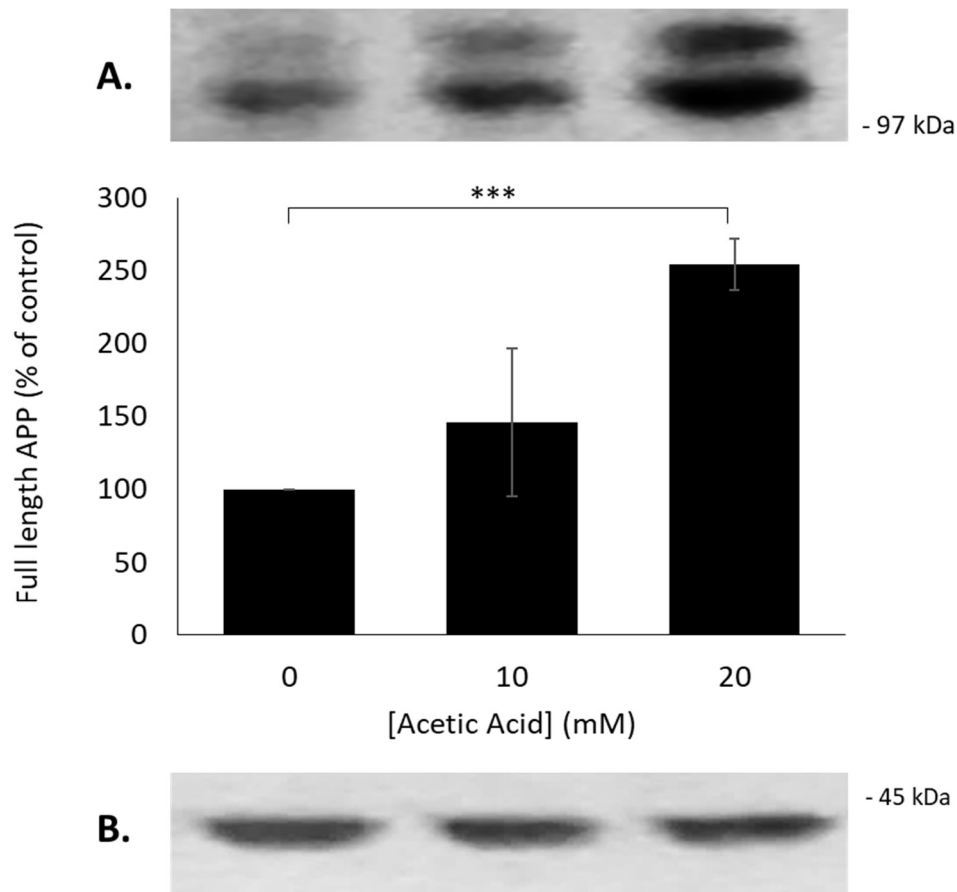


Figure 3.21. The effect of 24 h acetic acid treatment on the expression of full-length APP in SH-SY5Y cells. SH-SY5Y cells were treated with acetic acid at the concentrations indicated for 24 h. Equal amounts of lysate protein were then immunoblotted with **(A)** anti-APP C-terminal and **(B)** anti-actin antibodies. Results are means \pm S.D. (n=3). Significant results are indicated: *** = significant at $p \leq 0.005$.

When 24 h acetic acid-treated cell lysates were immunoblotted with anti-p53 antibody (Fig. 3.22.), significant decreases in the levels of this protein were observed in cells treated with both 10 and 20 mM acetic acid (26.32 ± 7.00 and 46.74 ± 15.40 % reductions, respectively, relative to controls). This was similar to the results obtained from sodium acetate treatments (which also reduced p53 levels), but the complete opposite to those obtained from DCA treated cells (which enhanced p53 levels). Therefore, it was clear that the DCA-induced alterations in p53 levels were not simply related to changes in extracellular pH.

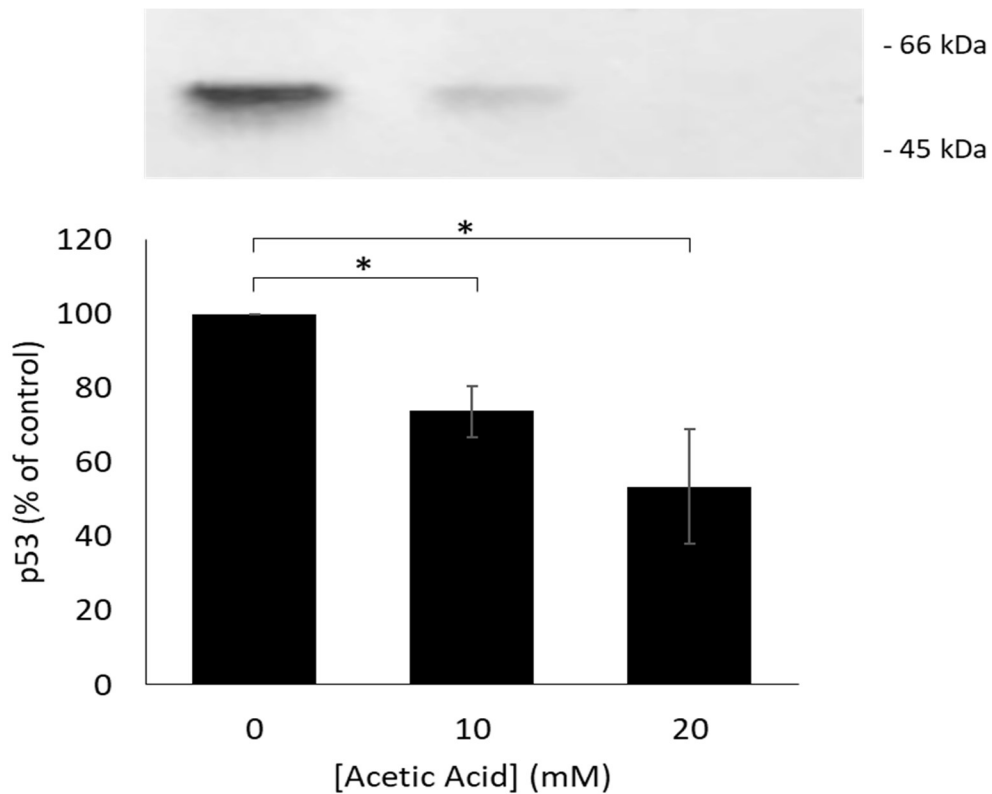


Figure 3.22. The effect of 24 h acetic acid treatment on the levels of p53 in SH-SY5Y cells. SH-SY5Y cells were treated with acetic acid at the concentrations indicated for 24 h. Equal amounts of lysate protein were then immunoblotted with anti-p53 antibody. Results are means \pm S.D. (n=3). Significant results are indicated: * = significant at $p \leq 0.05$.

Next, conditioned medium from the 24 h acetic acid-treated cells was immunoblotted with anti-APP 6E10 antibody in order to detect sAPP α . Initially, the results were quantified in terms of the absolute amount of the protein fragment released by cells (Fig. 3.23A.). Here, no significant change was observed in either sAPP751/770 α or sAPP695 α . The results were also standardised to account for the decreases observed previously in cell viability (Fig. 3.20.). These latter results (Fig. 3.23B.) showed that there was a significant increase in sAPP695 α production by cells treated with both 10 and 20 mM acetic acid (28.67 ± 4.15 and 138.17 ± 11.61 % increases, respectively, relative to controls). These results also showed that cells treated with 20 mM saw a significant increase in sAPP751/770 α production (179.86 ± 37.06

% increase, relative to controls). It is, therefore, worth noting that acetic acid treatments led to similar increases in sAPP α production to DCA treatments, despite having the opposite effect on extracellular pH.

The same conditioned medium samples were then immunoblotted for sAPP β and the results (Fig. 3.24.) showed a significant increase in sAPP β generation in acetic acid-treated cells. Non-standardised results (Fig. 3.24A.) revealed 41.15 ± 8.73 and 55.89 ± 14.90 % increases in sAPP β production in cells treated with 10 and 20 mM acetic acid, respectively, relative to controls. When these results were corrected to account for changes in cell viability (Fig. 3.24B.), these differences were even more apparent. Therefore, as previously observed with sodium acetate treated cells, acetic acid treatment also increased sAPP β production despite the opposing effects of the two compounds on pH.

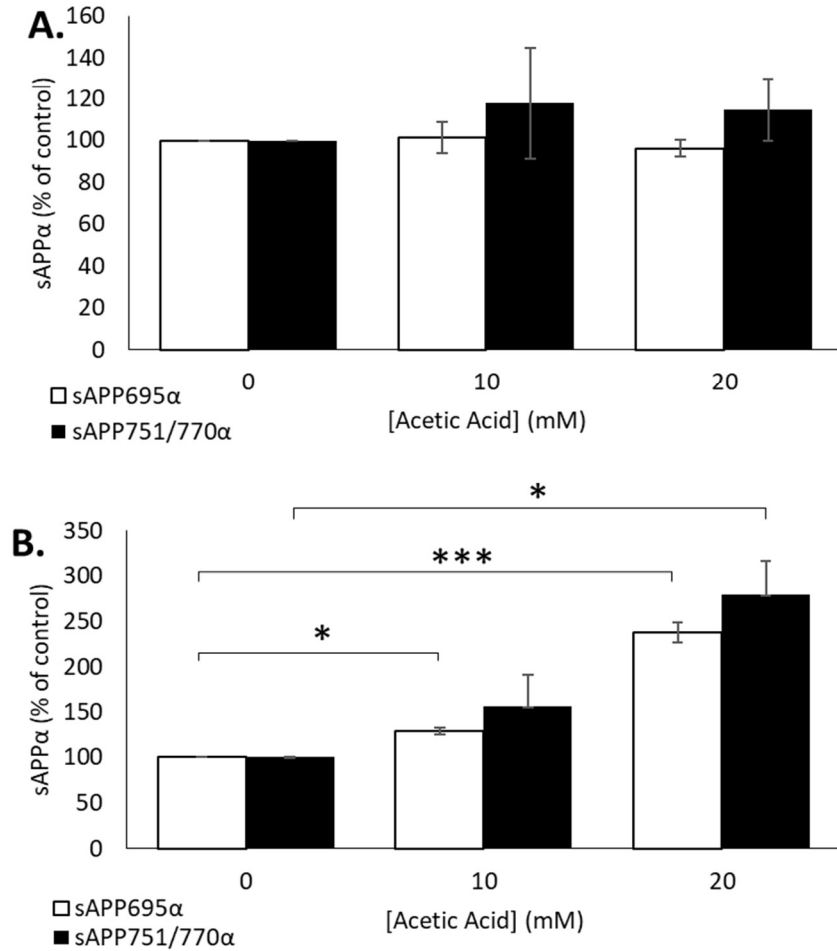
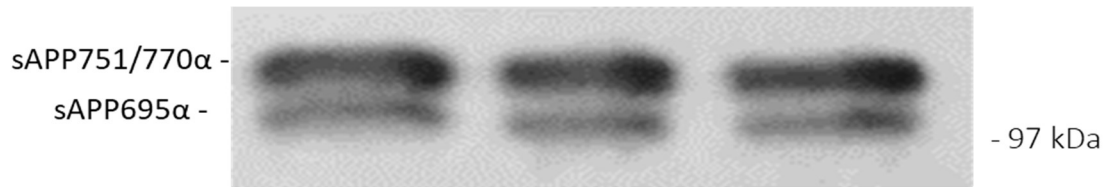


Figure 3.23. The effect of 24 h acetic acid treatment on the production of sAPP α by SH-SY5Y cells. SH-SY5Y cells were treated with acetic acid at the concentrations indicated for 24 h. Equal volumes of concentrated medium were then immunoblotted with the anti-sAPP α 6E10 antibody. **(A)** Standard results and **(B)** viability corrected results. Results are means \pm S.D. (n=3). Significant results are indicated: * = significant at $p \leq 0.05$, *** = significant at $p \leq 0.005$.

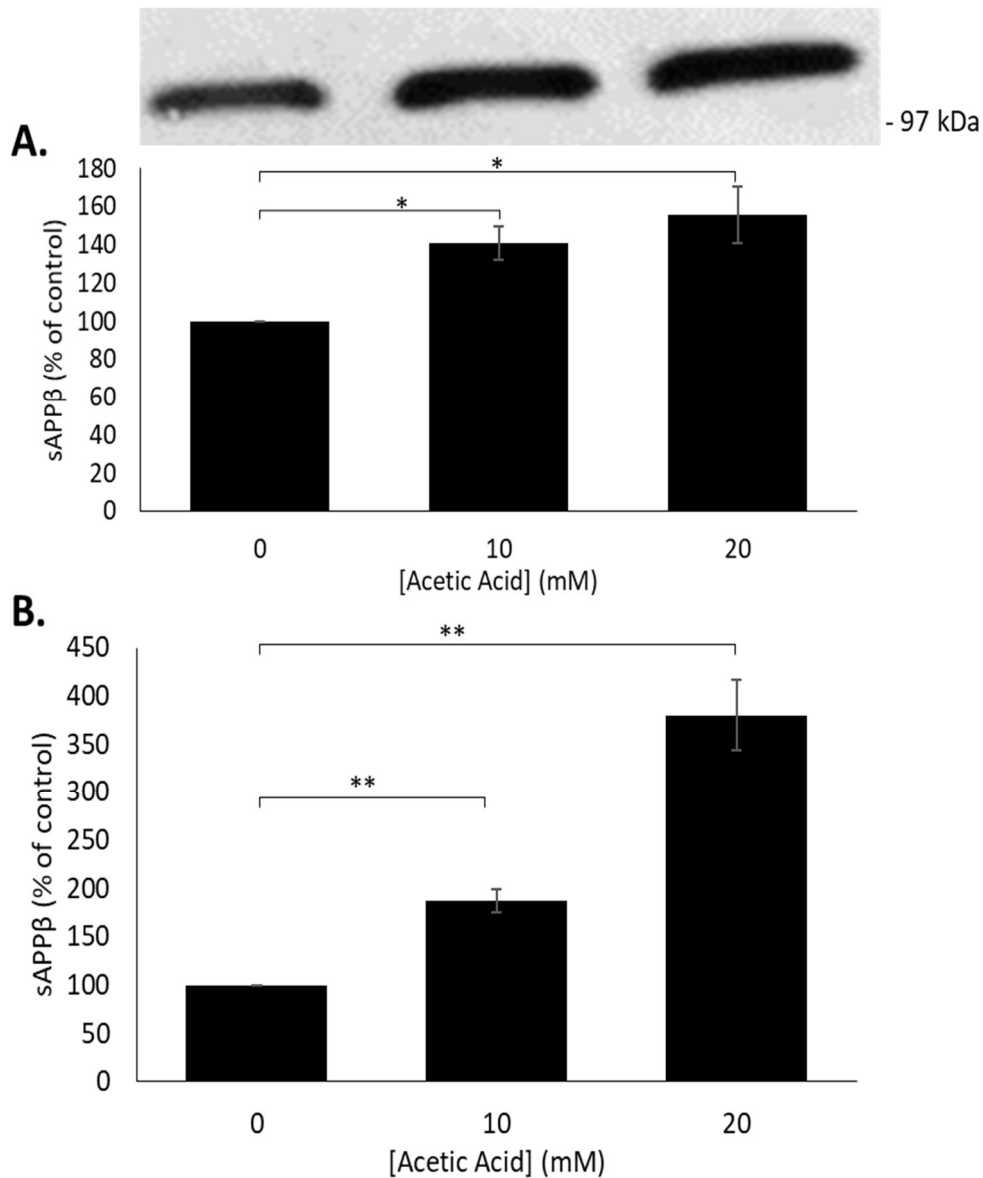


Figure 3.24. The effect of 24 h acetic acid treatment on the production of sAPPβ by SH-SY5Y cells. SH-SY5Y cells were treated with acetic acid at the concentrations indicated for 24 h. Equal volumes of concentrated medium were then immunoblotted with the anti-sAPPβ antibody. **(A)** Standard results and **(B)** corrected viability results. Results are means ± S.D. (n=3). Significant results are indicated: * = significant at $p \leq 0.05$, ** = significant at $p \leq 0.01$.

3.3. Summary.

The initial aim of this chapter was to reproduce previous data (Parkin *et al.*, unpublished) showing that DCA, at concentrations of 10 and 20 mM, enhanced non-amyloidogenic and impaired amyloidogenic processing of APP. The results in the current study also showed that 10 mM DCA was the minimum effective concentration of the drug in these respects. The same concentrations of DCA also enhanced p53 levels, although there was little effect on cell viability. Notably, when cells were treated with sodium acetate, similar changes in pH and cell viability were observed and the non-amyloidogenic production of sAPP α was also increased slightly. However, the effects of this compound on sAPP β generation and p53 levels were the complete opposite of those observed with DCA (i.e. sodium acetate enhanced production of sAPP β and decreased p53 levels whereas DCA impaired production of the former fragment and enhanced p53 levels). As such it is apparent that the effects of DCA on APP processing are not simply the consequence of an increase in the alkalinity of medium. When SH-SY5Y cells were treated with 10 and 20 mM concentrations of acetic acid, the pH of the conditioned medium, as one would expect for an acid, decreased in an exact opposite fashion to the effect mediated by DCA and sodium acetate. This drop in pH caused considerable decreases in cell viability although any cell death was probably not of an apoptotic manner as acetic acid also decreased p53 levels. Here, the increased acidity of the medium enhanced sAPP α generation (as seen with DCA and sodium acetate despite these compounds having an opposite effect to acetic acid on pH) and also enhanced sAPP β generation.

It is, therefore, apparent, given the different effects of DCA, sodium acetate and acetic acid on the proteolysis of APP, that the effect of the former drug in this respect cannot simply be mediated by changes in extracellular pH.

Chapter 4.

**DCA-mediated changes in p53 levels and the regulation of APP
proteolysis.**

4. DCA-mediated changes in p53 levels and the regulation of APP proteolysis.

In the preceding results section, it was demonstrated that DCA enhanced levels of p53 expression in SH-SY5Y cell lysates (Fig. 3.3.). It has previously been shown that there is a reciprocal relationship between APP and p53 levels (Alves da Costa *et al.*, 2006; Cuesta *et al.*, 2009). Therefore, in the current study, it was hypothesised that the changes in APP expression/proteolysis mediated by DCA might be related to cellular p53 levels. As such, the levels of the latter protein were experimentally manipulated and the effects of these changes on APP expression/proteolysis in DCA-treated cells were monitored.

4.1. Reactivating p53 and Inducing Tumour Apoptosis (RITA) enhancement of p53 levels.

Reactivating p53 and Inducing Tumour Apoptosis (RITA) is a drug in development for the treatment of cancer due to its ability to enhance cellular p53 levels (Merkel *et al.*, 2017). The drug works by inducing a conformational change in the N-terminal region of p53, which impedes the bindings of regulators (such as MDM2) and results in p53 stabilisation and activation (Enge *et al.*, 2009). Therefore, in the current study, RITA was used to enhance p53 levels in SH-SY5Y cells and to examine the effects of this change on APP expression/proteolysis both in the absence or presence of DCA.

4.1.1. Optimisation of RITA concentrations.

Before assessing whether RITA could modify the effects of DCA on APP expression/proteolysis, it was necessary to determine which concentrations of the former drug enhanced p53 levels in SH-SY5Y cells and what effects these concentrations had on cell viability. Ideally, the subsequent experiments using DCA could then be performed using a RITA concentration that enhanced p53 expression without impacting too severely on cell viability. Initially, cells were grown to confluence and treated with a range of RITA concentrations between 0-25 μM (this range was adopted from Issaeva *et al.*, 2004). After 24 h, cell viability was determined using the MTS assay as described in the Materials and Methods section. The results (Fig. 4.1.) showed that RITA concentrations at or below 5 μM had no significant effect on cell viability, whilst drug concentrations of 10 and 25 μM decreased viability by 22.50 ± 7.05 and 27.50 ± 9.47 %, respectively, relative to controls.

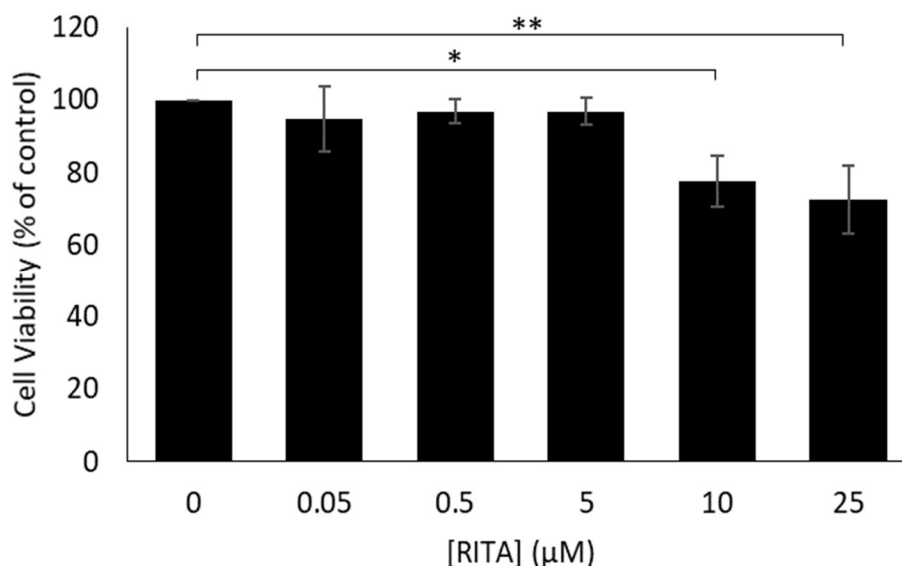


Figure 4.1. The effect of 24 h RITA treatment on SH-SY5Y cell viability. SH-SY5Y cells were treated with RITA at the concentrations indicated for 24 h. An MTS assay was then performed *in situ*. Results are means \pm S.D. (n=3). Significant results are indicated: * = significant at $p \leq 0.05$, ** = significant at $p \leq 0.01$.

Lysates prepared from RITA-treated cells were then also subjected to immunoblotting using the anti-p53 antibody. The results (Fig. 4.2.) showed no significant changes in p53 levels at RITA concentrations lower than 5 μM . However, cells treated with 5, 10 and 25 μM RITA exhibited increases in levels of the protein of 64.97 ± 17.07 , 79.71 ± 17.23 , and 124.21 ± 37.60 %, respectively, relative to controls.

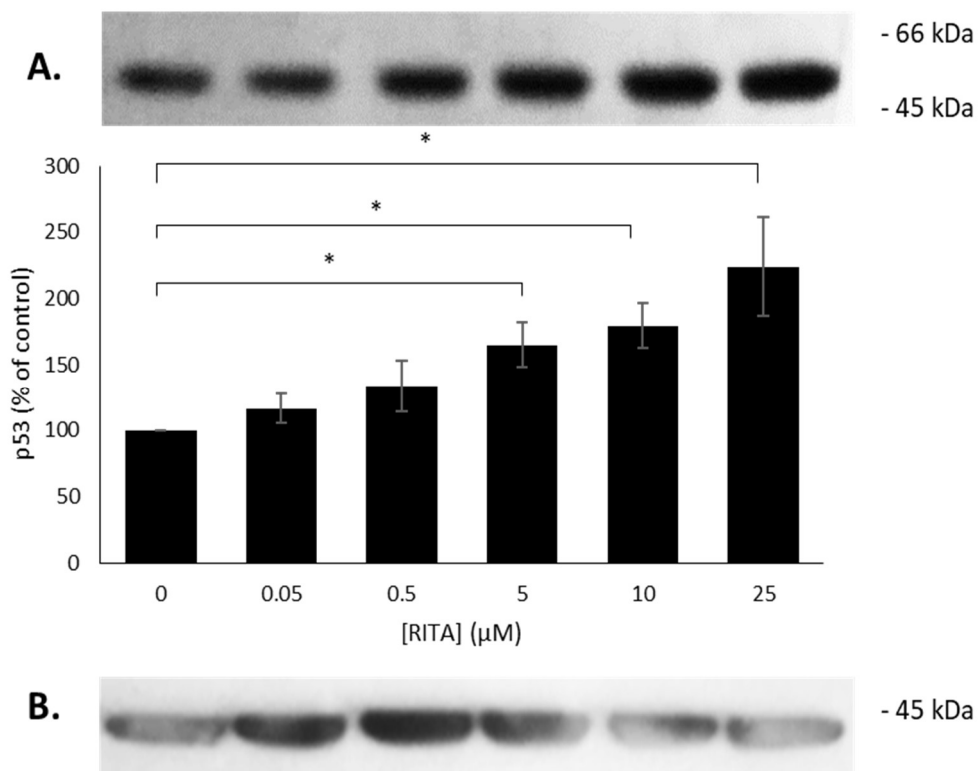


Figure 4.2. The effect of 24 h RITA treatment on the levels of p53 in SH-SY5Y cells. SH-SY5Y cells were treated with RITA at the concentrations indicated for 24 h. Cell lysates were then prepared, and equal amounts of protein were resolved and immunoblotted with **(A)** anti-p53 and **(B)** anti-actin antibodies. Results are means \pm S.D. (n=3). Significant results are indicated: * = significant at $p \leq 0.05$.

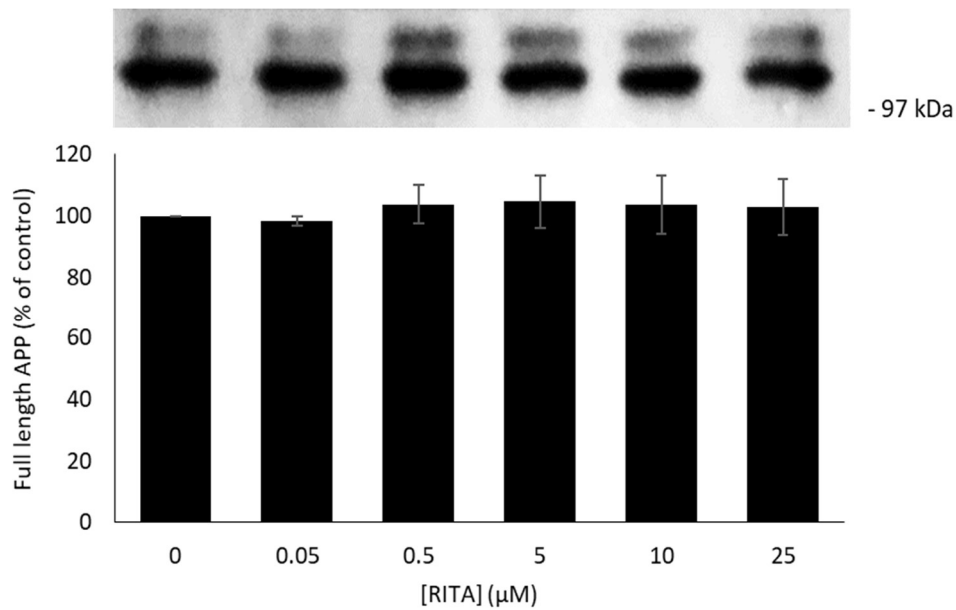


Figure 4.3. The effect of 24 h RITA treatment on the expression of full-length APP in SH-SY5Y cells. Cells were treated with RITA at the concentrations indicated for 24 h. Equal amounts of lysate protein were then immunoblotted with the anti-APP C-terminal antibody. Results are means \pm S.D. (n=3).

In order to assess the effect of this range of RITA concentrations on APP expression, the lysate samples were also immunoblotted with the anti-APP C-terminal antibody (Fig. 4.3.) but the results showed no significant effect of the drug on full-length APP expression.

Conditioned medium from 24 h RITA-treated cells was then immunoblotted with anti-APP 6E10 antibody to determine whether the drug had any effect on the non-amyloidogenic processing of APP. However, the results (Fig. 4.4.) revealed no changes in the levels of sAPP695 α and sAPP751/770 α generated by RITA-treated cells, regardless of whether or not levels of these fragments were corrected in order to account for RITA-induced changes in cell viability.

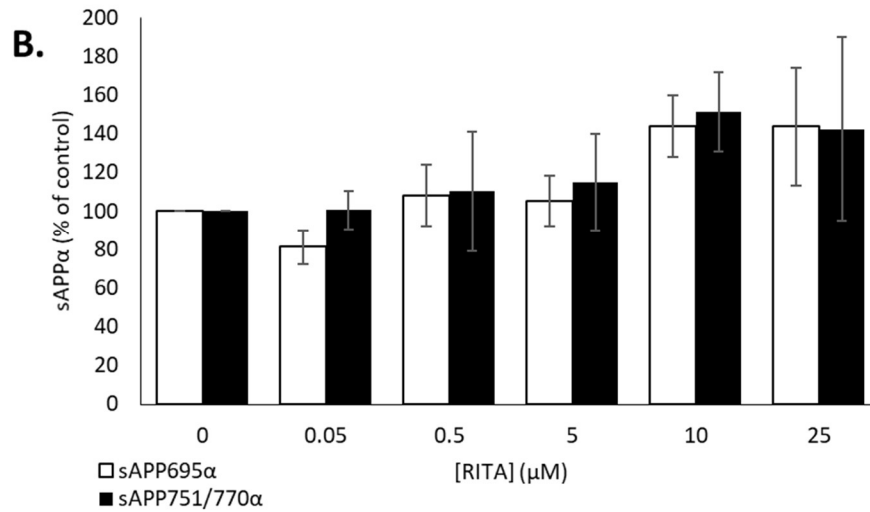
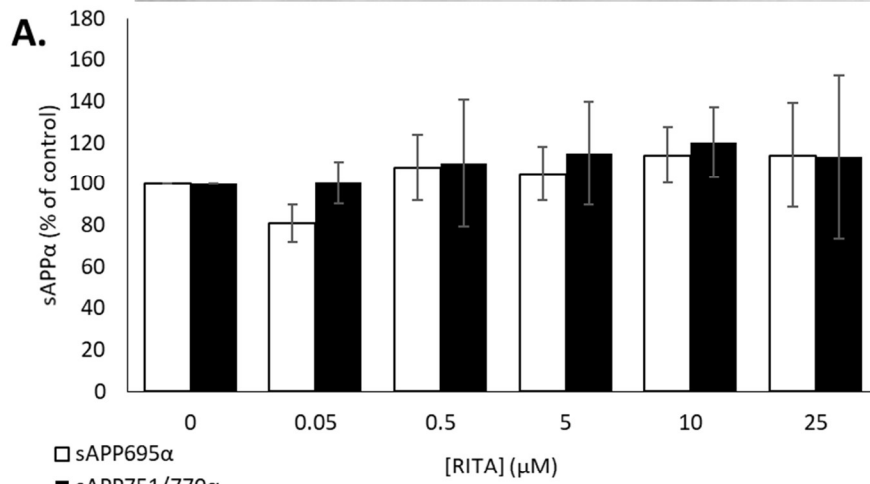
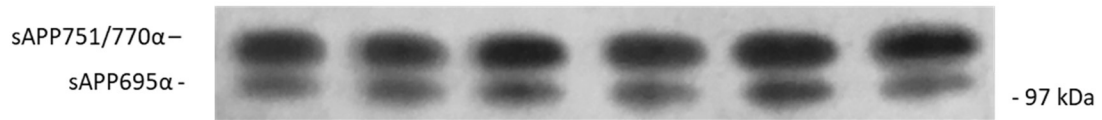


Figure 4.4. The effect of 24 h RITA treatment on the production of sAPPα. SH-SY5Y cells were treated with RITA at the concentrations indicated for 24 h. Equal volumes of concentrated medium were then immunoblotted with the anti-sAPPα 6E10 antibody. **(A)** Standard results and **(B)** viability corrected results. Results are means ± S.D. (n=3).

When concentrated medium from 24 h RITA-treated cells was immunoblotted with the anti-sAPP β antibody, the results (Fig. 4.5.) also showed no significant differences in sAPP β production in cells treated with RITA at any concentration.

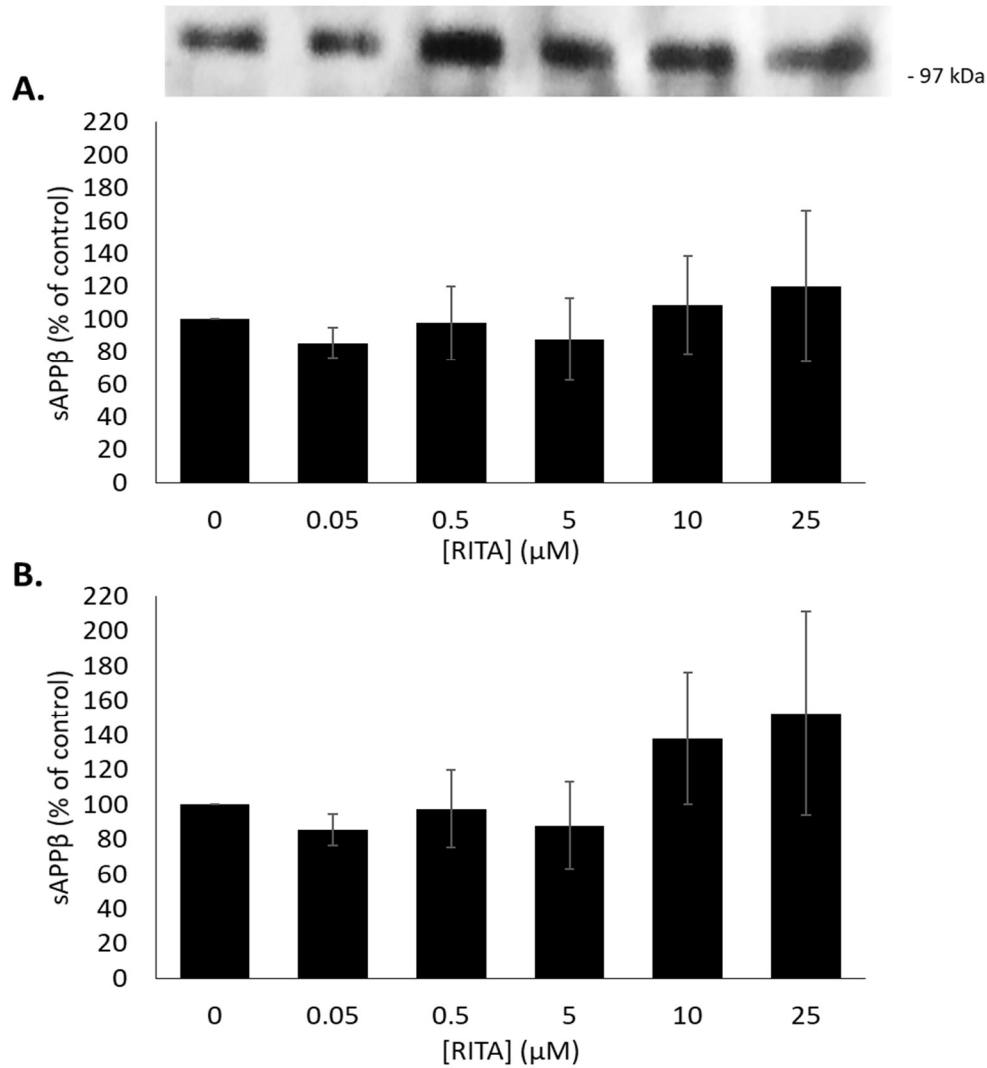


Figure 4.5. The effect of 24 h RITA treatment on the production of sAPP β . SH-SY5Y cells were treated with RITA at the concentrations indicated for 24 h. Equal volumes of concentrated medium were then immunoblotted with the anti-sAPP β antibody. **(A)** Standard results and **(B)** viability corrected results. Results are means \pm S.D. (n=3).

Interestingly, as RITA concentrations increased so too did the levels of a band detected by the anti-sAPP β antibody at around 30 kDa (Fig. 4.6A.). Given that the fragment must have contained the C-terminal neoepitope generated on sAPP β following β -secretase processing to be detected by this antibody, it was hypothesised that the fragment may result from an unknown protease cleavage of sAPP β . Such a cleavage would also, in theory, lead to the generation of a correspondingly truncated N-terminal fragment generated from sAPP β of around 70 kDa (full-length sAPP β being about 100 kDa). As such, the same medium samples were also immunoblotted with antibody 22C11 which detects an epitope in the N-terminal region of APP. However, the results (Fig. 4.6B.) showed no accumulation of a band around 70 kDa following RITA treatment. Interestingly though, a range of smaller (possibly N-terminal) fragments did accumulate in the range of 15-30 kDa suggesting possible degradation products of an N-terminal fragment.

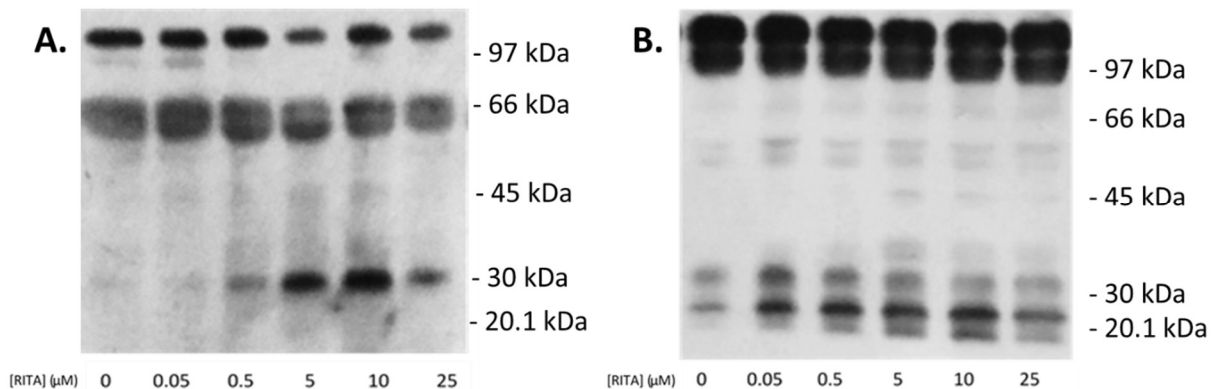


Figure 4.6. The effect of 24 h RITA treatment on the production of APP fragments by SH-SY5Y cells. SH-SY5Y cells were treated with RITA at the concentrations indicated for 24 h. Equal volumes of concentrated medium were then immunoblotted with **(A)** anti-sAPP β antibody and **(B)** antibody 22C11. (n=3).

4.1.2. The effect of RITA on the DCA-mediated regulation of APP expression/proteolysis.

In the preceding section, it was determined that a RITA concentration of 5 μ M substantially enhanced p53 levels in SH-SY5Y cells without leading to statistically significant decreases in cell viability. Therefore, despite the fact that RITA had no effect on APP expression or proteolysis when used alone, it was decided to examine whether this concentration of the drug might still be able to modify these events when used in combination with DCA. To this end, cells were grown to confluence and treated for 24 h with UltraMEM containing 10 mM DCA and/or 5 μ M RITA before conducting an MTS cell viability assay as described in the Materials and Methods section. The results (Fig. 4.7.) showed that, as previously observed using this technique, DCA (10 mM) did not cause a decrease in viability nor did RITA when used on its own at 5 μ M. However, when the two drugs were used in combination there was a 24.56 ± 6.64 % reduction in viability (relative to controls) which, interestingly, was significantly different not only from controls but also cultures treated with DCA or RITA on their own.

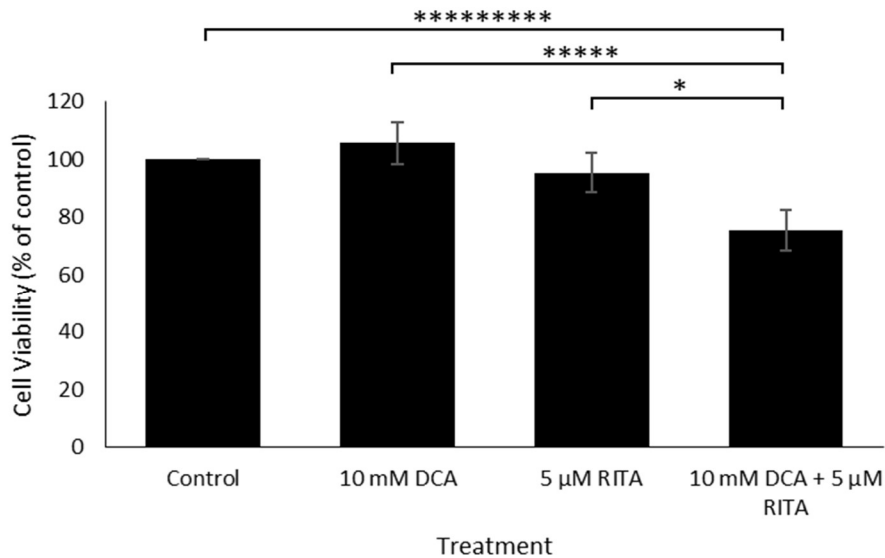


Figure 4.7. The effect of RITA and/or DCA treatment on the viability of SH-SY5Y cells. SH-SY5Y cells were treated with DCA and/or RITA at the concentrations indicated for 24 h. Cell viability was then assessed using an MTS assay *in situ*. Results are means \pm S.D. (n=3). Significant results are indicated: * = significant at $p \leq 0.05$, **** = significant at $p \leq 0.0005$, **** = significant at $p \leq 0.00005$.

The cell lysates were then immunoblotted with anti-p53 antibody and the results (Fig. 4.8.) showed that when used singularly, as previously observed, both DCA and RITA caused significant increases in cellular p53 levels. Interestingly, when used in combination, the two drugs seemed to have an additive effect on p53 levels leading to a 172.29 ± 36.17 % increase in p53 levels, relative to controls.

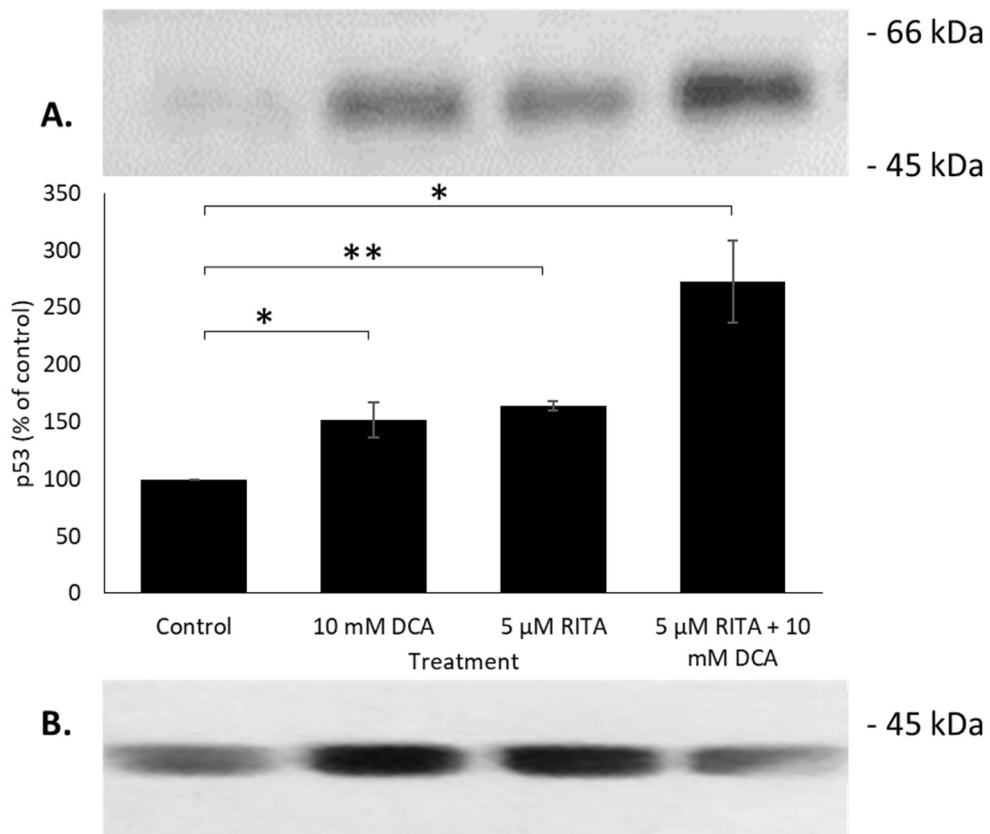


Figure 4.8. The effect of RITA and/or DCA treatment on p53 expression. SH-SY5Y cells were treated with DCA and/or RITA for 24 h. Cell lysates containing the same concentration of protein were then blotted with **(A)** anti-p53 and **(B)** anti-actin antibody. Results are means \pm S.D. (n=3). Significant results are indicated: * = significant at $p \leq 0.05$, ** = significant at $p \leq 0.01$.

Next, the effects of combined RITA and DCA treatments on APP expression and proteolysis were examined. The lysates from the previous experiment were also immunoblotted with the anti-APP C-terminal antibody but the results (Fig. 4.9.) showed no changes in APP expression.

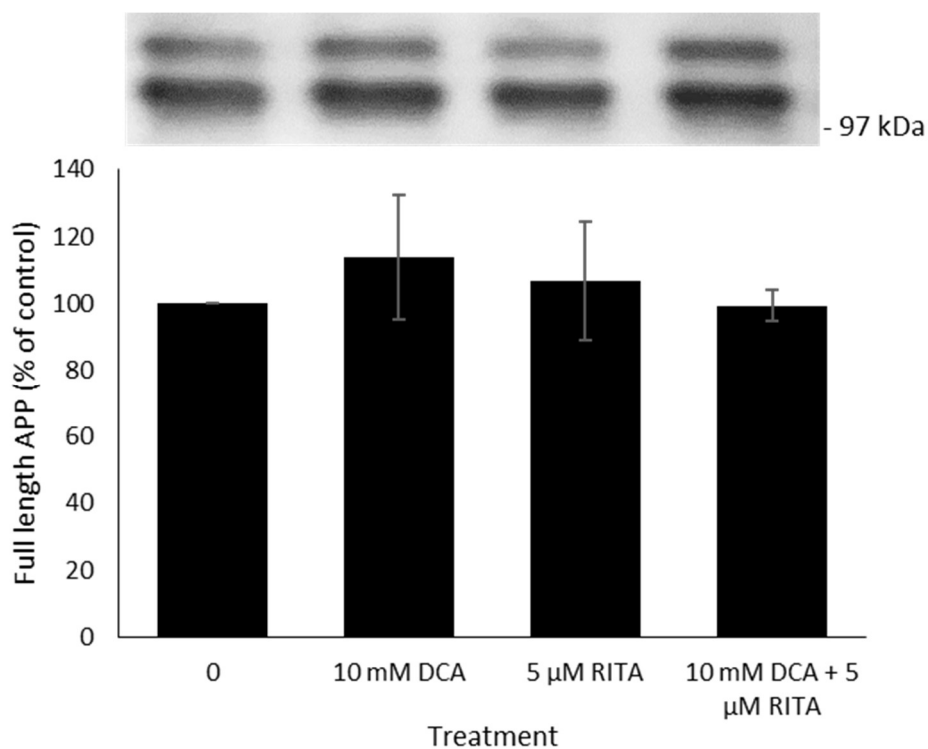


Figure 4.9. The effect of RITA and/or DCA treatment on full-length APP expression. SH-SY5Y cells were treated with DCA and/or RITA for 24 h. Cell lysates containing the same concentration of protein were then blotted with the anti-APP C-terminal antibody. Results are means \pm S.D. (n=3).

In order to see whether RITA might modify the effects of DCA on APP proteolysis, the conditioned medium from the same experiment was also immunoblotted with the anti-APP 6E10 and anti-sAPP β antibodies. However, the results (Fig. 4.10. and Fig. 4.11.) showed that whilst DCA, as previously observed, enhanced sAPP α and decreased sAPP β production, RITA did not modify these effects in any way.

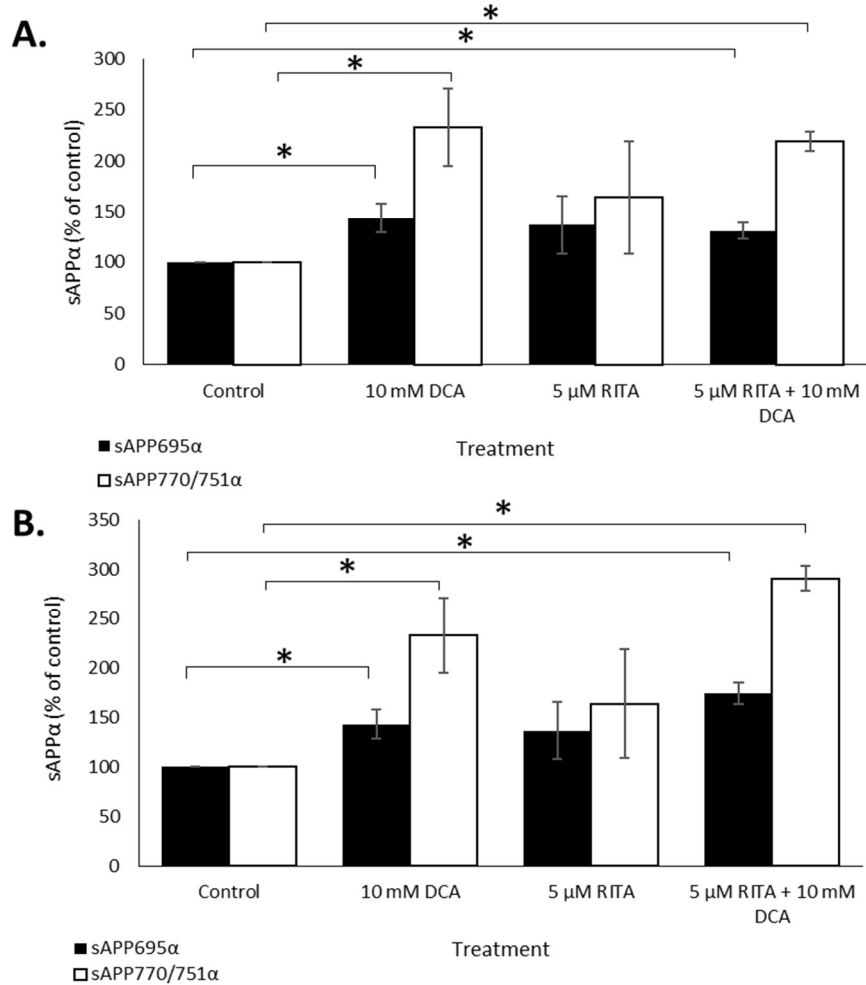
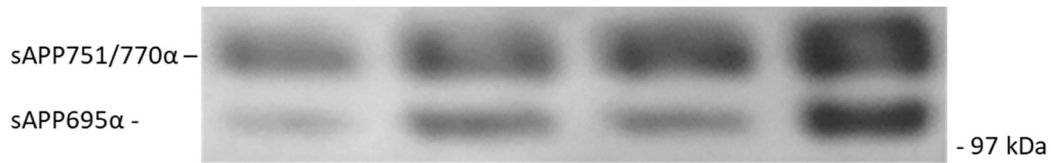


Figure 4.10. The effect of RITA and/or DCA treatment on the generation of sAPP α by SH-SY5Y cells. Cells were treated for 24 h with RITA and/or DCA. Equal volumes of concentrated conditioned medium were then blotted with the anti-sAPP α 6E10 antibody. **(A)** Standard results. **(B)** Viability corrected results. Results are means \pm S.D. (n=3). Significant results are indicated: * = significant at $p \leq 0.05$.

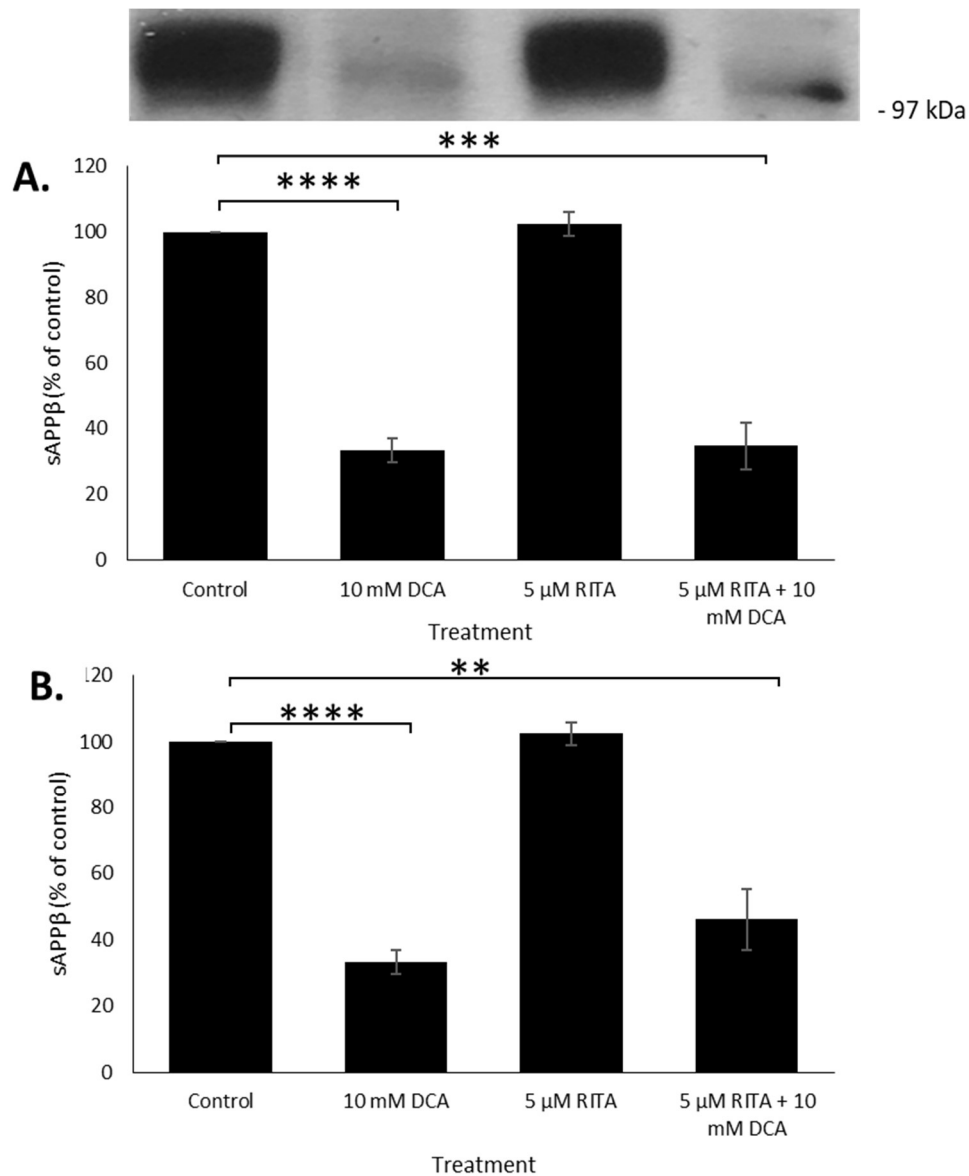


Figure 4.11. The effect of RITA and/or DCA treatment on the generation of sAPP β by SH-SY5Y cells. Cells were treated for 24 h with RITA and/or DCA. Equal volumes of concentrated conditioned medium were then blotted with the anti-sAPP β antibody. **(A)** Standard results. **(B)** Viability corrected results. Results are means \pm S.D. (n=3). Significant results are indicated: ** = significant at $p \leq 0.01$, *** = significant at $p \leq 0.005$, **** = significant at $p \leq 0.001$.

4.2. siRNA knockdown of p53.

Next, the effects of depleting p53 using siRNA on the DCA-mediated regulation of APP expression/proteolysis were examined.

4.2.1. Transfection optimisation.

Initially, suitable concentrations of transfection reagents and siRNA that gave sufficient p53 knockdown whilst not affecting cell viability were determined. SH-SY5Y cells were grown to 70 % confluence and the growth medium was then replaced with UltraMEM containing Dharmafect transfection reagent in the range 0-5 $\mu\text{l/ml}$ (final culture medium concentrations) before culturing the cells for a further 24 h. An MTS assay was then performed to evaluate the effect of the transfection reagent on cell viability (see Materials and Methods). The results (Fig. 4.12.) showed that Dharmafect concentrations of 2.5 and 5 $\mu\text{l/ml}$ resulted in significant cytotoxicity (32.20 ± 3.77 and 40.50 ± 4.69 % decreases in viability, respectively, relative to controls). As such, the highest non-toxic concentration of 1 $\mu\text{l/ml}$ was chosen for subsequent experiments.

Next, the concentration of siRNA required to give suitable p53 knockdown without appreciable decreases in viability was ascertained. Here, the final 1 $\mu\text{l/ml}$ Dharmafect concentration was employed in all samples but the final concentration of p53 siRNA was varied in the range 0-37.5 nM. As such, siRNA transfection was performed along with subsequent MTS analysis of cell viability and immunoblot analysis of p53 levels in cell lysates, according to the Materials and Methods section. The results (Fig. 4.13.) showed that none of the siRNA concentrations employed had a significant impact on cell viability.

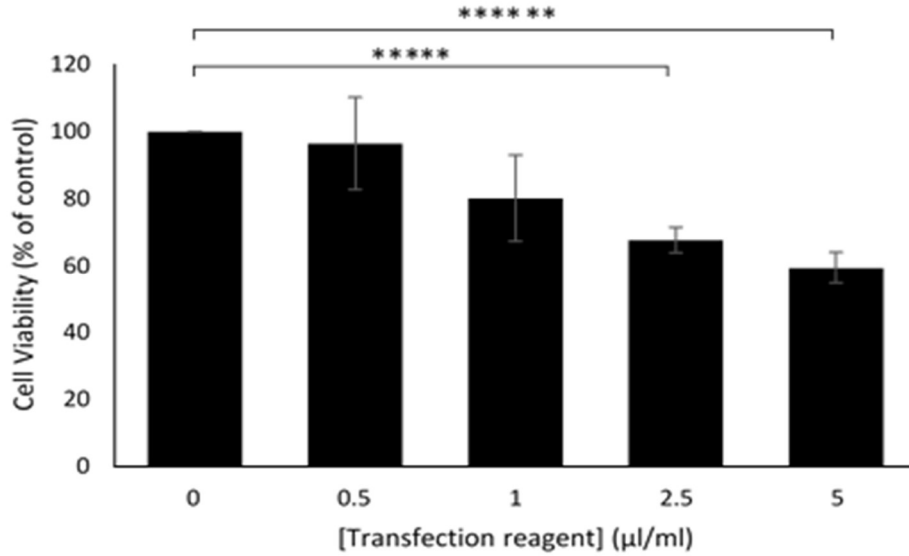


Figure 4.12. The effect of Dharmafect transfection reagent on the viability of SH-SY5Y cells. Cells were grown to 70% confluence before treating with Dharmafect transfection reagent at the concentrations indicated in growth medium lacking antibiotic for 24 h. An MTS viability assay was then performed *in situ*. Results are means \pm S.D. (n=3). Significant results are indicated: ***** = significant at $p \leq 0.0005$, ***** = significant at $p \leq 0.00001$.

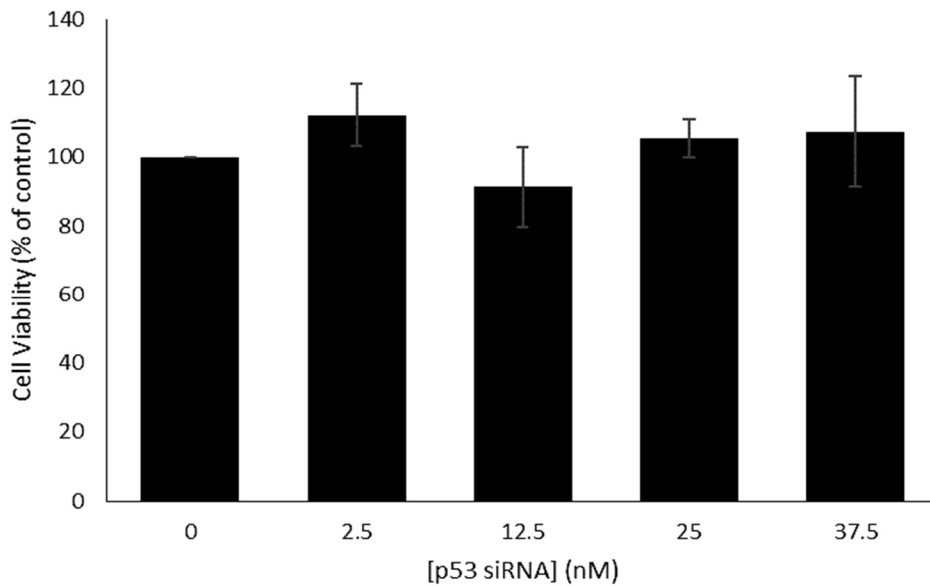


Figure 4.13. The effect of p53 siRNA transfection on the viability of SH-SY5Y cells. Cells were grown to 70 % confluence and transfected with the final siRNA concentrations indicated as described in the Materials and Methods section. An MTS assay was then performed *in situ*. Results are means \pm S.D. (n=3).

When p53 expression levels in cell lysates were analysed, the results (Fig. 4.14.) showed that the lowest siRNA concentration (2.5 nM) had no impact on p53 expression. However, 12.5, 25 and 37.5 nM concentrations reduced expression by 38.92 ± 14.05 , 45.29 ± 13.13 and 78.87 ± 3.64 %, respectively. Given that none of these siRNA concentrations caused significant toxicity, it was, therefore, decided that the highest (37.5 nM) concentration would be used for subsequent experiments.

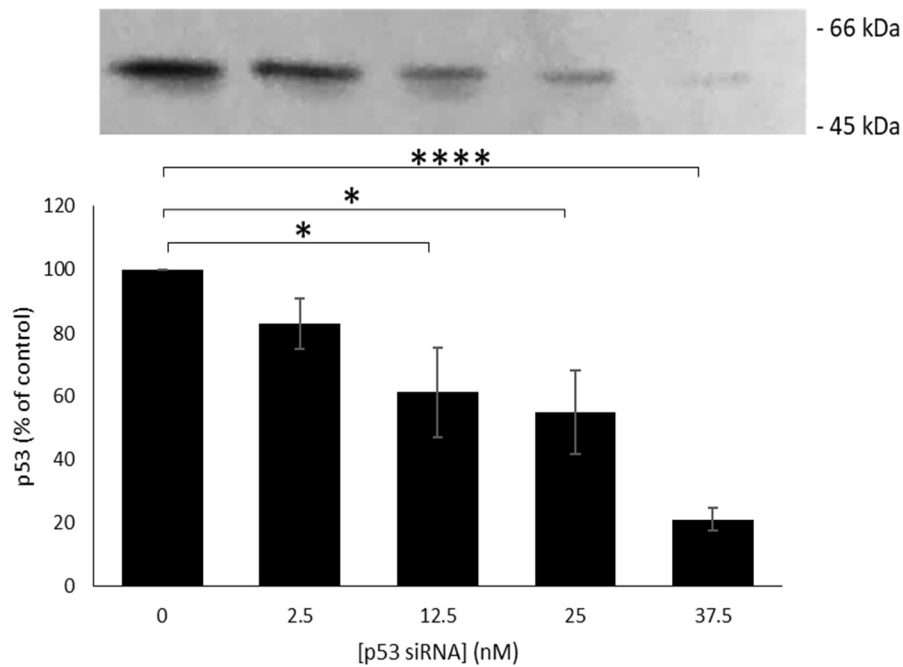


Figure 4.14. The effect of p53 siRNA concentrations on the expression of p53 in SH-SY5Y cells. Cells were grown to 70 % confluence and transfected with the final siRNA concentrations indicated as described in the Materials and Methods section. Equal amounts of cell lysate protein were then subjected to SDS-PAGE and immunoblotting using the anti-p53 antibody (see Materials and Methods). Results are means \pm S.D. (n=3). Significant results are indicated: * = significant at $p \leq 0.05$, **** = significant at $p \leq 0.001$.

4.2.2. The effect of p53 siRNA knockdown on DCA-mediated changes in APP expression/proteolysis.

Next, the effect of siRNA depletion of p53 on the ability of DCA to regulate APP expression/proteolysis was examined. To this end, SH-SY5Y cells were grown to 70 % confluence before transfection, using a final Dharmafect concentration of 1 μ l/ml and a final siRNA concentration of 37.5 nM. After a penultimate 48 h incubation in complete medium (containing antibiotics), the cells were further incubated for 24 h in UltraMEM in the absence or presence of 10 mM DCA. As might be expected from the previous experiments, none of these incubations resulted in significant decreases in cell viability (Fig. 4.15.).

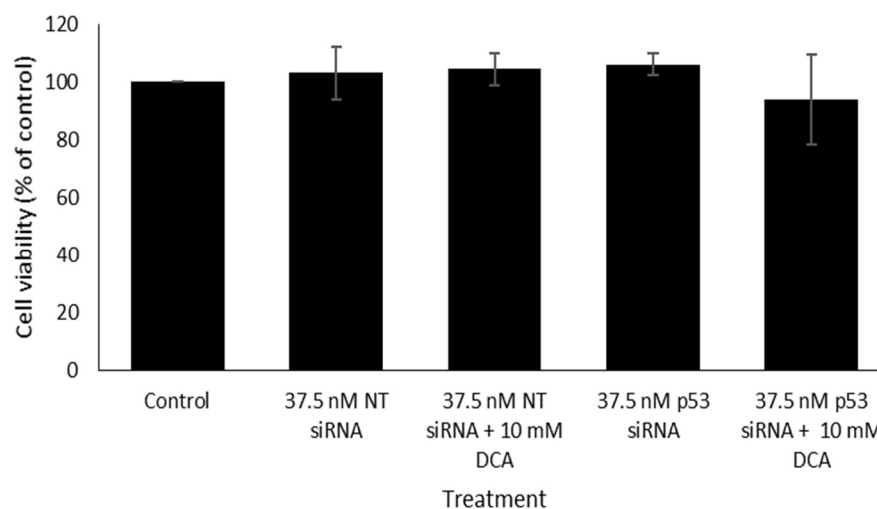


Figure 4.15. The effect of siRNA and DCA treatment on the viability of SH-SY5Y cells. Cells were grown to 70 % confluence and then transfected with either non-targeting (NT) or p53 siRNA as described in the Materials and Methods section. After a penultimate 48 h incubation in complete growth medium, the cells were incubated for a further 24 h in UltraMEM in the absence or presence of 10 mM DCA. An MTS assay was then performed *in situ*. Results are means \pm S.D. (n=3).

Cell lysates were then immunoblotted with the anti-p53 antibody and the results (Fig. 4.16.) showed that, as previously observed, DCA enhanced endogenous p53 expression (in the presence of non-targeting (NT) siRNA in this instance) (46.81 ± 17.58 % increase, relative to controls). Treatment with p53 siRNA virtually completely ablated expression of this protein in cells that were not treated with DCA but, interestingly, this did not prevent the ability of DCA to promote p53 expression to the same level as in the NT siRNA cells treated with the drug. This may well suggest that the ability of DCA to promote p53 expression lies at a post-translational level and perhaps in an ability to prevent degradation of the protein. Note that this experiment was repeated to further verify the result with p53 siRNA (see Appendix I).

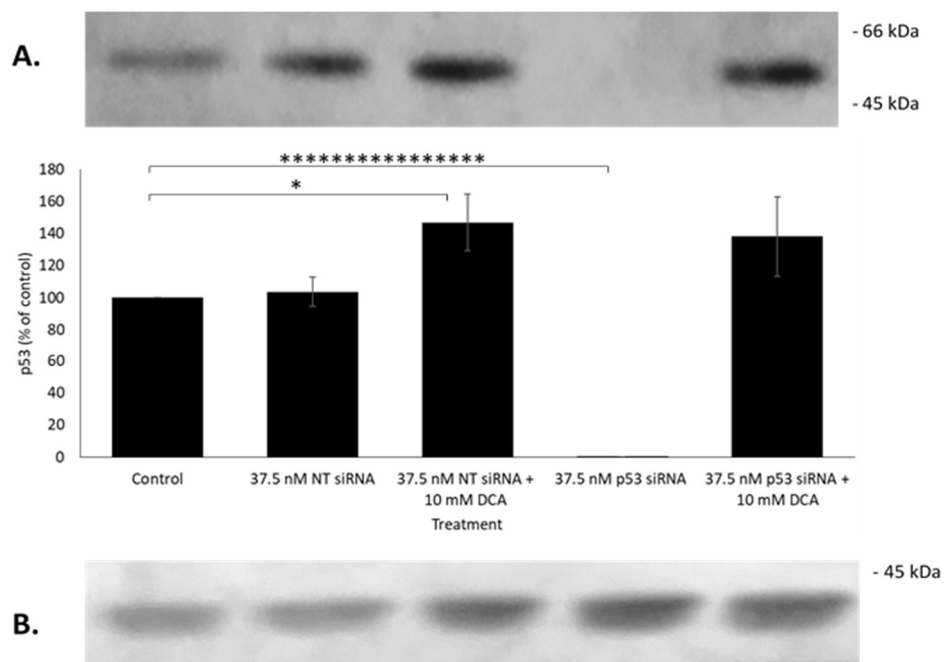


Figure 4.16. The effect of p53 knockout on DCA-mediated changes in p53 expression. SH-SY5Y cells were grown to 70 % confluence and then transfected with either non-targeting (NT) or p53 siRNA as described in the Materials and Methods section. After a penultimate 48 h incubation in complete growth medium, the cells were incubated for a further 24 h in UltraMEM in the absence or presence of 10 mM DCA. Equal amounts of cell lysate protein were then subjected to SDS-PAGE and immunoblotting using **(A)** anti-p53 and **(B)** anti-actin antibodies (see Materials and Methods). Results are means \pm S.D. (n=3). Significant results are indicated: * = significant at $p \leq 0.05$, ***** = significant at $p \leq 0.00000001$.

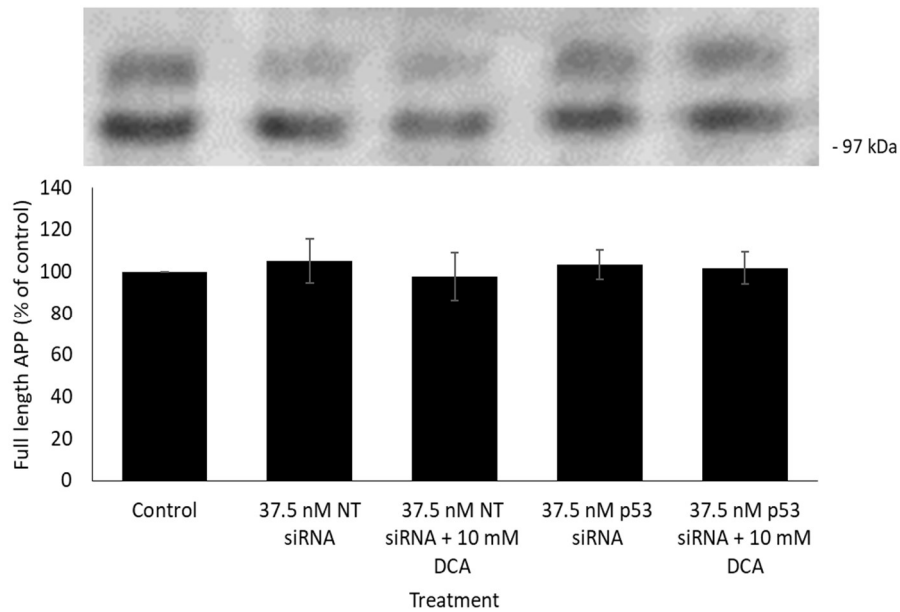


Figure 4.17. The effect of siRNA treatment on DCA-mediated changes in full-length APP expression. SH-SY5Y cells were grown to 70 % confluence and then transfected with either non-targeting (NT) or p53 siRNA as described in the Materials and Methods section. After a penultimate 48 h incubation in complete growth medium, the cells were incubated for a further 24 h in UltraMEM in the absence or presence of 10 mM DCA. Equal amounts of cell lysate protein were then subjected to SDS-PAGE and immunoblotting using the anti-APP C-terminal antibody (see Materials and Methods). Results are means \pm S.D. (n=3).

Next, the same cell lysates were immunoblotted with the anti-APP C-terminal antibody in order to determine how the combinations of siRNA and DCA treatments might impact on the expression of the protein. The results, however, showed no significant changes in APP expression (Fig. 4.17.).

The concentrated medium from the final 24 h DCA incubation was then immunoblotted with the anti-sAPP α 6E10 and anti-sAPP β antibodies to characterise any changes in the production of these fragments. However, the results (Fig. 4.18. and Fig. 4.19.), whilst corroborating previous observations in this study showing that DCA enhanced non-amyloidogenic whilst impairing amyloidogenic APP processing, did not reveal any impact of the siRNA treatments on the effects of DCA in these respects.

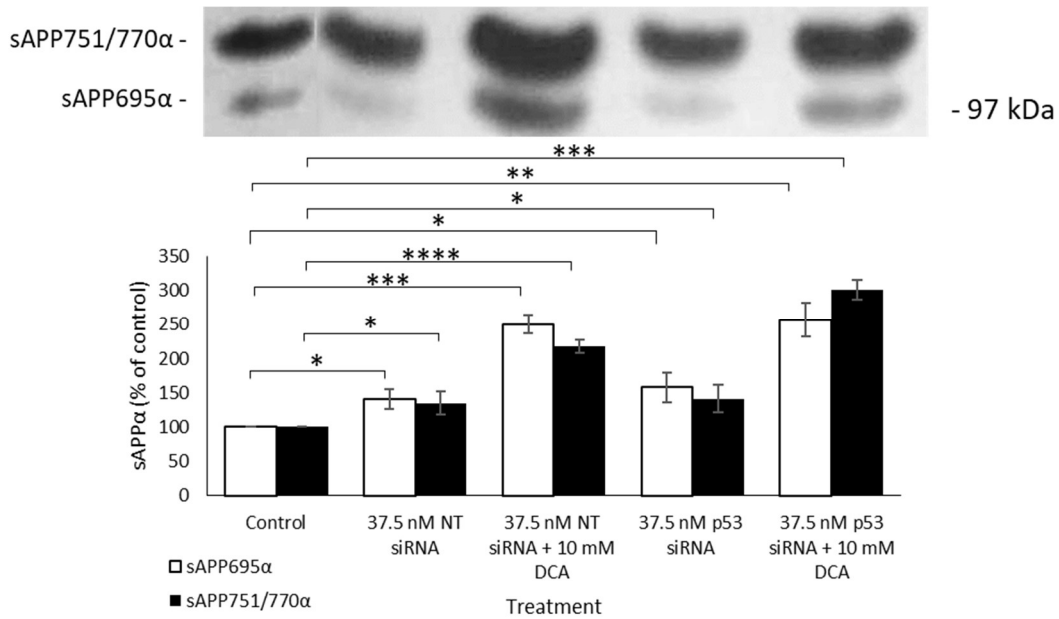


Figure 4.18. The effect of siRNA treatment on DCA-mediated changes in sAPP α production. SH-SY5Y cells were grown to 70 % confluence and then transfected with either non-targeting (NT) or p53 siRNA as described in the Materials and Methods section. After a penultimate 48 h incubation in complete growth medium, the cells were incubated for a further 24 h in UltraMEM in the absence or presence of 10 mM DCA. The conditioned medium from the final 24 h incubation was then concentrated, and equal volumes were subjected to SDS-PAGE and immunoblotting with anti-sAPP α 6E10 antibody as described in the Materials and Methods section. Results are means \pm S.D. (n=3). Significant results are indicated: * = significant at $p \leq 0.05$, ** = significant at $p \leq 0.01$, *** = significant at $p \leq 0.005$, **** = significant at $p \leq 0.001$.

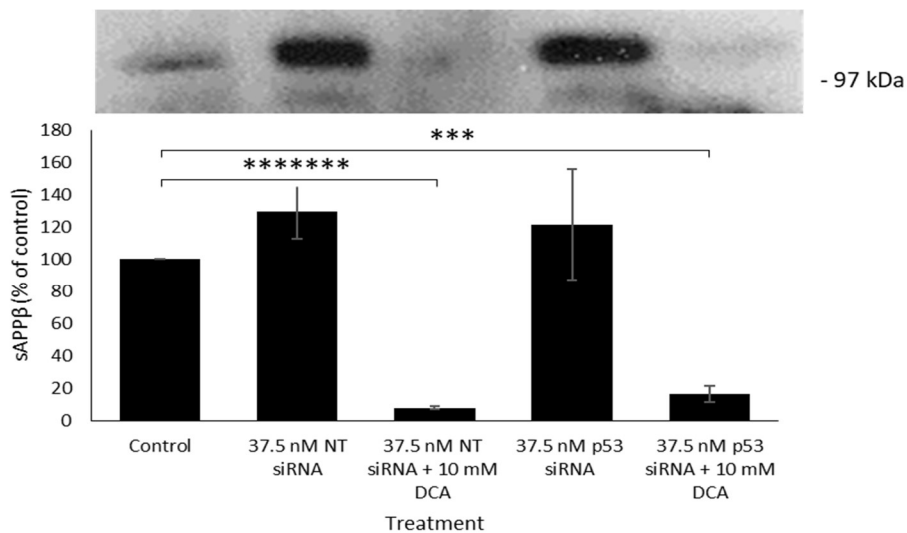


Figure 4.19. The effect of siRNA treatment on DCA-mediated changes in sAPP β production. SH-SY5Y cells were grown to 70 % confluence and then transfected with either non-targeting (NT) or p53 siRNA as described in the Materials and Methods section. After a penultimate 48 h incubation in complete growth medium, the cells were incubated for a further 24 h in UltraMEM in the absence or presence of 10 mM DCA. The conditioned medium from the final 24 h incubation was then concentrated, and equal volumes were subjected to SDS-PAGE and immunoblotting with anti-sAPP β antibody as described in the Materials and Methods section. Results are means \pm S.D. (n=3). Significant results are indicated: *** = significant at $p \leq 0.005$, **** = significant at $p \leq 0.0001$.

4.3. Summary.

The aim of these experiments was to determine whether DCA-mediated changes in p53 levels might be responsible for the corresponding changes seen in APP expression/proteolysis. Treatment of cells with RITA resulted in a synergistic cytotoxic effect with DCA and an additive effect on the expression of p53. However, RITA did not alter the ability of DCA to alter APP metabolism. Interestingly, when siRNA was employed to deplete p53 expression, whilst working very effectively in the absence of DCA treatment, p53 siRNA did not result in a decreased expression of the protein in DCA-treated cells. This would suggest that the ability of DCA to enhance p53 expression works via a post-translational mechanism. Rather unsurprisingly, given the fact p53 expression in DCA-treated cells was not impacted on by prior p53 siRNA treatment, these siRNA treatments did not modify the effects of DCA on APP expression/proteolysis either.

Chapter 5.

Altered pyruvate and lactic acid metabolism as factors in the DCA-mediated regulation of APP proteolysis.

5. Altered pyruvate and lactic acid metabolism as factors in the DCA-mediated regulation of APP proteolysis.

Previous studies have clearly demonstrated that DCA inhibits pyruvate dehydrogenase kinase, thereby impairing the phosphorylation and activation of PDH (Man *et al.*, 2000; Li *et al.*, 2009). The latter enzyme is responsible for the conversion of pyruvate to acetyl-CoA, thereby depleting the substrate for another enzyme, lactate dehydrogenase (LDH), which itself is responsible for the interconversion of pyruvate and lactate (Valvona *et al.*, 2016). Therefore, in the current study, it was hypothesised that changes in the levels of lactate and/or pyruvate in DCA-treated SH-SY5Y cells might, in turn, regulate APP expression/proteolysis. As such, the metabolism of the protein was investigated in cells treated with these compounds or with LDH inhibitors.

5.1. Lactate dehydrogenase inhibition.

As LDH-A is responsible for the conversion of pyruvate to lactate and LDH-B is largely responsible for the reciprocal reaction, inhibitors of both forms of the enzyme were investigated in terms of their ability to regulate APP expression/proteolysis. The first inhibitor used, GSK2837808A, inhibits both LDH-A and LDH-B with IC₅₀ values of 1.9 and 14 nM, respectively (Massey, 2017). The second inhibitor used, FX11, has a K_i of 8 μM for LDH-A but does not affect LDH-B even at higher concentrations (Le *et al.*, 2010).

5.1.1. GSK2837808A (LDH-A and LDH-B inhibitor).

Initially, the effect of this compound on the viability of SH-SY5Y cells was determined. Cells were grown to confluence and treated for 24 h with UltraMEM containing 0, 2, 5, 10, 15, or 25 nM concentrations of the inhibitor before analysing cell viability using the MTS assay, as described in the Materials and Methods section. The results (Fig. 5.1.) showed no significant effect on viability at any concentration.

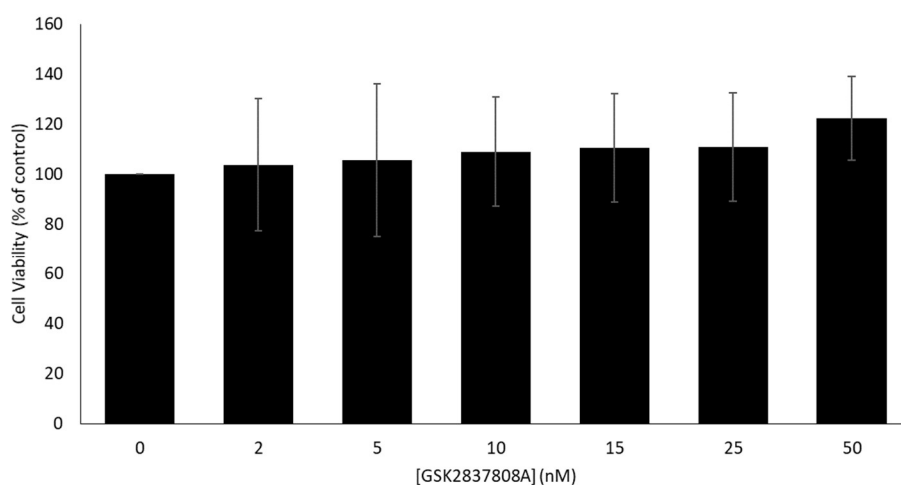


Figure 5.1. The effect of GSK2837808A (LDH-A and LDH-B inhibitor) on SH-SY5Y cell viability. Cells were grown to confluence and treated with the indicated inhibitor concentrations in UltraMEM for 24 h. Cell viability was then determined using the MTS assay, as described in the Materials and Methods section. Results are means \pm S.D. (n=6).

Given that DCA also altered p53 levels (see preceding results chapters), the effect of GSK2837808A on the level of this protein was also monitored in the current experiments. As such, lysates were prepared from inhibitor-treated cells and subjected to immunoblot analysis using the anti-p53 antibody. However, the results (Fig. 5.2.) showed no effect of GSK2837808A on the levels of this protein.

Next, the effects of GSK2837808A on APP expression and proteolysis were investigated. The lysates from the previous experiment were initially immunoblotted with the anti-APP C-terminal antibody and the results, as with p53, showed no significant change in APP expression (Fig. 5.3.).

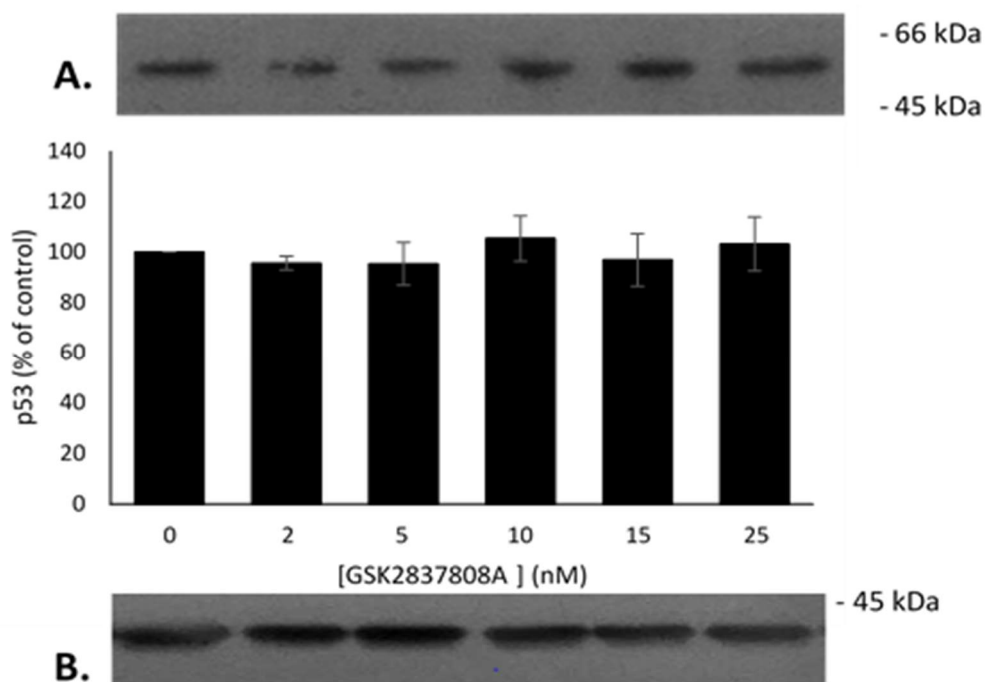


Figure 5.2. The effect of GSK2837808A (LDH-A and LDH-B inhibitor) on p53 levels. SH-SY5Y cells were grown to confluence and treated with the indicated inhibitor concentrations in UltraMEM for 24 h. Cell lysates were prepared, and equal amounts of protein were subjected to SDS-PAGE and immunoblotting using the (A) anti-p53 and (B) anti-actin antibodies, as described in the Materials and Methods section. Results are means \pm S.D. (n=6).

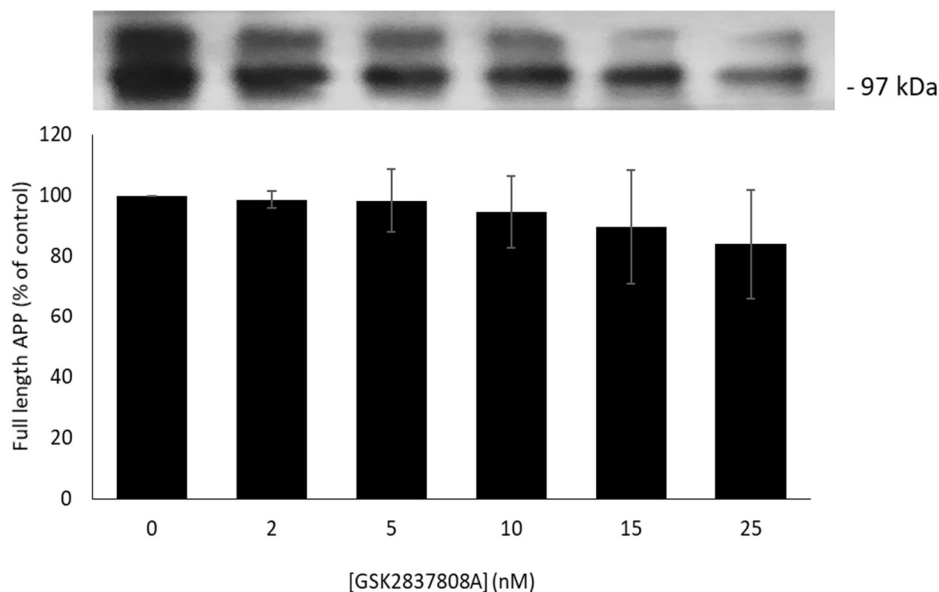


Figure 5.3. The effect of GSK2837808A (LDH-A and LDH-B inhibitor) on APP expression. SH-SY5Y cells were grown to confluence and treated with the indicated inhibitor concentrations in UltraMEM for 24 h. Cell lysates were prepared, and equal amounts of protein were subjected to SDS-PAGE and immunoblotting using the anti-APP C-terminal antibody, as described in the Materials and Methods section. Results are means \pm S.D. (n=6).

The effects of GSK2837808A on the generation of sAPP α and sAPP β were also monitored by immunoblotting equal volumes of concentrated conditioned medium with antibodies against these protein fragments. Results using the anti-APP 6E10 antibody (Fig. 5.4.) revealed a significant decrease in both sAPP695 α and sAPP751/770 α production by cells treated with 25 nM GSK2837808A (19.42 ± 6.05 and 30.22 ± 7.55 % decreases relative to controls, respectively). However, no significant differences were observed in the production of either fragment in cells treated with all other concentrations of GSK2836808A.

Next, the same medium samples were immunoblotted with the anti-sAPP β antibody. The results (Fig. 5.5.) showed a significant increase in sAPP β production in cells treated with GSK2837808A at concentrations of 10, 15 and 25 nM (335.46 ± 68.77 , 416.80 ± 92.83 and

400.53 ± 109.67 % increases, respectively). However, cells treated with 2 and 5 nM GSK2837808A saw no significant difference in sAPP β production.

In summary, GSK2837808A appears to reduce sAPP α (at the highest concentration) and enhance sAPP β production, the exact opposite of previous observations in DCA-treated cells. What this data does show, however, is that the inhibition of LDH does have the potential to alter both amyloidogenic and non-amyloidogenic APP processing, as was the case for DCA.

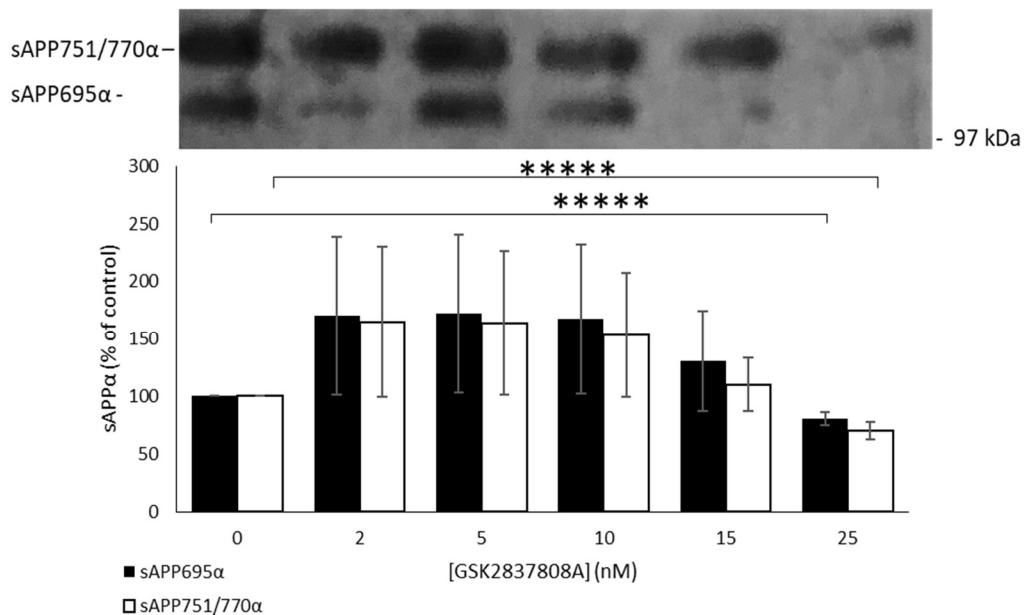


Figure 5.4. The effect of GSK2837808A (LDH-A and LDH-B inhibitor) on the production of sAPP α by SH-SY5Y cells. Cells were grown to confluence and then treated with the indicated inhibitor concentrations in UltraMEM for 24 h. Conditioned medium was then processed and subjected to SDS-PAGE and immunoblotting using the anti-sAPP α 6E10 antibody, as described in the Materials and Methods section. Results are means ± S.D. (n=6). Significant results are indicated: **** = significant at $p \leq 0.0005$.

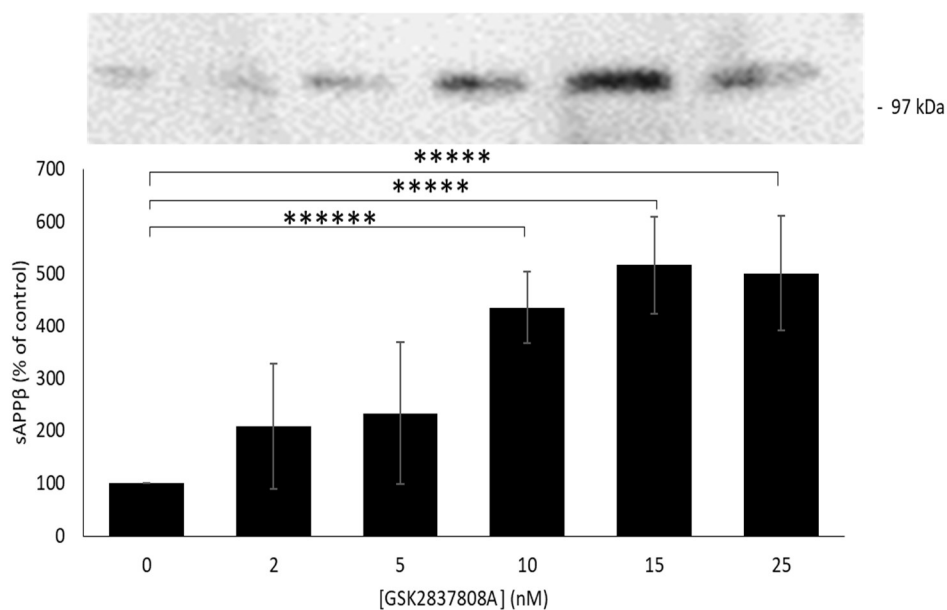


Figure 5.5. The effect of GSK2837808A (LDH-A and LDH-B inhibitor) on the production of sAPP β by SH-SY5Y cells. Cells were grown to confluence and then treated with the indicated inhibitor concentrations in UltraMEM for 24 h. Conditioned medium was then processed and subjected to SDS-PAGE and immunoblotting using the anti-sAPP β antibody, as described in the Materials and Methods section. Results are means \pm S.D. (n=6). Significant results are indicated: **** = significant at $p \leq 0.0005$, ***** = significant at $p \leq 0.0001$.

5.1.2. FX11 (LDH-A inhibitor).

The experiments in the preceding sections were repeated using FX11, which is a specific LDH-A inhibitor (K_i of 8 μ M). Again, cells were grown to confluence and treated for 24 h with inhibitor before analysing cell viability using the MTS assay (Fig. 5.6.). Unlike GSK2837808A, cultures treated with FX11 exhibited significantly decreased viability at inhibitor concentrations of 10, 50 and 100 μ M (27.08 ± 15.27 , 54.01 ± 11.50 , 93.92 ± 7.45 % decreases, respectively, relative to controls).

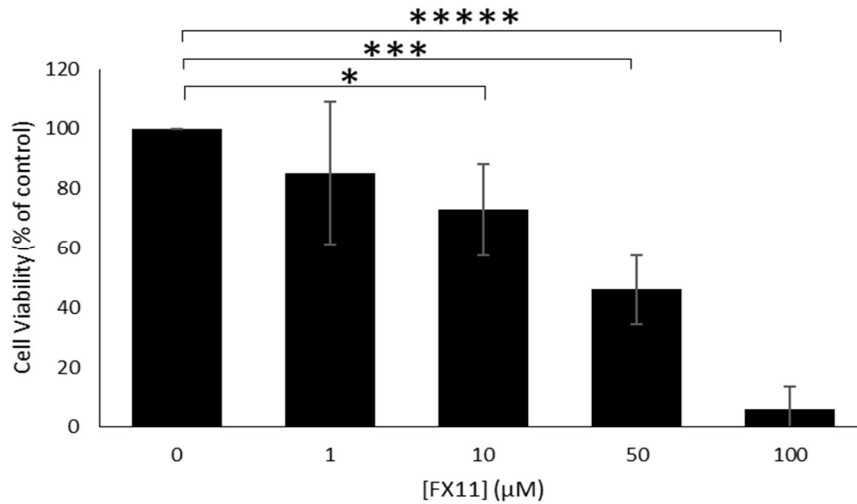


Figure 5.6. The effect of FX11 (LDH-A specific inhibitor) on SH-SY5Y cell viability. Cells were grown to confluence and then treated with the indicated inhibitor concentrations in UltraMEM for 24 h. Cell viability was then determined using the MTS assay as described in the Materials and Methods section. Results are means \pm S.D. (n=3). Significant results are indicated: * = significant at $p \leq 0.05$, *** = significant at $p \leq 0.005$, **** = significant at $p \leq 0.0005$.

Next, the effects of FX11 on p53 levels in cell lysates was analysed. Note that only inhibitor concentrations of 1 and 10 μM were investigated in this respect due to the dramatic decreases in cell viability observed previously at higher inhibitor concentrations. The results (Fig. 5.7.) revealed a significant increase in p53 levels in cells treated with 10 μM FX11 (172.40 ± 40.80 % increase, relative to controls), perhaps reflective of significant cell death occurring at this higher inhibitor concentration.

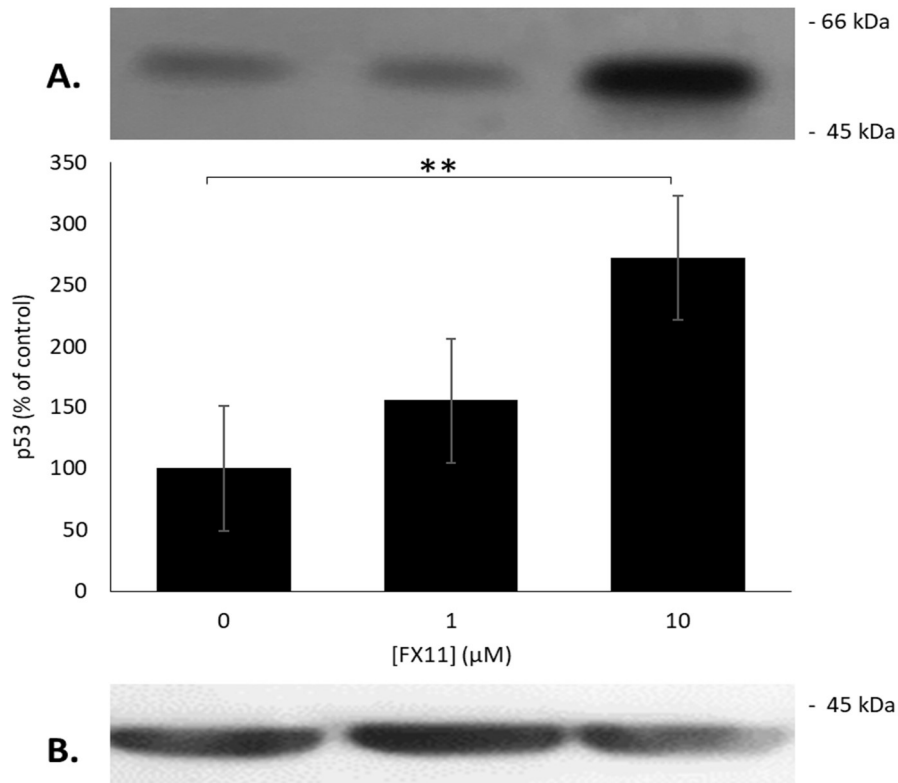


Figure 5.7. The effect of FX11 (LDH-A inhibitor) on p53 levels. SH-SY5Y cells were grown to confluence and then treated with the indicated inhibitor concentrations in UltraMEM for 24 h. Cell lysates were prepared, and equal amounts of protein were subjected to SDS-PAGE and immunoblotting using the **(A)** anti-p53 and **(B)** anti-actin antibodies as described in the Materials and Methods section. Results are means \pm S.D. (n=3). Significant results are indicated: ** = significant at $p \leq 0.01$.

Lysates from the same experiments were also immunoblotted with the anti-APP C-terminal antibody and the results (Fig. 5.8.) showed no effect of 1 and 10 μM FX11 on full-length APP expression.

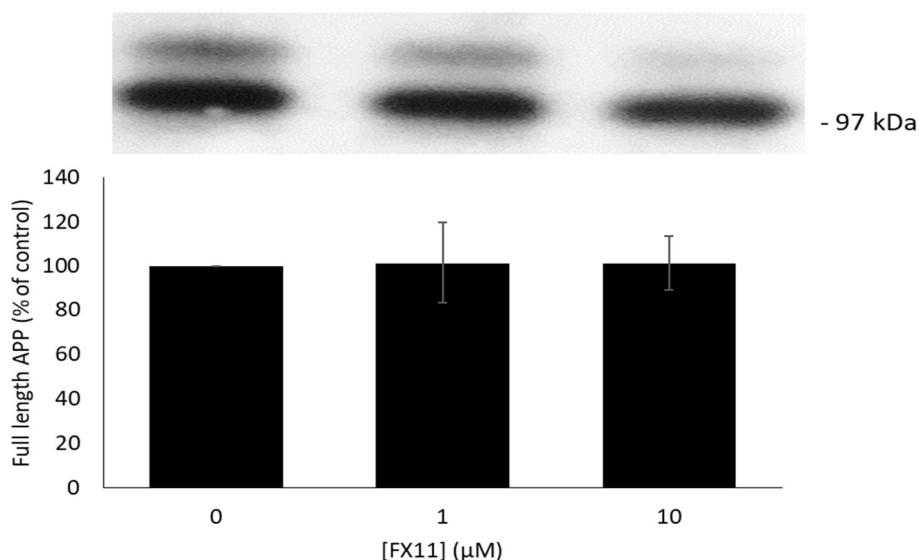


Figure 5.8. The effect of FX11 (LDH-A inhibitor) on APP expression. SH-SY5Y cells were grown to confluence and then treated with the indicated inhibitor concentrations in UltraMEM for 24 h. Cell lysates were prepared, and equal amounts of protein were subjected to SDS-PAGE and immunoblotting using the anti-APP C-terminal antibody as described in the Materials and Methods section. Results are means \pm S.D. (n=3).

The effects of the inhibitor on APP proteolysis were also investigated by immunoblotting concentrated conditioned medium from these experiments with anti-APP 6E10 and anti-sAPP β antibodies. Again, it is worth noting that only the results using the lower 1 and 10 μ M FX11 concentrations are shown due to high levels of toxicity at the higher inhibitor concentrations. The results (Fig. 5.9A.) showed that cells treated with 1 μ M FX11 generated significantly more sAPP751/770 α (28.03 ± 11.00 % increase, relative to controls) and this difference even remained significant when the results were adjusted to account for changes in cell viability (Fig. 5.9B.). Contrastingly, cells treated with 10 μ M FX11 exhibited decreases in both sAPP695 α and sAPP751/770 α production (Fig. 5.9A.) (24.34 ± 7.18 , and 65.76 ± 12.27 % decreases, respectively). However, only the difference in sAPP751/770 α remained significant at this concentration once the results were adjusted for cell viability (Fig. 5.9B.). The corresponding results for sAPP β showed no significant changes in the production of this fragment when the cells were treated with either 1 or 10 μ M FX11 (Fig. 5.10.).

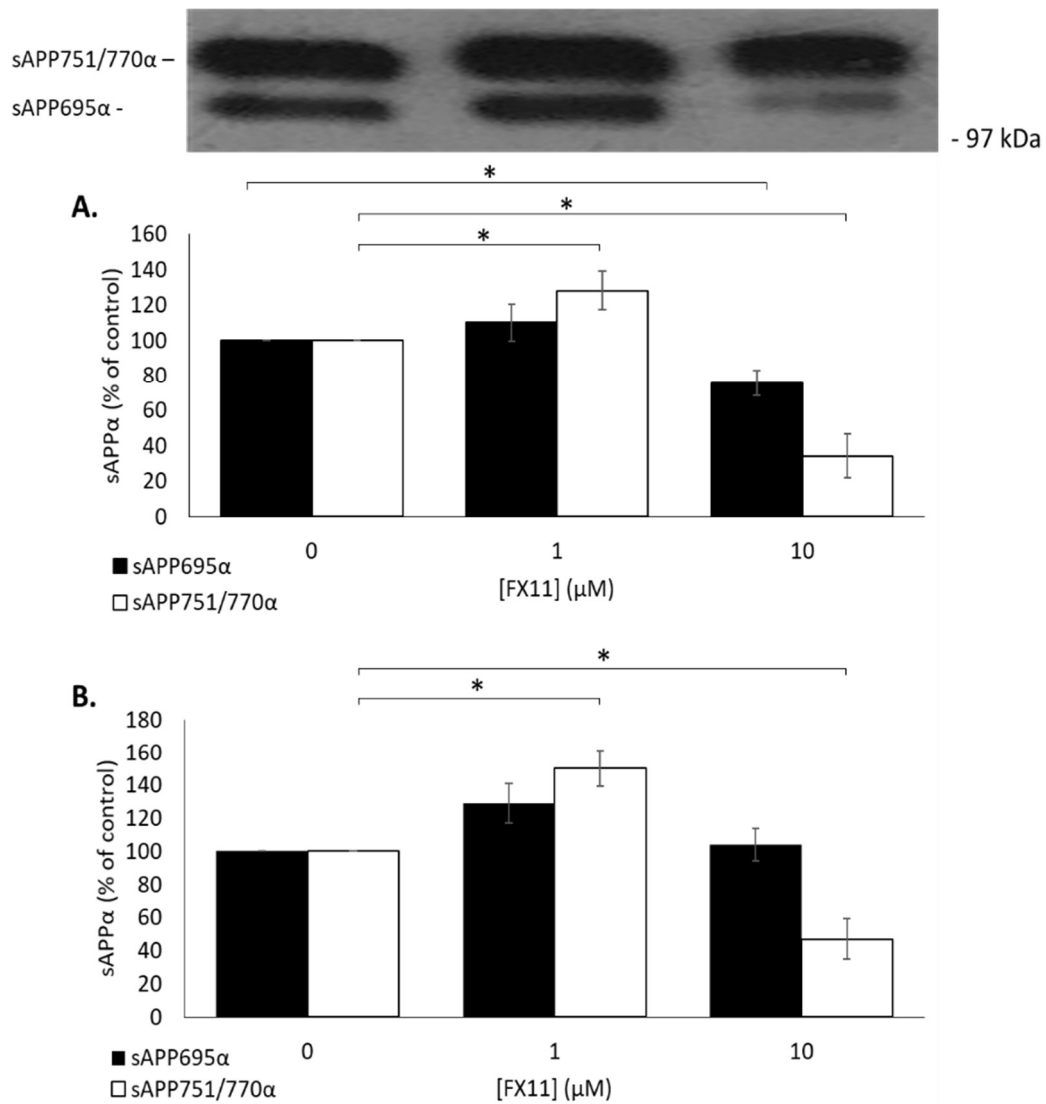


Figure 5.9. The effect of FX11 (LDH-A inhibitor) on the production of sAPPα by SH-SY5Y cells. Cells were grown to confluence and then treated with the indicated inhibitor concentrations in UltraMEM for 24 h. Equal volumes of concentrated medium were then immunoblotted with anti-sAPPα 6E10 antibody. Results are means ± S.D. (n=3). **(A)** Standard results and **(B)** viability corrected results. Significant results are indicated: * = significant at $p \leq 0.05$.

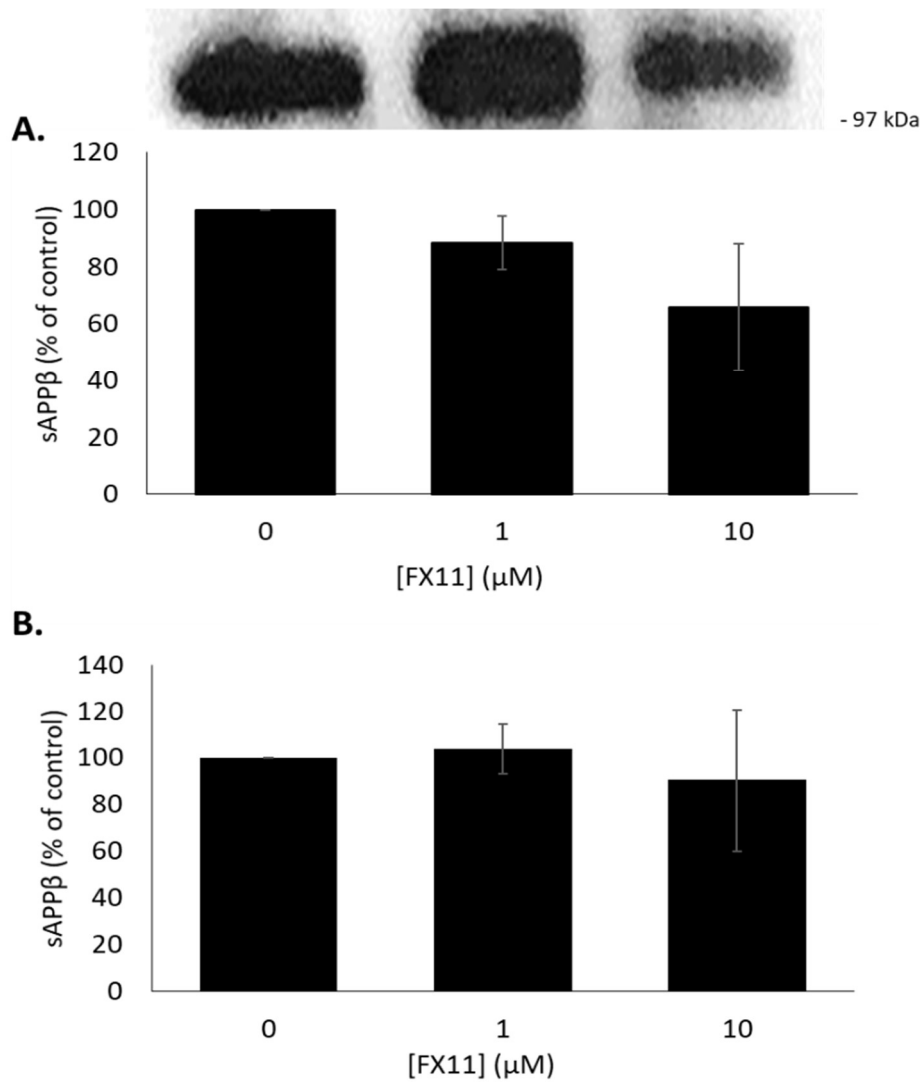


Figure 5.10. The effect of FX11 (LDH-A inhibitor) on the production of sAPPβ by SH-SY5Y cells. Cells were grown to confluence and then treated with the indicated inhibitor concentrations in UltraMEM for 24 h. Equal volumes of concentrated medium were then immunoblotted with anti-sAPPβ antibody. Results are means ± S.D. (n=3). **A)** Standard results and **(B)** viability corrected results.

5.2. Pyruvate and lactic acid supplementation.

Previous studies have shown that DCA activates PDH, leading to a greater conversion of pyruvate to acetyl-coA and a possible decrease in the cellular pool of the former compound (Mann *et al.*, 2000; Li *et al.*, 2009). The lack of pyruvate has also been shown to result in the depletion of cellular lactic acid levels (Stacpoole *et al.*, 2003). Furthermore, Xiang *et al.* (2010) showed that lactic acid treatment decreased non-amyloidogenic APP processing in SH-SY5Y cells. Consequently, in the current study, it was hypothesised that changes in the levels of these metabolites might be responsible for the observed effects of DCA on APP expression/proteolysis. As such, SH-SY5Y cells were supplemented with these compounds and APP metabolism was subsequently monitored.

5.2.1. Pyruvate.

Cells were grown to confluence and treated for 24 h with UltraMEM containing pyruvate in the concentration range 1-100 mM. Note that the basal pyruvate concentration in UltraMEM is 1 mM; as such this concentration was used as the control in this set of experiments. Following the pyruvate treatment, cell viability was monitored using the MTS assay as described in the Materials and Methods section. The results (Fig. 5.11.) showed that there was a significant increase in viability when the cells were treated with 10 mM pyruvate (23.27 ± 7.11 % increase, relative to controls). However, cells treated with 50 and 100 mM pyruvate exhibited decreased viability (35.08 ± 3.61 and 68.59 ± 7.72 % decreases, respectively, relative to controls).

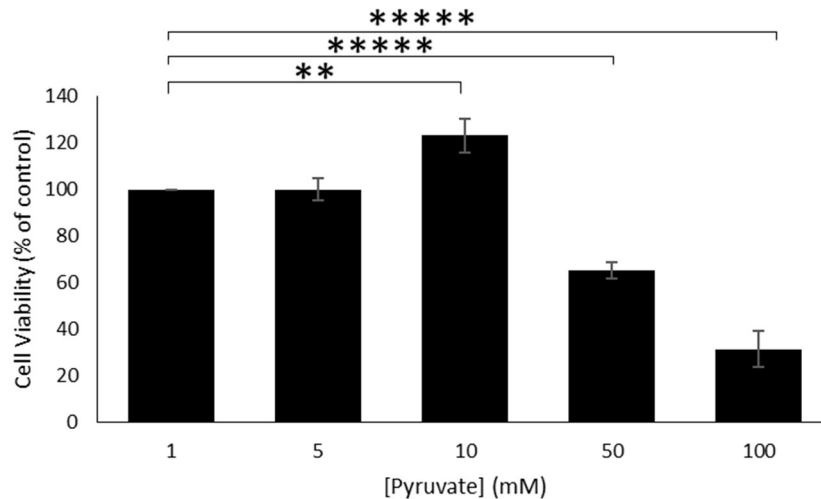


Figure 5.11. The effect of pyruvate on SH-SY5Y cell viability. Cells were grown to confluence and then treated with the indicated pyruvate concentrations in UltraMEM for 24 h. Cell viability was then determined using the MTS assay as described in the Materials and Methods section. Results are means \pm S.D. (n=3). Significant results are indicated: ** = significant at $p \leq 0.01$, **** = significant at $p \leq 0.0005$.

Next, the effect of pyruvate concentration on the p53 levels in cell lysates was evaluated by immunoblotting. The results (Fig. 5.12.) demonstrated unaltered levels of the protein at the lower pyruvate concentrations but levels did increase significantly at 50 and 100 mM concentrations (100.64 ± 37.86 and 93.44 ± 21.10 % increases, respectively, relative to controls). Note that this latter observation might well have been linked to the large decreases in cell viability observed at higher pyruvate concentrations (Fig. 5.11.).

The expression of APP was also quantified in lysates from cells treated with pyruvate. However, the results (Fig. 5.13.) showed no significant changes in the expression of this protein following pyruvate treatment.

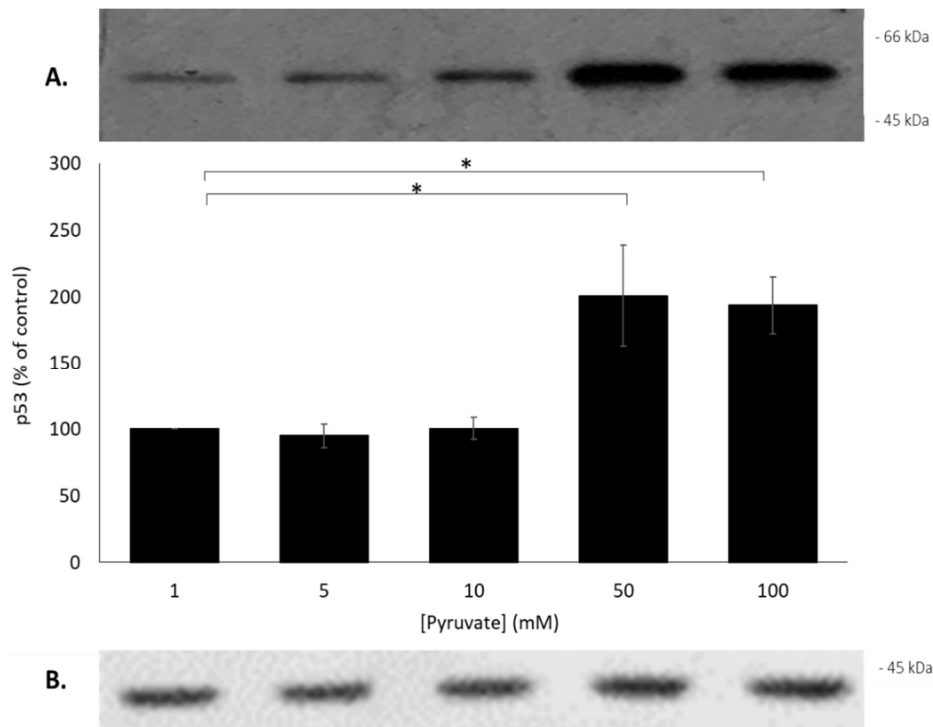


Figure 5.12. The effect of pyruvate on p53 levels. SH-SY5Y cells were grown to confluence and then treated with the indicated pyruvate concentrations in UltraMEM for 24 h. Cell lysates were prepared, and equal amounts of protein were subjected to SDS-PAGE and immunoblotting using the (A) anti-p53 and (B) anti-actin antibodies as described in the Materials and Methods section. Results are means \pm S.D. (n=3). Significant results are indicated: * = significant at $p \leq 0.05$.

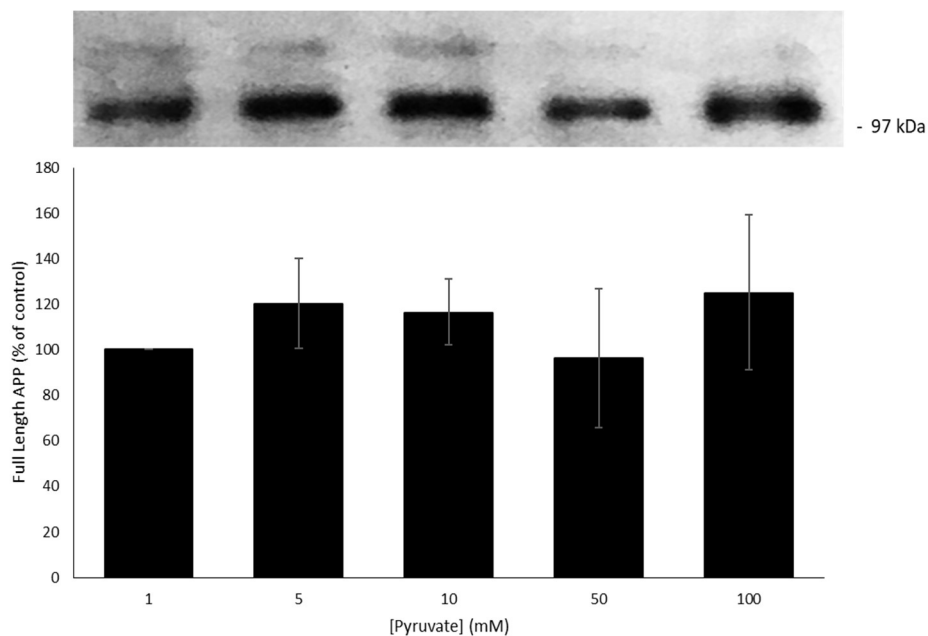


Figure 5.13. The effect of pyruvate on APP expression. SH-SY5Y cells were grown to confluence and then treated with the indicated pyruvate concentrations in UltraMEM for 24 h. Cell lysates were prepared, and equal amounts of protein were subjected to SDS-PAGE and immunoblotting using the anti-APP C-terminal antibody as described in the Materials and Methods section. Results are means \pm S.D. (n=3).

Next, the effects of pyruvate concentration on the levels of sAPP α and sAPP β generated by SH-SY5Y cells were investigated. Note that, given the high levels of toxicity at 50 and 100 mM pyruvate, these latter results are only shown for 1, 5 and 10 mM pyruvate-treated cells. Concentrated conditioned medium was initially immunoblotted with anti-APP 6E10 antibody and the results (Fig. 5.14A.) showed that sAPP α levels remained unchanged at pyruvate treatment concentrations of 5 mM (relative to 1mM controls). However, there was a significant decrease in the production of sAPP751/770 α (but not sAPP695 α) when cells were treated with 10 mM pyruvate and values were adjusted in order to take into account cell viability (55.17 ± 20.85 % reduction, relative to controls) (Fig. 5.14B.). Interestingly, when the same medium samples were immunoblotted in order to detect sAPP β , a corresponding increase in sAPP β levels was observed (Fig. 5.15A.) although significance was lost when the samples were adjusted for cell viability (Fig. 5.15B).

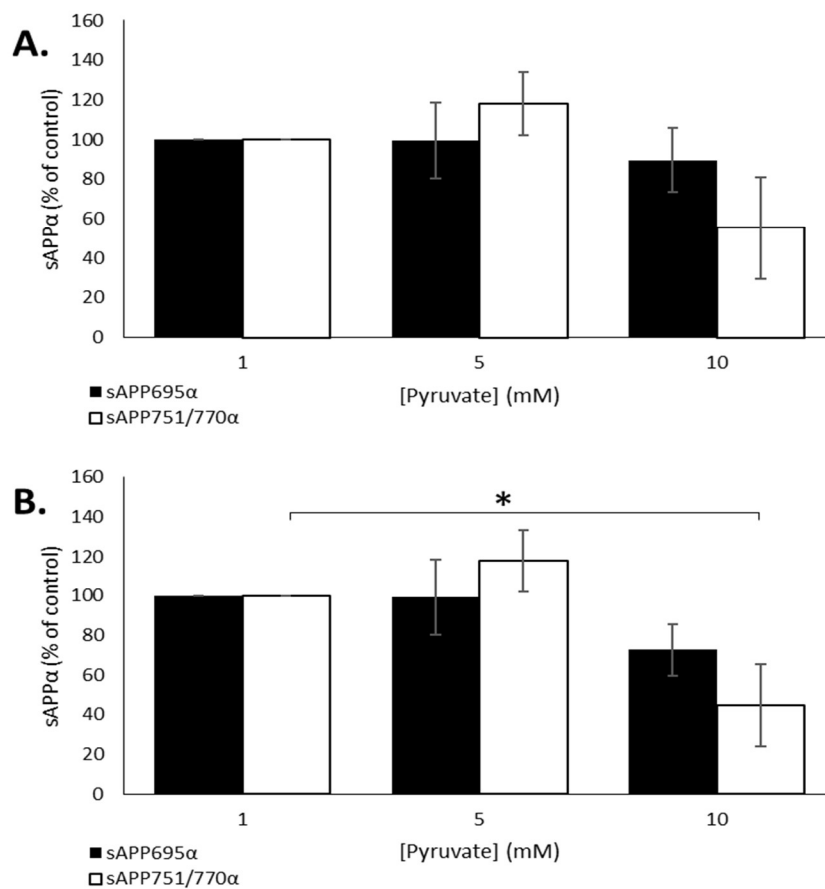
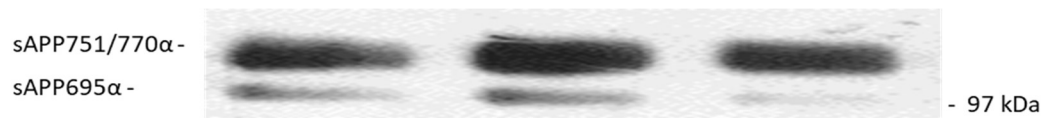


Figure 5.14. The effect of pyruvate on the production of sAPP α by SH-SY5Y cells. Cells were grown to confluence and then treated with the indicated pyruvate concentrations in UltraMEM for 24 h. Equal volumes of concentrated medium were then immunoblotted with anti-sAPP α 6E10 antibody. Results are means \pm S.D. (n=3). **(A)** Standard results and **(B)** viability corrected results. Significant results are indicated: * = significant at $p \leq 0.05$.

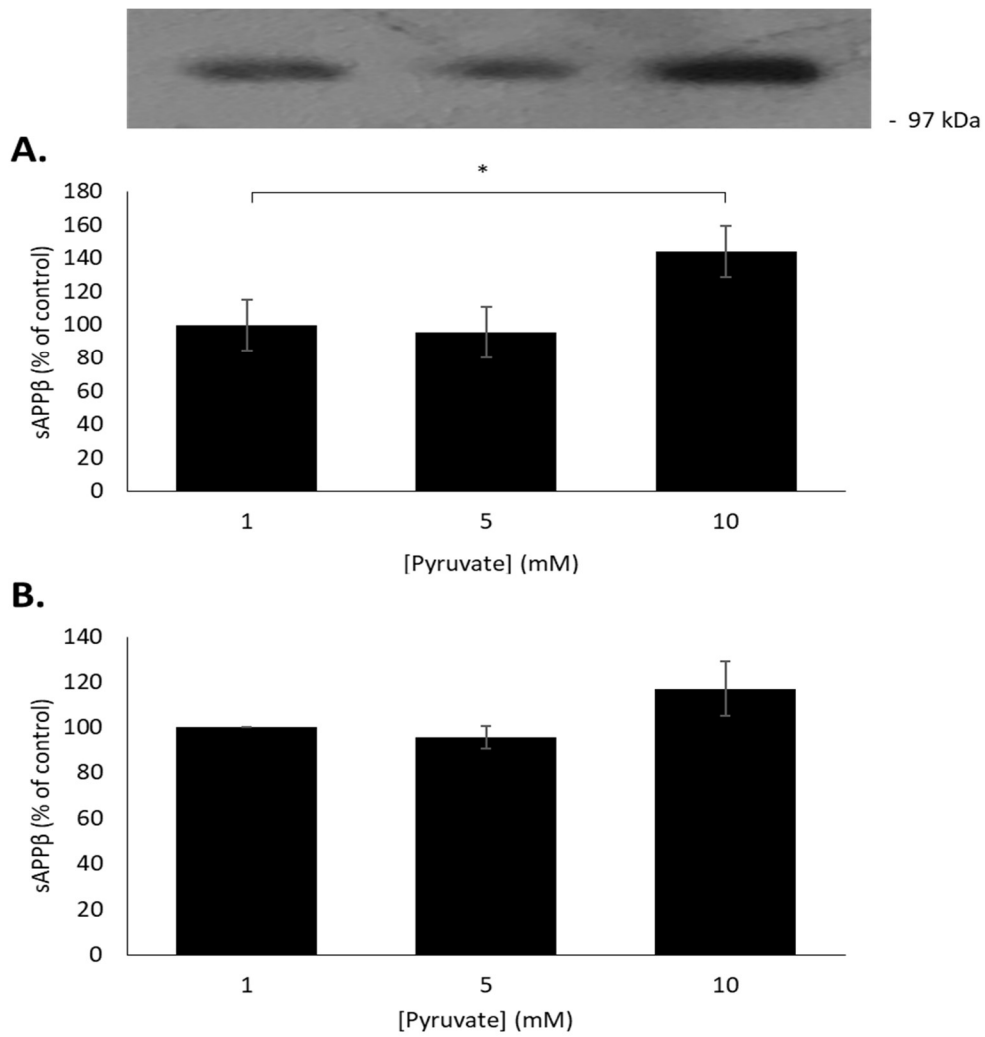


Figure 5.15. The effect of pyruvate on the production of sAPP β by SH-SY5Y cells. Cells were grown to confluence and then treated with the indicated pyruvate concentrations in UltraMEM for 24 h. Equal volumes of concentrated medium were then immunoblotted with anti-sAPP β antibody. Results are means \pm S.D. (n=3). **(A)** Standard results and **(B)** viability corrected results. Significant results are indicated: * = significant at $p \leq 0.05$.

5.2.2. Lactic acid.

Here, the ability of lactic acid (either singularly or in combination with DCA) to alter APP expression/proteolysis was investigated. Lactic acid concentrations of 6 and 12 mM were chosen based on a previous study by Xiang *et al.* (2010) where the authors demonstrated an increase in non-amyloidogenic APP processing at these concentrations. In the current study, SH-SY5Y cells were grown to confluence and treated for 24 h with either DCA (10 mM) or lactic acid (6 mM or 12 mM) or combinations of the two compounds. Cell viability was then analysed using the MTS assay as described in the Materials and Methods section. The results (Fig. 5.16.) demonstrated that, as previously observed, DCA alone (10 mM) did not result in any decrease in cell viability. However, when the drug was used in combination with 6 mM lactic acid there was a 9.57 ± 3.39 % decrease in cell viability relative to controls. Similarly, there were also small but significant decreases in viability when the cells were treated with either 12 mM lactic acid alone or in combination with DCA (11.92 ± 0.79 and 13.93 ± 1.19 % reductions, respectively, relative to controls).

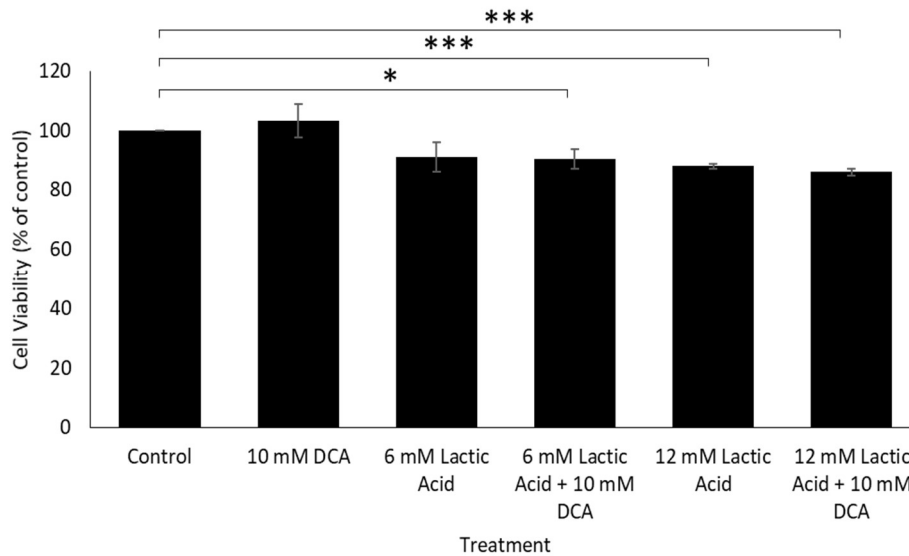


Figure 5.16. The effect of DCA and lactic acid on SH-SY5Y cell viability. Cells were grown to confluence and then treated with the indicated DCA and lactic acid concentrations in UltraMEM for 24 h. Cell viability was then determined using the MTS assay as described in the Materials and Methods section. Results are means \pm S.D. (n=3). Significant results are indicated: * = significant at $p \leq 0.05$, *** = significant at $p \leq 0.005$.

Next, the effect of lactic acid/DCA treatments on p53 in cell lysates was examined by immunoblotting (Fig. 5.17.). As previously observed, DCA caused an increase in p53 levels when used on its own (123.65 ± 20.87 % increase relative to controls). Perhaps more interestingly, lactic acid, when used on its own at 6 and 12 mM, also enhanced p53 levels (143.82 ± 42.38 and 109.53 ± 14.84 % increases, respectively, relative to controls). Notably these increases were not additive in the presence of DCA where lactic acid (at 6 and 12 mM) increased p53 levels by 146.32 ± 37.13 and 121.95 ± 26.46 %, respectively, relative to controls.

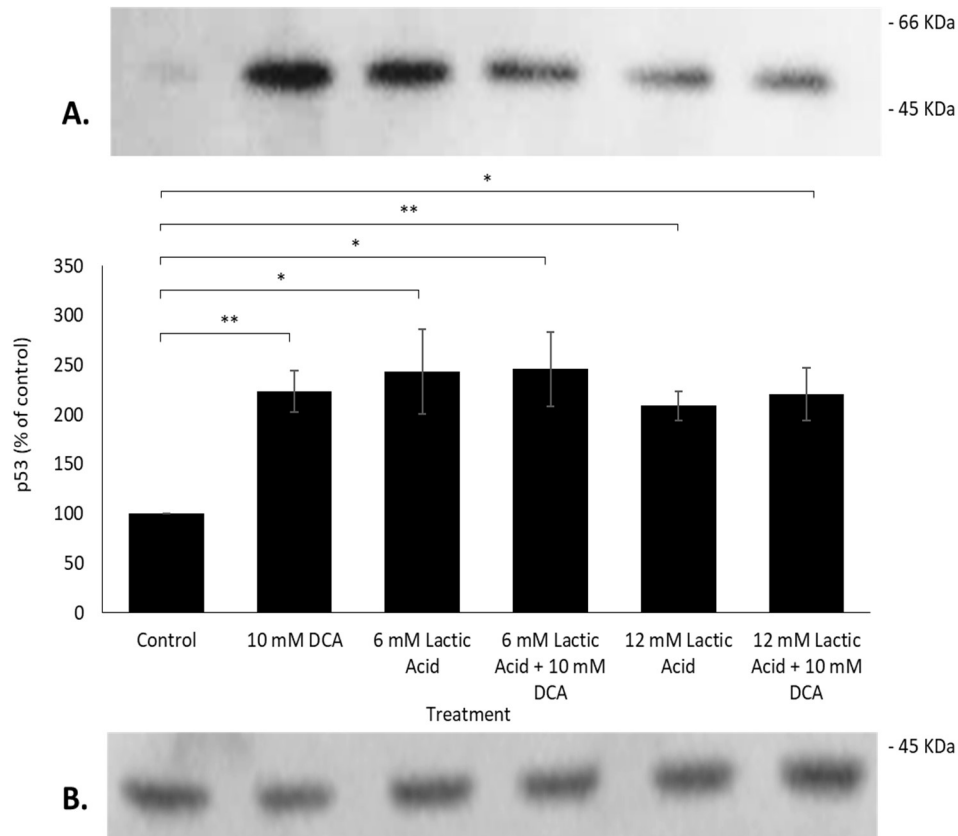


Figure 5.17. The effect of DCA and lactic acid on p53 levels. SH-SY5Y cells were grown to confluence and then treated with the indicated DCA and lactic acid concentrations in UltraMEM for 24 h. Cell lysates were prepared, and equal amounts of protein were subjected to SDS-PAGE and immunoblotting using the (A) anti-p53 and (B) anti-actin antibodies as described in the Materials and Methods section. Results are means \pm S.D. (n=3). Significant results are indicated: * = significant at $p \leq 0.05$, ** = significant at $p \leq 0.01$.

The same lysate samples from DCA/lactic acid-treated cells were then also immunoblotted with the anti-APP C-terminal antibody in order to examine full-length APP expression. The results (Fig. 5.18.) showed that neither compound either alone or in combination had any significant effect on APP expression at the concentrations employed.

Next, the effects of DCA/lactic acid on the proteolysis of APP were investigated by immunoblotting concentrated conditioned medium samples from the preceding experiments with anti-APP 6E10 and anti-sAPP β antibodies.

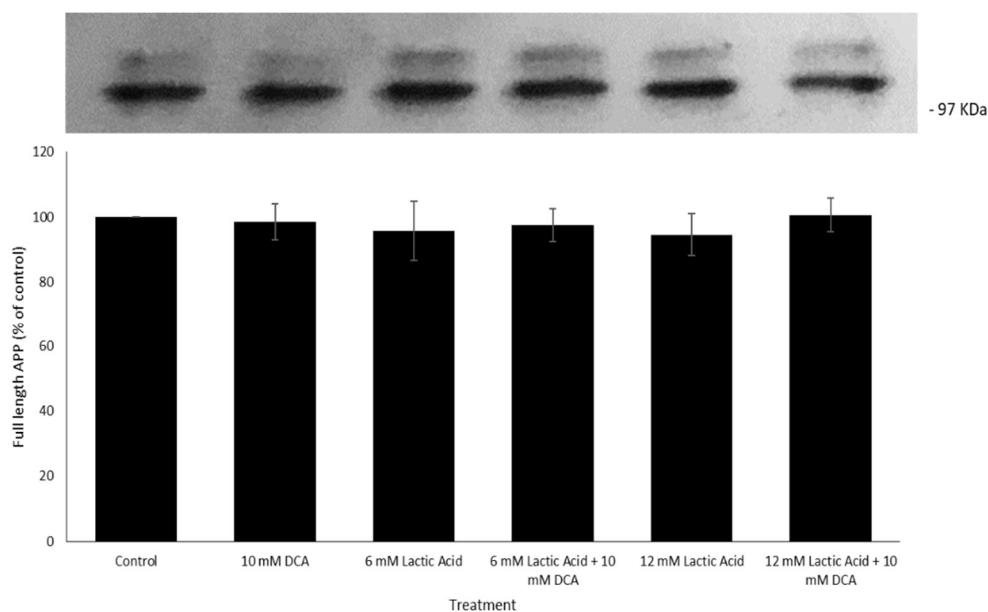


Figure 5.18. The effect of DCA and lactic acid on APP expression. SH-SY5Y cells were grown to confluence and then treated with the indicated DCA and lactic acid concentrations in UltraMEM for 24 h. Cell lysates were prepared, and equal amounts of protein were subjected to SDS-PAGE and immunoblotting using the anti-APP C-terminal antibody as described in the Materials and Methods section. Results are means \pm S.D. (n=3).

The results using the former antibody (Fig. 5.19.) showed that, whilst DCA (as previously observed) enhanced sAPP α production, lactic acid had no effect in this respect when used alone at either 6 or 12 mM concentrations. Furthermore, the combination of DCA and lactic acid had no additive effects over and above the effect of the former drug alone in relation to sAPP α production. Results using the anti-sAPP β antibody (Fig. 5.20.) showed that, as previously observed, DCA decreased sAPP β production. Interestingly, when used at the lower 6 mM (and not 12 mM) concentration, lactic acid alone enhanced sAPP β production (Fig. 5.20A.; 51.35 ± 28.45 % increase), a difference that remained when the values were adjusted to consider the minor alterations observed in cell viability (Fig. 5.20B.). Notably, when the cells were co-treated with DCA and lactic acid, the latter compound did not significantly modify the ability of DCA to reduce sAPP β production.

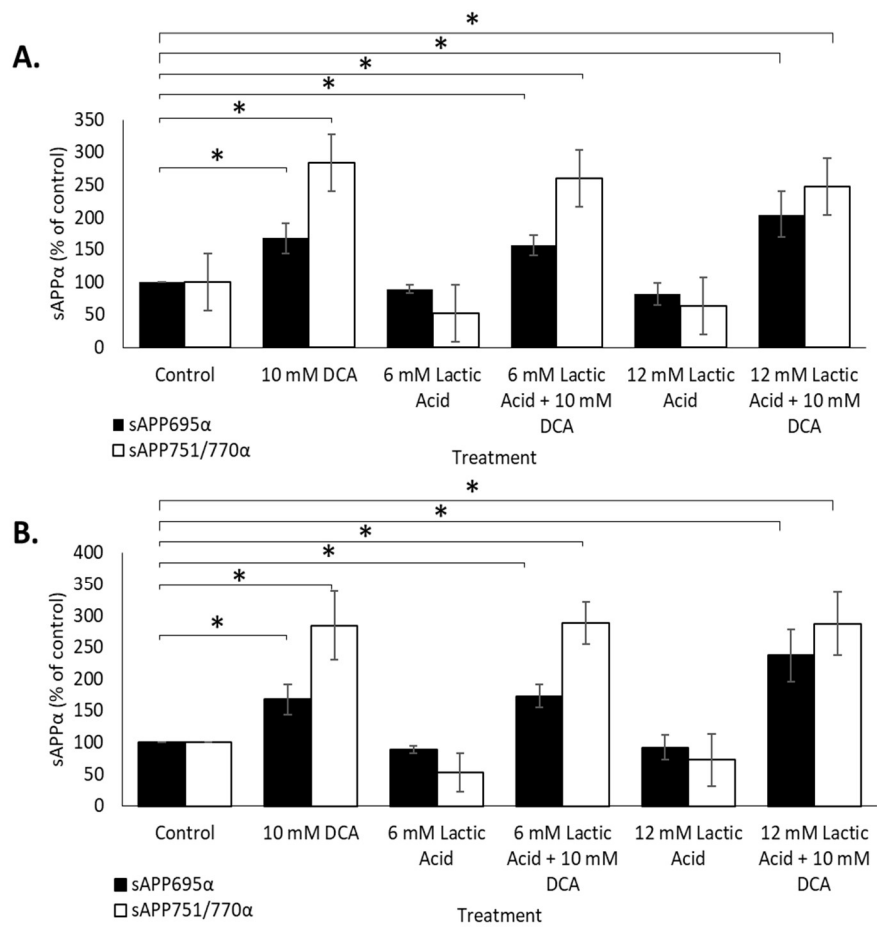
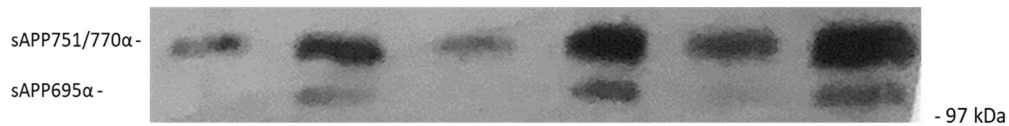


Figure 5.19. The effect of DCA and lactic acid on the production of sAPP α by SH-SY5Y cells. Cells were grown to confluence and then treated with the indicated DCA and lactic acid concentrations in UltraMEM for 24 h. Equal volumes of concentrated medium were then immunoblotted with anti-sAPP α 6E10 antibody. **(A)** Standard results and **(B)** viability corrected results. Results are means \pm S.D. (n=3). Significant results are indicated: * = significant at $p \leq 0.05$.

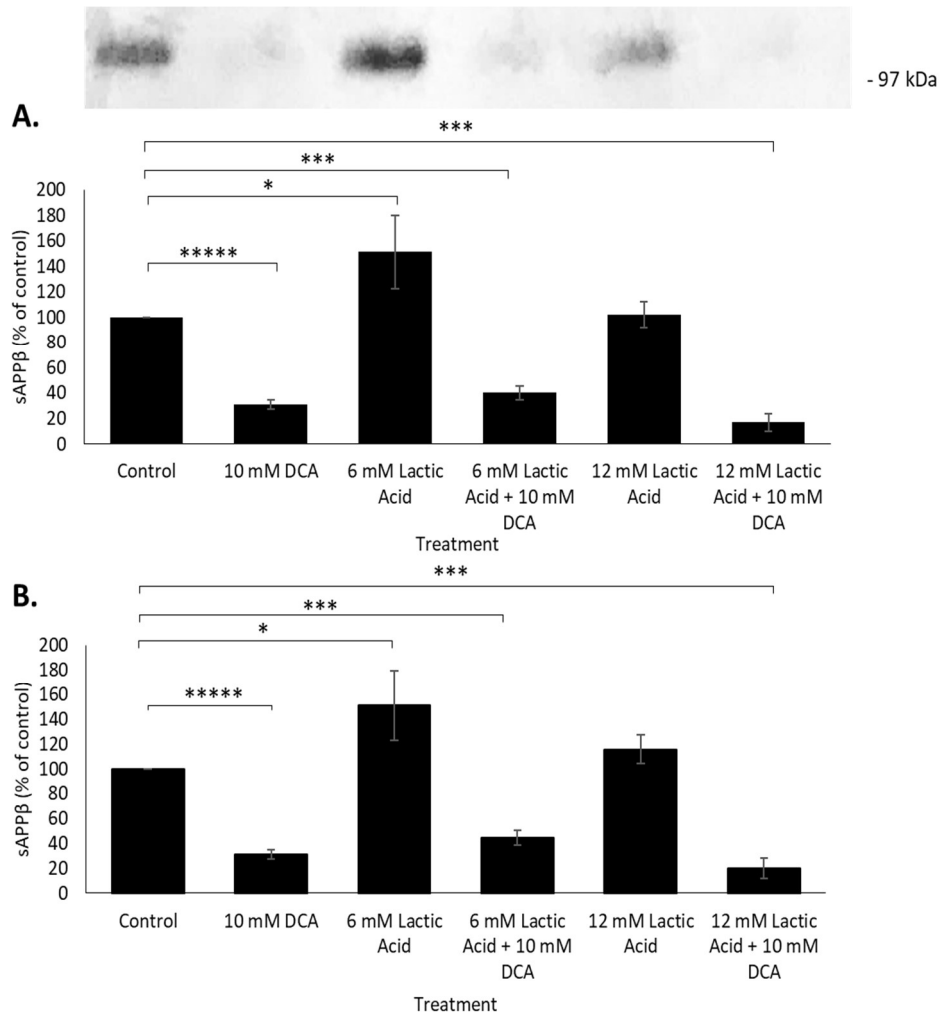


Figure 5.20. The effect of DCA and lactic acid on the production of sAPP β by SH-SY5Y cells. Cells were grown to confluence and then treated with the indicated DCA and lactic acid concentrations in UltraMEM for 24 h. Equal volumes of concentrated medium were then immunoblotted with anti-sAPP β antibody. **(A)** Standard results and **(B)** viability corrected results. Results are means \pm S.D. (n=3). Significant results are indicated: * = significant at $p \leq 0.05$, *** = significant at $p \leq 0.005$, **** = significant at $p \leq 0.0005$.

As mentioned previously, Xiang *et al.* (2010) reported a significant increase in sAPP α generation in SH-SY5Y cells following lactic acid treatment. In the current study, we chose initially to incubate SH-SY5Y cells with lactic acid for 24 h as this tied in with previous experiments using 24 h DCA treatments. However, it was subsequently noted that Xiang *et al.* conducted their treatments over just a 6 h treatment and, as such, it was hypothesised that the observed lack of effect on sAPP α generation (Fig. 5.19.) in the previous study might have been due to the differences in time scales employed. Therefore, the DCA/lactic acid treatment experiments were repeated but using a shorter 6 h incubation period.

Viability results (Fig. 5.21.) indicated that there was a very slight but significant decrease in viability observed in cells treated with 6 mM and 12 mM lactic acid for 6 h, both alone and in combination with DCA.

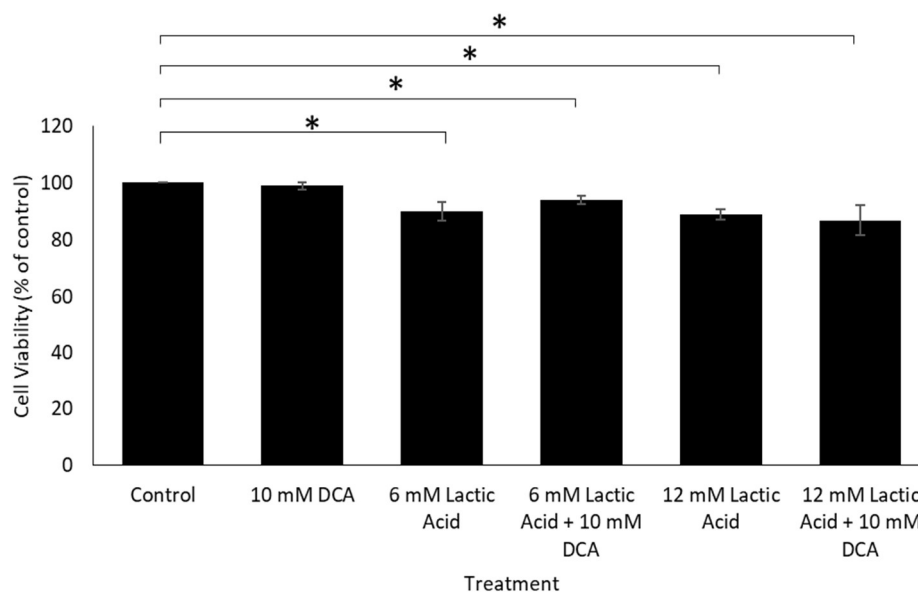


Figure 5.21. The effect of 6h DCA and lactic acid treatment on SH-SY5Y cell viability. Cells were grown to confluence and then treated with the indicated DCA and lactic acid concentrations in UltraMEM for 6 h. Cell viability was then determined using the MTS assay as described in the Materials and Methods section. Results are means \pm S.D. (n=3). Significant results are indicated: * = significant at $p \leq 0.05$.

Next, cell lysates from 6 h DCA/lactic acid-treated cells were immunoblotted in order to monitor p53 levels. The results (Fig. 5.22.) showed that DCA, when used alone, enhanced p53 levels even after this much shorter treatment duration (168.84 ± 6.63 % increase relative to controls). As observed with the longer (24 h) treatments, lactic acid alone also enhanced p53 levels at 6 h (83.64 ± 23.85 and 60.24 ± 26.97 % increases relative to controls for 6 and 12 mM lactic acid, respectively). Although, notably this effect was not significant at the higher lactic acid concentration. Combining lactic acid with DCA did not modify the ability of the latter compound to alter p53 levels.

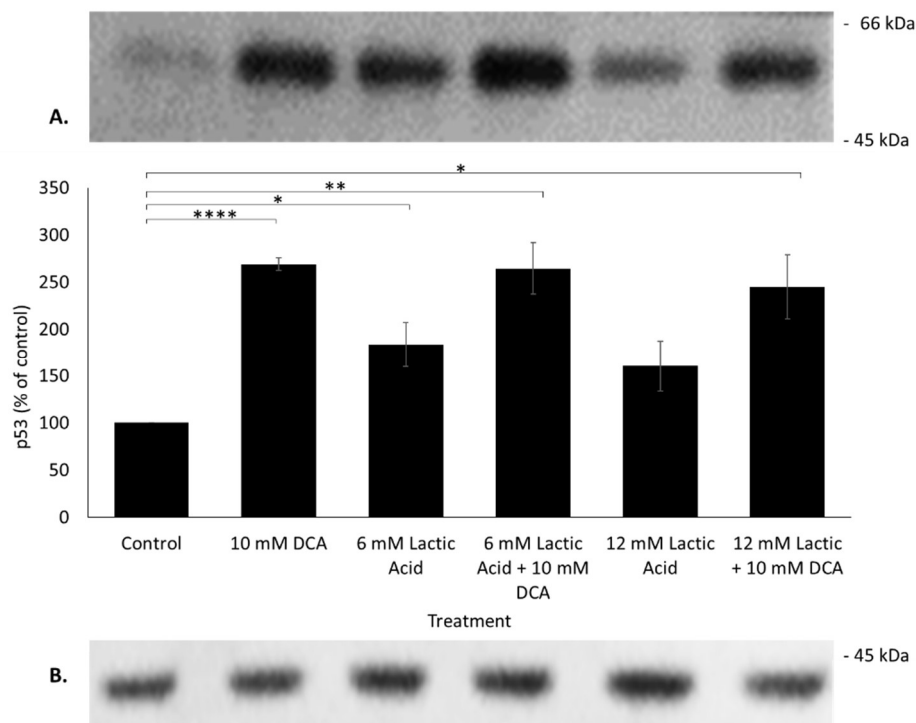


Figure 5.22. The effect of shorter (6 h) DCA and lactic acid treatments on p53 levels. SH-SY5Y cells were grown to confluence and then treated with the indicated DCA and lactic acid concentrations in UltraMEM for 6 h. Cell lysates were prepared, and equal amounts of protein were subjected to SDS-PAGE and immunoblotting using (A) anti-p53 and (B) anti-actin antibodies as described in the Materials and Methods section. Results are means \pm S.D. (n=3). Significant results are indicated: * = significant at $p \leq 0.05$, ** = significant at $p \leq 0.01$, **** = significant at $p \leq 0.001$.

The same lysate samples were then immunoblotted with the anti-APP C-terminal antibody to monitor APP expression. The results (Fig. 5.23.) showed a significant increase in full-length APP expression in cells treated with 10 mM DCA following this 6 h treatment (91.84 ± 20.57 % relative to controls) perhaps suggesting that such an increase might be transient given the fact that previous experiments had shown no change in APP expression in 10 mM DCA-treated cells at 24 h. Similarly, whereas earlier experiments (Fig. 5.18.) had shown no change in APP expression after 24 h lactic acid treatment, in this later 6 h experiment, expression was increased by 72.84 ± 15.50 and $72.67 \pm 9.86\%$, respectively, at 6 and 12 mM lactic acid. However, again, the combination of both DCA and lactic acid did not alter the ability of each compound individually to alter APP expression.

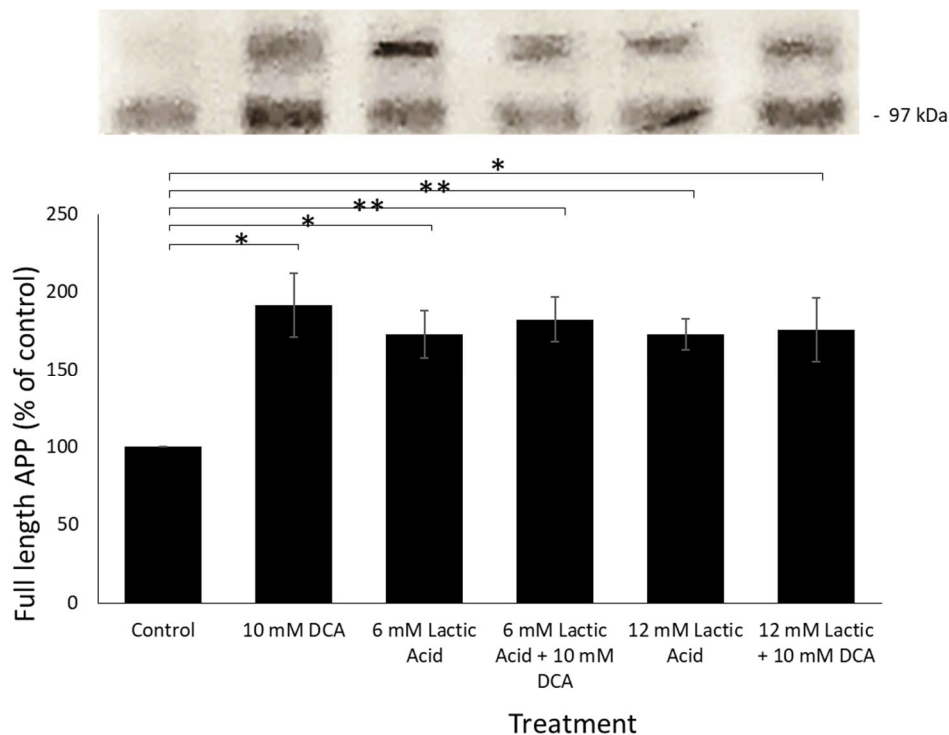


Figure 5.23. The effect of shorter (6 h) DCA and lactic acid treatments on APP expression. SH-SY5Y cells were grown to confluence and then treated with the indicated DCA and lactic acid concentrations in UltraMEM for 6 h. Cell lysates were prepared, and equal amounts of protein were subjected to SDS-PAGE and immunoblotting using the anti-APP C-terminal antibody as described in the Materials and Methods section. Results are means \pm S.D. (n=3). Significant results are indicated: * = significant at $p \leq 0.05$, ** = significant at $p \leq 0.01$.

Next, the conditioned medium from the 6 h DCA/lactic acid treatments was immunoblotted in order to quantify the effects of this shorter incubation time on sAPP α and sAPP β generation. In terms of sAPP α production, the results (Fig. 5.24.) again showed an increase in the generation of this fragment following DCA treatment. However, lactic acid did not modify the effect of DCA and additionally failed to enhance the generation of this product once the results were altered to account for viability. In relation to sAPP β , the results (Fig. 5.25.) showed that, as with previous 24 h incubations, DCA reduced the generation of this fragment after only 6 h. However, again, lactic acid failed to have any effect on this aspect of APP proteolysis, nor did it modify the ability of DCA in this respect.

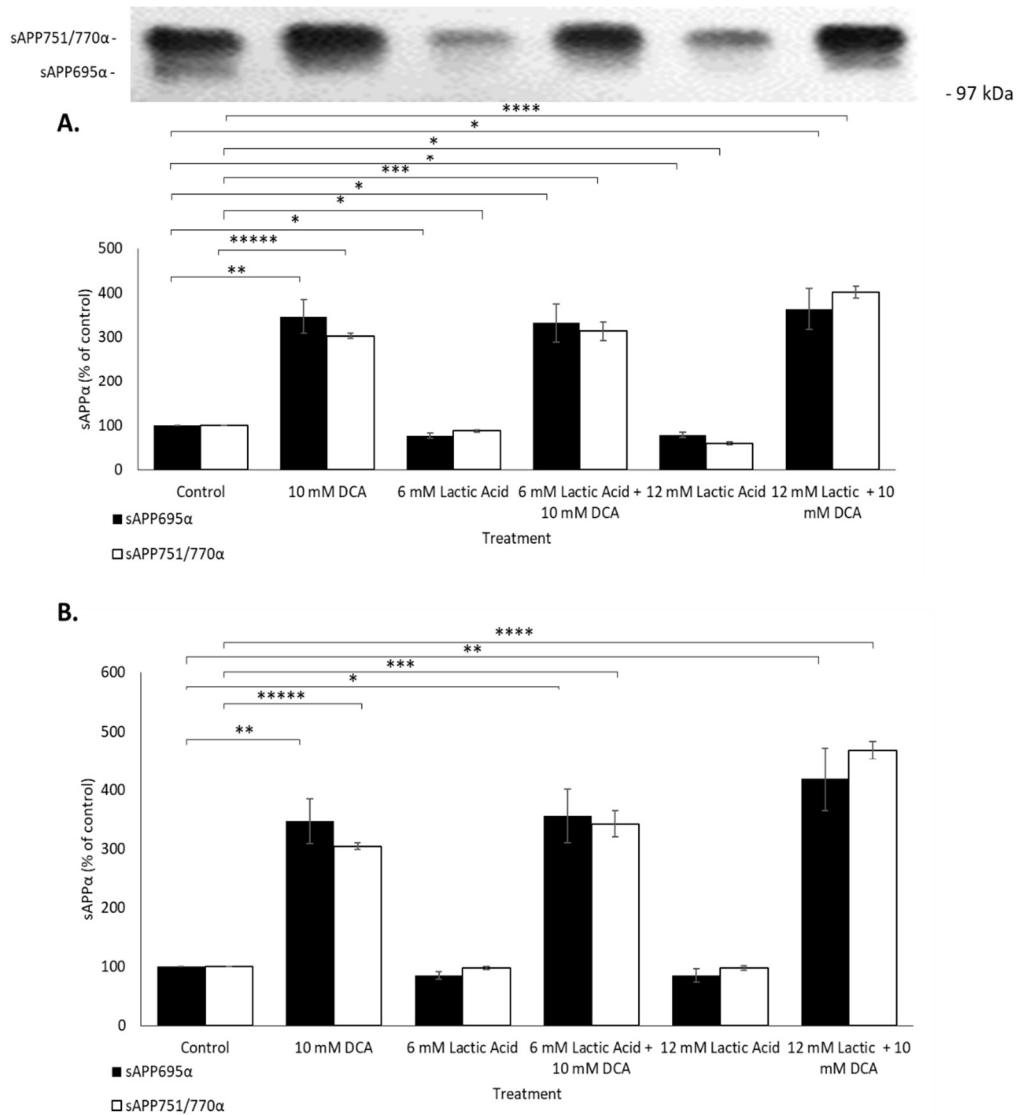


Figure 5.24. The effect of shorter (6 h) DCA and lactic acid treatments on the production of sAPP α by SH-SY5Y cells. Cells were grown to confluence and then treated with the indicated DCA and lactic acid concentrations in UltraMEM for 24 h. Equal volumes of concentrated medium were then immunoblotted with anti-sAPP α 6E10 antibody. **(A)** Standard results and **(B)** viability corrected results. Results are means \pm S.D. (n=3). Significant results are indicated: * = significant at $p \leq 0.05$, ** = significant at $p \leq 0.01$, *** = significant at $p \leq 0.005$, **** = significant at $p \leq 0.001$, ***** = significant at $p \leq 0.0005$.

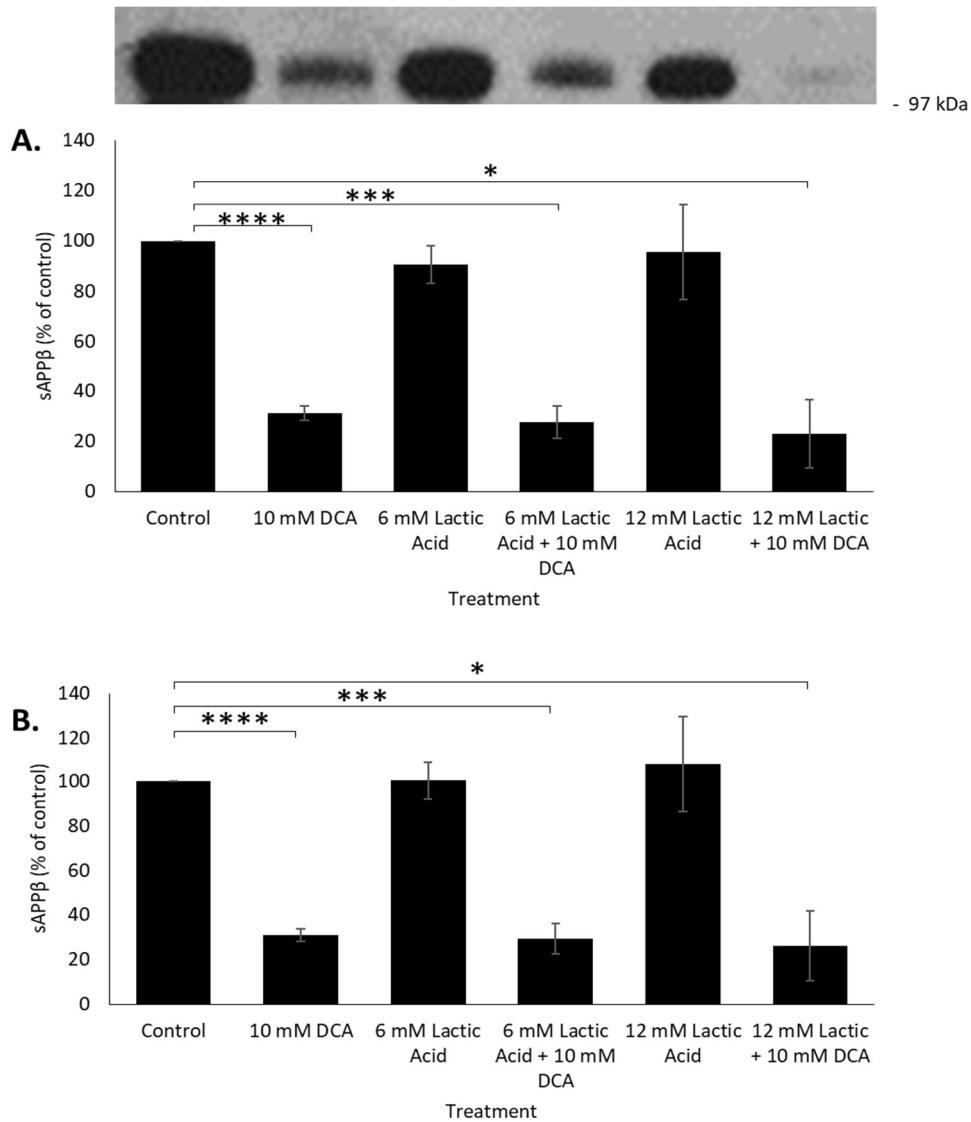


Figure 5.25. The effect of shorter (6 h) DCA and lactic acid treatments on the production of sAPPβ by SH-SY5Y cells. Cells were grown to confluence and then treated with the indicated DCA and lactic acid concentrations in UltraMEM for 24 h. Equal volumes of concentrated medium were then immunoblotted with anti-sAPPβ antibody. **(A)** Standard results and **(B)** viability corrected results. Results are means ± S.D. (n=3). Significant results are indicated: * = significant at $p \leq 0.05$, *** = significant at $p \leq 0.005$, **** = significant at $p \leq 0.001$

5.3. Summary.

The overarching aim of this chapter was to investigate whether DCA was able to regulate APP expression/proteolysis through alterations in cellular pyruvate and/or lactic acid concentrations.

Initially, two inhibitors of LDH were employed, GSK2837808A (an inhibitor of both LDH-A and LDH-B) and FX11 (a specific inhibitor of LDH-A). The former compound saw no significant effect on viability at any concentration, whilst the latter was toxic at all but the lowest concentration employed. This toxicity was reflected in terms of p53 levels in that GSK2837808A did not alter expression and FX11 enhanced expression at the point at which the compound became toxic to cells. Neither compound affected full-length APP expression, whilst FX11 saw an increase in sAPP α production at sub-toxic inhibitor concentrations and GSK2837808A saw a decrease in sAPP α production at the highest concentration. Interestingly, GSK2837808A enhanced sAPP β production at concentrations over 10 nM, whereas FX11 had no significant effect in this respect at non-toxic concentrations of the inhibitor. Clearly, there is a complex relationship between these two LDH inhibitors and APP proteolysis; this relationship is discussed further in the Discussion section of this report.

Pyruvate supplementation of SH-SY5Y cells had a biphasic effect on cell viability, increasing viability at 10 mM whilst becoming toxic at higher concentrations. The toxic effect of pyruvate above 10 mM was reflected in the increased p53 levels observed in cells treated with 50 and 100 mM concentrations of this metabolite. Pyruvate did not modify APP expression but did slightly decrease sAPP α generation at 10 mM whilst having no significant effect on sAPP β generation (after adjusting for viability changes).

Perhaps the most interesting results in the current chapter came from the lactic acid supplementation experiments. Here, following 24 h incubations, the metabolite effected a very small but significant decrease in the viability of cell cultures. Interestingly, despite only these small viability changes, lactic acid dramatically enhanced p53 levels (to a similar extent as DCA). However, the effects of DCA and lactic acid on p53 levels were not additive. Neither DCA nor lactic acid altered APP expression following a 24 h incubation. As previously observed, 24 h DCA treatments enhanced non-amyloidogenic and inhibited amyloidogenic APP processing. However, lactic acid did not regulate these proteolytic events when used singularly nor did it modify the ability of DCA to regulate these events.

It is notable that the changes in p53 levels mediated by lactic acid were a relatively rapid event as the expression of this protein also increased following a much shorter 6 h incubation of cells with the metabolite. Similarly, it is also notable that both lactic acid and DCA (alone or in combination, although the effect was not additive) enhanced APP expression over 6 h whereas neither compound altered the expression of this protein over the longer 24 h time course. This might suggest an initial burst in APP expression following 6 h lactic acid and/or DCA treatment with a subsequent return to control values by 24 h. Even at this shorter time point, however, lactic acid alone did not alter APP proteolysis, nor did it impact on the ability of DCA to regulate proteolysis (although DCA still enhanced non-amyloidogenic and impaired amyloidogenic processing even at the shorter 6 h time point).

Chapter 6.

**The effects of DCA on BACE1 activity and APP subcellular
localisation.**

6. The effects of DCA on BACE1 activity and APP subcellular localisation.

Previous studies have demonstrated that the inhibition of BACE1 leads to enhanced non-amyloidogenic processing and reduced amyloidogenic processing of APP (Cai *et al.*, 2001; Ohno *et al.*, 2004; McConlogue *et al.*, 2007; Yan *et al.*, 2014). Additionally, changes in the subcellular localisation of APP are known to affect proteolytic processing of the protein due to altered exposure of the substrate to BACE1 (Perez *et al.*, 1999; Carey *et al.*, 2005; Sano *et al.*, 2006; Choy *et al.*, 2012).

In the current study, it was, therefore, hypothesised that DCA might act either by reducing BACE1 activity (note that previous studies in our laboratory have shown that ADAM10 activity was unaffected by DCA; Parkin *et al.*, unpublished data) and/or by altering the subcellular distribution of the APP substrate.

6.1. The effect of DCA on BACE1 activity.

In order to determine whether DCA altered BACE1 activity in SH-SY5Y cells, a fluorescence-based assay was employed (see Materials and Methods). Cells were grown to confluence and treated for 24 h with 0, 10 or 20 mM DCA in UltraMEM. Cell lysates were prepared according to the manufacturer's instructions and assayed for BACE1 activity. Following the assay, protein concentrations in the lysates were determined and the results adjusted in order to account for minor differences in protein concentrations between the lysate samples. The results (Fig. 6.1.) were conclusive in that they clearly showed that DCA did not alter total cellular BACE1 activity.

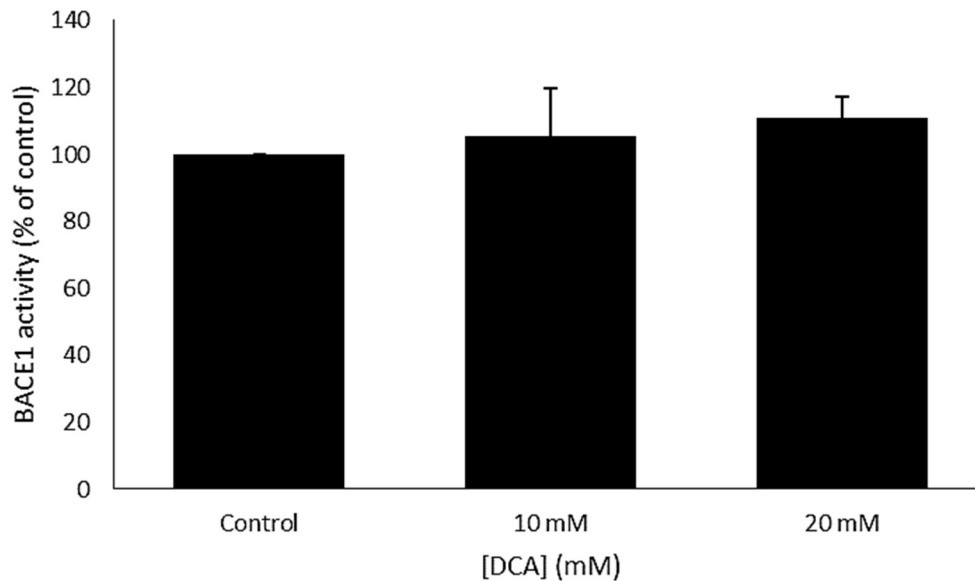


Figure 6.1. The effect of DCA treatment on BACE1 activity in SH-SY5Y cells. Confluent SH-SY5Y cells were treated with DCA at the concentrations indicated for 24 h. Lysates were then prepared and assayed using a BACE1 activity assay kit according to the manufacturer's instructions. Results were adjusted to account for differing protein levels and are means \pm S.D. (n=3).

6.2. The effect of DCA on APP subcellular localisation.

It was hypothesised that DCA may alter the subcellular localisation of APP resulting in differing exposure to the enzymes of the non-amyloidogenic and amyloidogenic processing pathways. In order to test this hypothesis, immunofluorescence microscopy was used to analyse APP subcellular distribution in the absence or presence of 10 mM DCA.

Initially, the working dilution of the anti-APP antibody WO2 stock was optimised and the manufacturer recommended concentrations of antibodies against organelle marker proteins for lysosomes (LAMP1), cis-Golgi (GM130) and late endosomes (Rab6A) were tested. Cells were grown to 60 % confluence (a lower level of confluence was employed to visualise individual cells) and processed for immunofluorescence as described in the Materials and Methods section (note that the cells were not treated with DCA in this first experiment). The results (Fig. 6.2A-E) showed that, whilst a strong perinuclear staining was achieved at the supplier recommendation of 1 in 20 dilution of the anti-APP WO2 antibody (Fig. 6.2A.), equally

(if not better) clarity could be achieved at a 1 in 50 dilution (Fig. 6.2B.). As such, this latter dilution was adopted for subsequent experiments primarily for economic reasons. As far as the organelle marker antibodies were concerned, the recommended concentrations of LAMP1 (Fig. 6.2F.) and Rab6A (Fig. 6.2H), clearly stained defined structures likely corresponding to lysosomes and late endosomes, respectively. However, the anti-GM130 antibody, at the recommended concentration (Fig. 6.2G.) gave somewhat inconsistent staining between cells; as such, a higher concentration of 40 µg/ml was adopted for subsequent experiments.

To gain an idea as to whether the anti-APP WO2 antibody was detecting APP and not cross-reacting with another protein, the hydroxamic acid inhibitor batimastat was employed. Here, the hypothesis was that this compound would inhibit shedding of APP by ADAM10 at the cell surface thereby leading to changes in the subcellular distribution of the former protein. If the WO2 antibody was picking up another protein (other than ADAM substrates) then batimastat would not lead to any changes in the subcellular fluorescence following immunodetection with the WO2 antibody. To this end, cells were again grown to 60 % confluence and then treated for 24 h in the absence or presence of batimastat (5 µM) before processing for immunofluorescence microscopy (see Materials and Methods). The control images (i.e. no batimastat) (Fig. 6.3.) revealed that APP showed little co-localisation with the lysosomal marker, LAMP1 and the strongest co-localisation with the cis-Golgi marker, GM130. There was also an intermediate level of co-localisation with the late endosomal marker, Rab6A. However, when the SH-SY5Y cells were pre-treated for 24 h with batimastat (Fig. 6.4.) there was a much greater co-localisation of APP with the lysosomal marker, LAMP1, a visible decrease in cis-Golgi localisation and a more defined localisation in the endosomes.

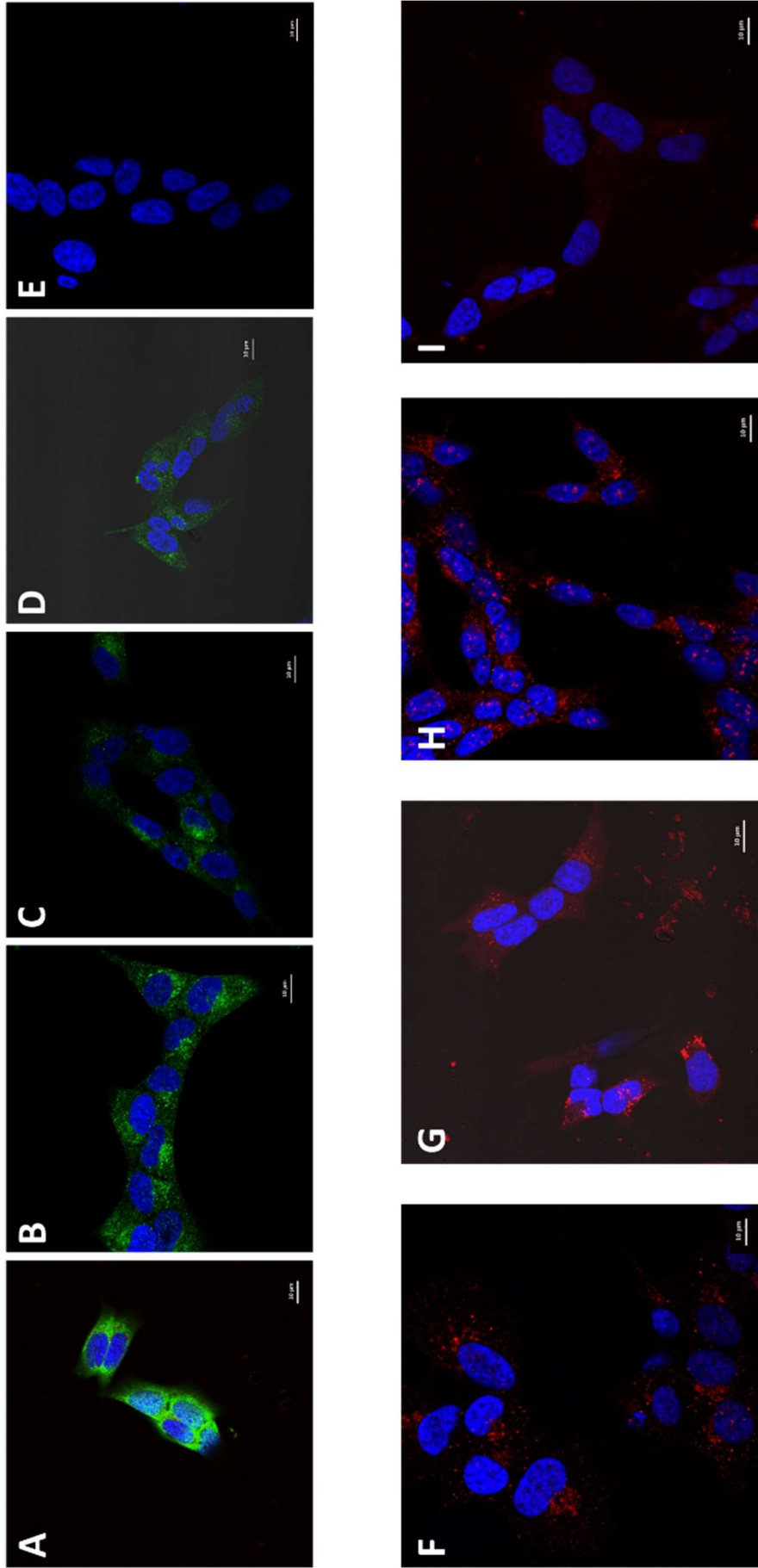


Figure 6.2. Optimisation of antibody concentrations used for immunofluorescence. SH-SY5Y cells were initially grown to 60 % confluence. Cells were then prepared *in situ* and fluorescently probed as described in the Materials and Methods section: **A-D**, Anti-APP WO2 antibody at stock dilutions of 1 in 20, 1 in 50, 1 in 100 and 1 in 200, respectively. **E**, Secondary antibody only control (1 in 200 dilutions of goat anti-mouse IgG H+L (AlexaFluor 488)). **F**, Anti-LAMP1 at a concentration of 5 $\mu\text{g/ml}$. **G**, Anti-GM130 at a concentration of 5 $\mu\text{g/ml}$. **H**, Anti-Rab6A at a concentration of 10 $\mu\text{g/ml}$. **I**, Secondary antibody only control (1 in 200 dilutions of goat anti-rabbit IgG H+L (AlexaFluor 594)).

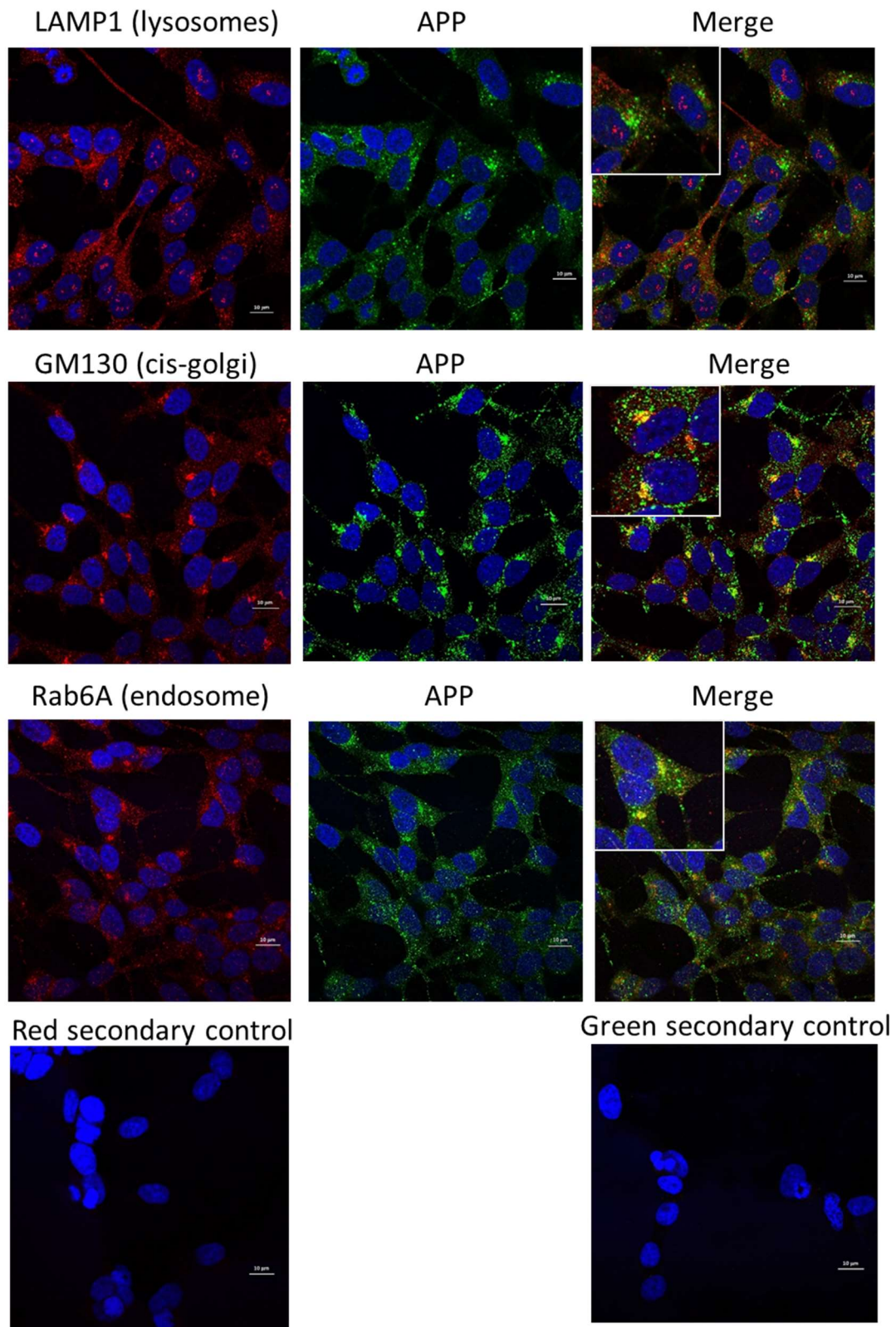


Figure 6.3. The localisation of APP in control SH-SY5Y cells. Human SH-SY5Y cells were initially grown to 60 % confluence before the medium was replaced with ultraMEM for a further 24 h incubation. Cells were then prepared *in situ* and immunolabelled as indicated.

As such, it was apparent that inhibiting APP release from the cell surface with batimastat did indeed result in a change in the subcellular distribution of immunofluorescence observed using the anti-APP WO2 antibody. This would suggest a degree of APP specificity to the antibody.

Having, optimised the immunofluorescence conditions, the effect of DCA on the subcellular localisation of APP was investigated. Here, cells were pre-incubated for 24 h with 10 mM DCA. Note that both the batimastat and these DCA treatments were performed in the same experiment and, as such, the control images for the latter treatments are those already described in Fig. 6.3. The images from DCA-treated cells (Fig. 6.5.) showed no major changes in APP subcellular localisation compared to the control cells (Fig. 6.3.), with a possible decrease in cis-Golgi localisation. Therefore, it is unlikely that the drug regulates APP proteolysis by mediating the subcellular localisation of APP.

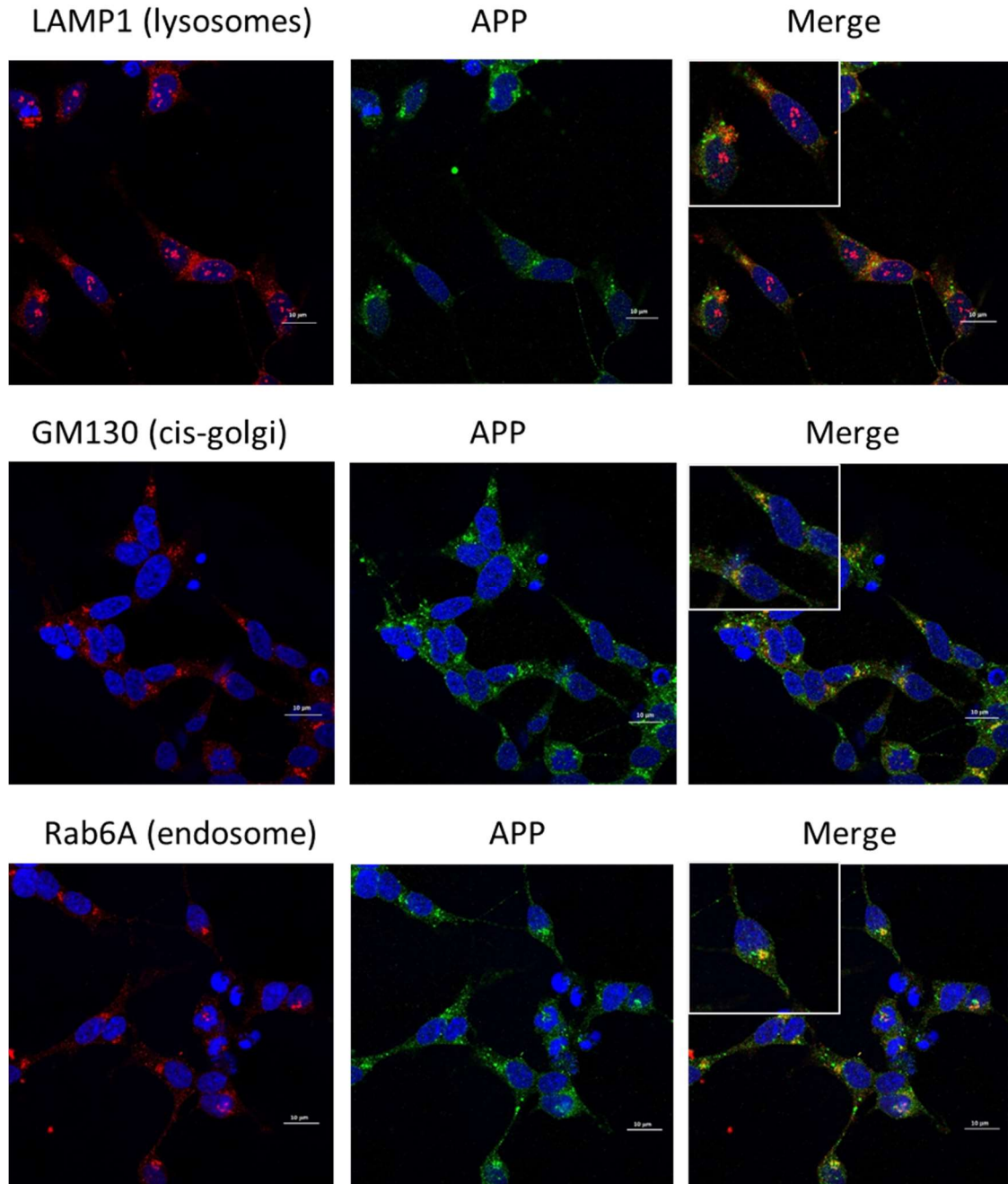


Figure 6.4. The localisation of APP in batimastat-treated SH-SY5Y cells. Human SH-SY5Y cells were initially grown to 60 % confluence before the medium was replaced with ultraMEM containing 5 μ M batimastat for a further 24 h incubation. Cells were then prepared *in situ* and immunolabelled as indicated.

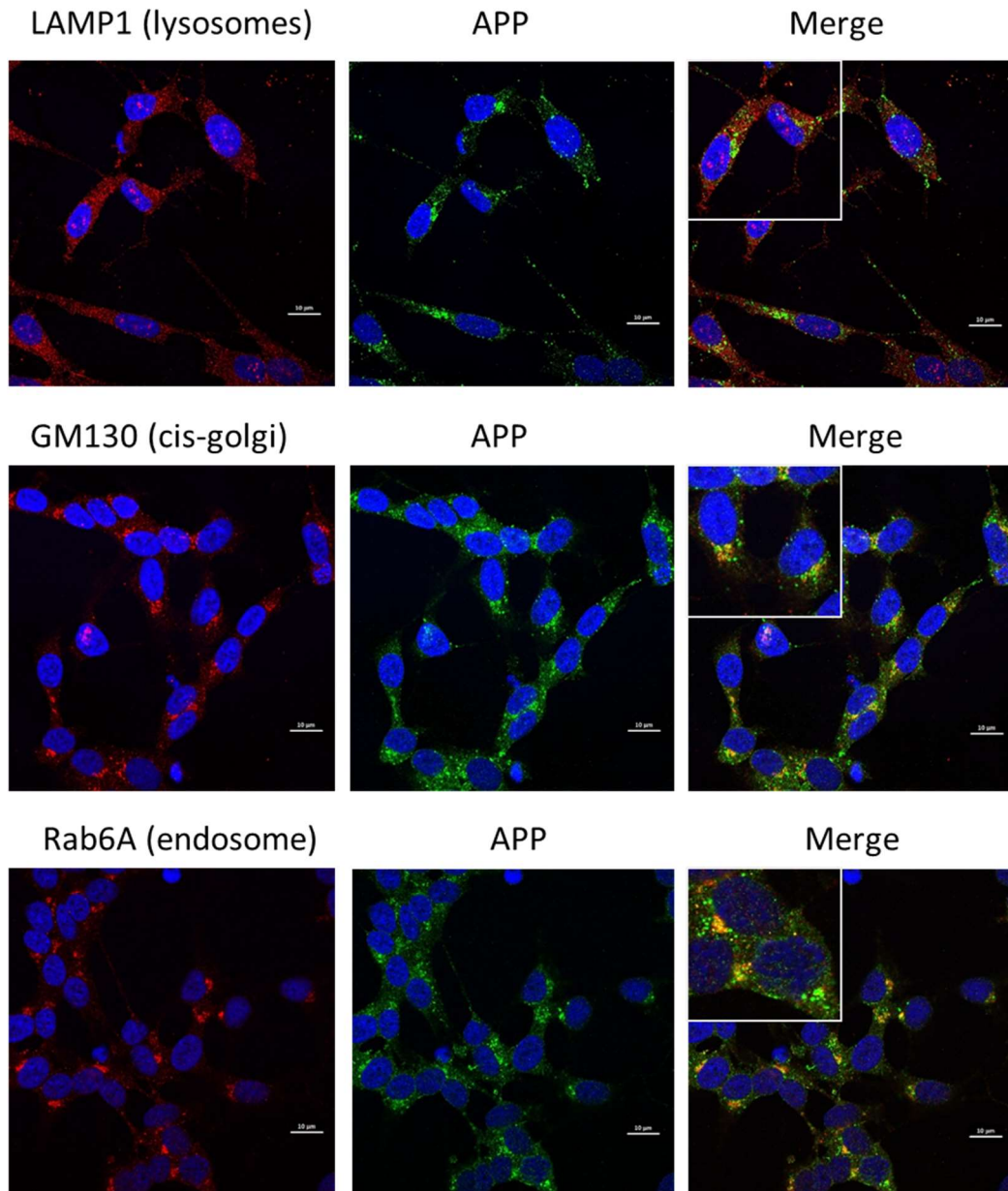


Figure 6.5. The localisation of APP in DCA-treated SH-SY5Y cells. Human SH-SY5Y cells were initially grown to 60 % confluence before the medium was replaced with ultraMEM containing 10 mM for a further 24 h incubation. Cells were then prepared *in situ* and immunolabelled as indicated.

6.3. Summary.

The results in the current chapter clearly show that DCA did not alter overall cellular BACE1 activity although caution should be applied in interpreting this result as this does not preclude the possibility that the drug alters activity of the protein in different intracellular compartments.

A reliable method for the subcellular visualisation of APP distribution has been established and ADAM inhibition using batimastat clearly impacted on this distribution suggesting that APP was, indeed, being specifically visualised. However, the results also show that DCA exhibited no major effect on APP subcellular distribution. As such, it is unlikely that the drug regulates proteolysis of the protein via changes in its subcellular distribution.

Chapter 7.

Mitochondrial autophagy and oxidative stress as possible mechanisms through which DCA regulates APP proteolysis.

7. Mitochondrial autophagy and oxidative stress as possible mechanisms through which DCA regulates APP proteolysis.

It has recently been demonstrated that DCA induces mitochondrial autophagy in SH-SY5Y cells (Pajuelo-Reguera *et al.*, 2015). Prior studies have also identified a link between mitophagy and APP processing (Cole *et al.*, 1989; Siman *et al.*, 1993) and have implicated mitophagy in the progression of AD (Manczak *et al.*, 2006; Chen *et al.*, 2007; Petersen *et al.*, 2008).

DCA has also been shown to enhance oxidative stress (Hassoun and Cearfoss, 2011; Dai *et al.*, 2014) and it is well established that oxidative stress plays a role both in the development of AD and in APP proteolysis (Smith *et al.*, 2007; Chen *et al.*, 2008; Tamagno *et al.*, 2008; Guglielmotto *et al.*, 2009; Mouton Liger *et al.*, 2012; Arimon *et al.*, 2015; Muche *et al.*, 2017; Cheignon *et al.*, 2018).

Therefore, in the current study, it was hypothesised that DCA might be regulating its effects on APP proteolysis through changes in mitochondrial autophagy and/or the enhancement of oxidative stress. To this end, SH-SY5Y cells were treated with DCA in the presence of mitophagy inhibitors or detoxifying free radical scavengers and the resultant effects on APP processing were characterised.

7.1. Mitochondrial autophagy and DCA-regulated APP processing.

To explore mitophagy as a potential mechanism by which DCA regulates APP proteolysis, SH-SY5Y cells were treated with two inhibitors of mitochondrial autophagy (ammonium chloride and chloroquine) and the effects of these compounds on the ability of

DCA to regulate APP proteolysis were monitored. The theory here was that, if the inhibitors prevented the mitophagy changes associated with DCA treatment, then they would also ablate the effects of the latter compound on APP proteolysis.

7.1.1. Ammonium chloride.

Here, SH-SY5Y cells were initially grown to confluence and treated for 24 h with UltraMEM containing DCA (10 mM) and/or ammonium chloride (10 mM). The concentration of the latter compound was adopted as it had previously been shown to block terminal autophagy phases in SH-SY5Y cells (Pajuelo-Reguera *et al.*, 2015). Cell viability was then determined using the MTS assay as described in the Materials and Methods section. The results (Fig. 7.1.) showed that, as previously observed, DCA (10 mM) alone caused no decrease in cell viability. Furthermore, ammonium chloride did not alter viability either when used singularly or in combination with DCA.

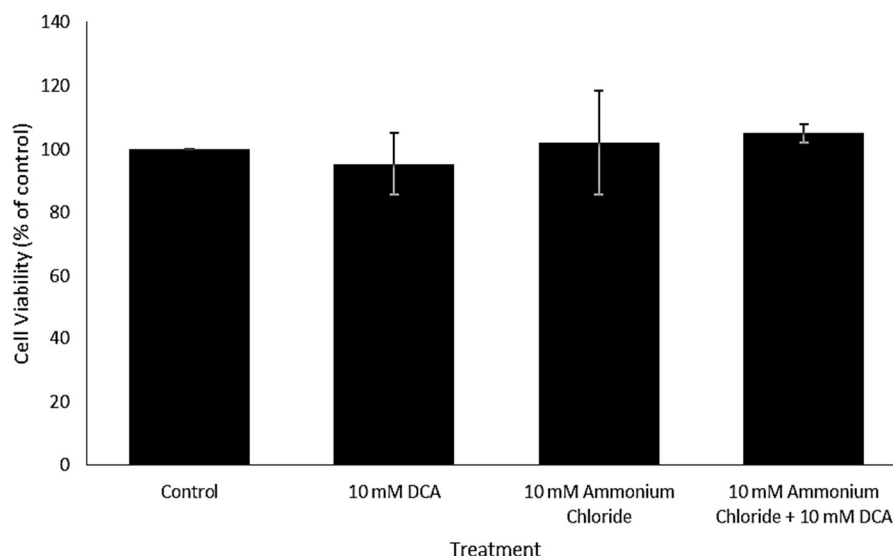


Figure 7.1. The effect of DCA and/or ammonium chloride treatment on SH-SY5Y cell viability. Cells were grown to confluence and then treated with DCA and/or ammonium chloride at the concentrations indicated in UltraMEM for 24 h. Cells were then quantified using an MTS assay *in situ*. Results are means \pm S.D. (n=3).

The same experiment was repeated but, this time, cells and conditioned medium were harvested. Cell lysates were prepared and immunoblotted to examine p53 levels. The results (Fig. 7.2.) show that, as previously observed, DCA alone enhanced p53 levels (113.17 ± 7.76 % increase relative to controls). In contrast, ammonium chloride alone had no effect on p53 levels nor did it alter the ability of DCA to promote levels of the protein.

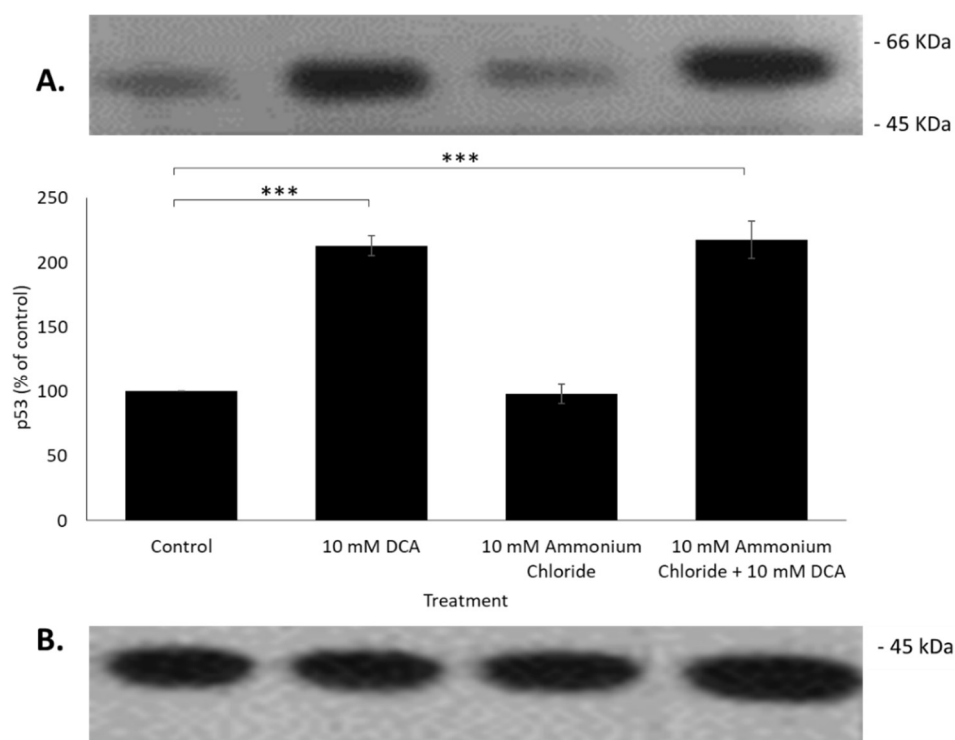


Figure 7.2. The effect of DCA and/or ammonium chloride treatment on the levels of p53 in SH-SY5Y cells. Cells were grown to confluence and then treated with DCA and/or ammonium chloride at the concentrations indicated in UltraMEM for 24 h. Cell lysates were then prepared and immunoblotted using the (A) anti-p53 and (B) anti-actin antibody as described in the Materials and Methods section. Results are means \pm S.D. (n=3). Significant results are indicated: *** = significant at $p \leq 0.005$.

The same lysates were also immunoblotted with the anti-APP C-terminal antibody to monitor any changes in the expression of full-length APP. The results (Fig. 7.3.) showed small increases in APP expression when cells were treated with DCA either alone or in combination with ammonium chloride (20.51 ± 3.55 and 26.08 ± 1.26 % increases, respectively, relative to controls). Cells treated with ammonium chloride did not exhibit altered APP expression nor did the compound modify the effect of DCA in this respect.

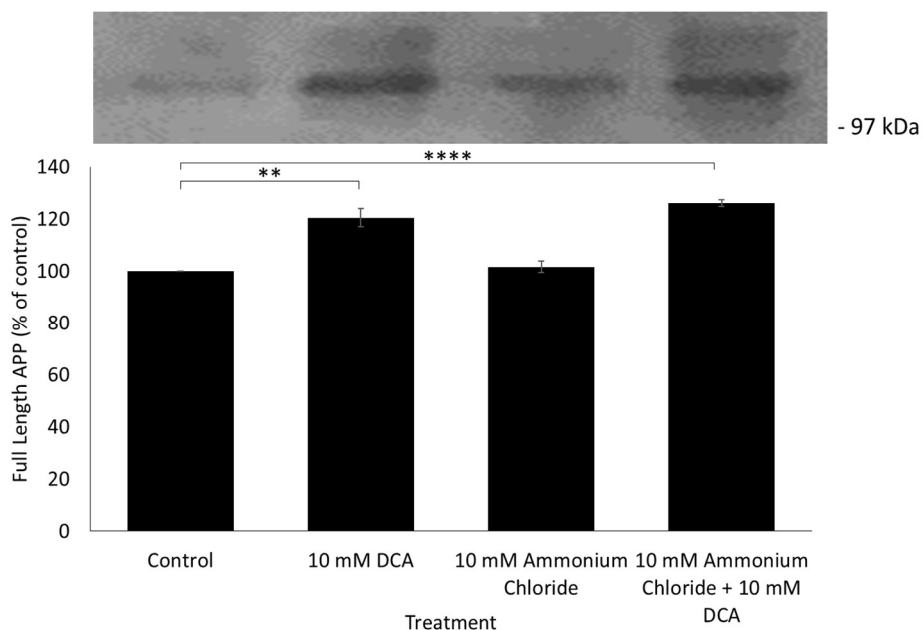


Figure 7.3. The effect of DCA and/or ammonium chloride treatment on the expression of APP in SH-SY5Y cells. Cells were grown to confluence and then treated with DCA and/or ammonium chloride at the concentrations indicated in UltraMEM for 24 h. Cell lysates were then prepared and immunoblotted using the anti-APP C-terminal antibody as described in the Materials and Methods section. Results are means \pm S.D. (n=3). Significant results are indicated: ** = significant at $p \leq 0.01$, **** = significant at $p \leq 0.001$.

Next, the effect of ammonium chloride and DCA on the proteolysis of APP was examined. To this end, concentrated conditioned medium from the preceding experiments was initially immunoblotted with anti-sAPP α 6E10 antibody. The results (Fig. 7.4.) showed that, as previously observed, DCA enhanced sAPP α production by cells (142.95 ± 56.14 and 392.81 ± 18.33 % increases for sAPP695 α and sAPP751/770 α , respectively, relative to controls). Similarly, ammonium chloride treatment led to a 67.98 ± 16.23 % increase in the production of sAPP695 α ; however, the production of sAPP751/770 α by these cells was not altered. Finally, whilst co-treatment of cells with DCA and ammonium chloride also resulted in enhanced sAPP695 α and sAPP751/770 α generation relative to controls (131.21 ± 41.99 % and 398.12 ± 69.15 %, respectively, for the two isoform groupings), these increments were not statistically different from the levels of these fragments generated when the cells were

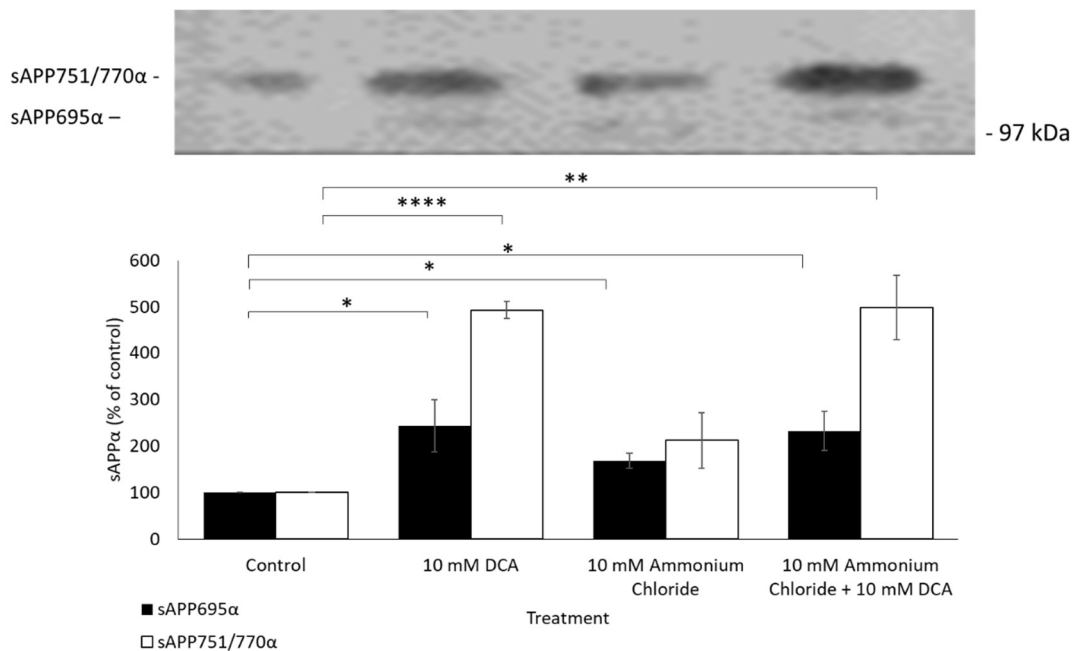


Figure 7.4. The effect of DCA and/or ammonium chloride treatment on the production of sAPP α by SH-SY5Y cells. Cells were treated with DCA and/or ammonium chloride at the concentrations indicated for 24 h. Equal volumes of concentrated medium were then immunoblotted with the anti-sAPP α 6E10 antibody. Results are means \pm S.D. (n=3). Significant results are indicated: * = significant at $p \leq 0.05$, ** = significant at $p \leq 0.01$, **** = significant at $p \leq 0.001$.

treated with DCA alone. As such, it was apparent that, whilst ammonium chloride had a minimal but significant effect on sAPP α production, it did not modify the ability of DCA to promote shedding of these fragments.

Finally, the conditioned medium from these experiments was immunoblotted to quantify the relative levels of sAPP β generated by cells. As observed previously, DCA inhibited the production of this fragment (Fig. 7.5.) (78.70 ± 2.24 % decrease relative to controls). However, ammonium chloride had no effect in this respect nor did it alter the ability of DCA to inhibit sAPP β production.

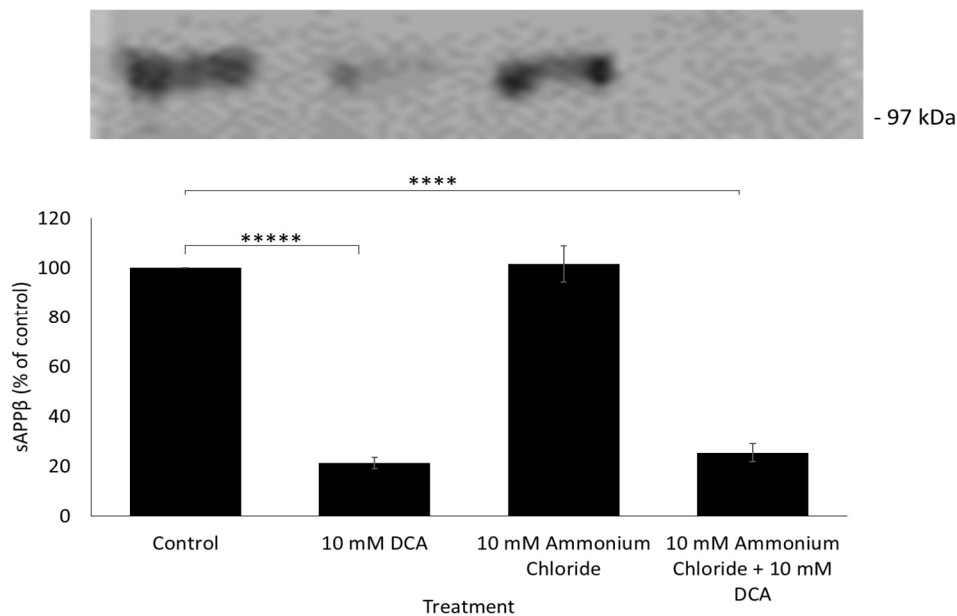


Figure 7.5. The effect of DCA and/or ammonium chloride treatment on the production of sAPP β by SH-SY5Y cells. Cells were treated with DCA and/or ammonium chloride at the concentrations indicated for 24 h. Equal volumes of concentrated medium were then immunoblotted with the anti-sAPP β antibody. Results are means \pm S.D. (n=3). Significant results are indicated: **** = significant at $p \leq 0.001$, ***** = significant at $p \leq 0.0005$.

7.1.2. Chloroquine.

To further investigate the potential role of mitochondrial autophagy as a mechanism underlying the effects of DCA on APP proteolysis, the mitophagy inhibitor, chloroquine, was also studied. Cells were initially grown to confluence and treated for 24 h with UltraMEM containing DCA and/or chloroquine diphosphate (50 μ M). Again, the concentration of the latter compound was adopted due to its previously demonstrated ability to block mitophagy in SH-SY5Y cells at this concentration (Pajuelo-Reguera *et al.*, 2015). After 24 h, the viability of cultures was assessed using the MTS assay as described in the Materials and Methods section. The results (Fig. 7.6.) demonstrated that neither DCA nor the chloroquine diphosphate, used singularly or in combination, had any significant effect on cell viability.

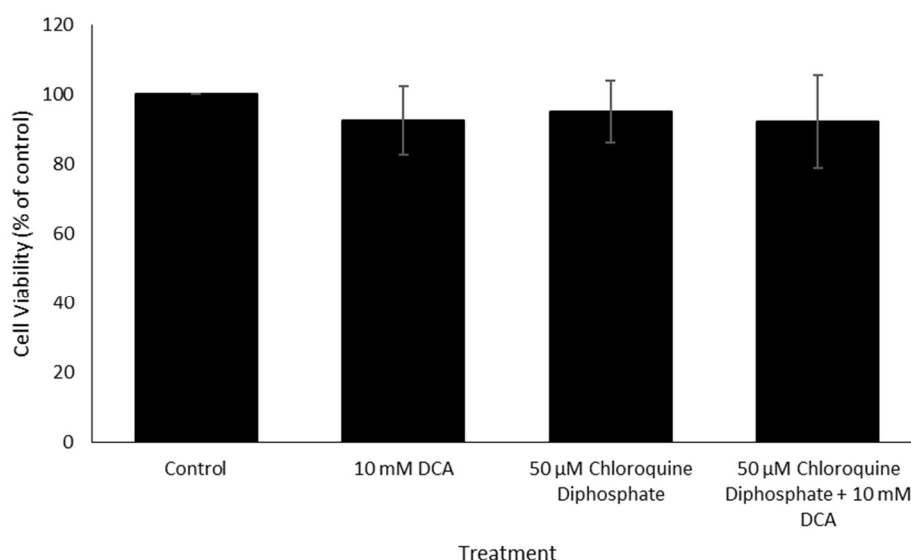


Figure 7.6. The effect of DCA and/or chloroquine diphosphate treatment on SH-SY5Y cell viability. Cells were treated with DCA and/or chloroquine diphosphate at the concentrations indicated for 24 h. Cells were then quantified using an MTS assay *in situ*. Results are means \pm S.D. (n=3).

The preceding experiments were repeated but, this time, cells and conditioned medium were harvested and processed for immunoblotting. Initially, equal amounts of lysate protein were immunoblotted with the anti-p53 antibody. The results (Fig. 7.7.) show that, as previously observed, DCA enhanced p53 levels (108.15 ± 9.70 % increase relative to controls) but chloroquine diphosphate did not alter the levels of this protein. The latter compound also failed to modify the ability of DCA to enhance p53 levels (116.13 ± 27.81 % increase, relative to controls).

The same cell lysates were also immunoblotted with the anti-APP C-terminal antibody to quantify relative levels of APP holoprotein expression. The results (Fig. 7.8.), in this instance, showed no significant change in APP expression.

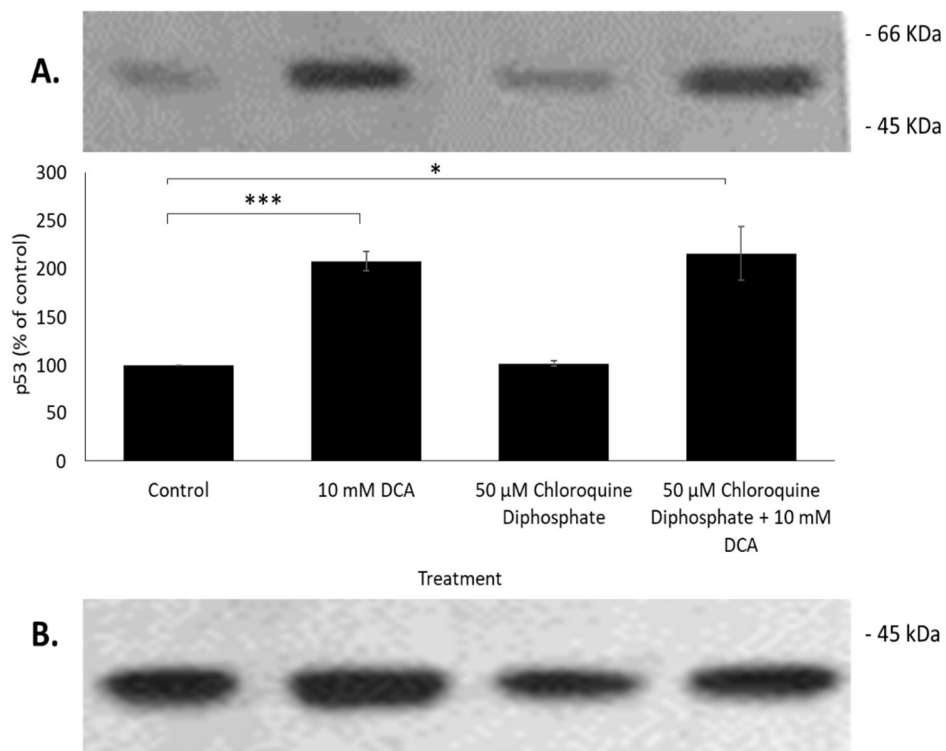


Figure 7.7. The effect of DCA and/or chloroquine diphosphate treatment on the levels of p53 in SH-SY5Y cells. Cells were grown to confluence and then treated with DCA and/or chloroquine diphosphate at the concentrations indicated in UltraMEM for 24 h. Cell lysates were then prepared and immunoblotted using the (A) anti-p53 and (B) anti-actin antibodies as described in the Materials and Methods section. Results are means \pm S.D. (n=3). Significant results are indicated: * = significant at $p \leq 0.05$, *** = significant at $p \leq 0.005$.

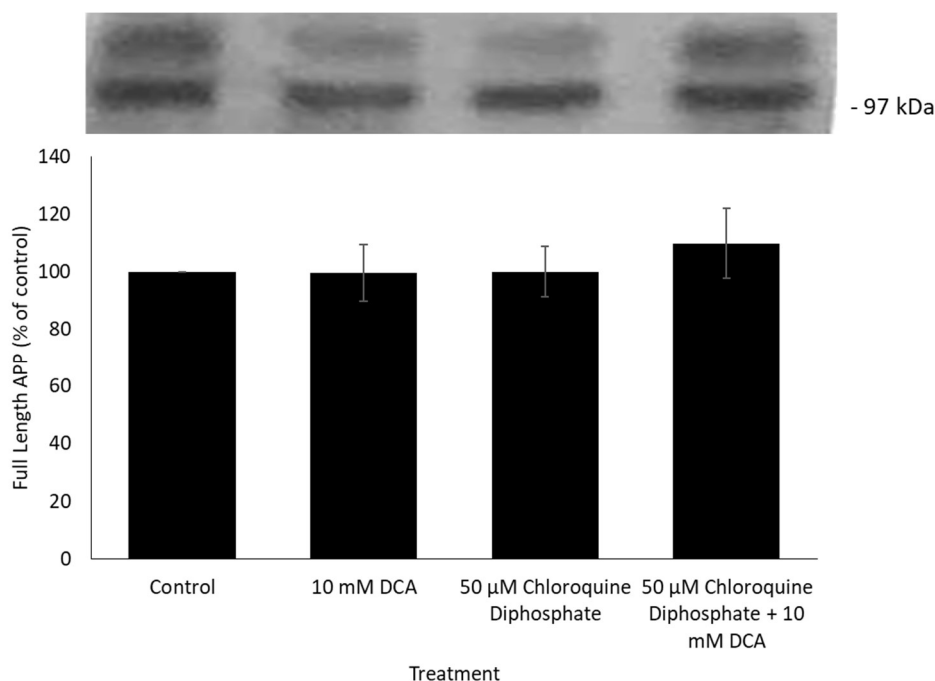


Figure 7.8. The effect of DCA and/or chloroquine diphosphate treatment on the expression of APP in SH-SY5Y cells. Cells were grown to confluence and then treated with DCA and/or chloroquine diphosphate at the concentrations indicated in UltraMEM for 24 h. Cell lysates were then prepared and immunoblotted using the anti-APP C-terminal antibody as described in the Materials and Methods section. Results are means \pm S.D. (n=3).

The concentrated conditioned medium from the preceding experiments was then immunoblotted to quantify the generation of sAPP α and sAPP β . The samples were first immunoblotted with the anti-sAPP α 6E10 antibody and the results (Fig. 7.9.) showed that, as previously observed, DCA enhanced the generation of sAPP α (99.18 ± 34.94 and 129.67 ± 37.64 % increases, respectively, for sAPP695 α and sAPP751/770 α , relative to controls). When used alone, chloroquine diphosphate slightly enhanced sAPP751/770 α generation (75.18 ± 28.31 % increase relative to controls) but had no significant effect on the generation of sAPP695 α . Notably, the co-treatment of cells with both DCA and chloroquine diphosphate did not alter the ability of DCA to promote sAPP α generation.

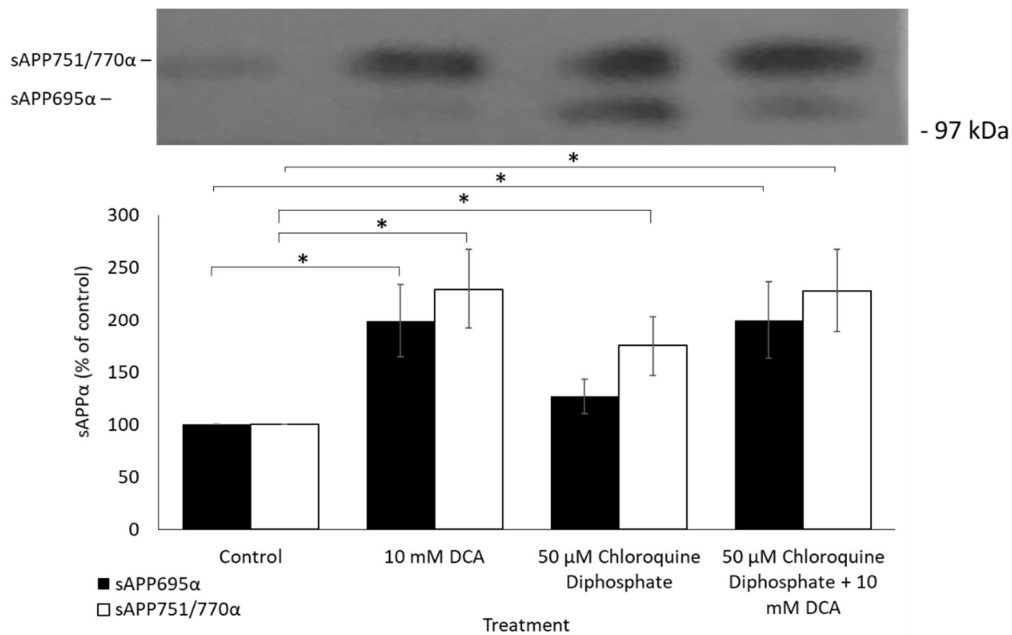


Figure 7.9. The effect of DCA and/or chloroquine diphosphate treatment on the production of sAPP α by SH-SY5Y cells. Cells were treated with DCA and/or chloroquine diphosphate at the concentrations indicated for 24 h. Equal volumes of concentrated medium were then immunoblotted with the anti-sAPP α 6E10 antibody. Results are means \pm S.D. (n=3). Significant results are indicated: * = significant at $p \leq 0.05$.

When the conditioned medium was immunoblotted with the sAPP β antibody the results (Fig. 7.10.) again demonstrated the ability of DCA to inhibit production of this fragment. However, used singularly, chloroquine diphosphate did not alter the generation of this fragment nor did it modify the effect of DCA in this respect.

Collectively, these results indicate that DCA does not alter APP proteolysis via mechanisms linked to cellular mitophagy with the caveat that the latter event was not quantified in the current experiments.

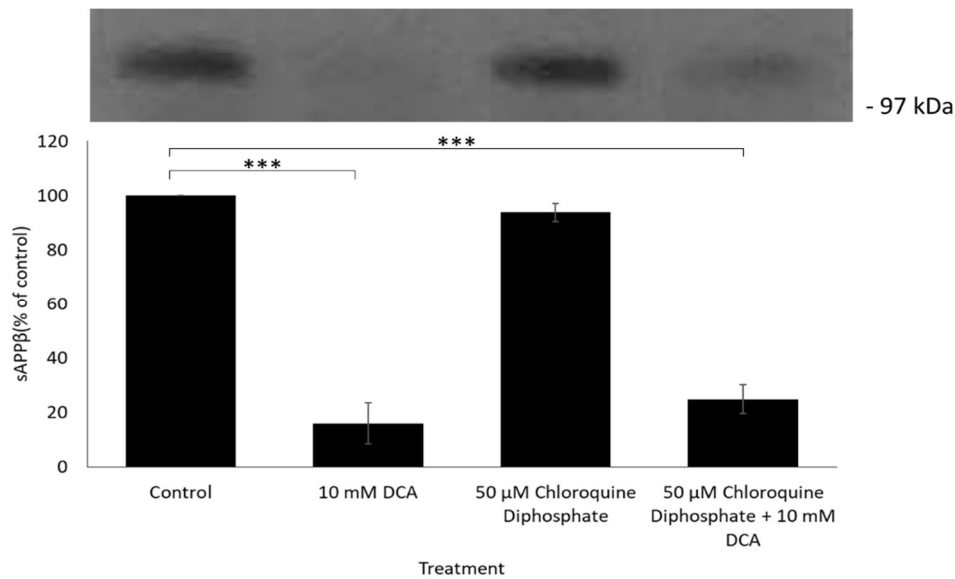


Figure 7.10. The effect of DCA and/or chloroquine diphosphate treatment on the production of sAPP β by SH-SY5Y cells. Cells were treated with DCA and/or chloroquine diphosphate at the concentrations indicated for 24 h. Equal volumes of concentrated medium were then immunoblotted with the anti-sAPP β antibody. Results are means \pm S.D. (n=3). Significant results are indicated: *** = significant at $p \leq 0.005$.

7.2. Oxidative stress and DCA-regulated APP processing.

A previous study by Hassoun and Cearfoss (2011) demonstrated that DCA enhances oxidative stress and ROS production. Given that oxidative stress has also been shown to alter APP proteolysis (Chen *et al.*, 2008; Tamagno *et al.*, 2008; Guglielmotto *et al.*, 2009; Mouton Liger *et al.*, 2012; Kanamaru *et al.*, 2015; Muche *et al.*, 2017) it was, therefore, hypothesised in the current study that DCA might regulate APP proteolysis through the enhancement of oxidative stress. To this end, the abilities of two free radical scavengers, dimethyl sulfoxide (DMSO) and N-acetylcysteine (NAC), to modify the effects of DCA on APP proteolysis were examined.

7.2.1. DMSO.

Initially, SH-SY5Y cells were grown to confluence and treated with UltraMEM containing DCA and/or DMSO (3 mM) for 24 h. This DMSO concentration was adopted as previous studies have demonstrated a free radical scavenging protective effect at similar concentrations (Jorns *et al.*, 1999). Initially, cell viability was determined using the MTS assay as described in the Materials and Methods section. The results (Fig. 7.11.) showed that neither DCA nor DMSO affected viability when the reagents were used singularly. However, when the cells were co-treated with both reagents, there was a 37.36 ± 8.13 % decrease in viability (relative to controls), which was significantly different from controls, DCA alone and DMSO alone.

The same experiments were then repeated on a larger scale and this time cells and conditioned medium were harvested. Cell lysates were prepared and equal amounts of protein from these samples were immunoblotted with the anti-p53 antibody. The results (Fig. 7.12.) show that, as previously observed, DCA enhanced p53 levels (76.72 ± 15.52 %,

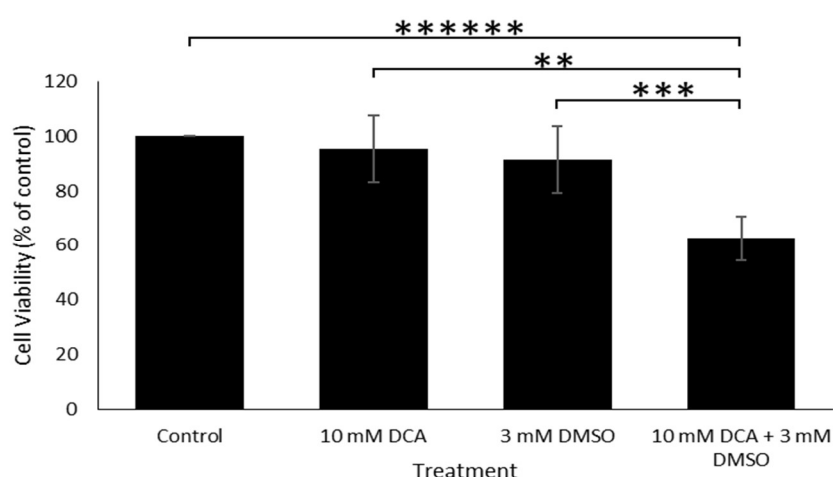


Figure 7.11. The effect of DCA and/or DMSO treatment on SH-SY5Y cell viability. Cells were treated with DCA and/or DMSO at the concentrations indicated for 24 h. Cells were then quantified using an MTS assay *in situ*. Results are means \pm S.D. (n=3). Significant results are indicated: **** = significant at $p \leq 0.0001$.

relative to controls). However, DMSO alone did not impact on p53 levels nor did it modify the ability of DCA to enhance levels of the protein when the two compounds were used in combination (70.85 ± 17.40 % increase, relative to controls).

The cell lysate samples were then immunoblotted with the anti-APP C-terminal antibody to identify any changes in APP holoprotein expression. However, the results showed no significant changes in APP expression in these experiments (Fig. 7.13.).

The effects of DCA and DMSO on APP proteolysis were then assessed by immunoblotting equal volumes of concentrated conditioned medium samples with the anti-APP 6E10 and anti-sAPP β antibodies.

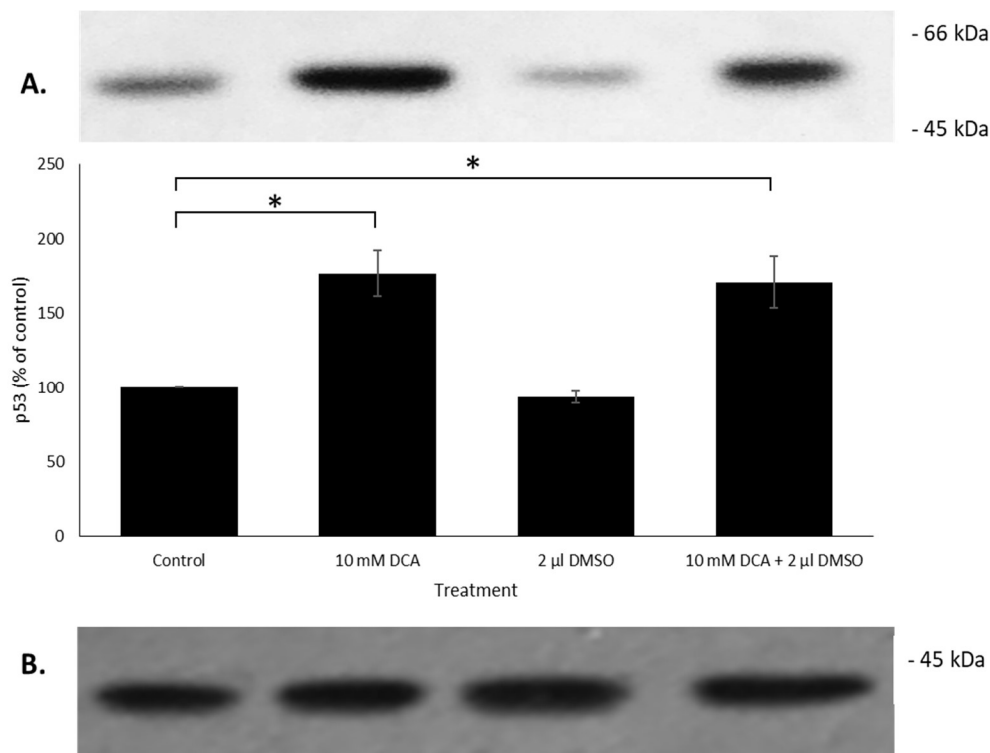


Figure 7.12. The effect of DCA and/or DMSO treatment on the expression of p53 in SH-SY5Y cells. Cells were grown to confluence and then treated with DCA and/or DMSO at the concentrations indicated in UltraMEM for 24 h. Cell lysates were then prepared and immunoblotted using the (A) anti-p53 and (B) anti-actin antibodies as described in the Materials and Methods section. Results are means \pm S.D. (n=3). Significant results are indicated: * = significant at $p \leq 0.05$.

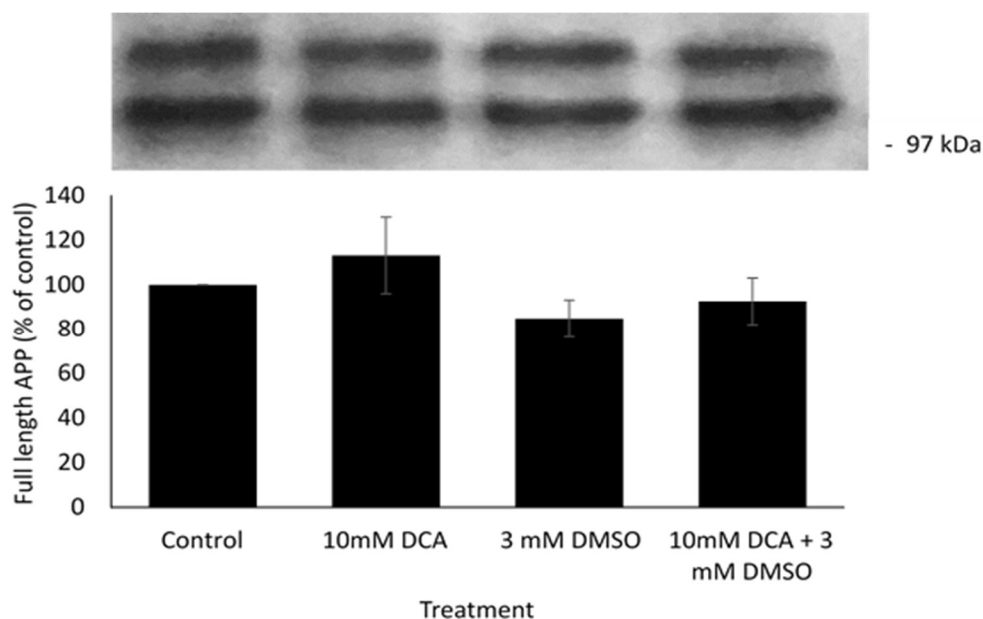


Figure 7.13. The effect of DCA and/or DMSO treatment on the expression of APP in SH-SY5Y cells. Cells were grown to confluence and then treated with DCA and/or DMSO at the concentrations indicated in UltraMEM for 24 h. Cell lysates were then prepared and immunoblotted using the anti-APP C-terminal antibody as described in the Materials and Methods section. Results are means \pm S.D. (n=3).

Initial results using the former antibody (Fig. 7.14A.) showed that DCA enhanced sAPP α production (156.73 ± 39.46 and 112.20 ± 28.01 % increases, respectively, for sAPP695 α and sAPP751/770 α relative to controls). DMSO did not modify the ability of DCA in this respect and used singularly had no effect on the production of these fragments, before and after viability correction (Fig. 7.14B.).

The conditioned medium was then immunoblotted with the anti-sAPP β antibody. The results (Fig. 7.15A.) showed that there were significant decreases in sAPP β production in cells treated with both DCA and DCA with DMSO (66.38 ± 11.72 and 77.50 ± 11.50 % reductions, respectively, relative to controls). These differences remained after correcting for cell viability (Fig. 7.15B.) (66.38 ± 11.72 and 63.77 ± 18.51 %). However, DMSO alone did not alter sAPP β production nor did it modify the ability of DCA to reduce the production of this fragment.

sAPP751/770 α -
sAPP695 α -

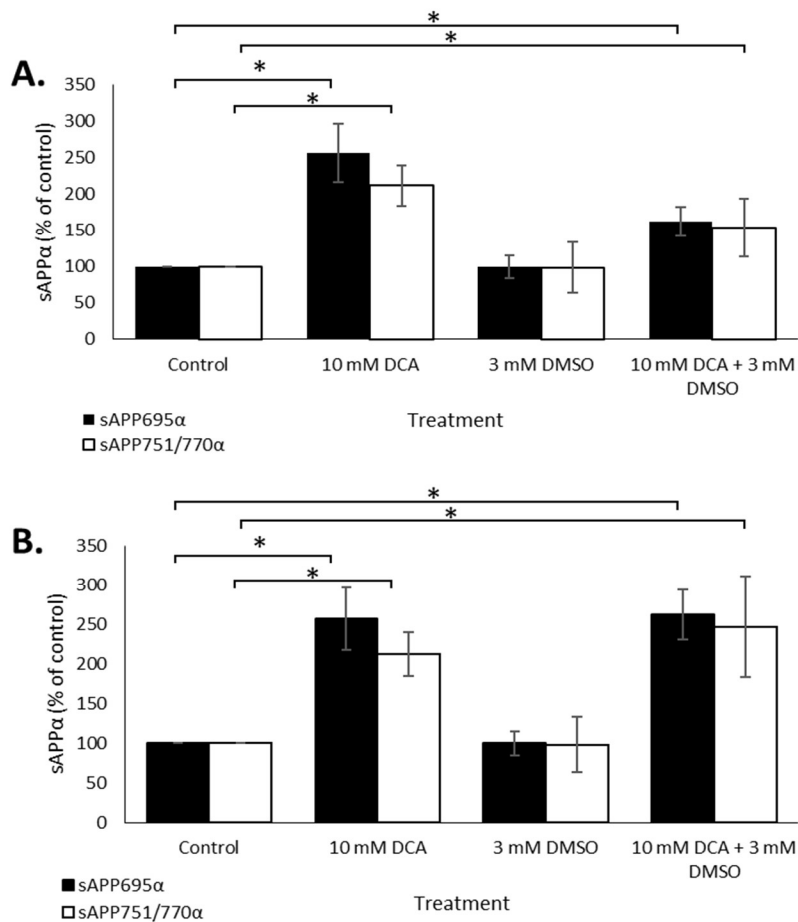
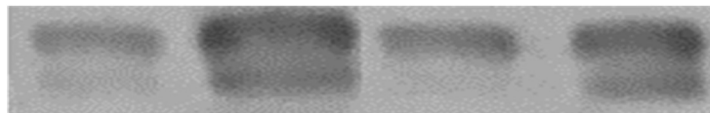


Figure 7.14. The effect of DCA and/or DMSO treatment on the production of sAPP α by SH-SY5Y cells. Cells were treated with DCA and/or DMSO at the concentrations indicated for 24 h. Equal volumes of concentrated medium were then immunoblotted with the anti-sAPP α 6E10 antibody. **(A)** Standard results. **(B)** Viability corrected results. Results are means \pm S.D. (n=3). Significant results are indicated: * = significant at $p \leq 0.05$.

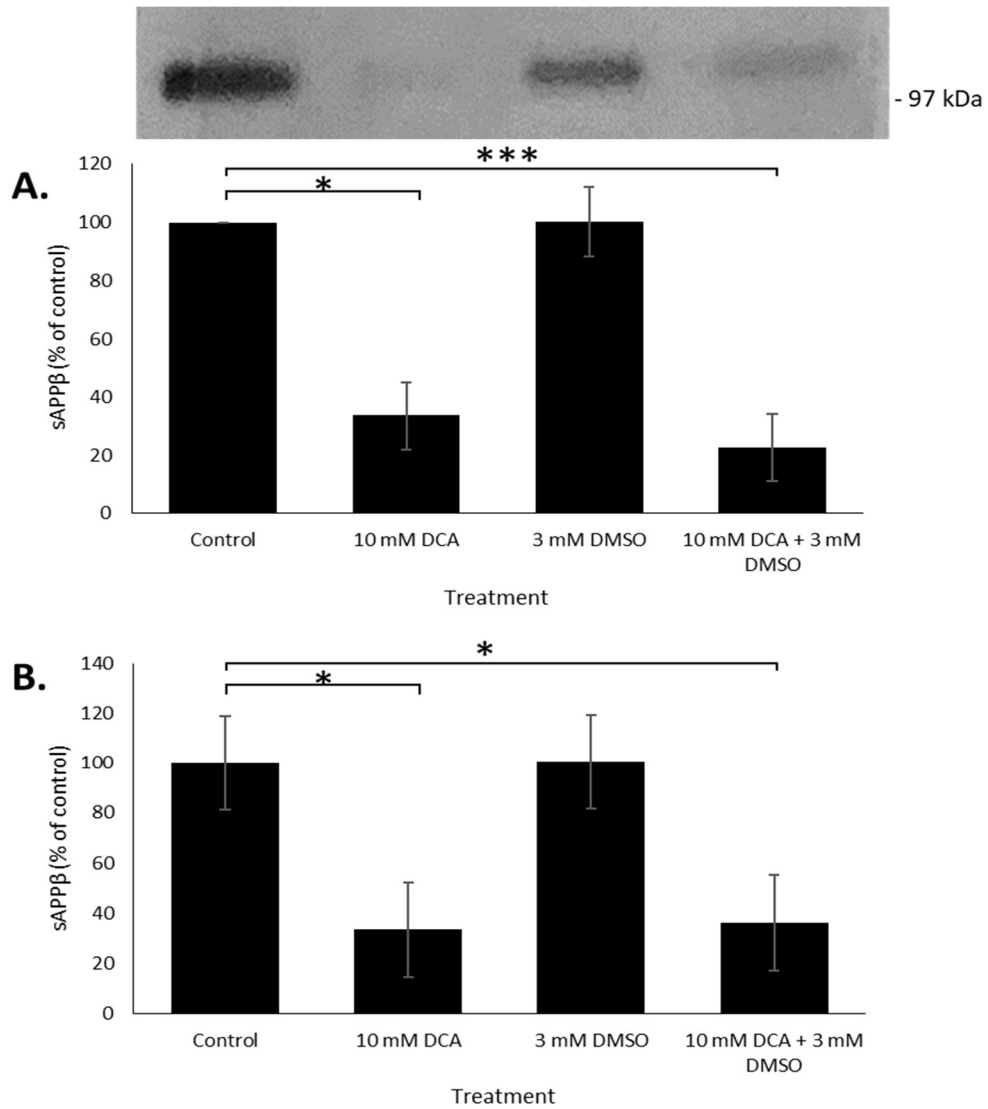


Figure 7.15. The effect of DCA and/or DMSO treatment on the production of sAPP β by SH-SY5Y cells. Cells were treated with DCA and/or DMSO at the concentrations indicated for 24 h. Equal volumes of concentrated medium were then immunoblotted with the anti-sAPP β antibody. **(A)** Standard results. **(B)** Viability corrected results. Results are means \pm S.D. (n=3). Significant results are indicated: * = significant at $p \leq 0.05$, *** = significant at $p \leq 0.005$.

7.2.2. NAC.

To further investigate the potential role of oxidative stress and ROS production as a mechanism by which DCA alters APP proteolysis, a second free radical scavenger, N-acetyl cysteine (NAC), was employed. These experiments were conducted in an identical manner to those in the preceding section except that the DMSO was replaced with 1 mM NAC (concentration adopted from Stephenson *et al.*, 2013).

Cell viability results (Fig. 7.16.) showed that, used singularly, neither DCA nor NAC influenced cell viability. However, as was the case with DMSO, the free radical scavenger NAC, appeared to work synergistically with DCA to reduce cell viability (54.01 ± 6.19 % decrease, relative to controls).

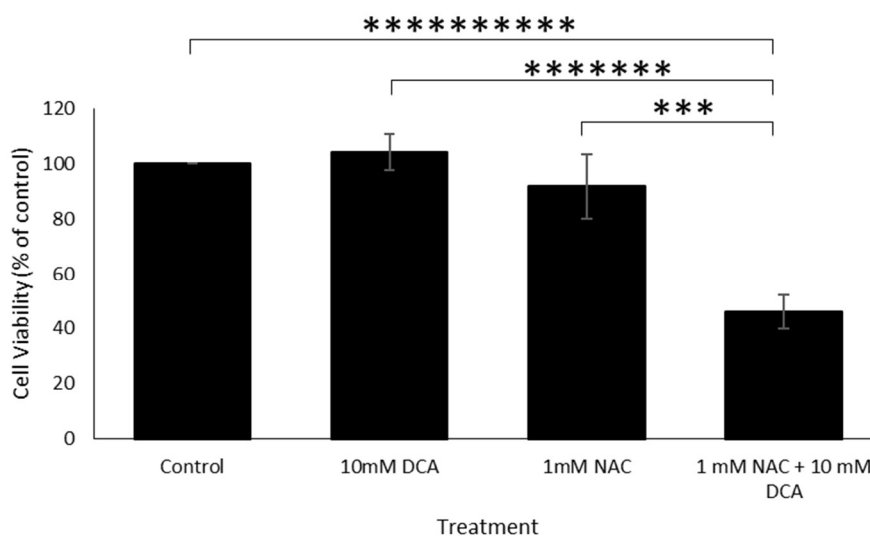


Figure 7.16. The effect of DCA and/or NAC treatment on SH-SY5Y cell viability. Cells were treated with DCA and/or NAC at the concentrations indicated for 24 h. Cells were then quantified using an MTS assay *in situ*. Results are means \pm S.D. (n=3). Significant results are indicated: *** = significant at $p \leq 0.005$, **** = significant at $p \leq 0.00005$, **** = significant at $p \leq 0.000005$.

Next, the effects of NAC and DCA treatment on the levels of p53 in cell lysates were investigated. The results (Fig. 7.17.) showed that DCA alone enhanced p53 levels by 205.97 ± 74.80 %, relative to controls. Interestingly, NAC, used singularly, also enhanced p53 levels (155.94 ± 53.95 %, relative to controls). However, the effects of the two compounds were not additive in that co-treatment of cells enhanced p53 levels to the same extent as either compound used singularly (144.52 ± 35.34 % relative to controls).

The same cell lysates were also immunoblotted with the anti-APP C-terminal antibody. However, the results (Fig. 7.18.) showed no significant changes in APP expression.

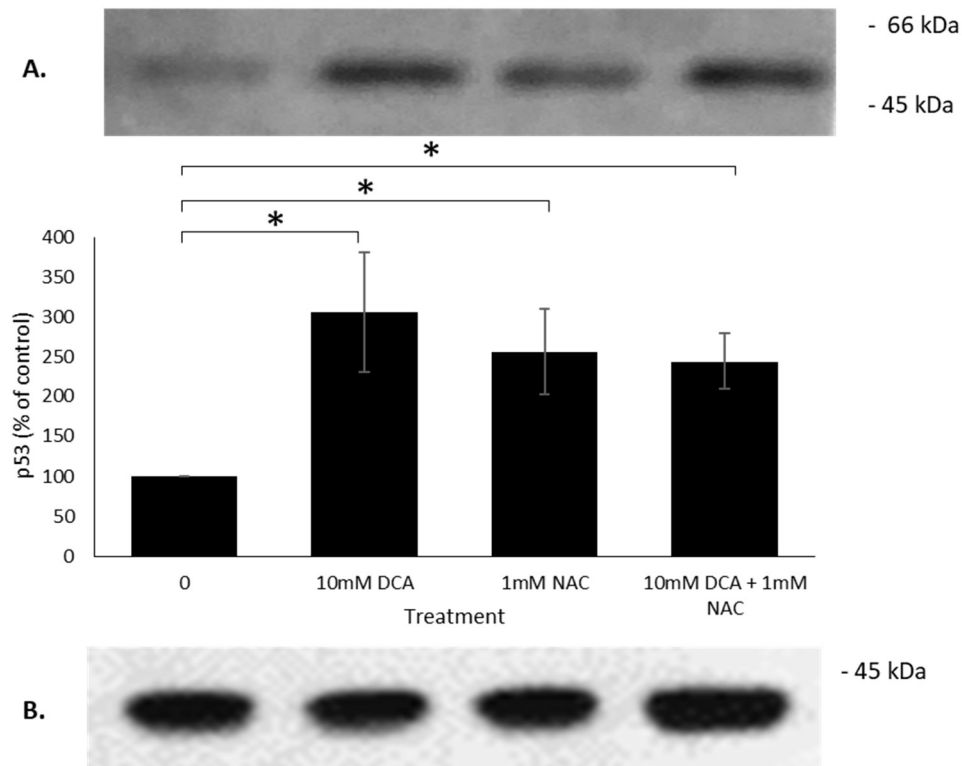


Figure 7.17. The effect of DCA and/or NAC treatment on the levels of p53 in SH-SY5Y cells. Cells were grown to confluence and then treated with DCA and/or NAC at the concentrations indicated in UltraMEM for 24 h. Cell lysates were then prepared and immunoblotted using the **(A)** anti-p53 and **(B)** anti-actin antibody as described in the Materials and Methods section. Results are means \pm S.D. (n=3). Significant results are indicated: * = significant at $p \leq 0.05$.

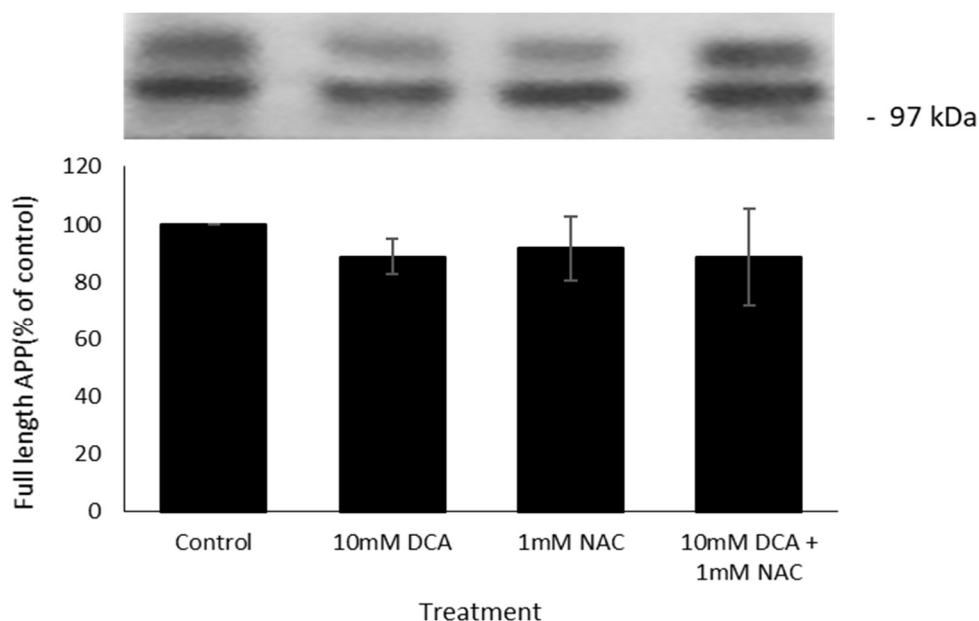


Figure 7.18. The effect of DCA and/or NAC treatment on the expression of APP in SH-SY5Y cells. Cells were grown to confluence and then treated with DCA and/or NAC at the concentrations indicated in UltraMEM for 24 h. Cell lysates were then prepared and immunoblotted using the anti-APP C-terminal antibody as described in the Materials and Methods section. Results are means \pm S.D. (n=3).

Next, the levels of sAPP α in concentrated conditioned medium samples were analysed. The results (Fig. 7.19A.) showed that, as usual, DCA enhanced the production of both sAPP695 α and sAPP751/770 α (44.39 ± 17.84 and 33.38 ± 9.02 % increases, respectively, relative to controls); the significance of these results also remained after adjusting for changes in cell viability (Fig. 7.19B.). These changes were not affected by NAC treatment and, when used on its own, NAC had no effect on the production of sAPP α .

The same conditioned medium samples were then immunoblotted with the anti-sAPP β antibody. The results (Fig. 7.20.) show that, as previously observed, DCA prevented the accumulation of this fragment but NAC had no significant effect in this respect, nor did it alter the ability of DCA to reduce levels of the fragment.

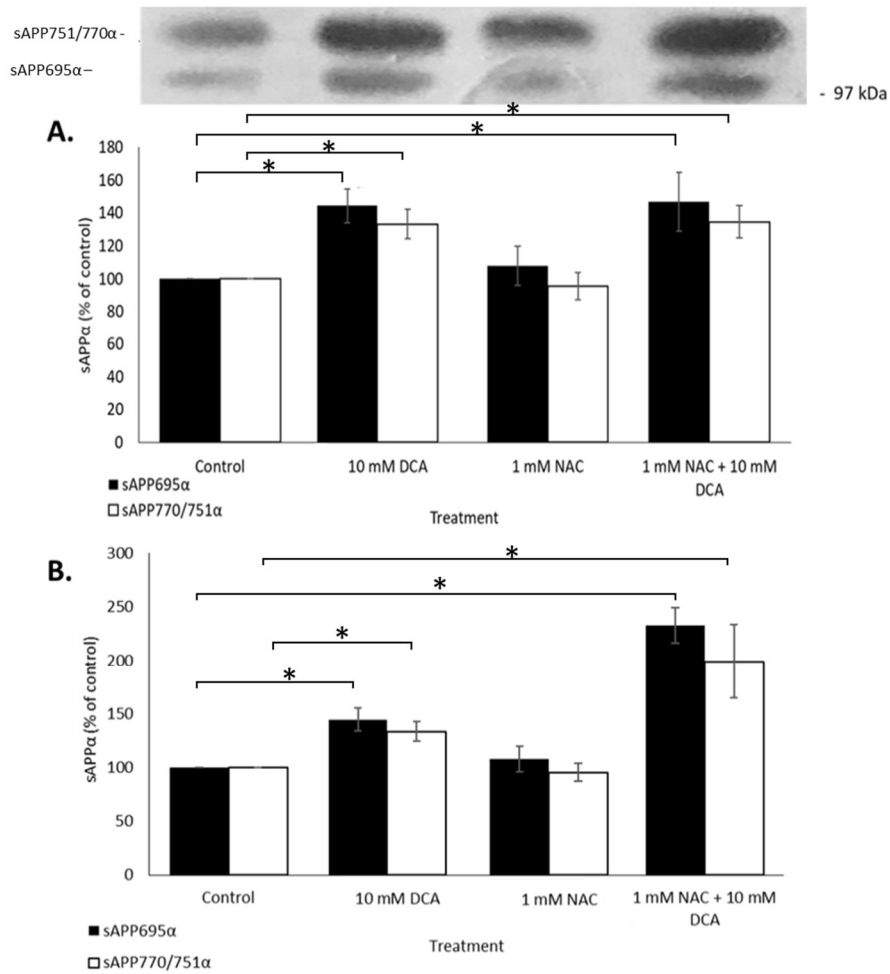


Figure 7.19. The effect of DCA and/or NAC treatment on the production of sAPP α by SH-SY5Y cells. Cells were treated with DCA and/or NAC at the concentrations indicated for 24 h. Equal volumes of concentrated medium were then immunoblotted with the anti-sAPP α 6E10 antibody. **(A)** Standard results. **(B)** Viability corrected results. Results are means \pm S.D. (n=3). Significant results are indicated: * = significant at $p \leq 0.05$.

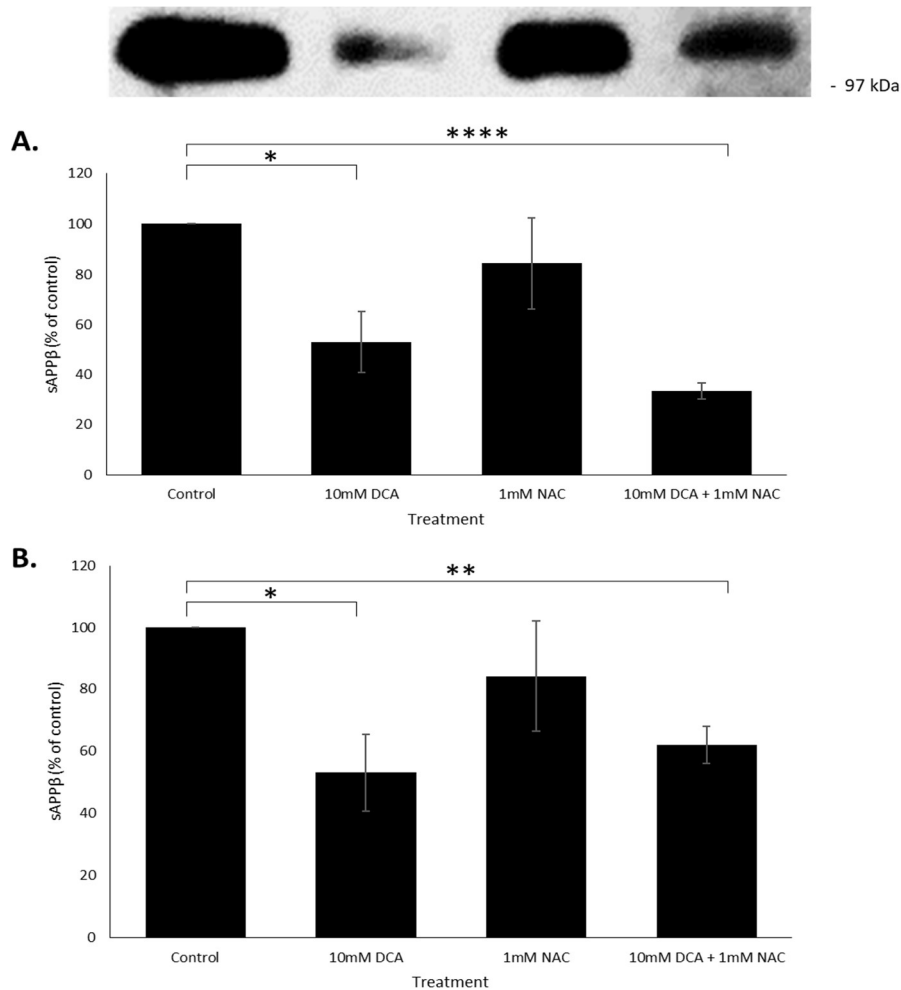


Figure 7.20. The effect of DCA and/or NAC treatment on the production of sAPP β by SH-SY5Y cells. Cells were treated with DCA and/or NAC at the concentrations indicated for 24 h. Equal volumes of concentrated medium were then immunoblotted with the anti-sAPP β antibody. **(A)** Standard results. **(B)** Viability corrected results. Results are means \pm S.D. (n=3). Significant results are indicated: * = significant at $p \leq 0.05$, ** = significant at $p \leq 0.01$, **** = significant at $p \leq 0.001$.

7.3. Summary.

The first part of this chapter investigated the ability of inhibitors of terminal mitophagy (ammonium chloride and chloroquine diphosphate) to modify the effects of DCA on APP proteolysis. Neither of these compounds had any effect on cell viability whether used singularly or in combination with DCA. Similarly, whereas DCA routinely enhanced p53 levels, the two mitophagy inhibitors had no effect in this respect, nor did they modify the ability of

DCA to alter p53 levels. Similarly, neither ammonium chloride nor chloroquine diphosphate had any effect on APP holoprotein expression. When used singularly, both compounds resulted in small but significant increases in sAPP α production. However, neither compound significantly modified the effects of DCA in this respect. Similarly, neither compound altered the ability of DCA to reduce sAPP β production. With the caveat that mitochondrial autophagy was not actually monitored in the current study, it would seem that these inhibitors of the process did not affect the ability of DCA to modify APP proteolysis. As such, these data would seem to support the fact that mitochondrial autophagy is not mechanistically involved in the effects of DCA in this context.

In terms of oxidative stress, it is notable that, whilst neither free radical scavenger (DMSO or NAC) had any impact on cell viability when used singularly, both seemed to work synergistically with DCA to reduce viability. Interestingly though, DMSO did not modify p53 levels whether used singularly or in conjunction with DCA (the latter being compared to treatments using DCA alone). In contrast, NAC enhanced p53 levels when used singularly but did not further enhance the ability of DCA to enhance the levels of this protein. Neither of the two free radical scavengers modified APP expression, sAPP α or sAPP β production, or the ability of DCA to alter production of either fragment. In conclusion, despite minor changes in APP proteolysis, it is unlikely that the effects of DCA in this respect are mechanistically linked to oxidative stress.

Chapter 8.

Discussion.

8. Discussion.

The orphan drug dichloroacetate has recently been shown to minimise the detrimental amyloidogenic APP processing pathway, whilst enhancing the neuroprotective non-amyloidogenic APP processing pathway (Parkin *et al.*, unpublished). However, the mechanism underlying these changes has not been determined. The current project, therefore, aimed to establish how, at the molecular level, DCA exerts its effects on APP proteolysis.

8.1. Characterisation of DCA action in SH-SY5Y cells.

Initially, the effects of DCA on cell viability, p53 and APP expression/proteolysis were fully characterised in SH-SY5Y cells. The drug did not reduce cell viability at either of the two (10 or 20 mM) concentrations used (Fig. 3.1.), contrasting with previous reports (Pajuelo-Regura *et al.*, 2015) which demonstrated significant decreases in SH-SY5Y cell viability even at 5 mM DCA. Whilst there is no obvious explanation for these differences, factors such as the degree of cell confluency may dictate the sensitivity of SH-SY5Y cells to DCA toxicity (entirely confluent cells were used in the current study). It is notable, however, that slight decreases in viability were observed when using the alternate Trypan blue method for determining cell viability (Fig. 3.1.), suggesting that some cells may have undergone apoptosis, detached from the flask base and been replaced by other cells in the confluent layer. This may also be indicated by the fact that DCA appeared to enhance p53 expression in the current study, an observation that corroborates previous reports (Agnoletto *et al.*, 2014).

The most interesting results here are that DCA enhanced non-amyloidogenic and inhibited amyloidogenic APP processing (Figs. 3.4, 3.5, 3.8, and 3.9.). Given that apoptosis has previously been associated with the amyloidogenic processing of APP and A β generation (reviewed by Obulesu and Lakshmi, 2014), these observations are somewhat counterintuitive in this respect.

8.2. pH as a possible mediator of DCA action.

Sodium dichloroacetate is a conjugate base of dichloroacetic acid and, as was observed in the current study, might be expected to increase the pH of conditioned cell culture medium (Fig. 3.10.). Alternatively, previous work has attributed the DCA-mediated increases in extracellular and intracellular pH to reductions in lactate levels due to PDH stimulation (Robey and Martin, 2011; Albatany *et al.*, 2018). Regardless of the cause of the pH alteration, however, the current study hypothesised that such a change might be responsible for the observed effects of DCA on APP proteolysis. To this end, the effects of two related compounds (sodium acetate and acetic acid) on pH and APP proteolysis were examined.

As would be expected for another conjugate base, sodium acetate resulted in similar increases in the pH of conditioned medium to those affected by DCA (Fig. 3.12.) and only minor decreases in cell viability (Fig. 3.13.). It is interesting to note that sodium acetate actually decreased cellular p53 levels (Fig. 3.15.), compared to the enhanced levels caused by DCA. This would indicate that DCA affected the levels of the protein via a mechanism unrelated to pH change; possibly linked to PDH inhibition, promotion of mitochondrial respiration/function and ROS production (Wong *et al.*, 2008). However, the fact remains that

sodium acetate actually impaired p53 expression, possibly by increasing the alkalinity of the extracellular solution, although there is scant information in the literature to support or refute this hypothesis.

In contrast to both DCA and sodium acetate, the treatment of cells with acetic acid led to the expected acidification of medium (Fig. 3.19.) with an associated decrease in cell viability (Fig. 3.20.). Notably, however, the levels of p53 were decreased rather than increased (Fig. 3.22.), suggesting that the observed decreases in cell viability were due to necrotic rather than apoptotic cell death, as the former form is not commonly associated with p53 (reviewed by Ying and Padanilam, 2016).

Turning to the effects of the three compounds on APP expression, it was notable that both DCA and acetic acid enhanced expression despite having opposing effects on pH (Figs. 3.2. and 3.21.), whilst sodium acetate did not alter APP expression (Fig. 3.14.) despite affecting pH in the same manner as DCA. Previous observations (Schrader-Fischer *et al.*, 1996) suggested that alkalinising agents may result in an accumulation of APP, which corroborates the DCA results but contrasts with the sodium acetate results in the current study. As these compounds had a similar effect on pH but opposing effects on APP expression, this clearly demonstrates that any observed effects of DCA upon APP expression in this study are not simply correlated to changes in pH.

As far as non-amyloidogenic APP processing is concerned, both alkalinising agents used in the current study enhanced sAPP α production by cells (Figs. 3.4. and 3.16.), albeit the changes with sodium acetate were not in the same order of magnitude as with DCA. This suggests that the effect of DCA in this respect may be mediated by enhanced pH, agreeing with previous observations (Schrader-Fischer *et al.*, 1996) which suggested alkalinising

treatments increased non-amyloidogenic APP processing. However, it should be noted that acetic acid also enhanced sAPP α production in the current study (Fig. 3.23.), suggesting a more complex relationship between pH and non-amyloidogenic APP processing.

Regarding amyloidogenic APP processing, the alkalisising agents had opposing effects, with sodium acetate increasing and DCA reducing sAPP β production (Figs. 3.5. and 3.17.). Previous investigations (Schrader-Fischer *et al.*, 1996) reported reduced amyloidogenic processing following alkalisising treatments, corroborating the DCA results but again contrasting with sodium acetate results in the current study. These differences may be explained by differential treatment times (4 h in the case of Schrader-Fischer *et al.* and 24 h in the current study), or the effects of different pH-modulating compounds (Schrader-Fischer *et al.* used ammonium chloride).

An increase in sAPP β production was also observed following acetic acid treatment in the current study (Fig. 3.24.). This is consistent with previous studies which reported enhanced amyloidogenic processing following acidifying treatments, attributed to optimal BACE-1 activity at pH 6 (Brown *et al.*, 1998; Lin *et al.*, 2000; Xiang *et al.*, 2010).

Overall, as sodium acetate and acetic acid had similar effects on APP proteolysis (despite having opposing effects on pH), and DCA and sodium acetate had different effects on APP proteolysis (despite having similar effects on pH), it is clear that the effects of DCA on APP expression/proteolysis are not simply the consequence of increased extracellular pH.

8.3. The interaction between p53 and APP expression/proteolysis.

As DCA enhanced p53 levels in the current study, the ability of RITA to upregulate levels of this protein and alter APP proteolysis in SH-SY5Y cells was examined. As would be expected in cells with enhanced levels of apoptotic-regulating p53, decreases in viability were observed at RITA concentrations $\geq 10 \mu\text{M}$ (Fig. 4.1.). In contrast, a previous report (Burmakin *et al.*, 2013) observed significant decreases in SH-SY5Y viability at just $1 \mu\text{M}$ RITA. These conflicting results, however, may be due to several differing factors, such as total treatment time (48 h used by Burmakin *et al.* and 24 h used in the current study) and degree of confluency (cells treated at the point of seeding by Burmakin *et al.* compared to 100 % confluency in the current study).

Interestingly, RITA and DCA appeared to act synergistically to dramatically decrease viability (Fig. 4.7.). This might be explained by the additive increase in p53 levels following co-treatment with the two compounds (Fig. 4.8.).

RITA did not alter APP expression (Fig. 4.3.) or modify the DCA-associated changes in this respect (Fig. 4.9.). This seems to contrast with previous work by Cuesta *et al.* (2009), who observed increased APP expression following p53 accumulation. However, the authors treated SH-SY5Y cells with camptothecin, leading to a much stronger accumulation and activation of p53 (10-fold increase in p53 compared to the 2/3-fold increase with RITA and/or DCA treatments in the current study). In the context of the current study, as RITA treatments did not enhance APP expression despite enhancing p53 levels to a similar degree as DCA, it is unlikely that the latter compound regulates APP expression through the enhancement of p53 levels.

When the effects of RITA on the proteolysis of APP were investigated, no significant differences in sAPP α or sAPP β production were observed (Figs. 4.4. and 4.5.). Interestingly, Checler *et al.* (2010) suggested that increased p53 expression regulated γ -secretase activity, with enhanced PS1 and PEN-2 expression and transactivation of several members of the complex. Although these observations could explain the parallel increases in p53 and A β aggregation observed within the brains of AD patients (Ohyagi *et al.*, 2005), the current study suggests that enhancing p53 levels does not mediate APP proteolysis or modify the DCA-associated changes (Figs. 4.10. and 4.11.).

It was noted that the sAPP β blots from the RITA experiments in the current study contained an increase in an unknown band located at 30 kDa (Fig. 4.6A.). It was hypothesised that this fragment might be generated from a cleavage of sAPP β , resulting in the production of two fragments; a C-terminal 30 kDa fragment (containing the sAPP β antibody epitope) and an N-terminal 70 kDa fragment. Although previous literature has suggested alternative pathways of APP proteolysis (Andrew *et al.*, 2016), a 30 kDa sAPP β fragment has not been reported. Upon immunoblotting with the 22C11 antibody, no corresponding 70 kDa N-terminal fragment was observed (Fig. 4.6B.) but numerous smaller fragments around 15-20 kDa were detected following RITA treatment. This raised the possibility that the N-terminal fragment produced may have been rapidly degraded and, therefore, not detected as an intact 70 kDa band.

In the current study, siRNA experiments were also employed to examine the effects of p53 depletion on APP expression/proteolysis. Interestingly, siRNA treatment almost completely ablated cellular p53 levels in the absence of DCA treatment. However, when cells were subjected to p53 siRNA treatment followed by treatment with DCA, control levels of the

p53 protein were restored (Fig. 4.16.). A prior investigation (Agnolotto *et al.*, 2014) demonstrated increased p53 levels following DCA treatment, suggesting it was a result of enhanced TP53 gene transcription. In the current study, however, *de novo* production of p53 was inhibited and yet levels still increased, suggesting that DCA enhances levels of the protein via a post-translational mechanism. Several other drugs have been shown to enhance p53 levels by hindering the degradation of the protein; for example, Nutlins hinder degradation by preventing interaction between p53 and MDM2, whilst MDM2 E3 ubiquitin ligase inhibitors prevent ubiquitinylation of p53 and hence prevent degradation via the proteasome (Wang and Sun, 2010). Therefore, it is possible that DCA may also control p53 at the level of turnover.

Depleting p53 expression in the current study did not affect APP expression, with or without DCA treatment (Fig. 4.17.). This contrasts with previous work (Cuesta *et al.*, 2009), which demonstrated an increase in APP promoter activity following the expression of a dominant-negative p53 mutant. Furthermore, p53 siRNA did not mediate the DCA-associated changes in APP proteolysis products (Figs. 4.18. and 4.19.). However, as DCA treatments returned the levels of p53 to control levels following p53 siRNA treatments, the contribution of lower p53 levels on the metabolism of APP cannot be fully assessed.

Overall, the current study indicates that p53 is not responsible for the changes in APP proteolysis mediated by DCA.

8.4. The association between lactic acid, pyruvate and APP processing.

In the current study, cells were treated with LDH inhibitors to alter the levels of lactate and pyruvate and determine the subsequent effects on APP expression/proteolysis. Whilst

the GSK2837808A inhibitor had no effect on SH-SY5Y cell viability and p53 levels (Figs. 5.1. and 5.2.), FX11 treatment dramatically reduced viability at higher concentrations ($\geq 10 \mu\text{M}$) and increased p53 levels (Figs. 5.6. and 5.7.). These findings suggest that LDH-A inhibition stimulates apoptosis, agreeing with previous observations that LDH-A inhibition blocks aerobic glycolysis (Brighenti *et al.*, 2017) and stimulates oxidative stress and cellular death (Le *et al.*, 2010). As these toxic effects were not observed in cells treated with the GSK2837808A inhibitor, this suggests that the inhibition of LDH-B possibly outweighed the effects of LDH-A inhibition and protected cells from viability changes.

GSK2837808A-treated cells exhibited decreased sAPP α production, whilst FX11-treated cells exhibited increased sAPP α production at sub-toxic (1 μM) levels of the inhibitor and decreased production at toxic (10 μM) levels (Figs. 5.4. and 5.9.). Comparatively, sAPP β production was enhanced at all concentrations $\geq 10 \text{ nM}$ in GSK2837808A-treated cells, but not altered in FX11 cells (Figs. 5.5. and 5.10.). Therefore, as with DCA, the results are somewhat counterintuitive in terms of apoptosis, with no viability differences observed at sAPP β -enhancing GSK2837808A concentrations but apoptosis observed in FX11 treatments where sAPP β was not altered. It is also interesting to note that amyloidogenic processing of APP only increased when both LDH-A and LDH-B were inhibited, suggesting that inhibition of LDH-B was responsible for these changes. Whereas previous studies have reported enhanced LDH-A activity in AD patients (Bigl *et al.*, 1999) and A β resistance in patients with enhanced LDH activity (Soucek *et al.*, 2003), our results demonstrate a complex interaction between LDH-A, LDH-B and the processing of APP.

Cells were next treated with pyruvate and the effects on APP expression/proteolysis were characterised. Viability was dramatically reduced in cells treated with pyruvate at higher

concentrations (Fig. 5.11.), correlating with increased p53 levels (Fig. 5.12.), suggesting enhanced apoptosis. A previous study by Wszelaki and Melzig (2013) actually identified a protective effect of pyruvate against neurotoxicity in SH-SY5Y cells and saw no viability changes up to 1 mM pyruvate. However, toxic concentrations identified in the current study were much higher (50 and 100 mM), and 10 mM pyruvate actually enhanced viability, agreeing with the suggested protective role of the compound.

In terms of APP proteolysis products, pyruvate yielded the opposite effects to those of DCA, with reduced sAPP α production following viability correction and increased sAPP β production before viability correction (Figs. 5.14. and 5.15.). It was therefore hypothesised that DCA may alter APP processing by enhancing PDH activity and consequentially lowering pyruvate levels. However, as no prior studies have investigated a link between the levels of pyruvate and APP expression/proteolysis, this hypothesis cannot be confirmed nor refuted.

The next stage of the current study involved the treatment of cells with lactic acid in the presence of DCA and the characterisation of the resultant effects on APP expression/proteolysis. Very slight but significant decreases in viability were observed in cells treated for 24 h with DCA and lactic acid (at both 6 and 12 mM concentrations), and 12 mM lactic acid alone (Fig. 5.16.). This contrasts with prior observations (Xiang *et al.*, 2010) in which no viability differences were obtained following 6 h treatments with lactic acid at the same concentrations.

Interestingly, although lactic acid did not impact on the DCA-mediated increase in p53, cells treated with lactic acid alone also exhibited enhanced p53 levels (Fig. 5.17.). No prior studies have directly demonstrated an increase in p53 expression following lactic acid treatment and so these results cannot be confirmed nor refuted.

In terms of APP, lactic acid did not alter the DCA-mediated effects upon APP expression and proteolysis (Figs. 5.18-5.20.). Furthermore, neither APP expression nor sAPP α production were altered by lactic acid treatment, contrasting with a previous report (Xiang *et al.*, 2010) in which lactic acid increased levels of APP and A β , and decreased levels of sAPP α . However, as this paper had treated cells for 6 h with lactic acid (rather than 24 h), it was hypothesised that lactic acid may have been metabolised after 6 h, losing the effects on APP. Therefore, the studies in the current report were repeated over a 6 h time course. Again, very small but significant decreases in viability were observed in cells treated with lactic acid alone or in combination with DCA (Fig. 21.), accompanied by p53 level increases (Fig. 5.22.). This contrasts with the viability data from Xiang *et al.* (2010), who identified no viability changes at the same concentrations. However, the data presented in this latter paper did demonstrate a general trend for decreasing viability with large error bars which may have prevented the identification of significance.

The 6 h time course lactic acid experiments in the current study demonstrated a decreased cellular generation of sAPP α after lactic acid treatment akin to that observed by Xiang *et al.* (2010). However, it is notable that the latter authors did not identify and adjust their result for cell viability; when the results in the current study were adjusted in this respect, any effect of lactic acid on sAPP α generation lost significance. This may have resulted in an artefactual lactic acid-mediated effect on APP proteolysis.

Overall, these results suggest complex interactions between LDH activity, lactic acid, pyruvate and APP processing. As pyruvate treatment appeared to enhance amyloidogenic processing in the current study, DCA may mediate APP proteolysis via enhancing PDH activity

and thereby lowering pyruvate levels. Future studies should, therefore, investigate if pyruvate pre-treatment circumvents the DCA-mediated effects on APP proteolysis.

8.5. DCA and APP localisation.

In the current study, cells were treated with DCA and the effects on APP localisation were investigated. Control cells (Fig. 6.3.) contained APP within the early endosomes and the cis-Golgi, agreeing with previous papers (Greenfield *et al.*, 1999; Haass *et al.*, 2012). However, very minimal APP was observed within the lysosomes, contrasting with previous work which demonstrated that APP localises within the lysosomes before it is degraded (Haass *et al.*, 1992; Lorenzen *et al.*, 2010). However, Haass *et al.* prevented the breakdown of the APP within the lysosomes with leupeptin, and Lorenzen *et al.* used APP-transfected cells. Therefore, APP in the current study may have been rapidly degraded following internalisation in the lysosome or the amount may have been too small to be detected.

When cells were treated with batimastat (which prevents APP shedding) (Fig. 6.4.), a much stronger localisation of the APP within the endosome was observed. Furthermore, these cells were the only samples which identified APP within the lysosomes, potentially explained by less APP shedding via α -secretase leading to more reinternalisation.

Finally, when cells treated with DCA (Fig. 6.5.) were compared to control cells (Fig. 6.3.), the results showed a marginal decrease in APP within the cis-Golgi. However, no other significant changes in APP location were identified, suggesting that DCA does not mediate APP processing by altering the subcellular localisation of the APP secretase substrate.

It is worth noting that the effect of DCA on BACE1 localisation was not investigated in the current study due to the exceedingly low endogenous BACE1 levels in SH-SY5Y cells. Although this issue may have been overcome by using BACE1-overexpressing SH-SY5Y cells, previous work in our laboratories (Parkin *et al.*, unpublished) demonstrated that BACE1 overexpression negated the effects of DCA.

8.6. DCA-induced mitophagy and APP expression/proteolysis.

In the current study, cells were treated with DCA in the presence of autophagy inhibitors (adopted from Pajuelo-Reguera *et al.*, 2015) to investigate the role of this phenomenon in the DCA-regulated proteolysis of APP. Viability decreases were observed in cells treated with both 10 mM ammonium chloride and 50 μ M chloroquine, both alone and in combination with DCA (Figs. 7.1. and 7.6.). However, no significant increases in p53 levels were observed in cells treated with either inhibitor (Figs. 7.2. and 7.7.), potentially suggesting that these viability differences were due to necrosis, as this form of cell death is not commonly associated with changes in p53 levels (reviewed by Ying and Padanilam, 2016).

Cellular treatments with ammonium chloride or chloroquine also revealed no effects upon APP expression/proteolysis (Figs. 7.3-7.5. and 7.8-7.10.), contrasting with previous studies where autophagy inhibition reduced A β production (Cole *et al.*, 1989; Siman *et al.*, 1993). These differences, however, may be due to several factors; for example, these papers used cell lines overexpressing APP (PC12 and HCT293), which were treated with higher ammonium chloride concentrations (50 mM) for longer treatment periods (48 h). The current results, therefore, suggest that the mechanism by which DCA mediates APP proteolysis is not

related to mitochondrial autophagy, with the caveat that the ability of ammonium chloride and chloroquine to impair autophagy in the current study was not qualified.

8.7. ROS production as a potential mediator of DCA-regulated APP proteolysis.

In the current study, the free radical scavengers DMSO and NAC both demonstrated synergistic cytotoxicity when used in combination with DCA (Figs. 7.11. and 7.16.). However, cells co-treated with DCA and DMSO or NAC exhibited similar increases in p53 levels to those treated with DCA alone (Figs. 7.12. and 7.17.), suggesting that the synergistic toxicity was a result of necrosis rather than apoptosis.

Neither DMSO nor NAC altered APP expression/proteolysis or modified the effects of DCA in these respects (Figs. 7.13-7.15. and 7.18-7.20.) which leads to the conclusion that DCA does not mediate such processes via oxidative stress and ROS production.

8.8. Concluding remarks and future perspectives.

In the current study, the possible mechanisms behind the DCA-mediated changes in APP proteolysis have been investigated. Although the mechanism has not been identified, we have demonstrated that these changes are not attributed to changes relating to culture medium pH, p53 activity, lactic acid/pyruvate metabolism, mitochondrial morphology, BACE1 activity, APP localisation or production of ROS. However, several mechanistic possibilities still

require further investigation, such as the effect of DCA on BACE1 localisation and the effects of pyruvate and DCA co-treatment on the proteolysis of APP.

Additionally, this current study has led to several interesting results in relation to possible cancer treatments. For example, the cytotoxic synergism between RITA and DCA and their additive effects on p53 levels, the potential post-translational effects of DCA on p53, the induction of apoptosis and p53 expression via LDH-A inhibition, the enhancement of p53 expression via lactic acid, and the synergistic effects of DMSO/NAC and DCA on cytotoxicity.

Overall, the findings in the current study (and previous unpublished data) have demonstrated that DCA enhances non-amyloidogenic processing and reduces amyloidogenic processing. Therefore, future investigations into the mechanism could still provide key insights into APP processing.

Chapter 9.

Appendices.

9. Appendices.

9.1. Appendix I.

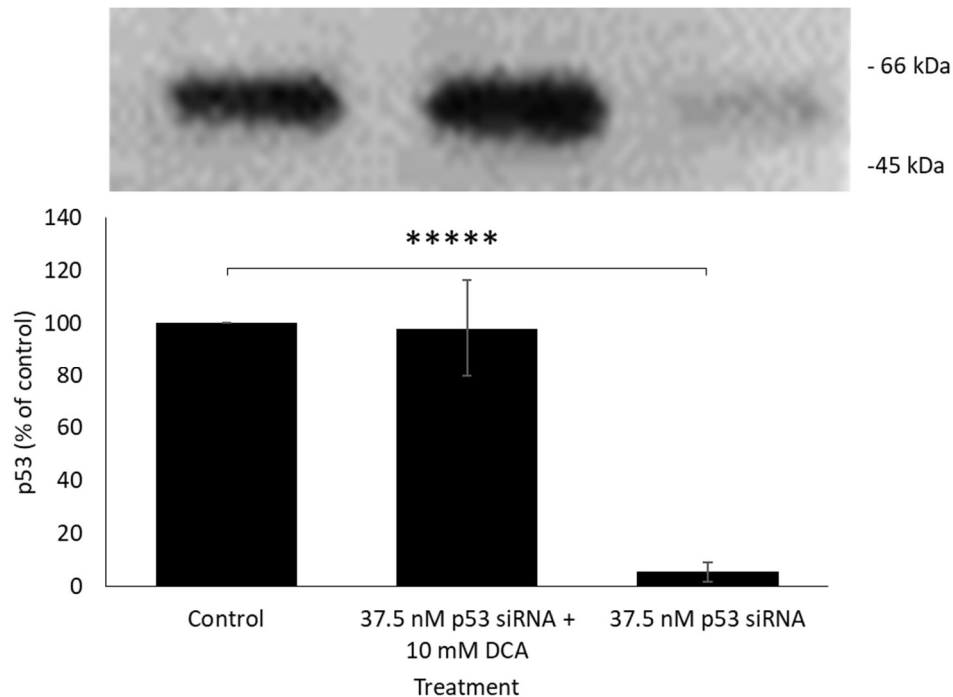


Figure 8.1. DCA circumvents the decrease in p53 expression mediated by p53 siRNA. SH-SY5Y cells were grown to 70 % confluence and then transfected with p53 siRNA as described in the Materials and Methods section. After a penultimate 48 h incubation in complete growth medium, the cells were incubated for a further 24 h in UltraMEM in the absence or presence of 10 mM DCA. Equal amounts of cell lysate protein were then subjected to SDS-PAGE and immunoblotting using anti-p53 (see Materials and Methods). Results are means \pm S.D. (n=3). Significant results are indicated: **** = significant at $p \leq 0.0005$.

Chapter 10.

References.

10. References.

- Acevedo, K. M., Hung, Y. H., Dalziel, A. H., Li, Q. X., Laughton, K., Wikhe, K., Rembach, A., Roberts, B., Masters, C. L., Bush, A. I. & Camakaris, J. 2011. Copper Promotes the Trafficking of the Amyloid Precursor Protein. *Journal of Biological Chemistry*, 286(10), 8252-8262.
- Agnoletto, C., Melloni, E., Casciano, F., Rigolin, G. M., Rimondi, E., Celeghini, C., Brunelli, L., Cuneo, A., Secchiero, P. & Zauli, G. 2014. Sodium Dichloroacetate Exhibits Anti-Leukemic Activity in B-Chronic Lymphocytic Leukemia (B-CLL) and Synergizes with the P53 Activator Nutlin-3. *Oncotarget*, 5(12), 4347-4360.
- Aguayo-Ortiz, R. & Dominguez, L. 2017. Generation of Amyloid-Beta Peptides by Gamma-Secretase. *Israel Journal of Chemistry*, 57(7-8), 574-585.
- Aguayo-Ortiz, R. & Dominguez, L. 2018. Simulating the Gamma-Secretase Enzyme: Recent Advances and Future Directions. *Biochimie*, 147, 130-135.
- Albatany, M., Li, A., Meakin, S. & Bartha, R. 2018. Dichloroacetate Induced Intracellular Acidification in Glioblastoma: In Vivo Detection Using Acid-Cest Mri at 9.4 Tesla. *Journal of Neuro-Oncology*, 136(2), 255-262.
- Alvarez, G., Ramos, M., Ruiz, F., Satrustegui, J. & Bogonez, E. 2003. Pyruvate Protection against Beta-Amyloid-Induced Neuronal Death: Role of Mitochondrial Redox State. *Journal of Neuroscience Research*, 73(2), 260-269.
- Andrew, R. J., Kellett, K. A. B., Thinakaran, G. & Hooper, N. M. 2016. A Greek Tragedy: The Growing Complexity of Alzheimer Amyloid Precursor Protein Proteolysis. *Journal of Biological Chemistry*, 291(37), 19235-19244.
- Araki, W. 2016. Post-Translational Regulation of the Beta-Secretase Bace1. *Brain Research Bulletin*, 126, 170-177.

- Arimon, M., Takeda, S., Post, K. L., Svirsky, S., Hyman, B. T. & Berezovska, O. 2015. Oxidative Stress and Lipid Peroxidation Are Upstream of Amyloid Pathology. *Neurobiology of Disease*, 84, 109-119.
- Atwood, C. S., Moir, R. D., Huang, X. D., Scarpa, R. C., Bacarra, N. M. E., Romano, D. M., Hartshorn, M. K., Tanzi, R. E. & Bush, A. I. 1998. Dramatic Aggregation of Alzheimer a Beta by Cu(II) Is Induced by Conditions Representing Physiological Acidosis. *Journal of Biological Chemistry*, 273(21), 12817-12826.
- Bhatt, J. & Mukhopadhyay, S. 2018. Alzheimer's - Current Strategies for Its Diagnosis and Treatment. *Indo American Journal of Pharmaceutical Sciences*, 5(4), 2881-2896.
- Bigl, M., Bruckner, M. K., Arendt, T., Bigl, V. & Eschrich, K. 1999. Activities of Key Glycolytic Enzymes in the Brains of Patients with Alzheimer's Disease. *Journal of Neural Transmission*, 106(5-6), 499-511.
- Blennow, K., De Leon, M. J. & Zetterberg, H. 2006. Alzheimer's Disease. *Lancet*, 368(9533), 387-403.
- Bowen, D. M. & Davison, A. N. 1986. Biochemical-Studies of Nerve-Cells and Energy-Metabolism in Alzheimers-Disease. *British Medical Bulletin*, 42(1), 75-80.
- Brannstrom, K., Ohman, A., Nilsson, L., Pihl, M., Sandblad, L. & Oloisson, A. 2014. The N-Terminal Region of Amyloid Beta Controls the Aggregation Rate and Fibril Stability at Low Ph through a Gain of Function Mechanism. *Journal of the American Chemical Society*, 136(31), 10956-10964.
- Brewer, G. J. 1997. Effects of Acidosis on the Distribution and Processing of the Beta-Amyloid Precursor Protein in Cultured Hippocampal Neurons. *Molecular and Chemical Neuropathology*, 31(2), 171-186.
- Brighenti, E., Carnicelli, D., Brigotti, M. & Fiume, L. 2017. The Inhibition of Lactate Dehydrogenase a Hinders the Transcription of Histone 2b Gene Independently from the Block of Aerobic Glycolysis. *Biochemical and Biophysical Research Communications*, 485(4), 742-745.

- Brown, A. M., Potempska, A., Tummolo, D., Spruyt, M. A., Jacobsen, J. S. & Sonnenberg-Reines, J. 1998. Characterization of Endogenous App Processing in a Cell-Free System. *Age*, 21(1), 15-23.
- Burmakin, M., Shi, Y., Hedstrom, E., Kogner, P. & Selivanova, G. 2013. Dual Targeting of Wild-Type and Mutant P53 by Small Molecule Rita Results in the Inhibition of N-Myc and Key Survival Oncogenes and Kills Neuroblastoma Cells in Vivo and in Vitro. *Clinical Cancer Research*, 19(18), 5092-5103.
- Bursavich, M. G., Harrison, B. A. & Blain, J. F. 2016. Gamma Secretase Modulators: New Alzheimer's Drugs on the Horizon? *Journal of Medicinal Chemistry*, 59(16), 7389-7409.
- Buxbaum, J. D., Liu, K. N., Luo, Y. X., Slack, J. L., Stocking, K. L., Peschon, J. J., Johnson, R. S., Castner, B. J., Cerretti, D. P. & Black, R. A. 1998. Evidence That Tumor Necrosis Factor Alpha Converting Enzyme Is Involved in Regulated Alpha-Secretase Cleavage of the Alzheimer Amyloid Protein Precursor. *Journal of Biological Chemistry*, 273(43), 27765-27767.
- Caccamo, A., Oddo, S., Billings, L. M., Green, K. N., Martinez-Coria, H., Fisher, A. & Laferla, F. M. 2006. M1 Receptors Play a Central Role in Modulating Ad-Like Pathology in Transgenic Mice. *Neuron*, 49(5), 671-682.
- Cai, H. B., Wang, Y. S., Mccarthy, D., Wen, H. J., Borchelt, D. R., Price, D. L. & Wong, P. C. 2001. Bace1 Is the Major Beta-Secretase for Generation of a Beta Peptides by Neurons. *Nature Neuroscience*, 4(3), 233-234.
- Carey, R. M., Balcz, B. A., Lopez-Coviella, I. & Slack, B. E. 2005. Inhibition of Dynamin-Dependent Endocytosis Increases Shedding of the Amyloid Precursor Protein Ectodomain and Reduces Generation of Amyloid Beta Protein. *Bmc Cell Biology*, 6.
- Cha, M. Y., Han, S. H., Son, S. M., Hong, H. S., Choi, Y. J., Byun, J. & Mook-Jung, I. 2012. Mitochondria-Specific Accumulation of Amyloid Beta Induces Mitochondrial Dysfunction Leading to Apoptotic Cell Death. *Plos One*, 7(4).

- Checler, F. 2011. Acid Controls P53 and Regulates Beta App Processing. *Journal of Neurochemistry*, 118, 172-172.
- Checler, F., Dunys, J., Pardossi-Piquard, R. & Da Costa, C. A. 2010. P53 Is Regulated by and Regulates Members of the Gamma-Secretase Complex. *Neurodegenerative Diseases*, 7(1-3), 50-55.
- Cheignon, C., Tomas, M., Bonnefont-Rousselot, D., Faller, P., Hureau, C. & Collin, F. 2018. Oxidative Stress and the Amyloid Beta Peptide in Alzheimer's Disease. *Redox Biology*, 14, 450-464.
- Chen, C. H., Zhou, W. H., Liu, S. C., Deng, Y., Cai, F., Tone, M., Tone, Y., Tong, Y. G. & Song, W. H. 2012. Increased Nf-Kappa B Signalling up-Regulates Bace1 Expression and Its Therapeutic Potential in Alzheimer's Disease. *International Journal of Neuropsychopharmacology*, 15(1), 77-90.
- Chen, H. C., Mccaffery, J. M. & Chan, D. C. 2007. Mitochondrial Fusion Protects against Neurodegeneration in the Cerebellum. *Cell*, 130(3), 548-562.
- Chen, L. J., Na, R., Gu, M. J., Richardson, A. & Ran, Q. 2008. Lipid Peroxidation Up-Regulates Bace1 Expression in Vivo: A Possible Early Event of Amyloidogenesis in Alzheimer's Disease. *Journal of Neurochemistry*, 107(1), 197-207.
- Chen, Z. C. & Zhong, C. J. 2014. Oxidative Stress in Alzheimer's Disease. *Neuroscience Bulletin*, 30(2), 271-281.
- Chira, S., Gulei, D., Hajitou, A. & Berindan-Neagoe, I. 2018. Restoring the P53 'Guardian' Phenotype in P53-Deficient Tumor Cells with Crispr/Cas9. *Trends in Biotechnology*, 36(7), 653-660.
- Choy, R. W. Y., Cheng, Z. L. & Schekman, R. 2012. Amyloid Precursor Protein (App) Traffics from the Cell Surface Via Endosomes for Amyloid Beta (a Beta) Production in the Trans-Golgi Network. *Proceedings of the National Academy of Sciences of the United States of America*, 109(30), E2077-E2082.

- Coburger, I., Dahms, S. O., Roeser, D., Guhrs, K. H., Hortschansky, P. & Than, M. E. 2013. Analysis of the Overall Structure of the Multi-Domain Amyloid Precursor Protein (App). *Plos One*, 8(12).
- Cole, G. M., Huynh, T. V. & Saitoh, T. 1989. Evidence for Lysosomal Processing of Amyloid Beta-Protein Precursor in Cultured-Cells. *Neurochemical Research*, 14(10), 933-939.
- Cook, D. G., Forman, M. S., Sung, J. C., Leight, S., Kolson, D. L., Iwatsubo, T., Lee, V. M. Y. & Doms, R. W. 1997. Alzheimer's a Beta(1-42) Is Generated in the Endoplasmic Reticulum/Intermediate Compartment of Nt2n Cells. *Nature Medicine*, 3(9), 1021-1023.
- Coric, V., Salloway, S., Van Dyck, C. H., Dubois, B., Andreasen, N., Brody, M., Curtis, C., Soininen, H., Thein, S., Shiovitz, T., Pilcher, G., Ferris, S., Colby, S., Kerselaers, W., Dockens, R., Soares, H., Kaplita, S., Luo, F., Pachai, C., Bracoud, L., Mintun, M., Grill, J. D., Marek, K., Seibyl, J., Cedarbaum, J. M., Albright, C., Feldman, H. H. & Berman, R. M. 2015. Targeting Prodromal Alzheimer Disease with Avagacestat a Randomized Clinical Trial. *Jama Neurology*, 72(11), 1324-1333.
- Coronel, R., Bernabeu-Zornoza, A., Palmer, C., Muniz-Moreno, M., Zambrano, A., Cano, E. & Liste, I. 2018. Role of Amyloid Precursor Protein (App) and Its Derivatives in the Biology and Cell Fate Specification of Neural Stem Cells. *Molecular Neurobiology*, 55(9), 7107-7117.
- Cuesta, A., Zambrano, A., Royo, M. & Pascual, A. 2009. The Tumour Suppressor P53 Regulates the Expression of Amyloid Precursor Protein (App). *Biochemical Journal*, 418, 643-650.
- Da Costa, C. A., Sunyach, C., Pardossi-Piquard, R., Sevalle, J., Vincent, B., Boyer, N., Kawarai, T., Girardot, N., George-Hyslop, P. S. & Checler, F. 2006. Presenilin-Dependent Gamma-Secretase-Mediated Control of P53-Associated Cell Death in Alzheimer's Disease. *Journal of Neuroscience*, 26(23), 6377-6385.
- Dai, Y. H., Xiong, X. P., Huang, G., Liu, J. J., Sheng, S. L., Wang, H. J. & Qin, W. X. 2014. Dichloroacetate Enhances Adriamycin-Induced Hepatoma Cell Toxicity in Vitro and in Vivo by Increasing Reactive Oxygen Species Levels. *Plos One*, 9(4).

- Dawson, D. M., Kaplan, N. O. & Goodfriend, T. L. 1964. Lactic Dehydrogenases - Functions of 2 Types - Rates of Synthesis of 2 Major Forms Can Be Correlated with Metabolic Differentiation. *Science*, 143(360), 929-&.
- De Strooper, B., Saftig, P., Craessaerts, K., Vanderstichele, H., Guhde, G., Annaert, W., Von Figura, K. & Van Leuven, F. 1998. Deficiency of Presenilin-1 Inhibits the Normal Cleavage of Amyloid Precursor Protein. *Nature*, 391(6665), 387-390.
- Dementia Statistics Hub. 2018. *Global prevalence | Dementia Statistics Hub*. [online] Available at: <https://www.dementiastatistics.org/statistics/global-prevalence/>
- Ding, J., Karp, J. E. & Emadi, A. 2017. Elevated Lactate Dehydrogenase (Ldh) Can Be a Marker of Immune Suppression in Cancer: Interplay between Hematologic and Solid Neoplastic Clones and Their Microenvironments. *Cancer Biomarkers*, 19(4), 353-363.
- Doody, R. S., Raman, R., Farlow, M., Iwatsubo, T., Vellas, B., Joffe, S., Kieburtz, K., He, F., Sun, X. Y., Thomas, R. G., Aisen, P. S., Siemers, E., Sethuraman, G. & Mohs, R. 2013. A Phase 3 Trial of Semagacestat for Treatment of Alzheimer's Disease. *New England Journal of Medicine*, 369(4), 341-350.
- Duggan, S. P. & Mccarthy, J. V. 2016. Beyond Gamma-Secretase Activity: The Multifunctional Nature of Presenilins in Cell Signalling Pathways. *Cellular Signalling*, 28(1), 1-11.
- Egan, M. F., Kost, J., Tariot, P. N., Aisen, P. S., Cummings, J. L., Vellas, B., Sur, C., Mukai, Y., Voss, T., Furtek, C., Mahoney, E., Mozley, L. H., Vandenberghe, R., Mo, Y. & Michelson, D. 2018. Randomized Trial of Verubecestat for Mild-to-Moderate Alzheimer's Disease. *New England Journal of Medicine*, 378(18), 1691-1703.
- Eggert, S., Thomas, C., Kins, S. & Hermey, G. 2018. Trafficking in Alzheimer's Disease: Modulation of App Transport and Processing by the Transmembrane Proteins Lrp1, Sorla, Sorcs1c, Sortilin, and Calsyntenin. *Molecular Neurobiology*, 55(7), 5809-5829.
- Enge, M., Bao, W. J., Hedstrom, E., Jackson, S. P., Moumen, A. & Selivanova, G. 2009. Mdm2-Dependent Downregulation of P21 and Hnrnp K Provides a Switch between Apoptosis and Growth Arrest Induced by Pharmacologically Activated P53. *Cancer Cell*, 16(1), 79-79.

- Fraering, P. C., Ye, W. J., Strub, J. M., Dolios, G., Lavoie, M. J., Ostaszewski, B. L., Van Dorsselaer, A., Wang, R., Selkoe, D. J. & Wolfe, M. S. 2004. Purification and Characterization of the Human Gamma-Secretase Complex. *Biochemistry*, 43(30), 9774-9789.
- Francis, R., Mcgrath, G., Zhang, J. H., Ruddy, D. A., Sym, M., Apfeld, J., Nicoll, M., Maxwell, M., Hai, B., Ellis, M. C., Parks, A. L., Xu, W., Li, J. H., Gurney, M., Myers, R. L., Himes, C. S., Hiesch, R., Ruble, C., Nye, J. S. & Curtis, D. 2002. Aph-1 and Pen-2 Are Required for Notch Pathway Signaling, Gamma-Secretase Cleavage of Beta App, and Presenilin Protein Accumulation. *Developmental Cell*, 3(1), 85-97.
- Ganju, N., Wands, J. R. & De La Monte, S. M. 1998. Increased Apoptosis with up-Regulation of the P53 Gene in Ad Brains. *Journal of Neuropathology and Experimental Neurology*, 57(5), 496-496.
- Glenner, G. G. & Wong, C. W. 1984. Alzheimers-Disease and Downs-Syndrome - Sharing of a Unique Cerebrovascular Amyloid Fibril Protein. *Biochemical and Biophysical Research Communications*, 122(3), 1131-1135.
- Goldgaber, D., Lerman, M. I., Mcbride, O. W., Saffiotti, U. & Gajdusek, D. C. 1987. Characterization and Chromosomal Localization of a Cdna-Encoding Brain Amyloid of Alzheimers-Disease. *Science*, 235(4791), 877-880.
- Greenfield, J. P., Tsai, J., Gouras, G. K., Hai, B., Thinakaran, G., Checler, F., Sisodia, S. S., Greengard, P. & Xu, H. X. 1999. Endoplasmic Reticulum and Trans-Golgi Network Generate Distinct Populations of Alzheimer Beta-Amyloid Peptides. *Proceedings of the National Academy of Sciences of the United States of America*, 96(2), 742-747.
- Gu, T., Wu, W. Y., Dong, Z. X., Yu, S. P., Sun, Y., Zhong, Y., Lu, Y. T. & Li, N. G. 2017. Development and Structural Modification of Bace1 Inhibitors. *Molecules*, 22(1).
- Guglielmotto, M., Aragno, M., Autelli, R., Giliberto, L., Novo, E., Colombatto, S., Danni, O., Parola, M., Smith, M. A., Perry, G., Tamagno, E. & Tabaton, M. 2009. The up-Regulation of Bace1 Mediated by Hypoxia and Ischemic Injury: Role of Oxidative Stress and Hif1 Alpha. *Journal of Neurochemistry*, 108(4), 1045-1056.

- Haass, C., Kaether, C., Thinakaran, G. & Sisodia, S. 2012. Trafficking and Proteolytic Processing of App. *Cold Spring Harbor Perspectives in Medicine*, 2(5).
- Haass, C., Koo, E. H., Mellon, A., Hung, A. Y. & Selkoe, D. J. 1992. Targeting of Cell-Surface Beta-Amyloid Precursor Protein to Lysosomes - Alternative Processing into Amyloid-Bearing Fragments. *Nature*, 357(6378), 500-503.
- Hardy, J. 1992. Framing Beta-Amyloid. *Nature Genetics*, 1(4), 233-234.
- Hardy, J. & Allsop, D. 1991. Amyloid Deposition as the Central Event in the Etiology of Alzheimers-Disease. *Trends in Pharmacological Sciences*, 12(10), 383-388.
- Hardy, J. & Selkoe, D. J. 2002. Medicine - the Amyloid Hypothesis of Alzheimer's Disease: Progress and Problems on the Road to Therapeutics. *Science*, 297(5580), 353-356.
- Hassoun, E. A. & Cearfoss, J. 2011. Dichloroacetate- and Trichloroacetate-Induced Modulation of Superoxide Dismutase, Catalase, and Glutathione Peroxidase Activities and Glutathione Level in the Livers of Mice after Subacute and Subchronic Exposures. *Toxicological and Environmental Chemistry*, 93(2), 332-344.
- Henley, D. B., May, P. C., Dean, R. A. & Siemers, E. R. 2009. Development of Semagacestat (Ly450139), a Functional Gamma-Secretase Inhibitor, for the Treatment of Alzheimer's Disease. *Expert Opinion on Pharmacotherapy*, 10(10), 1657-1664.
- Hoefgen, S., Dahms, S. O., Oertwig, K. & Than, M. E. 2015. The Amyloid Precursor Protein Shows a Ph-Dependent Conformational Switch in Its E1 Domain. *Journal of Molecular Biology*, 427(2), 433-442.
- Holsinger, R. M. D., Goense, N., Bohorquez, J. & Strappe, P. 2013. Splice Variants of the Alzheimer's Disease Beta-Secretase, Bace1. *Neurogenetics*, 14(1), 1-9.
- Huse, J. T., Liu, K. N., Pijak, D. S., Carlin, D., Lee, V. M. Y. & Doms, R. W. 2002. Beta-Secretase Processing in the Trans-Golgi Network Preferentially Generates Truncated Amyloid Species That Accumulate in Alzheimer's Disease Brain. *Journal of Biological Chemistry*, 277(18), 16278-16284.

- Issaeva, N., Bozko, P., Enge, M., Protopopova, M., Verhoef, L., Masucci, M., Pramanik, A. & Selivanova, G. 2004. Small Molecule Rita Binds to P53, Blocks P53-Hdm-2 Interaction and Activates P53 Function in Tumors. *Nature Medicine*, 10(12), 1321-1328.
- James, M. O. & Stacpoole, P. W. 2016. Pharmacogenetic Considerations with Dichloroacetate Dosing. *Pharmacogenomics*, 17(7), 743-753.
- Jiang, S. T., Li, Y. F., Zhang, X., Bu, G. J., Xu, H. X. & Zhang, Y. W. 2014. Trafficking Regulation of Proteins in Alzheimer's Disease. *Molecular Neurodegeneration*, 9.
- Jorissen, E., Prox, J., Bernreuther, C., Weber, S., Schwanbeck, R., Serneels, L., Snellinx, A., Craessaerts, K., Thathiah, A., Tesseur, I., Bartsch, U., Weskamp, G., Blobel, C. P., Glatzel, M., De Strooper, B. & Saftig, P. 2010. The Disintegrin/Metalloproteinase Adam10 Is Essential for the Establishment of the Brain Cortex. *Journal of Neuroscience*, 30(14), 4833-4844.
- Jorns, A., Tiedge, M., Lenzen, S. & Munday, R. 1999. Effect of Superoxide Dismutase, Catalase, Chelating Agents, and Free Radical Scavengers on the Toxicity of Alloxan to Isolated Pancreatic Islets in Vitro. *Free Radical Biology and Medicine*, 26(9-10), 1300-1304.
- Kaether, C., Schmitt, S., Willem, M. & Haass, C. 2006. Amyloid Precursor Protein and Notch Intracellular Domains Are Generated after Transport of Their Precursors to the Cell Surface. *Traffic*, 7(4), 408-415.
- Kamat, P. K., Rai, S., Swarnkar, S., Shukla, R. & Nath, C. 2014. Molecular and Cellular Mechanism of Okadaic Acid (Oka)-Induced Neurotoxicity: A Novel Tool for Alzheimer's Disease Therapeutic Application. *Molecular Neurobiology*, 50(3), 852-865.
- Kanamaru, T., Kamimura, N., Yokota, T., Iuchi, K., Nishimaki, K., Takami, S., Akashiba, H., Shitaka, Y., Katsura, K., Kimura, K. & Ohta, S. 2015. Oxidative Stress Accelerates Amyloid Deposition and Memory Impairment in a Double-Transgenic Mouse Model of Alzheimer's Disease. *Neuroscience Letters*, 587, 126-131.
- Kankotia, S. & Stacpoole, P. W. 2014. Dichloroacetate and Cancer: New Home for an Orphan Drug? *Biochimica Et Biophysica Acta-Reviews on Cancer*, 1846(2), 617-629.

- Kato, M., Li, J., Chuang, J. L. & Chuang, D. T. 2007. Distinct Structural Mechanisms for Inhibition of Pyruvate Dehydrogenase Kinase Isoforms by Azd7545, Dichloroacetate, and Radicol. *Structure*, 15(8), 992-1004.
- Koike, H., Tomioka, S., Sorimachi, H., Saido, T. C., Maruyama, K., Okuyama, A., Fujisawa-Sehara, A., Ohno, S., Suzuki, K. & Ishiura, S. 1999. Membrane-Anchored Metalloprotease Mdc9 Has an Alpha-Secretase Activity Responsible for Processing the Amyloid Precursor Protein. *Biochemical Journal*, 343, 371-375.
- Kudo, T., Okumura, M., Imaizumi, K., Araki, W., Morihara, T., Tanimukai, H., Kamagata, E., Tabuchi, N., Kimura, R., Kanayama, D., Fukumori, A., Tagami, S., Okochi, M., Kubo, M., Tanii, H., Tohyama, M., Tabira, T. & Takeda, M. 2006. Altered Localization of Amyloid Precursor Protein under Endoplasmic Reticulum Stress. *Biochemical and Biophysical Research Communications*, 344(2), 525-530.
- Kumar, D., Ganeshpurkar, A., Modi, G., Gupta, S. K. & Singh, S. K. 2018. Secretase Inhibitors for the Treatment of Alzheimer's Disease: Long Road Ahead. *European Journal of Medicinal Chemistry*, 148, 436-452.
- Labuschagne, C. F., Zani, F. & Vousden, K. H. 2018. Control of Metabolism by P53-Cancer and Beyond. *Biochimica Et Biophysica Acta-Reviews on Cancer*, 1870(1), 32-42.
- Lammich, S., Kojro, E., Postina, R., Gilbert, S., Pfeiffer, R., Jasionowski, M., Haass, C. & Fahrenholz, F. 1999. Constitutive and Regulated Alpha-Secretase Cleavage of Alzheimer's Amyloid Precursor Protein by a Disintegrin Metalloprotease. *Proceedings of the National Academy of Sciences of the United States of America*, 96(7), 3922-3927.
- Le, A., Cooper, C. R., Gouw, A. M., Dinavahi, R., Maitra, A., Deck, L. M., Royer, R. E., Jagt, D. L. V., Semenza, G. L. & Dang, C. V. 2010. Inhibition of Lactate Dehydrogenase a Induces Oxidative Stress and Inhibits Tumor Progression. *Proceedings of the National Academy of Sciences of the United States of America*, 107(5), 2037-2042.
- Lee, S. F., Shah, S., Yu, C., Wigley, W. C., Li, H., Lim, M., Pedersen, K., Han, W. P., Thomas, P., Lundkvist, J., Hao, Y. H. & Yu, G. 2004. A Conserved Gxxxg Motif in Aph-1 Is Critical for Assembly and Activity of the Gamma-Secretase Complex. *Journal of Biological Chemistry*, 279(6), 4144-4152.

- Levy-Lahad, E., Wasco, W., Poorkaj, P., Romano, D. M., Oshima, J., Pettingell, W. H., Yu, C. E., Jondro, P. D., Schmidt, S. D., Wang, K., Crowley, A. C., Fu, Y. H., Guenette, S. Y., Galas, D., Nemens, E., Wijsman, E. M., Bird, T. D., Schellenberg, G. D. & Tanzi, R. E. 1995. Candidate Gene for the Chromosome-1 Familial Alzheimers-Disease Locus. *Science*, 269(5226), 973-977.
- Li, J., Kato, M. & Chuang, D. T. 2009. Pivotal Role of the C-Terminal Dw-Motif in Mediating Inhibition of Pyruvate Dehydrogenase Kinase 2 by Dichloroacetate. *Journal of Biological Chemistry*, 284(49), 34458-34467.
- Lin, X. L., Koelsch, C., Wu, S. L., Downs, D., Dashti, A. & Tang, J. 2000. Human Aspartic Protease Memapsin 2 Cleaves the Beta-Secretase Site of Beta-Amyloid Precursor Protein. *Proceedings of the National Academy of Sciences of the United States of America*, 97(4), 1456-1460.
- Lorenzen, A., Samosh, J., Vandewark, K., Anborgh, P. H., Seah, C., Magalhaes, A. C., Cregan, S. P., Ferguson, S. S. G. & Pasternak, S. H. 2010. Rapid and Direct Transport of Cell Surface App to the Lysosome Defines a Novel Selective Pathway. *Molecular Brain*, 3.
- Macdonald, R., Barnes, K., Hastings, C. & Mortiboys, H. 2018. Mitochondrial Abnormalities in Parkinson's Disease and Alzheimer's Disease: Can Mitochondria Be Targeted Therapeutically? *Biochemical Society Transactions*, 46, 891-909.
- Manczak, M., Anekonda, T. S., Henson, E., Park, B. S., Quinn, J. & Reddy, P. H. 2006. Mitochondria Are a Direct Site of a Beta Accumulation in Alzheimer's Disease Neurons: Implications for Free Radical Generation and Oxidative Damage in Disease Progression. *Human Molecular Genetics*, 15(9), 1437-1449.
- Mann, W. R., Dragland, C. J., Vinluan, C. C., Vedananda, T. R., Bell, P. A. & Aicher, T. D. 2000. Diverse Mechanisms of Inhibition of Pyruvate Dehydrogenase Kinase by Structurally Distinct Inhibitors. *Biochimica Et Biophysica Acta-Protein Structure and Molecular Enzymology*, 1480(1-2), 283-292.
- Massey, A. J. 2017. Modification of Tumour Cell Metabolism Modulates Sensitivity to Chk1 Inhibitor-Induced Dna Damage. *Scientific Reports*, 7.

- Masters, C. L., Simms, G., Weinman, N. A., Multhaup, G., McDonald, B. L. & Beyreuther, K. 1985. Amyloid Plaque Core Protein in Alzheimer-Disease and Down Syndrome. *Proceedings of the National Academy of Sciences of the United States of America*, 82(12), 4245-4249.
- Matsui, H., Ito, H., Taniguchi, Y., Takeda, S. & Takahashi, R. 2010. Ammonium Chloride and Tunicamycin Are Novel Toxins for Dopaminergic Neurons and Induce Parkinson's Disease-Like Phenotypes in Medaka Fish. *Journal of Neurochemistry*, 115(5), 1150-1160.
- Mattson, M. P., Cheng, B., Culwell, A. R., Esch, F. S., Lieberburg, I. & Rydel, R. E. 1993. Evidence for Excitoprotective and Intraneuronal Calcium-Regulating Roles for Secreted Forms of the Beta-Amyloid Precursor Protein. *Neuron*, 10(2), 243-254.
- McConlogue, L., Buttini, M., Anderson, J. P., Brigham, E. F., Chen, K. S., Freedman, S. B., Games, D., Johnson-Wood, K., Lee, M., Zeller, M., Liu, W., Motter, R. & Sinha, S. 2007. Partial Reduction of Bace1 Has Dramatic Effects on Alzheimer Plaque and Synaptic Pathology in App Transgenic Mice. *Journal of Biological Chemistry*, 282(36), 26326-26334.
- Merkel, O., Taylor, N., Prutsch, N., Staber, P. B., Moriggl, R., Turner, S. D. & Kenner, L. 2017. When the Guardian Sleeps: Reactivation of the P53 Pathway in Cancer. *Mutation Research-Reviews in Mutation Research*, 773, 1-13.
- Michaelis, M., Rothweiler, F., Agha, B., Barth, S., Voges, Y., Loschmann, N., Von Deimling, A., Breitling, R., Doerr, H. W., Rodel, F., Speidel, D. & Cinatl, J. 2012. Human Neuroblastoma Cells with Acquired Resistance to the P53 Activator Rita Retain Functional P53 and Sensitivity to Other P53 Activating Agents. *Cell Death & Disease*, 3.
- Michelakis, E. D., Webster, L. & Mackey, J. R. 2008. Dichloroacetate (DCA) as a Potential Metabolic-Targeting Therapy for Cancer. *British Journal of Cancer*, 99(7), 989-994.
- Mouton-Liger, F., Paquet, C., Dumurgier, J., Bouras, C., Pradier, L., Gray, F. & Hugon, J. 2012. Oxidative Stress Increases Bace1 Protein Levels through Activation of the Pkr-Eif2 Alpha Pathway. *Biochimica Et Biophysica Acta-Molecular Basis of Disease*, 1822(6), 885-896.

- Muche, A., Arendt, T. & Schliebs, R. 2017. Oxidative Stress Affects Processing of Amyloid Precursor Protein in Vascular Endothelial Cells. *Plos One*, 12(6).
- Neveu, M. A., De Preter, G., Joudiou, N., Bol, A., Brender, J. R., Saito, K., Kishimoto, S., Gregoire, V., Jordan, B. F., Krishna, M. C., Feron, O. & Gallez, B. 2016. Multi-Modality Imaging to Assess Metabolic Response to Dichloroacetate Treatment in Tumor Models. *Oncotarget*, 7(49), 81741-81749.
- Nitsch, R. M., Slack, B. E., Wurtman, R. J. & Growdon, J. H. 1992. Release of Alzheimer Amyloid Precursor Derivatives Stimulated by Activation of Muscarinic Acetylcholine-Receptors. *Science*, 258(5080), 304-307.
- Obulesu, M. & Lakshmi, M. J. 2014. Apoptosis in Alzheimer's Disease: An Understanding of the Physiology, Pathology and Therapeutic Avenues. *Neurochemical Research*, 39(12), 2301-2312.
- Ohno, M., Sametsky, E. A., Younkin, L. H., Oakley, H., Younkin, S. G., Citron, M., Vassar, R. & Disterhoft, J. F. 2004. Bace1 Deficiency Rescues Memory Deficits and Cholinergic Dysfunction in a Mouse Model of Alzheimer's Disease. *Neuron*, 41(1), 27-33.
- Ohyagi, Y., Asahara, H., Chui, D. H., Tsuruta, Y., Sakae, N., Miyoshi, K., Yamada, T., Kikuchi, H., Taniwaki, T., Murai, H., Ikezoe, K., Furuya, H., Kawarabayashi, T., Shoji, M., Checler, F., Iwaki, T., Makifuchi, T., Takeda, K., Kira, J. I. & Tabira, T. 2005. Intracellular α Beta 42 Activates P53 Promoter: A Pathway to Neurodegeneration in Alzheimer's Disease. *Faseb Journal*, 19(2), 255-257.
- Pajuelo-Reguera, D., Alan, L., Olejar, T. & Jezek, P. 2015. Dichloroacetate Stimulates Changes in the Mitochondrial Network Morphology Via Partial Mitophagy in Human Sh-Sy5y Neuroblastoma Cells. *International Journal of Oncology*, 46(6), 2409-2418.
- Pandey, P., Sliker, B., Peters, H. L., Tuli, A., Herskovitz, J., Smits, K., Purohit, A., Singh, R. K., Dong, J. X., Batra, S. K., Coulter, D. W. & Solheim, J. C. 2016. Amyloid Precursor Protein and Amyloid Precursor-Like Protein 2 in Cancer. *Oncotarget*, 7(15), 19430-19444.

- Parkin, E. & Harris, B. 2009. A Disintegrin and Metalloproteinase (Adam)-Mediated Ectodomain Shedding of Adam10. *Journal of Neurochemistry*, 108(6), 1464-1479.
- Perez, R. G., Soriano, S., Hayes, J. D., Ostaszewski, B., Xia, W. M., Selkoe, D. J., Chen, X. H., Stokin, G. B. & Koo, E. H. 1999. Mutagenesis Identifies New Signals for Beta-Amyloid Precursor Protein Endocytosis, Turnover, and the Generation of Secreted Fragments, Including a Beta 42. *Journal of Biological Chemistry*, 274(27), 18851-18856.
- Petersen, C. A. H., Alikhani, N., Behbahani, H., Wiehager, B., Pavlov, P. F., Alafuzoff, I., Leinonen, V., Ito, A., Winblad, B., Glaser, E. & Ankarcrona, M. 2008. The Amyloid Beta-Peptide Is Imported into Mitochondria Via the Tom Import Machinery and Localized to Mitochondrial Cristae. *Proceedings of the National Academy of Sciences of the United States of America*, 105(35), 13145-13150.
- Pirchl, M., Marksteiner, J. & Humpel, C. 2006. Effects of Acidosis on Brain Capillary Endothelial Cells and Cholinergic Neurons: Relevance to Vascular Dementia and Alzheimer's Disease. *Neurological Research*, 28(6), 657-664.
- Placido, A. I., Pereira, C. M. F., Duarte, A. I., Candeias, E., Correia, S. C., Santos, R. X., Carvalho, C., Cardoso, S., Oliveira, C. R. & Moreira, P. I. 2014. The Role of Endoplasmic Reticulum in Amyloid Precursor Protein Processing and Trafficking: Implications for Alzheimer's Disease. *Biochimica Et Biophysica Acta-Molecular Basis of Disease*, 1842(9), 1444-1453.
- Postina, R., Schroeder, A., Dewachter, I., Bohl, J., Schmitt, U., Kojro, E., Prinzen, C., Endres, K., Hiemke, C., Blessing, M., Flamez, P., Dequenne, A., Godaux, E., Van Leuven, F. & Fahrenholz, F. 2004. A Disintegrin-Metalloproteinase Prevents Amyloid Plaque Formation and Hippocampal Defects in an Alzheimer Disease Mouse Model. *Journal of Clinical Investigation*, 113(10), 1456-1464.
- Prox, J., Rittger, A. & Saftig, P. 2012. Physiological Functions of the Amyloid Precursor Protein Secretases Adam10, Bace1, and Presenilin. *Experimental Brain Research*, 217(3-4), 331-341.
- Querfurth, H. W. & Laferla, F. M. 2010. Mechanisms of Disease Alzheimer's Disease. *New England Journal of Medicine*, 362(4), 329-344.

- Robakis, N. K., Ramakrishna, N., Wolfe, G. & Wisniewski, H. M. 1987. Molecular-Cloning and Characterization of a Cdna-Encoding the Cerebrovascular and the Neuritic Plaque Amyloid Peptides. *Proceedings of the National Academy of Sciences of the United States of America*, 84(12), 4190-4194.
- Robey, I. F. & Martin, N. K. 2011. Bicarbonate and Dichloroacetate: Evaluating Ph Altering Therapies in a Mouse Model for Metastatic Breast Cancer. *Bmc Cancer*, 11.
- Robinson, N., Grabowski, P. & Rehman, I. 2018. Alzheimer's Disease Pathogenesis: Is There a Role for Folate? *Mechanisms of Ageing and Development*, 174, 86-94.
- Rogaev, E. I., Sherrington, R., Rogaeva, E. A., Levesque, G., Ikeda, M., Liang, Y., Chi, H., Lin, C., Holman, K., Tsuda, T., Mar, L., Sorbi, S., Nacmias, B., Piacentini, S., Amaducci, L., Chumakov, I., Cohen, D., Lannfelt, L., Fraser, P. E., Rommens, J. M. & Stgeorgehyslop, P. H. 1995. Familial Alzheimers-Disease in Kindreds with Missense Mutations in a Gene on Chromosome-1 Related to the Alzheimers-Disease Type-3 Gene. *Nature*, 376(6543), 775-778.
- Sabapathy, K. & Lane, D. P. 2018. Therapeutic Targeting of P53: All Mutants Are Equal, but Some Mutants Are More Equal Than Others. *Nature Reviews Clinical Oncology*, 15(1), 13-30.
- Salminen, A., Kaarniranta, K., Kauppinen, A., Ojala, J., Haapasalo, A., Soininen, H. & Hiltunen, M. 2013. Impaired Autophagy and App Processing in Alzheimer's Disease: The Potential Role of Beclin 1 Interactome. *Progress in Neurobiology*, 106, 33-54.
- Sanabria-Castro, A., Alvarado-Echeverria, I. & Monge-Bonilla, C. 2017. Molecular Pathogenesis of Alzheimer's Disease: An Update. *Annals of Neurosciences*, 24(1), 46-54.
- Sankaranarayanan, S., Price, E. A., Wu, G. X., Crouthamel, M. C., Shi, X. P., Tugusheva, K., Tyler, K. X., Kahana, J., Ellis, J., Jin, L., Steele, T., Stachel, S., Coburn, C. & Simon, A. J. 2008. In Vivo Beta-Secretase 1 Inhibition Leads to Brain a Beta Lowering and Increased Alpha-Secretase Processing of Amyloid Precursor Protein without Effect on Neuregulin-1. *Journal of Pharmacology and Experimental Therapeutics*, 324(3), 957-969.

- Sano, Y., Syuzo-Takabatake, A., Nakaya, T., Saito, Y., Tomita, S., Itohara, S. & Suzuki, T. 2006. Enhanced Amyloidogenic Metabolism of the Amyloid Beta-Protein Precursor in the X111-Deficient Mouse Brain. *Journal of Biological Chemistry*, 281(49), 37853-37860.
- Schellenberg, G. D., Bird, T. D., Wijsman, E. M., Orr, H. T., Anderson, L., Nemens, E., White, J. A., Bonnycastle, L., Weber, J. L., Alonso, M. E., Potter, H., Heston, L. L. & Martin, G. M. 1992. Genetic-Linkage Evidence for a Familial Alzheimers-Disease Locus on Chromosome-14. *Science*, 258(5082), 668-671.
- Schrader-Fischer, G. & Paganetti, P. A. 1996. Effect of Alkalinizing Agents on the Processing of the Beta-Amyloid Precursor Protein. *Brain Research*, 716(1-2), 91-100.
- Sheng, B. Y., Gong, K., Niu, Y., Liu, L. L., Yan, Y. F., Lu, G. Y., Zhang, L. H., Hu, M., Zhao, N. M., Zhang, X. F., Tang, P. F. & Gong, Y. D. 2009. Inhibition of Gamma-Secretase Activity Reduces a Beta Production, Reduces Oxidative Stress, Increases Mitochondrial Activity and Leads to Reduced Vulnerability to Apoptosis: Implications for the Treatment of Alzheimer's Disease. *Free Radical Biology and Medicine*, 46(10), 1362-1375.
- Sherrington, R., Rogaev, E. I., Liang, Y., Rogaeva, E. A., Levesque, G., Ikeda, M., Chi, H., Lin, C., Li, G., Holman, K., Tsuda, T., Mar, L., Foncin, J. F., Bruni, A. C., Montesi, M. P., Sorbi, S., Rainero, I., Pinessi, L., Nee, L., Chumakov, I., Pollen, D., Brookes, A., Sanseau, P., Polinsky, R. J., Wasco, W., Dasilva, H. A. R., Haines, J. L., Pericakvance, M. A., Tanzi, R. E., Roses, A. D., Fraser, P. E., Rommens, J. M. & Stgeorgehyslop, P. H. 1995. Cloning of a Gene Bearing Missense Mutations in Early-Onset Familial Alzheimers-Disease. *Nature*, 375(6534), 754-760.
- Siman, R., Mistretta, S., Durkin, J. T., Savage, M. J., Loh, T., Trusko, S. & Scott, R. W. 1993. Processing of the Beta-Amyloid Precursor - Multiple Proteases Generate and Degrade Potentially Amyloidogenic Fragments. *Journal of Biological Chemistry*, 268(22), 16602-16609.
- Slack, B. E., Ma, L. K. & Seah, C. C. 2001. Constitutive Shedding of the Amyloid Precursor Protein Ectodomain Is Up-Regulated by Tumour Necrosis Factor-Alpha Converting Enzyme. *Biochemical Journal*, 357, 787-794.
- Small, S. A. & Gandy, S. 2006. Sorting through the Cell Biology of Alzheimer's Disease: Intracellular Pathways to Pathogenesis. *Neuron*, 52(1), 15-31.

- Smith, D. G., Cappai, R. & Barnham, K. J. 2007. The Redox Chemistry of the Alzheimer's Disease Amyloid Beta Peptide. *Biochimica Et Biophysica Acta-Biomembranes*, 1768(8), 1976-1990.
- Soucek, T., Cumming, R., Dargusch, R., Maher, P. & Schubert, D. 2003. The Regulation of Glucose Metabolism by Hif-1 Mediates a Neuroprotective Response to Amyloid Beta Peptide. *Neuron*, 39(1), 43-56.
- Stacpoole, P. W. 2017. Therapeutic Targeting of the Pyruvate Dehydrogenase Complex/Pyruvate Dehydrogenase Kinase (Pdc/Pdk) Axis in Cancer. *Inci-Journal of the National Cancer Institute*, 109(11).
- Stacpoole, P. W., Abdelmalak, M., Lew, A., Ramezani, R., Shroads, A. L., Coats, B. S. & Shankar, M. N. 2012. Long-Term Safety of Dichloroacetate in Congenital Lactic Acidosis. *Mitochondrion*, 12(5), 557-557.
- Stacpoole, P. W., Nagaraja, N. V. & Hutson, A. D. 2003. Efficacy of Dichloroacetate as a Lactate-Lowering Drug. *Journal of Clinical Pharmacology*, 43(7), 683-691.
- Stacpoole, P. W., Wright, E. C., Baumgartner, T. G., Bersin, R. M., Buchalter, S., Curry, S. H., Duncan, C. A., Harman, E. M., Henderson, G. N., Jenkinson, S., Lachin, J. M., Lorenz, A., Schneider, S. H., Siegel, J. H., Summer, W. R., Thompson, D., Wolfe, C. L. & Zorovich, B. 1992. A Controlled Clinical-Trial of Dichloroacetate for Treatment of Lactic-Acidosis in Adults. *New England Journal of Medicine*, 327(22), 1564-1569.
- Stephenson, A. P., Schneider, J. A., Nelson, B. C., Atha, D. H., Jain, A., Soliman, K. F. A., Aschner, M., Mazzi, E. & Reams, R. R. 2013. Manganese-Induced Oxidative Dna Damage in Neuronal SH-SY5Y Cells: Attenuation of Thymine Base Lesions by Glutathione and N-Acetylcysteine. *Toxicology Letters*, 218(3), 299-307.
- Sun, J. C. & Roy, S. 2018. The Physical Approximation of App and Bace-1: A Key Event in Alzheimer's Disease Pathogenesis. *Developmental Neurobiology*, 78(3), 340-347.
- Sun, L. C., Suo, C. X., Li, S. T., Zhang, H. F. & Gao, P. 2018. Metabolic Reprogramming for Cancer Cells and Their Microenvironment: Beyond the Warburg Effect. *Biochimica Et Biophysica Acta-Reviews on Cancer*, 1870(1), 51-66.

- Takami, M., Nagashima, Y., Sano, Y., Ishihara, S., Morishima-Kawashima, M., Funamoto, S. & Ihara, Y. 2009. Gamma-Secretase: Successive Tripeptide and Tetrapeptide Release from the Transmembrane Domain of Beta-Carboxyl Terminal Fragment. *Journal of Neuroscience*, 29(41), 13042-13052.
- Tamagno, E., Guglielmotto, M., Aragno, M., Borghi, R., Autelli, R., Giliberto, L., Muraca, G., Danni, O., Zhu, X. W., Smith, M. A., Perry, G., Jo, D. G., Mattson, M. P. & Tabaton, M. 2008. Oxidative Stress Activates a Positive Feedback between the Gamma- and Beta-Secretase Cleavages of the Beta-Amyloid Precursor Protein. *Journal of Neurochemistry*, 104(3), 683-695.
- Tippmann, F., Hundt, J., Schneider, A., Endres, K. & Fahrenholz, F. 2009. Up-Regulation of the Alpha-Secretase Adam10 by Retinoic Acid Receptors and Acitretin. *Faseb Journal*, 23(6), 1643-1654.
- Toh, W. H., Tan, J. Z. A., Zulkefli, K. L., Houghton, F. J. & Gleeson, P. A. 2017. Amyloid Precursor Protein Traffics from the Golgi Directly to Early Endosomes in an Arl5b-and Ap4-Dependent Pathway. *Traffic*, 18(3), 159-175.
- Tousseyn, T., Thathiah, A., Jorissen, E., Raemaekers, T., Konietzko, U., Reiss, K., Maes, E., Snellinx, A., Serneels, L., Nyabi, O., Annaert, W., Saftig, P., Hartmann, D. & De Strooper, B. 2009. Adam10, the Rate-Limiting Protease of Regulated Intramembrane Proteolysis of Notch and Other Proteins, Is Processed by Adams-9, Adams-15, and the Gamma-Secretase. *Journal of Biological Chemistry*, 284(17), 11738-11747.
- Trimmer, P. A. & Borland, M. K. 2005. Differentiated Alzheimer's Disease Transmitochondrial Cybrid Cell Lines Exhibit Reduced Organelle Movement. *Antioxidants & Redox Signaling*, 7(9-10), 1101-1109.
- Valvona, C. J., Fillmore, H. L., Nunn, P. B. & Pilkington, G. J. 2016. The Regulation and Function of Lactate Dehydrogenase A: Therapeutic Potential in Brain Tumor. *Brain Pathology*, 26(1), 3-17.
- Vassar, R. 2004. Bace1 - the Beta-Secretase Enzyme in Alzheimer's Disease. *Journal of Molecular Neuroscience*, 23(1-2), 105-113.

- Vassar, R., Bennett, B. D., Babu-Khan, S., Kahn, S., Mendiaz, E. A., Denis, P., Teplow, D. B., Ross, S., Amarante, P., Loeloff, R., Luo, Y., Fisher, S., Fuller, L., Edenson, S., Lile, J., Jarosinski, M. A., Biere, A. L., Curran, E., Burgess, T., Louis, J. C., Collins, F., Treanor, J., Rogers, G. & Citron, M. 1999. Beta-Secretase Cleavage of Alzheimer's Amyloid Precursor Protein by the Transmembrane Aspartic Protease Bace. *Science*, 286(5440), 735-741.
- Von Arnim, C. A. F., Kinoshita, A., Peltan, I. D., Tangredi, M. M., Herl, L., Lee, B. M., Spoelgen, R., Hshieh, T. T., Ranganathan, S., Battey, F. D., Liu, C. X., Bacskai, B. J., Sever, S., Irizarry, M. C., Strickland, D. K. & Hyman, B. T. 2005. The Low Density Lipoprotein Receptor-Related Protein (Lrp) Is a Novel Beta-Secretase (Bace1) Substrate. *Journal of Biological Chemistry*, 280(18), 17777-17785.
- Wang, M. H., Liao, C. W., Hu, Y., Pan, Q. W. & Jiang, J. 2017. Sensitization of Breast Cancer Cells to Paclitaxel by Dichloroacetate through Inhibiting Autophagy. *Biochemical and Biophysical Research Communications*, 489(2), 103-108.
- Wang, X. L., Su, B., Siedlak, S. L., Moreira, P. I., Fujioka, H., Wang, Y., Casadesus, G. & Zhu, X. W. 2008. Amyloid-Beta Overproduction Causes Abnormal Mitochondrial Dynamics Via Differential Modulation of Mitochondrial Fission/Fusion Proteins. *Proceedings of the National Academy of Sciences of the United States of America*, 105(49), 19318-19323.
- Wang, Y. Q., Qu, D. H. & Wang, K. 2016. Therapeutic Approaches to Alzheimer's Disease through Stimulating of Non-Amyloidogenic Processing of Amyloid Precursor Protein. *European Review for Medical and Pharmacological Sciences*, 20(11), 2389-2403.
- Wang, Y. Z. & Xu, T. L. 2011. Acidosis, Acid-Sensing Ion Channels, and Neuronal Cell Death. *Molecular Neurobiology*, 44(3), 350-358.
- Warburg O, Wind F, Negelein E. 1927. THE METABOLISM OF TUMORS IN THE BODY. *J Gen Physiol.*, 8(6), 519-30.
- Wiegering, A., Matthes, N., Muhling, B., Koospal, M., Quenzer, A., Peter, S., Germer, C. T., Linnebacher, M. & Otto, A. 2017. Reactivating P53 and Inducing Tumor Apoptosis (Rita) Enhances the Response of Rita-Sensitive Colorectal Cancer Cells to Chemotherapeutic Agents 5-Fluorouracil and Oxaliplatin. *Neoplasia*, 19(4), 301-309.

- Willem, M., Garratt, A. N., Novak, B., Citron, M., Kaufmann, S., Rittger, A., Destrooper, B., Saftig, P., Birchmeier, C. & Haass, C. 2006. Control of Peripheral Nerve Myelination by the Beta-Secretase Bace1. *Science*, 314(5799), 664-666.
- Willem, M., Tahirovic, S., Busche, M. A., Ovsepijan, S. V., Chafai, M., Kootar, S., Hornburg, D., Evans, L. D. B., Moore, S., Daria, A., Hampel, H., Muller, V., Giudici, C., Nuscher, B., Wenninger-Weinzierl, A., Kremmer, E., Heneka, M. T., Thal, D. R., Giedraitis, V., Lannfelt, L., Muller, U., Livesey, F. J., Meissner, F., Herms, J., Konnerth, A., Marie, H. & Haass, C. 2015. Eta-Secretase Processing of App Inhibits Neuronal Activity in the Hippocampus. *Nature*, 526(7573), 443-450.
- Wong, J. Y. Y., Huggins, G. S., Debidda, M., Munshi, N. C. & De Vivo, I. 2008. Dichloroacetate Induces Apoptosis in Endometrial Cancer Cells. *Gynecologic Oncology*, 109(3), 394-402.
- World Health Organisation. 2018. The Epidemiology and Impact of Dementia: Current State and Future Trends. [online] Available at: <http://www.who.int/mentalhealth/neurology/dementia/dementiathematicbriefepidemiology.pdf>.
- Wszelaki, N. and Melzig, M. 2013. Additive Protective Effects of Luteolin and Pyruvate against 6-Hydroxydopamine and 3-Hydroxykynurenine Induced Neurotoxicity in SH-SY5Y Cells. *Pharmacology & Pharmacy*, 4 (4), 369-376.
- Wu, Z. F., Zhu, Y. S., Cao, X. S., Sun, S. F. & Zhao, B. L. 2014. Mitochondrial Toxic Effects of a Beta through Mitofusins in the Early Pathogenesis of Alzheimer's Disease. *Molecular Neurobiology*, 50(3), 986-996.
- Xiang, Y. W., Xu, G. L. & Weigel-Van Aken, K. A. K. 2010. Lactic Acid Induces Aberrant Amyloid Precursor Protein Processing by Promoting Its Interaction with Endoplasmic Reticulum Chaperone Proteins. *Plos One*, 5(11).
- Yan, R. Q., Bienkowski, M. J., Shuck, M. E., Miao, H. Y., Tory, M. C., Pauley, A. M., Brashler, J. R., Stratman, N. C., Mathews, W. R., Buhl, A. E., Carter, D. B., Tomasselli, A. G., Parodi, L. A., Heinrikson, R. L. & Gurney, M. E. 1999. Membrane-Anchored Aspartyl Protease with Alzheimer's Disease Beta-Secretase Activity. *Nature*, 402(6761), 533-537.

- Yan, R. Q. & Vassar, R. 2014. Targeting the Beta Secretase Bace1 for Alzheimer's Disease Therapy. *Lancet Neurology*, 13(3), 319-329.
- Yang, Y. N., Turner, R. S. & Gaut, J. R. 1998. The Chaperone Bip/Grp78 Binds to Amyloid Precursor Protein and Decreases a Beta 40 and a Beta 42 Secretion. *Journal of Biological Chemistry*, 273(40), 25552-25555.
- Yates, C. M., Butterworth, J., Tennant, M. C. & Gordon, A. 1990. Enzyme-Activities in Relation to Ph and Lactate in Post-mortem Brain in Alzheimer-Type and Other Dementias. *Journal of Neurochemistry*, 55(5), 1624-1630.
- Ying, Y. & Padanilam, B. J. 2016. Regulation of Necrotic Cell Death: P53, Parp1 and Cyclophilin D-Overlapping Pathways of Regulated Necrosis? *Cellular and Molecular Life Sciences*, 73(11-12), 2309-2324.
- Yu, G., Nishimura, M., Arawaka, S., Levitan, D., Zhang, L. L., Tandon, A., Song, Y. Q., Rogaeva, E., Chen, F. S., Kawaral, T., Supala, A., Levesque, L., Yu, H., Yang, D. S., Holmes, E., Millman, P., Liang, Y., Zhang, D. M., Xu, D. H., Sato, C., Rogaeve, E., Smith, M., Janus, C., Zhang, Y. N., Aebersold, R., Farrer, L., Sorbi, S., Bruni, A., Fraser, P. & St George-Hyslop, P. 2000. Nicastrin Modulates Presenilin-Mediated Notch/Glp-1 Signal Transduction and Beta App Processing. *Nature*, 407(6800), 48-54.
- Yuan, C., Gao, J. Y., Guo, J. C., Bai, L., Marshall, C., Cai, Z. Y., Wang, L. M. & Xiao, M. 2014. Dimethyl Sulfoxide Damages Mitochondrial Integrity and Membrane Potential in Cultured Astrocytes. *Plos One*, 9(9).
- Yuan, X. Z., Sun, S., Tan, C. C., Yu, J. T. & Tan, L. 2017. The Role of Adam10 in Alzheimer's Disease. *Journal of Alzheimers Disease*, 58(2), 303-321.
- Zhang, Q. Y., Tan, M. S., Yu, J. T. & Tan, L. 2016. The Role of Retromer in Alzheimer's Disease. *Molecular Neurobiology*, 53(6), 4201-4209.
- Zhang, X., Li, Y. F., Xu, H. X. & Zhang, Y. W. 2014. The Gamma-Secretase Complex: From Structure to Function. *Frontiers in Cellular Neuroscience*, 8.

Zhang, Y. W., Luo, W. J., Wang, H., Lin, P., Vetrivel, K. S., Liao, F., Li, F., Wong, P. C., Farquhar, M. G., Thinakaran, G. & Xu, H. A. 2005. Nicastrin Is Critical for Stability and Trafficking but Not Association of Other Presenilin/Gamma-Secretase Components. *Journal of Biological Chemistry*, 280(17), 17020-17026.

Zoltowska, K. M. & Berezovska, O. 2018. Dynamic Nature of Presenilin1/Gamma-Secretase: Implication for Alzheimer's Disease Pathogenesis. *Molecular Neurobiology*, 55(3), 2275-2284.